IDENTIFICATION OF HIGH COLLISION LOCATIONS FOR THE CITY OF REGINA USING GIS AND POST-NETWORK SCREENING ANALYSIS

A Thesis Submitted to the College of

Graduate Studies and Research

In Partial Fulfillment of the Requirements

For the Degree of Master of Science

In the Department of Civil and Geological Engineering

University of Saskatchewan

Saskatoon

By

Jason Young

PERMISSION TO USE

In presenting this thesis in partial fulfillment of the requirements for a Postgraduate degree from the University of Saskatchewan, I agree that the Libraries of this University may make it freely available for inspection. I further agree that permission for copying of this thesis in any manner, in whole or in part, for scholarly purposes may be granted by the professor or professors who supervised my thesis work or, in their absence, by the Head of the Department or the Dean of the College in which my thesis work was done. It is understood that any copying or publication or use of this thesis or parts thereof for financial gain shall not be allowed without my written permission. It is also understood that due recognition shall be given to me and to the University of Saskatchewan in any scholarly use which may be made of any material in my thesis.

Requests for permission to copy or to make other use of material in this thesis in whole or part should be addressed to:

Head of the Department of Civil and Geological Engineering
University of Saskatchewan
Engineering Building
57 Campus Drive
Saskatoon, Saskatchewan S7N 5A9
Canada

ABSTRACT

In 2010, the American Association of State Highway and Transportation Officials (AASHTO) released the first edition of the Highway Safety Manual (HSM). The HSM introduces a six-step safety management process which provides engineers with a systematic and scientific approach to managing road safety. The first step of this process, network screening, aims to identify the locations that will most benefit from a safety improvement program. The output obtained from network screening is simply a list of locations that have a high concentration of collisions, based on their potential for safety improvement. The ranking naturally tends to lead to the assumption that the most highly ranked locations are the obvious target locations where road authorities should allocate their often-limited road safety resources. Though these locations contain the highest frequency of collisions, they are often spatially unrelated, and scattered throughout the roadway network. Allocating safety resources to these locations may not be the most effective method of increasing road safety.

The purpose of this research is to investigate and validate a two-step method of post-network screening analysis, which identifies collision hotzones (i.e., groups of neighboring hotspots) on a road network. The first step is the network screening process described in the HSM. The second step is new and involves network-constrained kernel density estimation (KDE), a type of spatial analysis. KDE uses expected collision counts to estimate collision density, and outputs a graphical display that shows areas (referred to here as hotzones) with high collision densities. A particularly interesting area of application is the identification of high-collision corridors that may benefit from a program of systemic safety improvements. The proposed method was tested using five years of collision data (2005-2009) for the City of

Regina, Saskatchewan. Three different network screening measures were compared: 1) observed collision counts, 2) observed severity-weighted collision counts, and 3) expected severity-weighted collision counts. The study found that observed severity-weighted collision counts produced a dramatic picture of the City's hotzones, but this picture could be misleading as it could be heavily influenced by a small number of severe collisions. The results obtained from the expected severity-weighted collision counts smoothed the effects of the severity-weighting and successfully reduced regression-to-the-mean bias. A comparison was made between the proposed approach and the results of the HSM's existing network screening method. As the proposed approach takes the spatial association of roadway segments into account, and is not limited to single roadway segments, the identified hotzones capture a higher number of expected EPDO collisions than the existing HSM methodology. The study concludes that the proposed two-step method can help transportation safety professionals to prioritize hotzones within high-collision corridors more efficiently and scientifically.

Jurisdiction-specific safety performance functions (SPFs) were also developed over the course of this research, for both intersections (three-leg unsignalized, four-leg unsignalized, three and four-leg signalized), and roadway segments (major arterials, minor arterials, and collectors). These SPFs were compared to the base SPFs provided in the HSM, as well as calibrated HSM SPFs. To compare the different SPFs and find the best-fitting SPFs for the study region, the study used statistical goodness-of-fit (GOF) tests and cumulative residual (CURE) plots. Based on the results of this research, the jurisdiction-specific SPFs were found to provide the best fit to the data, and would be the best SPFs for predicting collisions at intersections and roadway segments in the City of Regina.

ACKNOWLEDGEMENTS

I've been fortunate enough to receive guidance from many talented and experienced people over the course of this journey. First and foremost, I would like to thank my advisor, Dr. Peter Park, for his dedication and support along the way. Thank you to my committee members: Dr. Curtis Berthelot, Dr. Gordon Sparks, Scott Thomas, and Dr. Moh Boulfiza. I'm also indebted to my fellow graduate students for their assistance and camaraderie, as well as Ms. Katie Yuan, my family, and friends.

Thank you to Saskatchewan Government Insurance, The Saskatchewan Centre of Excellence for Transportation and Infrastructure, and the City of Regina for the funding and cooperation that made this research possible.

TABLE OF CONTENTS

LIST OF FIGURES

LIST OF TABLES

CHAPTER 1. INTRODUCTION

1.1. Research Overview

With a population of 215,000, Regina is the second-largest city in Saskatchewan, and the eighteenth-largest in Canada (Statistics Canada, 2010). The city is located on the Trans-Canada Highway, as well as four provincial highways (No. 6, No. 11, No. 33 and No. 46). A perimeter expressway (Ring Road) currently encircles the city, and there are plans to build a highway bypass that will divert heavier vehicles from the existing road network (City of Regina, 2007). The city's road network plan is shown in Figure 1.

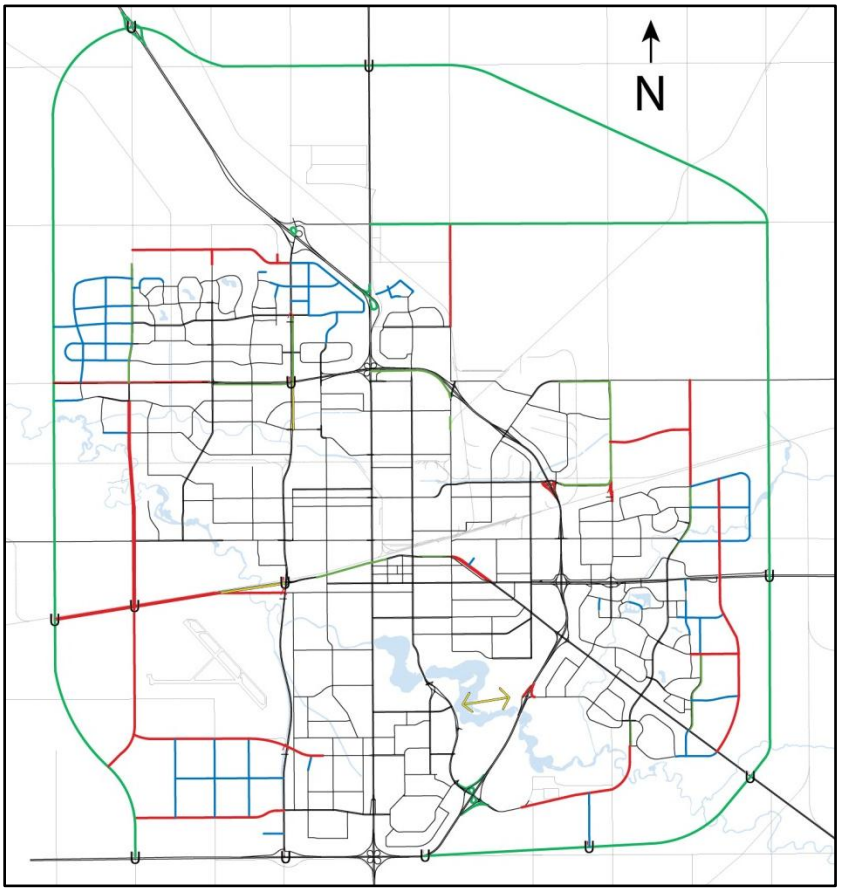

Figure 1: The City of Regina's Road Network Plan. (City of Regina, 2007)

According to Saskatchewan Government Insurance's (SGI) most recent collision data, Regina had the second-highest number of annual collisions in the province in 2009, with a total of 10,625 (as compared to Saskatoon's 13,409) (SGI, 2011). Figure 2 summarizes the reported PDO, injury, and fatal collisions in Regina for the most recent four years of available data.

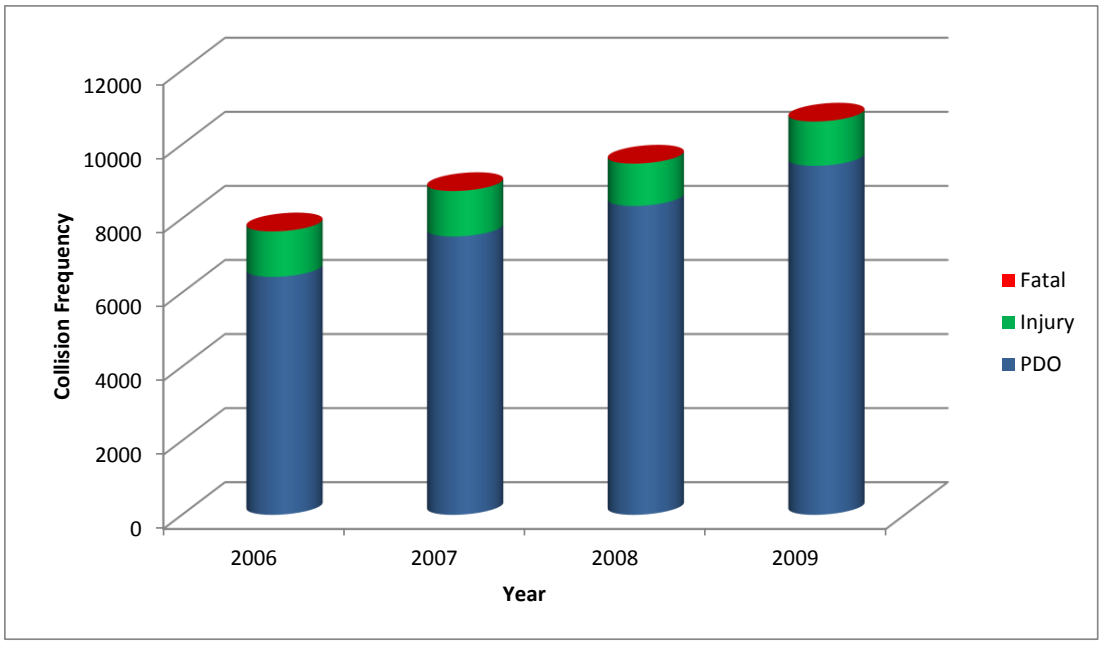

Figure 2: Collisions by Severity from 2006 to 2009.

As the figure shows, the number of collisions has been growing steadily in recent years. In 2006, there were a total of 7,659 collisions, and in 2009 that number increased to 10,625. The biggest contributor to this increase was property damage only (PDO) collisions, which increased from 6,426 in 2006 to 9,423 in 2009.

Using the societal collision costs provided in AASHTO's Highway Safety Manual (HSM), which are shown in Table 1, the cost of these collisions can be estimated. In 2009, the total cost to society was approximately $185 million.

Table 1: Societal Collision Costs (AASHTO, 2010).

Severity	Comprehensive Collision Cost
Fatality	$4,008,900
Injury	$82,600
PDO	$7,400

In order to reduce collisions, jurisdictions typically allocate resources to engineering projects that are aiming to reduce a certain type of collisions on roadway networks in their governing area. Unfortunately, the jurisdictions responsible for these engineering projects have limited resources; therefore, a system and/or tool is required to identify candidate projects that are expected to produce the greatest increase in safety. The six-step roadway safety management process described in the following sections can be viewed as a systematic and data-driven means of achieving these safety goals.

1.2. Roadway Safety Management Process

Recently, the American Association of State Highway and Transportation Officials (AASHTO) released the first edition of the Highway Safety Manual (HSM) (AASHTO, 2010). The HSM presents systematic tools and methodologies to aid transportation professionals in the area of roadway safety; one such tool is the roadway safety management process, which is made up of the following six steps:

1. *Safety Network Screening: Reviewing a transportation network to identify and rank sites based on the potential for reducing average collision frequency.*
2. *Diagnosis: Evaluating collision data, historic site data, and field conditions to identify collision patterns.*

3. *Select Countermeasures: Identifying factors that may contribute to collisions at a site and selecting possible countermeasures to reduce the average collision frequency.*
4. *Economic Appraisal: Evaluating the benefits and costs of the possible countermeasures and identifying individual projects that are cost effective or economically justified.*
5. *Prioritize Projects: Evaluating economically justified improvements at specific sites, and across multiple sites, to identify a set of improvement projects to meet objectives such as cost, mobility, or environmental impacts.*
6. *Safety Effectiveness Evaluation: Evaluating effectiveness of a countermeasure at one site or multiple sites in reducing collision frequency or severity.*

The proposed research will focus on "Safety Network Screening," which is described in detail in the following section.

1.3. Safety Network Screening

"Safety Network Screening" is described in the HSM as "...the process for reviewing a transportation network to identify and rank sites from most likely to least likely to benefit from safety improvements..." (AASHTO, 2010). The identification and ranking of sites is important, as jurisdictions typically have limited resources for addressing traffic safety concerns. For example, the City of Saskatoon states one of its traffic safety objectives in the 2011 preliminary budget as follows:

> *Conduct an independent review of three high collision intersections per year. Geometric improvements to intersections based on the review ... to improve the safety and collision rate* (City of Saskatoon, 2011).

With approximately 250 signalized intersections alone (City of Saskatoon, 2011), a systematic tool is required in order to select the sites what will result in the greatest increase in safety; "Safety Network Screening" is one such tool.

The HSM provides a set of mathematical formulas known as safety performance functions (SPFs) to be used in performing this screening. More specifically, SPFs are regression equations that can be used to estimate average collision frequencies, using traffic volumes and roadway lengths as primary input. An example expression of an SPF for single-vehicle crashes on urban/suburban arterials is given as follows:

$$N_{brsv} = \exp(a + b \times ln(AADT) + ln(L)) \qquad \text{[Equation 1]}$$

Where:

N_{brsv} = predicted average crash frequency of single-vehicle crashes for base conditions (collisions/year);

a = intercept regression coefficient;

b = AADT regression coefficient;

AADT = average annual daily traffic volume (vehicles per day) on roadway segment;

L = length of roadway segment (miles).

During the network screening process, SPFs are used to identify high-collision locations on the roadway network, for the specific roadway type being examined (e.g., signalized intersections, two-lane collectors). The selected sites can then be studied in more detail to identify collision patterns, contributing factors, and appropriate countermeasures. The HSM provides a number of network screening methods that incorporate SPFs into the decision-making process, including 'excess predicted average collision frequency,' 'expected average collision

frequency with empirical Bayes (EB) adjustment,' 'equivalent property damage only (EPDO) average collision frequency with EB adjustment,' and 'excess expected average collision frequency with EB adjustment.'

In North America, many road authorities currently use the safety network screening process outlined in the HSM. The locations identified during safety network screening are also known as hotspots, blackspots, sites with promise, or high risk locations where there are concentrations of collisions within a network. The locations typically refer to an intersection or road segment and may also refer to a location such as a ramp (Hauer, 1996). In recent decades, the questions surrounding the best way to identify hotspots and the best way to identify a manageable and appropriate number of locations have been the subject of great interest and discussion amongst safety engineers around the world (Montella, 2010; Park and Sahaji, 2013).

1.4. Post-Network Screening Analysis

Numerous network screening measures are available, including those described in the previous section. Whichever measures are used, the output obtained from network screening is simply a list of locations that have a high concentration of collisions. The locations are ranked from the riskiest to the least risky. The ranking naturally tends to lead to the assumption that the most highly ranked locations are the obvious target locations (hotspots) where road authorities should allocate their limited road safety resources.

Depending on the sophistication of the analysis selected for the network screening, the assumption that the most highly ranked locations must merit our attention may be naïve. In addition, the assumption may not be a practical and completely useful approach in the real world where road authorities do not necessarily go from one point location to another, but may wish to

employ a systemic approach to improving surface road infrastructure and road safety by working on longer sections of roadways that could potentially include multiple hotspots. The systemic approach is particularly important where it is possible or suspected that collisions are occurring due to weaknesses within the road system as well as or instead of weaknesses at particular spots.

When it comes to the safety diagnosis (the second step of the HSM's RSMP), it is also likely that a systemic approach can offer more cost-effective solutions to safety issues. A good example of a systemic approach that coordinates safety improvements for a group of neighboring hotspots would be a corridor-level safety improvement program that implements access control/management, median installations, and/or synchronized traffic signals for multiple intersections along a corridor. The group of neighboring hotspots is then treated as a "hotzone."

The current HSM's RSMP may need an additional step, referred to here as a post-network screening analysis, between the first step (network screening) and the second step (diagnosis) to encourage safety engineers to consider possible spatial associations involved in collisions occurring at neighboring hotspots. Post-network screening analysis can help road authorities to develop corridor-level surface infrastructure improvement programs. Examples of such programs in North America include "Safe Corridor Programs" for provinces/states (Nemmers et al, 2008; New Jersey DOT, 2008; New Mexico DOT, 2003; Washington DOT, 2009) and "Integrated Corridor Safety Plan/Program" for cities/municipalities (Popoff, 2005; Shimko and Walbaum, 2010).

Spatial data analysis using a geographic information system (GIS) offers an efficient methodology for conducting a post-network screening analysis that can bridge network screening and diagnosis. Kernel density estimation (KDE) is a spatial data analysis technique that divides

the road network into a number of units, which are then analyzed using a kernel function. The output of this type of analysis is a collision density map, which shows the hotzones that exist within a road network.

1.5. Research Goal

The primary goal of this research is to investigate the proposed two-step network screening approach using a network-constrained KDE technique, which takes the spatial association of neighbouring hotspots into account.

1.6. Objectives

The specific objectives for this research are as follows:

1. Develop safety performance functions for intersections and road segments for the major road classifications in the City of Regina.
2. Conduct network screenings on the City of Regina's intersections and road segments using the HSM's standard approach.
3. Compare the network screening results obtained using the HSM's standard approach with the results obtained from the proposed two-step network screening approach using a network-constrained KDE method.

1.7. Benefits of Research

The SPFs that were developed during the course of the research can be applied to road safety engineering projects in the City of Regina. Transportation engineers will be able to screen intersections and segments within the road network for hotspots (using the HSM's traditional network screening approach) as well as hotzones (using the proposed two-step post-network

screening approach). In addition to the jurisdiction-specific SPFs that are developed, calibration factors will also be generated for use with the HSM's base SPFs.

The proposed two-step network screening approach will also benefit road safety engineers who are involved with safety corridor projects, as the proposed network-constrained KDE approach (as well as the outcome of the analysis) will allow them to identify spatially-associated regions within the road network where corridor-level safety improvements may be of benefit. Instead of allocating road safety budgets to scattered locations within a roadway network, often-limited safety-related funds can be spent on road safety improvement projects that reduce collisions on adjacent, spatially-related roadways.

1.8. Scope

This study focused on the HSM's road safety management process, with particular emphasis on the "Network Screening" step.

Traffic and collision data were provided by the City of Regina and SGI, respectively; no new data was collected from the field for the purpose of this study. Research was performed on roadways currently maintained by the City of Regina.

SPFs were developed for the following intersection categories:

- three-leg unsignalized;
- four-leg unsignalized; and
- three- and four-leg signalized.

SPFs were developed for the following road segment categories:

- major arterials;
- minor arterials; and

- collectors.

1.9. Layout of Thesis

Chapter two of this thesis contains a literature review of the development of SPFs. Chapter three discusses the steps that were undertaken in order to develop and validate the jurisdiction-specific SPFs for the City of Regina. Chapter four presents the network screening results for the intersections and road segments in the City of Regina, using the jurisdiction-specific SPFs. Chapter five describes the proposed two-step post-network screening approach using network-constrained KDE. Chapter six contains the conclusions and recommendations of this thesis.

1.10. Chapter Summary

This study focused on the City of Regina, and the collisions that occurred within the roadway network from 2004 to 2009. The HSM's roadway safety management process was used, with particular emphasis on the first step, "Safety Network Screening". The primary goal of this research was to investigate the proposed two-step network screening approach using a network-constrained KDE technique, which takes the spatial association of neighbouring hotspots into account. This goal was reached by completing three objectives: developing jurisdiction-specific SPFs for the City of Regina; conducting network screening using the developed SPFs; and applying a network-constrained kernel density estimation method.

CHAPTER 2. LITERATURE REVIEW

2.1. Literature Review on Safety Performance Functions

Safety performance functions (SPF) are regression equations that can be used to estimate average collision frequencies, using traffic volumes and roadway lengths as primary input. The following sections contain a literature review on the HSM's usage of SPFs, as well as the development, validation, and transferability of jurisdiction-specific SPFs.

2.1.1. Safety Performance Functions in the Highway Safety Manual

The first edition of AASHTO's Highway Safety Manual (HSM) provides a number of safety performance functions (SPF) for use in the six-step roadway safety management process. These SPFs were developed using collision data from various U.S. states, including Texas, California, Washington, Minnesota, Michigan and North Carolina (Harwood et al., 2000; Harwood et al., 2007; Lord et al., 2008).

The HSM provides SPFs for three categories of roadways: rural two-lane roads, rural multi-lane highways, and urban/suburban arterials. Each of these two categories is broken down further, with separate SPFs provided for roadway segments and intersections. For urban/suburban arterials, for example, there are five types of SPFs provided for roadway segments (2-lane undivided arterials, 3-lane arterials including a center two-way left-turn lane, 4-lane undivided arterials, 4-lane divided arterials, and 5-lane arterials including a center two-way left-turn lane), and four types of SPFs for intersections (3-leg signalized intersections, 3-leg intersections with stop control on the minor-road approach, 4-leg signalized intersections, and 4-leg intersections with stop control on the minor-road approach).

Various collision types are accounted for with separate SPFs. For example, five types of collision SPFs for roadway segments are given in the HSM (multiple-vehicle non-driveway collisions, single-vehicle collisions, multiple-vehicle driveway-related collisions, vehicle-pedestrian collisions, and vehicle-bicycle collisions), while four types of collision SPFs for intersections are given (multiple-vehicle collisions, single-vehicle collisions, vehicle-pedestrian collisions, and vehicle-bicycle collisions).

The functional form of a roadway segment SPF for single-vehicle collisions is shown in Equation 2:

$$N_{brsv} = \exp(a + b \times ln(AADT) + ln(L)) \quad \text{[Equation 2]}$$

Where:

N_{brsv} = predicted average crash frequency of single-vehicle crashes for base conditions (collisions/year);

a = intercept regression coefficient;

b = AADT regression coefficient;

AADT = average annual daily traffic volume (vehicles per day) on roadway segment;

L = length of roadway segment (miles) (AASHTO, 2010).

As the equation shows, there is assumed to be a linear relationship between the segment length and the predicted number of collisions. To better represent local roadway conditions, driver characteristics, and geometric design more accurately, the HSM recommends the calibration of the provided SPFs. The calibration procedure described in the HSM specifies two criteria in the selection of a dataset: 1) a minimum of 30 to 50 sites, and 2) a minimum of 100 collisions (AASHTO, 2010).

Calibration factors (e.g., Ci for intersections) are obtained by calculating the ratio of the total number of observed collisions to the total number of predicted collisions obtained from the base SPFs. Therefore, the nominal value of the calibration factor (which would be the case if the observed collision frequency equaled the predicted crash frequency) is 1. When there are more collisions observed than are predicted by the default SPF, the calibration factor will be greater than 1. When there are fewer collisions observed than are predicted by the default SPF, the calibration factor will be less than 1. Once the required calibration factors are calculated, they can be applied to the default SPFs provided in the HSM.

2.1.2. Development of Safety Performance Functions

Safety performance functions are regression equations that are used to model the relationship between explanatory variables and a dependant variable (e.g., number of predicted collisions per year). A number of potential explanatory variables have been proposed, including the following: traffic volume (AADT), segment length, design or posted speed, horizontal curves, lane widths, lighting, median type, number and type of driveways, presence of curb parking, and older drivers/driver population characteristics (Harwood et al., 2007).

The output of the SPF (i.e., the dependant variable) is typically a predicted collision frequency for a specified time interval. In the past, collision rates have also been used, but have mostly been discontinued due to the implicit assumption that the number of collisions is related linearly to the traffic volume, which is not the case (Harwood et al., 2007).

SPFs can be developed using multinomial regression analysis; the negative-binomial (NB) model is one of the most commonly-used distributions for developing collision prediction models. The NB model (also referred to as the Poisson-gamma model) assumes that the Poisson

parameter follows the gamma distribution, and allows for overdispersion in the data, due to the presence of an overdispersion parameter (Lord & Mannering, 2010). Overdispersion is present when the variance in a given dataset is greater than the mean. The NB distribution function is given in the following form:

$$F(y) = \frac{\Gamma(y+k)}{\Gamma(y+1)\Gamma(k)} \frac{\left(\frac{1}{k}\mu\right)^{y}}{\left(1+\frac{1}{k}\mu\right)^{(y+k)}} \qquad \text{[Equation 3]}$$

Where:

k = dispersion parameter;

μ = mean;

Γ = gamma function; and

y = observed value (Hilbe, 2008).

By using jurisdiction-specific SPFs, road safety engineers may be able to better capture the unique collision characteristics of their study network in a particular region. Many recent studies have described the development of jurisdiction-specific SPFs for rural roadway segments (Sacchi et al., 2012; Brimley et al., 2012; Alluri & Ogle, 2012; Bornheimer at al., 2012), urban roadway segments (Alluri & Ogle, 2012; Lu et al., 2012), rural intersections (Tegge at al., 2010; Garber et al., 2011), and urban intersections (Tegge at al., 2010; Garber et al., 2011; Lyon et al, 2005).

Garber et al. (2011) developed jurisdiction-specific SPFs for four classifications of intersections (three/four legs, signalized/unsignalized) in Virginia, and found that these models performed better than the models included in SafetyAnalyst (a road safety management software package developed by AASHTO). An example is given in Figure 3, which shows a comparison

between an HSM-supplied SPF and a locally-developed model for the State of Virginia, using data from 568 intersections from 2003 to 2007. The roadways being examined are urban 4-leg signalized intersection, with minor street AADT of 8000.

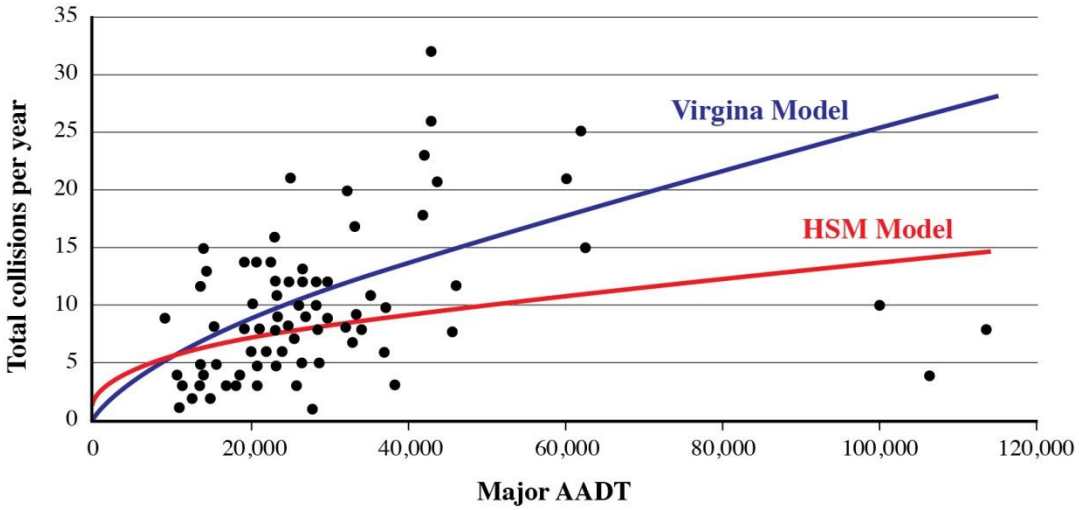

Figure 3: Comparison of Locally-Developed/HSM SPFs (Garber and Rivera, 2010).

The black triangles in the figure represent the observed number of collisions for the urban 4-leg signalized intersections. The pink line represents the predicted number of collisions per year using the built-in SPFs in HSM and the blue line represents the predicted number of collisions per year using the locally-developed SPF. It is clear from the figure that the HSM's SPF significantly underestimates the predicted number of collisions per year particularly for the signalized intersections with higher than 20,000 major street AADT. For the intersections with higher than 80,000 major street AADT, the HSM's SPF shows about 12 as the predicted value that is only about half of the value predicted (i.e., 23) by the locally-developed SPF.

Lu et al. (2012) developed jurisdiction-specific SPFs for urban freeways in Florida, and compared these SPFs to both calibrated and uncalibrated SPFs available in SafetyAnalyst. Selected results from this study are given in Figure 4.

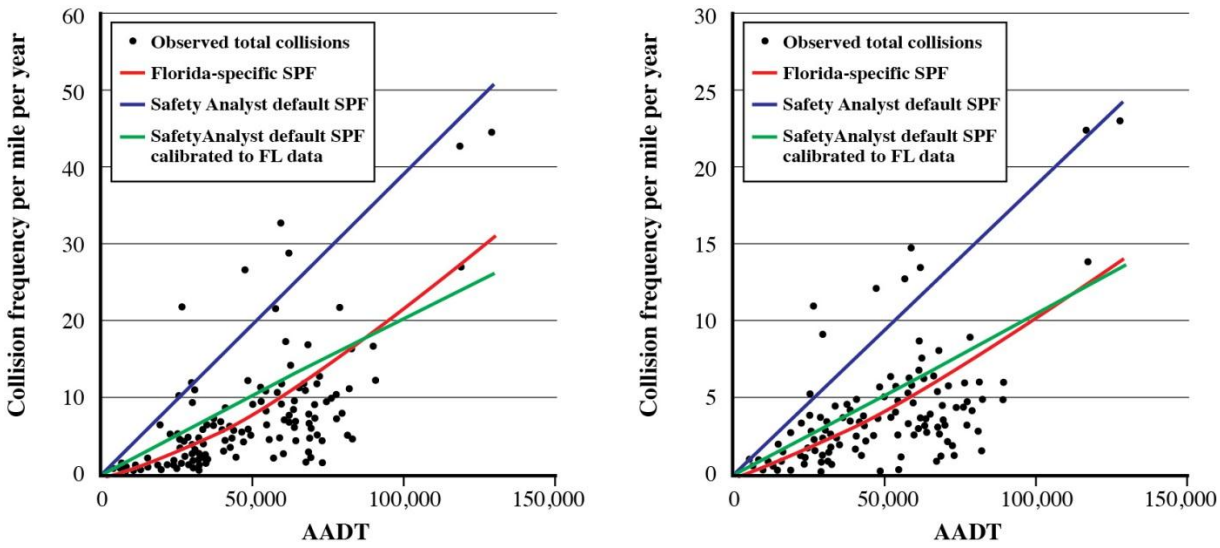

Figure 4: Observed Collisions and SPF Results for Total (Left) and FI (Right) Severity Levels (Lu et al, 2012).

As the figure shows, the uncalibrated SafetyAnalyst SPFs over-predicted the number of collisions by a wide margin, while the calibrated SafetyAnalyst SPFs and jurisdiction-specific SPFs fit the data more closely. The authors stated that the jurisdiction-specific SPFs fit the observed collision data the best, based on comparison of Freeman-Tukey R^2 values, and examination of the various models' overdispersion parameters (the jurisdiction-specific SPFs' overdispersion parameters were closer to zero than the other models).

Once SPFs are developed, a number of methods can be used to select the most appropriate model form, including the Akaike information criterion (AIC) and the Bayesian information criterion (BIC). The AIC is a relative measure of a statistical model's goodness of fit (GOF), first proposed by Hirotsugu Akaike (Akaike, 1974). This measure can be used to help determine the best-fitting model from several candidates – lower values are preferable – but provides no absolute information about a model's performance. The AIC is calculated using Equation 4 below.

$$AIC = 2 \times k - 2 \times \log(L)$$ [Equation 4]

where:

k = number of parameters in the statistical model; and

L = maximized value of the likelihood function for the estimated model.

The BIC, first proposed by Gideon Schwarz, is similar to the AIC, but includes a term to quantify the number of data points in the model (Schwarz, 1978). Like the AIC, lower values are preferable. The BIC is calculated using Equation 5 below.

$$BIC = k \times \log(n) - 2 \times \log(L)$$ [Equation 5]

where:

n = number of data points in the study dataset.

2.1.3. Validation of Safety Performance Functions

Washington et al. reported a series of statistical tests that can be used to validate models, and recommended that multiple GOF tests be assessed before making a decision in regards to a particular model's validity (Washington et al., 2005).

The mean square error (MSE) is applied to the estimation data. This test is a measure of the error associated with the model; smaller values are preferable to larger values. Equation 6 shows the formulation for this GOF test.

$$MSE = \frac{\sum_{i=1}^{n}(Y_i - \hat{Y}_i)^2}{n-p}$$ [Equation 6]

where:

Y = number of predicted collisions;

$\hat{Y}$ = number of observed collisions;

n = data sample size; and

p = number of parameters in the statistical model.

The mean prediction bias (MPB) is applied to the validation data. This test provides a measure of the magnitude and direction of the average model bias – the smaller the value, the better the model is at predicting observed data. The form of the MPB is given in Equation 7.

$$MPB = \frac{\sum_{i=1}^{n}(\hat{Y}_i - Y_i)}{n} \quad \text{[Equation 7]}$$

The mean absolute deviation (MAD) is applied to the validation data. This test gives a measure of the average magnitude of variability of prediction, and unlike the MPB, values can only be positive. Smaller values are preferable to larger values. The form of the MAD is given in Equation 8.

$$MAD = \frac{\sum_{i=1}^{n}|\hat{Y}_i - Y_i|}{n} \quad \text{[Equation 8]}$$

The mean square prediction error (MSPE) is applied to the validation data. This test can be compared to the MSE to check for over-fitting of models to estimation data (MSPE > MSE) or under-fitting models (MSPE < MSE). Similar MSPE and MSE values are desired; the form is shown in Equation 9.

$$MSPE = \frac{\sum_{i=1}^{n}(Y_i - \hat{Y}_i)^2}{n} \quad \text{[Equation 9]}$$

The Freeman Tukey R-Squared (R^2_{FT}) is applied to both estimation and validation data. This test measures GOF, with larger values indicating a better fit (Fridstrom et al., 1995). Equations 10 through 13 show the equations required to compute this value (Hamidi et al., 2010).

$$R_{FT}{}^2 = \frac{\sum_{i=1}^{n}(f_i-\bar{f})^2-\sum_{i=1}^{n}\hat{e}_i{}^2}{\sum_{i=1}^{n}(f_i-\bar{f})^2} \quad \text{[Equation 10]}$$

$$f_i = \sqrt{Y_i} + \sqrt{Y_i+1} \quad \text{[Equation 11]}$$

$$\bar{f} = \frac{\sum_{i=1}^{n}\left(\sqrt{Y_i}+\sqrt{Y_i+1}\right)}{n} \quad \text{[Equation 12]}$$

$$\hat{e}_i = \sqrt{Y_i} + \sqrt{Y_i+1} - \sqrt{4\times\hat{Y}_i+1} \quad \text{[Equation 13]}$$

An additional statistical test that can be applied to the estimation data is the likelihood ratio R-squared, R^2_{LR}, which is described as a measure of how much better the regression model fits the data than an intercept-only model (Magee, 1990). This test statistic is a function of the log likelihoods of both the full model and the intercept-only model, as well as the sample size of the dataset, and is presented in Equation 14.

$$R^2_{LR} = 1 - exp\left(-\left(2 * \log\left(\frac{L_U}{L_R}\right)\right)/n\right) \quad \text{[Equation 14]}$$

where:

L_U = likelihood of the full model;

L_R = likelihood of the restricted (intercept-only) model; and

n = data sample size.

Values range from 0 to 1, with higher values being more favourable; however, even lower values are indicative of a model that shows a better fit than the intercept-only version. This test statistic was also used by the developers of the SPFs found in the HSM, as a method of selecting the best-fitting candidate models (Harwood et al., 2007).

A graphical method known as CURE plot is used to compare different forms of SPFs (Hauer & Bamfo, 1997). In this method, each model's cumulative residuals (defined as the difference between the observed and predicted values for each site) are plotted horizontally. Residuals below zero indicate a model that over-estimates the predicted number of collision, while residuals above zero are indicative of a model that under-represents the predicted number of collisions. Additionally, good-fitting models can be identified by cumulative residuals that lie between the boundaries of two standard deviations, both above and below zero, which represent a 95% confidence limit. Figure 5 shows an example of a CURE plot, with the red line representing the cumulative residuals, and the blue and green lines showing the positive and negative two-standard deviation boundaries, respectively.

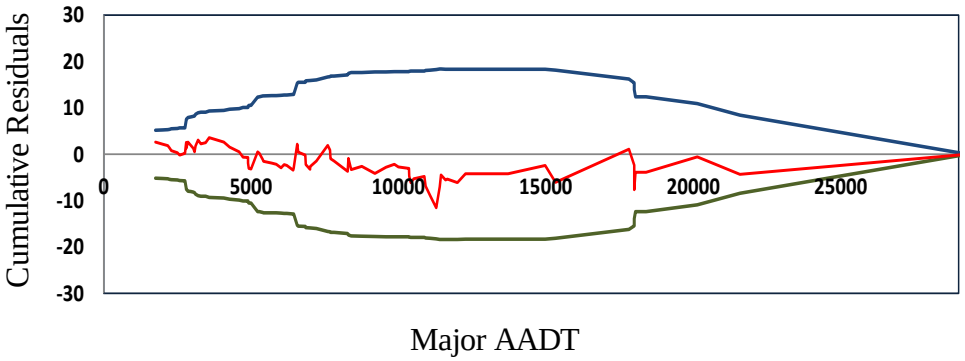

Figure 5: Sample CURE Plot of a Collision Prediction Model.

2.1.4. Transferability of Safety Performance Functions

In recent years, specific studies – known as transferability tests – have been undertaken to investigate the applicability of SPFs on regions other than the ones for which they were originally developed. Common comparison methods for these tests include visual plots (e.g., AADT/collision plots and CURE plots) and statistical goodness-of-fit tests, similar to the tests used to validate the SPFs developed for the City of Regina.

Garber et al. (2010) performed a transferability test for two-lane roadways in Virginia. The performance of SPFs developed using data from Ohio, Minnesota and Washington was compared using two measures: visual comparison of plots, as well as R^2 / Freeman-Tukey R^2 (R^2_{FT}) values. Figure 6 shows a sample result from this study.

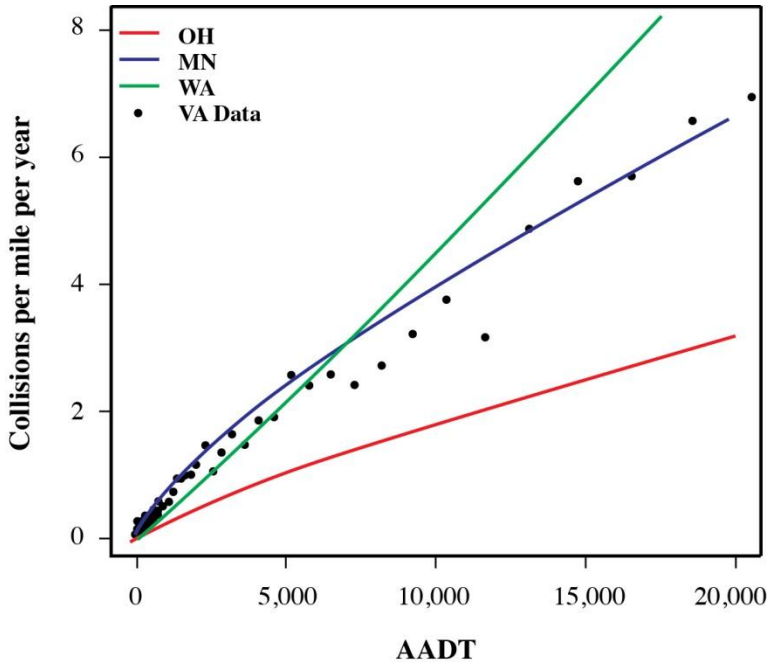

Figure 6: Urban Virginia Data (Total Collisions) Compared to SPFs from Ohio, Minnesota and Washington (Garber et al., 2010).

As the figure shows, the performance of out-of-state SPFs shows varying levels of performance, depending on the AADT range. For AADT values less than approximately 5,000, The Minnesota SPF appears to exhibit the best performance. For medium-range AADT values ($5000 < AADT \geq 12{,}000$), none of the SPFs seem to fit the Virginia data.

Table 2 shows the R^2 and R^2_{FT} results for the transferability test. As the authors of the study state, while Ohio SPFs – which were integrated into SafetyAnalyst – may be adequate for rural Virginia roadways, they are not at all transferable to urban locations. Probable reasons for the out-of-state SPFs' poor performance include differences that may exist between the roadside environments of Virginia and the other states, as well as differences that may exist between collision reporting thresholds between the different states (Garber et al., 2010).

Table 2: Fit of Virginia Total Collisions to Out-of-State SPFs (Garber et al., 2010).

	Rural Total Crashes				Urban Total Crashes		
	OH	MN	WA	NC	OH	MN	WA
R^2	0.35627	0.28727	0.48740	0.38128	-0.16281	0.33297	0.43931
R_{FT}^2	0.32400	0.14847	0.41205	0.35430	-0.34127	0.36350	0.36593

Persaud et al. (2002) investigated the transferability of SPFs developed in California and Vancouver to three and four-leg unsignalized intersections in Toronto. Similar to the study described above, both visual tests (including AADT/collision plots and CURE plots) and statistical measures (in this case, root mean squared prediction errors) were used to compare the models. While the authors found that the root mean squared prediction errors for the Vancouver (on three-leg unsignalized intersections) and California (on four-leg unsignalized intersections) models were similar to the SPFs developed using Toronto collision data, the out-of-province models tended to predict quite different collision frequencies for certain cases (e.g. low minor road AADTs using the California three-leg unsignalized intersections, and high minor road AADTs using the Vancouver four-leg unsignalized intersections). The authors concluded by stating that multiple calibration factors (based on various ranges of AADT) may be of benefit to SPF users.

2.2. Literature Review on Spatial Data Analysis

Spatial data analysis using a geographic information system (GIS) offers an efficient methodology for conducting a post-network screening analysis that can bridge network screening and diagnosis. The following sections contain a literature review on two methods of spatial data analysis used in the identification of high collision locations: planar kernel density estimation and network-constrained kernel density estimation.

2.2.1. Planar Kernel Density Estimation

Many road safety researchers have already used spatial data analysis techniques to identify hotzones amongst hotspots that are scattered across a study road network (Loo, 2009; Flahaut et al., 2003; Moons et al., 2009; Steenberghen et al., 2010).

Kernel density estimation (KDE) is one of the most popular spatial data analysis techniques. In the past, the most common form of KDE has been the two-dimensional planar approach. With planar KDE, the study area is divided into a grid with a user-specified cell size. A kernel function is then used to calculate the density of discrete events (in this case, collisions) within a user-specified search bandwidth (the search radius). The analysis results are a continuous surface that shows areas of high and low density of collisions (Yamada and Thill, 2004). An example of planar KDE is shown in Figure 7.

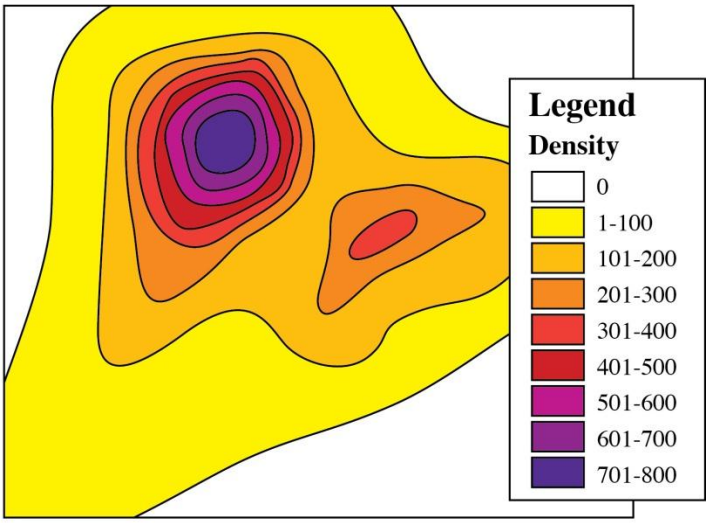

Figure 7: Planar KDE Example.

While planar KDE may be appropriate for occurrences that exist along a continuous surface (e.g. oil spills in a body of water, vegetation growth), in the case of events that are

constrained to a network space, the assumption of homogeneity of two-dimensional space does not stand up (Xie and Yan, 2008). In order to better approximate the true nature of network-based events, a network-constrained form of KDE can be utilized. This method is described in the following section.

2.2.2. Network-Constrained Kernel Density Estimation

Okabe et al. (2009) proposed a network-constrained KDE method that takes the spatial relationships of the roadway network into account. Network-constrained KDE calculates density using a linear unit whereas planar KDE calculates density using an area unit. As vehicle collisions are restrained to the network space, network-constrained KDE is a more appropriate method of analysis (Dai, 2012). The network-constrained KDE approach has been applied in recent years in the area of road safety in order to identify high-collision locations (Kuo et al., 2012; Mohaymany et al., 2013; Yamada and Thill, 2004). An example of planar KDE is shown in Figure 8.

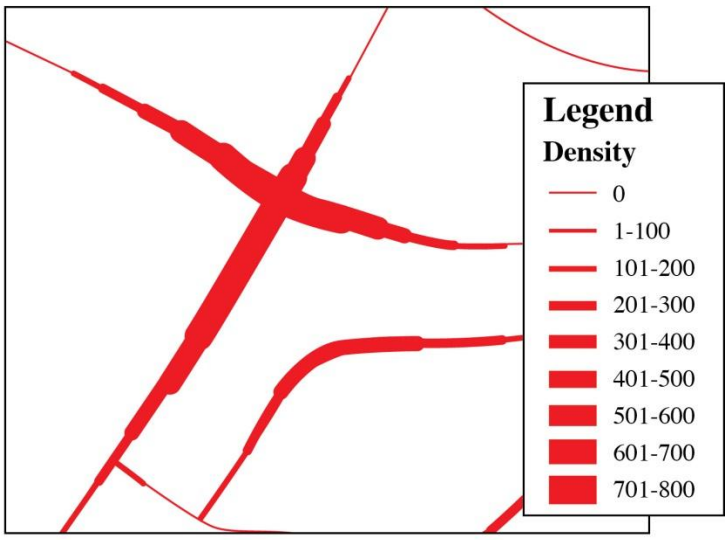

Figure 8: Network-Constrained KDE Example.

It may appear that studies that have used network-constrained KDE have successfully identified spatial associations (e.g., proximity) amongst collisions in the process of identifying hotspots and hotzones. Unfortunately, however, these studies neglected central issues in collision data analysis. Firstly, many existing studies that applied KDE failed to take into account different levels of collision severity and gave inadequate attention to severe collisions. The studies made no distinction between a PDO collision and a fatal collision, and simply treated the two collisions equally (Kuo et al., 2012; Yamada and Thill, 2004). Even more importantly, the studies simply used the observed collision counts (the raw collision data) from each location as an input for the KDE and resulting collision density maps without properly taking into account the issue of regression-to-the-mean (RTM).

As Elvik and Vaa (2004) and Park and Lord (2010) explain, RTM is an inevitable statistical phenomenon inherent in collision data and in many other data. In the case of collision data, RTM refers to the tendency for an unusually high number of collisions observed at a

location for a relatively short time period to return to a (lower) number closer to the long term average (expected) number of collisions for the location. Similarly, an unusually low number of collisions will return to a (higher) number closer to the long term average (expected) number of collisions at the location.

In practical terms, this means that if we base our spatial data analysis on the observed number of collisions collected over a given term period (e.g., three or five years), we should recognize that the output from the analysis shows only a snapshot of current hotspots/hotzones. Some of these hotspots/hotzones will not be genuine hotspots/hotzones as they are only short term problem sites. The snapshot obtained from the raw collision data may not be representative of the long term period and may make it impossible to draw meaningful conclusions about the long term impact of a safety improvement program for the hotspots/hotzones. There is clear consent amongst safety engineers that the decision to improve surface infrastructure should fully consider the long term safety impact of the proposed improvements. To measure the long term safety impact and to take into account the crucial issue of RTM, we need to use the long term average (expected) number of collisions. It is clear that the issue of RTM must be taken into account in any spatial data analysis, including KDE, designed to select hotspots/hotzones in a study network. Unfortunately, spatial data analysis studies have tended to use raw collision data and have therefore neglected the RTM issue. This is an important weakness in the spatial data analysis studies available (Yamada and Thill, 2004; De Pauw et al., 2011; Kuo et al., 2012).

The goal of this study is to improve road safety by using an improved network screening approach that identifies hotzones within corridors. The study introduces a post-network screening analysis that combines the standard HSM approach with spatial data analysis (using a network-constrained KDE technique) to identify the corridor hotzones. The

identification of corridor hotzones enables road authorities to improve road safety by developing efficient corridor-level programs for surface infrastructure improvement.

2.3. Chapter Summary

A literature review was performed for two specific topics: safety performance functions, and spatial data analysis.

The review of safety performance functions included a description of the roadway segment and intersection SPFs provided in the HSM. The development of SPFs was described, including the commonly-used negative binomial (Poisson-gamma) model, and relevant studies by past transportation safety researchers. The validation of SPFs was also described, including the statistical tests commonly used to determine the goodness of fit of both estimation and validation data. The first half of this chapter concluded with a description of transferability tests, with recent studies in both Canada and the United States summarized.

The section on spatial data analysis included an overview of relevant studies on planar kernel density estimation (where the study region is divided into a two-dimensional grid), and network-constrained kernel density estimation (where the study region is constrained to the network space).

CHAPTER 3. SAFETY PERFORMANCE FUNCTIONS

3.1. Study Data

Three types of information were required in order to perform the proposed research: road network information, traffic volume (AADT), and collision data (including severity and configuration information).

3.1.1. Road Network Basemap

The City of Regina maintains a geographic information system (GIS) of its current road network. Two ArcGIS shape files were supplied, one for intersections and one for roadway segments. These shape files contain information on each element's location, name, and other details; Table 3 shows several of the types of information available.

Table 3: Intersection and Roadway Segment Information Available in Supplied ArcGIS Shape Files.

Intersections	
Field	**Definition**
KEYNUMBER	Unique Identifier
LOCATION	Names of Intersecting Road Segments
TYPE	Signal Information
Roadway Segments	
Field	**Definition**
KEYNUMBER	Unique Identifier
FULL_NAME	Name of Road
ROAD_FUNC	Functional Classification
SPEED_LIM	Posted Speed Limit
ONE_WAY	One-Way Identifier
SHAPE_LEN	Segment Length (Metres)

The initial roadway segment data that was supplied included information on each segment's classification; further, more in-depth functional classification information was also supplied. These two sets of classification information are shown in Table 4.

Table 4: Roadway Segment Classifications.

Original Classifications
Arterial
Collector
Local
Private
Gravel
Ramp
Row
Highway
Expressway
Functional Classifications
Major Arterial
Minor Arterial
Major Collector
Minor Collector
Major Industrial/Commercial Local
Minor Industrial/Commercial Local
Major Residential Local
Minor Residential Local
Ramp
Expressway

Figure 9 shows the City of Regina's roadway network, as supplied.

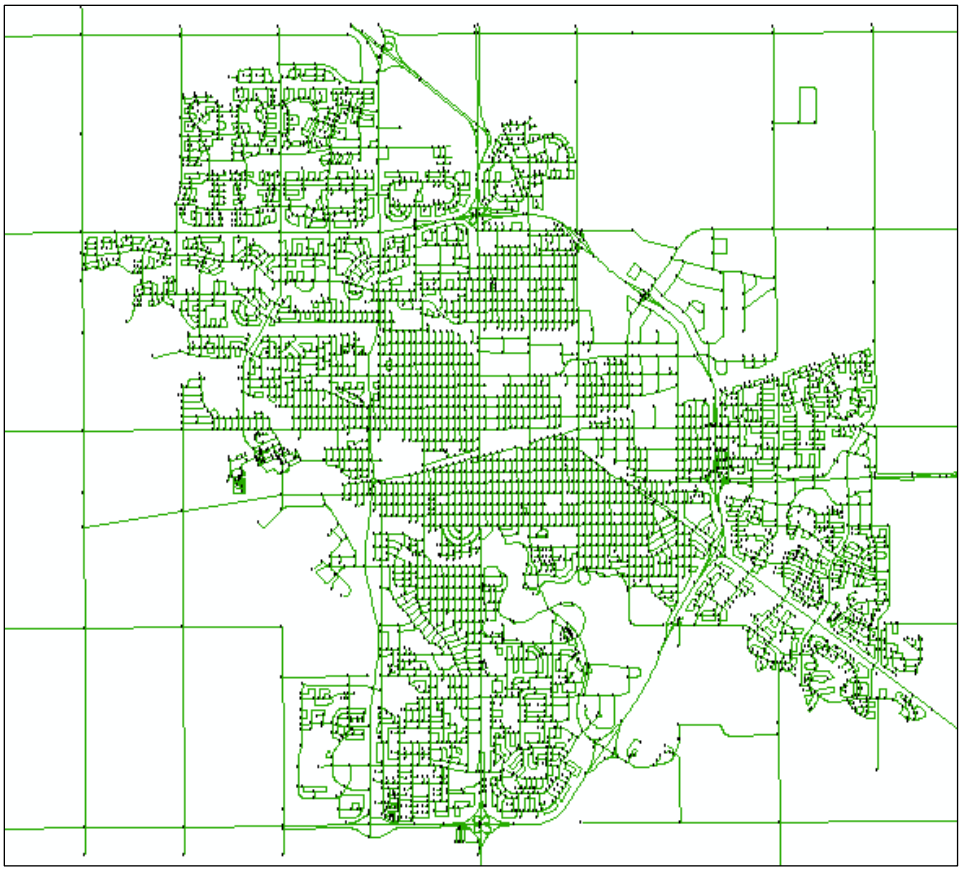

Figure 9: The City of Regina's Roadway Network Shape File.

3.1.2. Traffic Volume

Traffic volume data from the City of Regina exists in a series of spreadsheets from the years 2003, 2004, 2006, 2007, 2008, and 2009. Each traffic count location is referenced to a "UGRID," an urban grid code that can be referenced to a location in the city.

3.1.3. Collision Data

Collision data is provided in three separate databases that organize the collision records according to the following classifications: by collision (SASKAC), by vehicle (SASKVE), and by occupant (SASKOC). The databases are referenced to each other by a field entitled "Case Number," and include collisions from 2000 to 2009.

3.2. Database Management

Before the jurisdiction-specific SPFs could be developed, considerable work had to be done with the supplied databases in order to remove errors and inconsistencies, extract the required information, and accurately link the relevant pieces of information together. The steps undertaken in this regard are outlined in the following sections.

3.2.1. Road Network Basemap

The ArcGIS shape files provided by the City of Regina included a number of roadway segments which are not maintained by the City of Regina (i.e., driveways, private roads, gravel roads), and many of which share the same UGRIDs (for example, hundreds of private roads share the UGRID "1," and hundreds of gravel roads share the UGRID "3"). These road segments were identified by checking the shape file's road classification and UGRID fields.

The shape file for the City of Regina's road network also contained a high number of road segments with duplicate UGRIDs. In order to remove redundancies (which would affect the allocation of collisions and traffic volumes), each of the duplicate entries was manually checked, and where appropriate, merged using ArcGIS's "merge" function. Figure 10 shows three road segments with the same UGRID (155300), which were merged into a single segment.

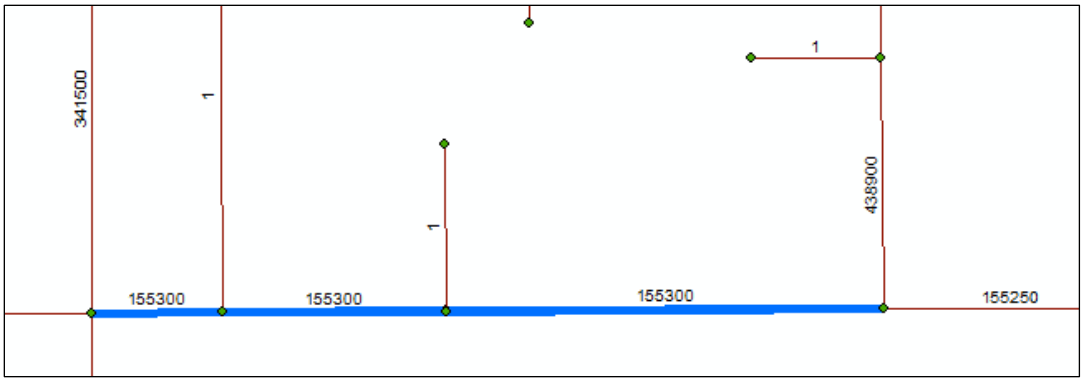

Figure 10: Road Segments with Duplicate UGRIDs.

Another issue arose due to the presence of several overpasses on Regina's perimeter road, Ring Road. Though the shape files had these overpasses labeled as intersections, in reality, no intersection-related collisions would occur at these grade-separated locations. Using Google Maps, overpass locations were determined, with the intersections labeled accordingly in ArcGIS. An example is shown in Figure 11, which shows the overpass at Ring Road and McDonald Street, both in ArcGIS and Google Maps.

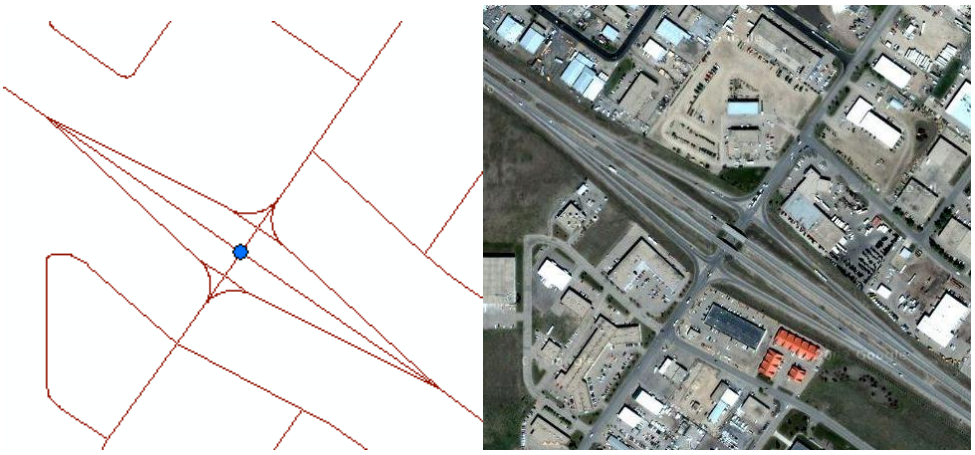

(a) **(b)**

Figure 11: (a) Intersection Representing an Overpass and (b) Google Maps View.

As supplied, the intersection shape file did not have road segments associated with each intersection. In order to make these associations (which would be required in the following steps), a Python script developed by Chad Coziahr was modified in order to spatially analyze the City of Regina's roadway network, and assign segments to each intersection location. Using this script, each intersection was classified as either 3-leg or 4-leg. This information was then integrated with a file that listed the city's signalized intersections, allowing disaggregation into the following categories: 3-leg signalized, 3-leg unsignalized, 4-leg signalized, and 4-leg unsignalized.

Two further pieces of information which were not available in the supplied databases were the number of lanes for each roadway segment, and information about whether or not each road was divided. As the City of Regina did not have a database showing the number of lanes, a surrogate measure was used in order to obtain this information. The city did have a pavement markings database, which included details on the road segments which had painted lines (e.g., dashed lines, shoulder markings, etc.). Table 5 presents a list of the supplied pavement marking types, along with the number of roadway segments that are represented by each category.

Table 5: Pavement Marking Types.

Pavement Marking Type	Quantity
Bike_Lanes	8
Centre	745
Centre Dual Dashed	3
Centre_Dashed	276
Centre_Dashed_Should	5
Centre_Left_Turn	3
Centre_Nshoulder	3
Centre_Shoulder	21
Centre_Shoulder_Hwy	1
Dashed	313
Dashed_Shoulder	40
Dashed-Shoulder_Hwy	34
Dual Dashed	33
Permanent	35
Permanent_Dashed	2
Permanent_Shoulder	16
Shoulder	51
Shoulder_Hwy	16

By using Google Maps, each of these categories of pavement marking could be assigned a number of lanes. For some of the categories, each roadway segment had to be examined individually, due to the possibility that different numbers of lanes could be represented. For example, Figure 12 shows two types of roadways that could have dashed lines painted between lanes – an undivided two lane roadway (shown on the left), or a divided four lane roadway (shown on the right). Once the visual inspection was completed, lane information was assigned to each road segment.

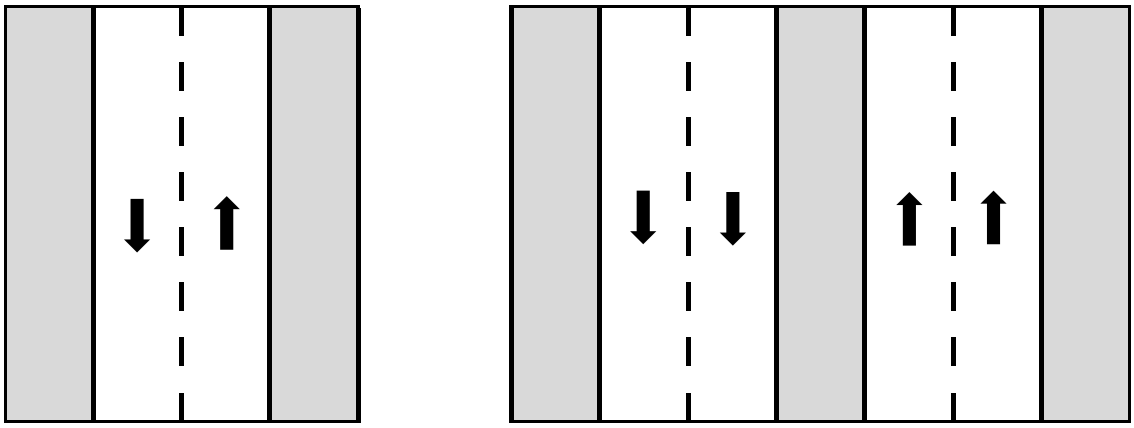

Figure 12: Examples of Different Street Types with Dashed Lane Markings: Two Lane Undivided (Left) and Four Lane Divided (Right).

In order to classify each street as divided or undivided, a city map which showed divided roadways was consulted. As Figure 13 shows, this map represented undivided roads as single lines, and divided roads as double lines.

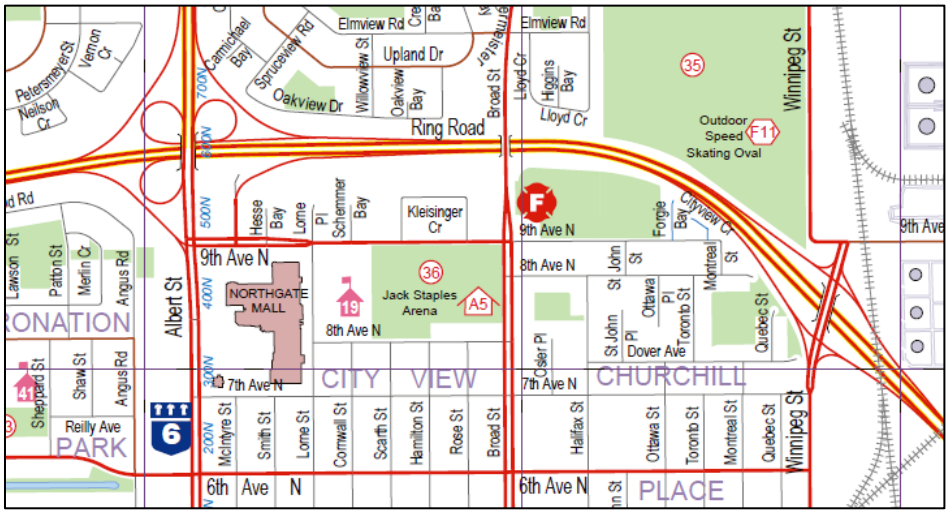

Figure 13: Street Map of Regina, Showing Divided Roadway Segments.

This information was manually added to the database; 451 roadway segments out of the 6,847 total segments were classified as divided. The divided roadway segments are shown in red on the map of Regina presented in Figure 14.

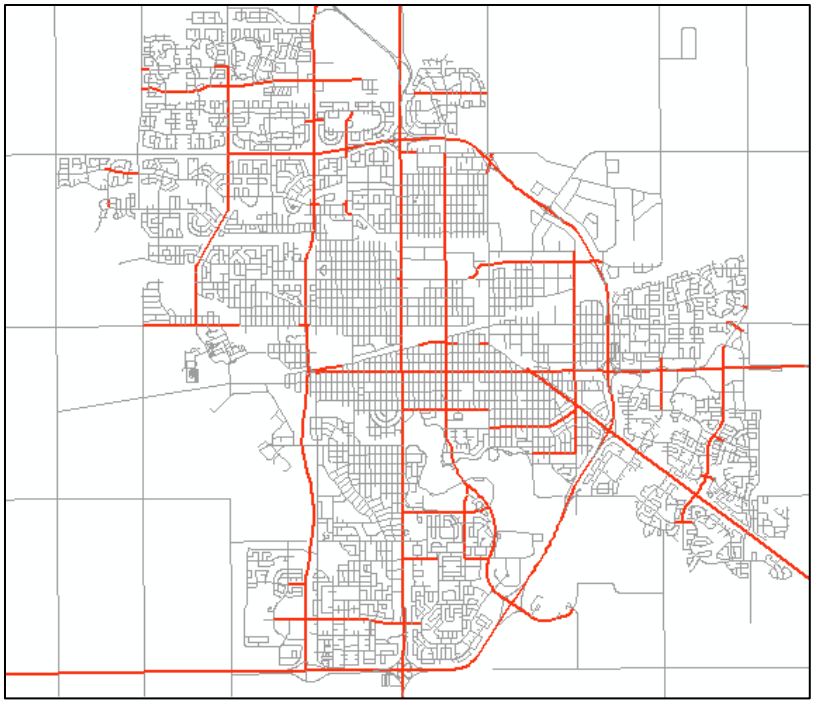

Figure 14: Divided Roadway Segments in the City of Regina Shown in Red.

3.2.2. Traffic Volume

Since traffic counts are not performed every year, for every segment, the estimation procedure described in the HSM was followed in order to generate volume information for missing years:

- If data is missing for one or more years between known traffic counts, linear interpolation is used to estimate the missing years' data; and

- If data is missing before or after the first or last recorded counts, this value is assumed to remain constant for the missing portion of the study period (AASHTO, 2010).

Using this procedure, a database of traffic volumes between the years 2003 and 2009 was developed for 1,920 roadway segments.

3.2.3. Collision Data

In order to extract the required collision information for the City of Regina, the three supplied collision databases (SASKAC, SASKVE and SASKOC) needed to be related to each other; this operation was possible through the use of the "Case Number" field, which linked individual collision occurrences together with the vehicles and occupants involved.

As the focus of this study is vehicle-only collisions, pedestrian and bicycle-related collisions needed to be separated. The OCCPOS field in the occupant database describes the position in or on the vehicle each occupant was located, based on the diagram filled out by arriving officers. A value of "09" in this field represents pedestrians, including people pushing a bike or riding in a wheelchair (SGI, 2007). This field could be queried in order to separate pedestrian entries from the database.

The VIDENT field in the vehicle database gives a description of each vehicle involved in a collision, based on its general design characteristics and body type. This field could be queried for entries which contained a value of "13" in this field, which represents bicycles, in order to separate the bicycle-related collisions from the vehicle-only collisions.

It was also necessary to correctly allocate collisions to roadway segments or intersections. While the collisions would eventually be assigned to UGRIDs belonging to either intersections or road segment, collisions that occurred on roadway segments may be intersection-related; a query of the collision database was required in order to identify these instances. Using MS Access, the ACCSITE field in the collision database was queried to identify all collisions that had the following values: "01" (Non-Intersection), "05" (Intersection With Private Approach, Driveway), "08" (Bridge or Overpass), "09" (Tunnel or Underpass), "11" (Passing

Lane or Climbing Lane), “13” (Off Roadway [Within Right of Way]), or “14” (Other). These collisions were categorized as being non-intersection-related, and could be assigned to roadway segment UGRIDs.

3.2.4. Integrated Database

Three separate databases (collision, traffic volume, and road basemap) were integrated into a final database for the following steps undertaken in this research. This database was broken down into two subsets: one for intersections (see Table 6 as an example) and one for road segments (see Table 7 as an example).

Table 6: Integrated Database Structure for Intersections.

Location	UGRID	Int. Type	Major AADT					Minor AADT					Fatal Collisions					Injury Collisions					PDO Collisions				
			2005	2006	2007	2008	2009	2005	2006	2007	2008	2009	2005	2006	2007	2008	2009	2005	2006	2007	2008	2009	2005	2006	2007	2008	2009
9th Ave N & McCarthy Blvd	RE688050	4S	19500	19500	21500	21500	21500	16100	16100	18900	18900	18900	0	0	0	0	0	11	3	9	7	9	26	17	28	29	48
Dewdney Ave & Lewvan Dr	RE697760	4S	33800	33800	33900	33900	33900	13900	13900	15700	15700	15700	0	0	0	0	0	12	11	9	7	9	22	26	28	44	23
4th Ave & Lewvan Dr	RE683430	4S	33400	33400	33400	33400	33400	11600	11600	11700	11700	11700	1	0	0	0	0	11	9	12	6	8	21	24	25	23	18
Park St & Victoria Ave	RE706920	4S	25900	25900	25900	25900	26200	18400	18400	18400	18400	18400	0	0	0	0	0	9	6	10	6	10	19	22	27	36	40
Prince Of Wales Dr & Victoria Ave	RE707580	4S	28450	29500	29500	29500	37600	11400	15100	15100	15100	15200	0	0	0	0	0	5	8	4	10	9	23	17	22	35	57
Fleet St & Victoria Ave N Srv Rd	RE700100	4U	17600	15600	15600	15600	24700	4000	4400	4400	4400	9400	0	0	0	0	0	3	3	2	2	2	12	16	11	17	13
Arcola Ave & Victoria Ave	RE689720	4S	27600	27600	27600	27600	28200	15400	15400	15400	15400	15400	0	0	0	0	0	2	8	9	6	8	24	14	19	30	52
Albert St & Saskatchewan Dr	RE689010	4S	32300	32300	32300	33100	33100	20800	20800	20800	17200	17200	0	0	0	0	0	8	5	7	8	11	23	31	33	32	54
Victoria Ave & Coleman Cres	RE696740	4S	29800	32200	32200	32200	52400	5800	5800	5800	5800	15400	0	0	0	0	0	7	5	3	6	6	13	14	11	24	13
Glencairn Rd & Victoria Ave N Srv Rd	RE701010	4U	6050	5800	5800	5800	9400	4500	4600	4600	4600	6200	0	0	0	0	0	0	0	1	3	3	15	14	12	17	16

Table 7: Integrated Database Structure for Road Segments.

Street Name	UGRID	Road Class	Length (m)	Traffic Volume					Fatal Collisions					Injury Collisions					PDO Collisions				
				2005	2006	2007	2008	2009	2005	2006	2007	2008	2009	2005	2006	2007	2008	2009	2005	2006	2007	2008	2009
Albert St	RE3400	MAJ	362	27500	27500	27500	27400	27400	0	0	0	0	0	3	3	4	3	1	10	10	8	17	15
Quance St	RE308275	COLL	575	5950	6600	3200	3200	4700	0	0	0	0	0	0	3	3	1	6	7	2	9	8	8
9th Ave N	RE900015	MAJ	810	16100	16100	18900	18900	18900	0	0	0	0	0	1	0	1	4	5	10	4	5	8	10
Broad St	RE38700	MAJ	488	21700	21700	21700	25300	24400	0	0	0	0	0	4	1	2	3	1	3	0	1	2	10
Albert St	RE7500	MAJ	406	22800	22800	22700	22700	22700	0	0	0	0	0	0	3	0	1	5	5	2	9	9	11
Albert St	RE3100	MAJ	231	25100	25100	25100	22100	22100	0	0	0	0	0	0	1	3	2	0	13	10	9	11	10
Saskatchewan Dr	RE350300	MAJ	315	20800	20800	20800	14600	14600	0	0	0	0	0	0	1	3	2	2	10	6	10	10	7
Quance St	RE308225	COLL	262	8400	8400	8400	8400	14600	0	0	0	0	0	0	2	0	0	1	8	3	7	7	7
Avonhurst Dr	RE28000	MAJ	210	13400	13400	15200	15200	15200	0	0	0	0	0	0	1	2	0	2	3	1	2	4	5
Albert St	RE6600	MAJ	135	35000	35000	34100	29000	29000	0	0	0	0	0	3	1	1	0	2	3	5	4	0	0

3.3. SPF Development

R-Language (a statistical computing program) was used to develop SPFs, using the negative binomial distribution. Programs were written to perform the regression analysis on comma separated variable (CSV) files, which contained information on each intersection and segment, including the most recent five years of traffic volume, collision history, and segment length. Models were developed for three severity categories: total collisions, fatal/injury (FI) collisions, and property damage only (PDO) collisions.

The developed programs performed a number of intermediate functions, including calculating the five-year averages for traffic volumes, summing the collisions, and calculating the natural log for the relevant variables. Traffic volumes were divided by 1,000 in order to make the resulting coefficients more user-friendly. Separate programs were created for intersections and segments, as these locations required different input variables, and unique functional forms. The following sections contain a description of the SPF development process for intersections and segments.

3.3.1. Intersection SPFs

The City of Regina's intersections were divided into four categories: 3-leg signalized, 3-leg unsignalized, 4-leg signalized, and 4-leg unsignalized. As a low number of 3-leg signalized intersections (28) existed in the study region, these intersections were aggregated with the 4-leg signalized intersections for the purposes of this study. Table 8 shows the number of intersections for each category that were used for the development of SPFs.

Table 8: City of Regina Intersection Categories.

Category	No. of Intersections
3-Leg Unsignalized	118
4-Leg Unsignalized	125
3 & 4-Leg Signalized	144

Each of these categories was divided into two subsections by random selection: estimation (70% of the data) and validation (30% of the data). The first set of data (estimation) was used in the negative-binomial regression, and the second set of data (validation) was later used to test the models' applicability to the observed data.

For each of the three severity categories, four candidate model forms were developed; Table 9 shows the initial model forms that were created.

Table 9: Initial Candidate Model Forms for Intersections.

Model No.	Model Form
1	$N = exp^{\beta_0} \cdot \left(\frac{AADT_{min}}{1000}\right)^{\beta_1} \cdot \left(\frac{AADT_{maj}}{1000}\right)^{\beta_2}$
2	$N = exp^{\beta_0} \cdot \left(\frac{AADT_{min}}{1000}\right)^{\beta_1} \cdot \left(\frac{AADT_{maj}}{1000}\right)^{\beta_2} \cdot exp^{\left(\beta_3 \frac{AADT_{min}}{1000}\right)}$
3	$N = exp^{\beta_0} \cdot \left(\frac{AADT_{min}}{1000}\right)^{\beta_1} \cdot \left(\frac{AADT_{maj}}{1000}\right)^{\beta_2} \cdot exp^{\left(\beta_3 \frac{AADT_{maj}}{1000}\right)}$
4	$N = exp^{\beta_0} \cdot \left(\frac{AADT_{min}}{1000}\right)^{\beta_1} \cdot \left(\frac{AADT_{maj}}{1000}\right)^{\beta_2} \cdot exp^{\left(\beta_3 \frac{AADT_{min}}{1000}\right)} \cdot exp^{\left(\beta_4 \frac{AADT_{maj}}{1000}\right)}$

A number of methods were used to select the most appropriate form of SPFs for each data category, including investigation of each model's p-values, Akaike information criterion (AIC), Bayesian information criterion (BIC), cumulative residual (CURE) plots, and dispersion

parameters. Regression results for each of the three intersection types are presented in Table 10 through Table 12. CURE plots for each of the models are shown in Figure 15 through Figure 17, with cumulative residuals shown on the vertical axis and major AADT (in thousands) shown on the horizontal axis.

Table 10: Regression Results for 3-Leg Unsignalized Intersections.

	Severity	Model	Regression Coefficients										Dispersion Parameter	AIC	BIC
			β_0	*p*-Value	β_1	*p*-Value	β_2	*p*-Value	β_3	*p*-Value	β_4	*p*-Value			
3-Leg Unsignalized	Total Collisions	1	-1.717	<0.001	0.826	<0.001	0.648	<0.001	NA	NA	NA	NA	2.525	493.0	500.4
		2	-1.698	<0.001	0.664	0.128	0.647	<0.001	0.044	0.692	NA	NA	2.536	494.8	504.1
		3	-1.623	<0.001	0.837	<0.001	0.537	0.077	0.012	0.688	NA	NA	2.534	494.8	504.1
		4	-1.612	<0.001	0.686	0.119	0.544	0.073	0.041	0.709	0.011	0.707	2.545	496.7	507.8
	FI Collisions	1	-3.786	<0.001	0.858	<0.001	0.709	<0.001	NA	NA	NA	NA	2.059	245.3	252.7
		2	-3.735	<0.001	0.600	0.396	0.711	<0.001	0.066	0.686	NA	NA	2.073	247.1	256.4
		3	-4.282	<0.001	0.804	0.001	1.200	0.032	-0.045	0.347	NA	NA	2.087	246.3	255.6
		4	-4.221	<0.001	0.540	0.444	1.194	0.031	0.067	0.683	-0.045	0.348	2.097	248.2	259.3
	PDO Collisions	1	-1.832	<0.001	0.825	<0.001	0.626	<0.001	NA	NA	NA	NA	2.398	471.7	479.1
		2	-1.812	<0.001	0.667	0.142	0.624	<0.001	0.042	0.717	NA	NA	2.407	473.5	482.8
		3	-1.643	<0.001	0.849	<0.001	0.403	0.200	0.023	0.435	NA	NA	2.427	473.1	482.4
		4	-1.633	<0.001	0.712	0.121	0.410	0.192	0.037	0.746	0.023	0.448	2.436	475.0	486.1

Table 11: Regression Results for 4-Leg Unsignalized Intersections.

	Severity	Model	Regression Coefficients										Dispersion Parameter	AIC	BIC
			β_0	*p*-Value	β_1	*p*-Value	β_2	*p*-Value	β_3	*p*-Value	β_4	*p*-Value			
4-Leg Unsignalized	Total Collisions	1	-1.007	<0.001	0.732	<0.001	0.605	<0.001	NA	NA	NA	NA	3.556	559.7	567.1
		2	-0.993	<0.001	1.145	<0.001	0.613	<0.001	-0.139	0.156	NA	NA	3.612	559.8	569.1
		3	-0.698	0.037	0.754	<0.001	0.254	0.420	0.041	0.235	NA	NA	3.649	560.2	569.5
		4	-0.715	0.034	1.129	<0.001	0.295	0.352	-0.127	0.192	0.037	0.286	3.692	560.6	571.7
	FI Collisions	1	-3.195	<0.001	0.241	0.234	0.959	<0.001	NA	NA	NA	NA	2.053	301.9	309.3
		2	-3.174	<0.001	0.656	0.218	0.955	<0.001	-0.138	0.403	NA	NA	2.076	303.2	312.4
		3	-2.721	<0.001	0.260	0.204	0.468	0.391	0.054	0.341	NA	NA	2.111	302.9	312.2
		4	-2.740	<0.001	0.622	0.243	0.508	0.358	-0.120	0.468	0.049	0.388	2.124	304.4	315.5
	PDO Collisions	1	-1.138	<0.001	0.799	<0.001	0.559	<0.001	NA	NA	NA	NA	3.893	532.0	539.4
		2	-1.130	<0.001	1.202	<0.001	0.566	<0.001	-0.133	0.173	NA	NA	3.954	532.2	541.5
		3	-0.824	0.014	0.825	<0.001	0.205	0.512	0.041	0.229	NA	NA	4.006	532.5	541.8
		4	-0.843	0.012	1.192	<0.001	0.241	0.444	-0.122	0.209	0.038	0.276	4.056	533.0	544.1

Table 12: Regression Results for 3 & 4-Leg Signalized Intersections.

	Severity	Model	Regression Coefficients										Dispersion Parameter	AIC	BIC
			β_0	*p*-Value	β_1	*p*-Value	β_2	*p*-Value	β_3	*p*-Value	β_4	*p*-Value			
3 & 4-Leg Signalized	Total Collisions	1	-0.929	<0.001	0.665	<0.001	0.684	<0.001	NA	NA	NA	NA	8.993	882.8	890.2
		2	-0.976	0.002	0.702	<0.001	0.688	<0.001	-0.004	0.818	NA	NA	9.005	884.7	894.0
		3	-0.636	0.336	0.661	<0.001	0.525	0.130	0.009	0.628	NA	NA	9.018	884.6	893.8
		4	-0.642	0.333	0.732	<0.001	0.486	0.192	-0.008	0.680	0.011	0.572	9.048	886.4	897.5
	FI Collisions	1	-3.011	<0.001	0.503	<0.001	0.945	<0.001	NA	NA	NA	NA	9.190	601.3	608.7
		2	-3.113	<0.001	0.582	0.010	0.951	<0.001	-0.009	0.696	NA	NA	9.315	603.2	612.5
		3	-2.260	0.014	0.496	<0.001	0.549	0.241	0.021	0.380	NA	NA	9.159	602.6	611.8
		4	-2.240	0.015	0.664	0.006	0.436	0.385	-0.018	0.436	0.027	0.287	9.428	604.0	615.1
	PDO Collisions	1	-1.067	<0.001	0.704	<0.001	0.630	<0.001	NA	NA	NA	NA	8.408	849.7	857.1
		2	-1.139	<0.001	0.760	<0.001	0.636	<0.001	-0.006	0.740	NA	NA	8.425	851.6	860.9
		3	-0.970	0.165	0.703	<0.001	0.577	0.114	0.003	0.877	NA	NA	8.413	851.7	860.9
		4	-0.979	0.162	0.773	<0.001	0.540	0.168	-0.008	0.697	0.005	0.799	8.440	853.5	864.6

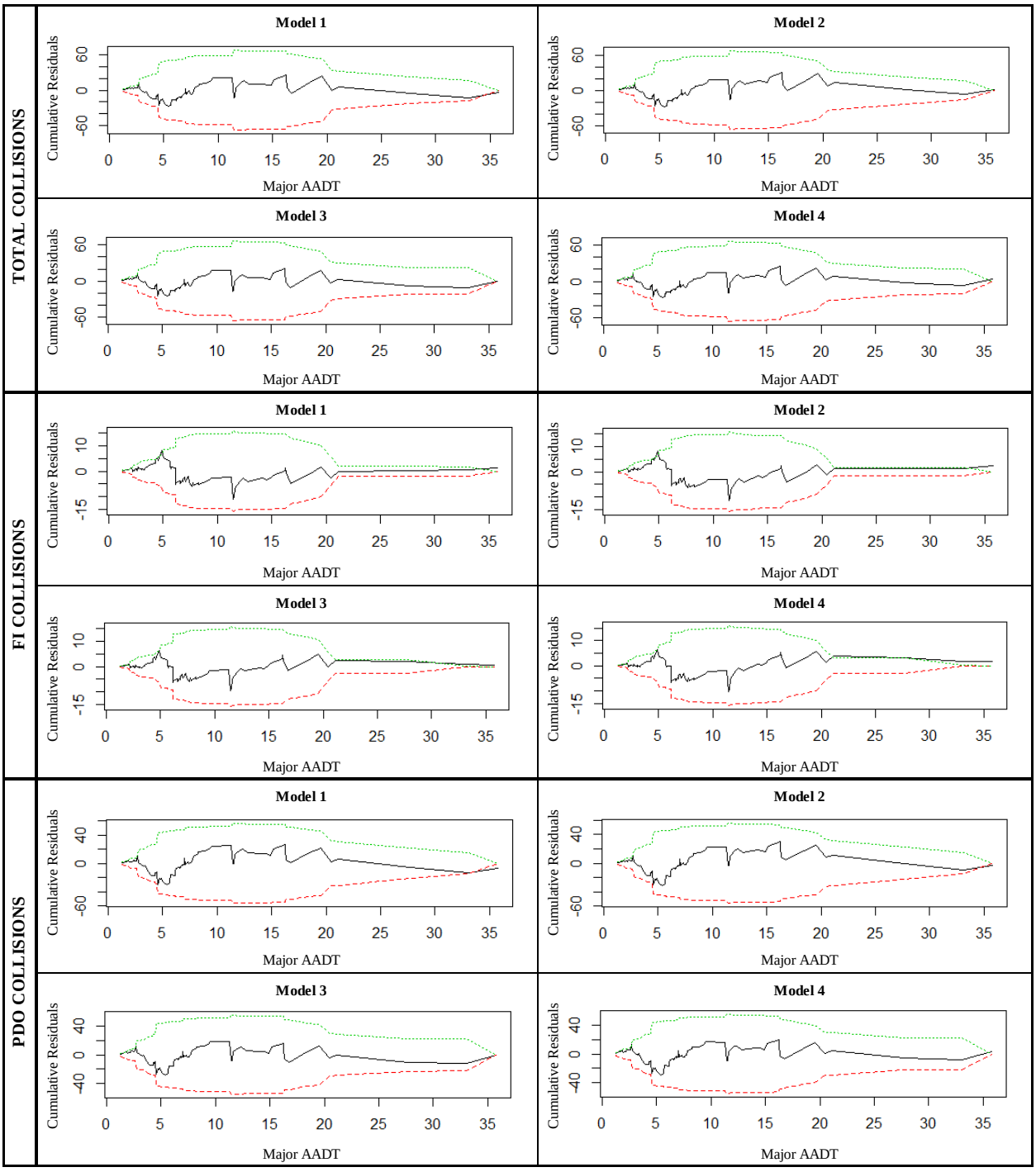

Figure 15: CURE Plots for 3-Leg Unsignalized Intersections.

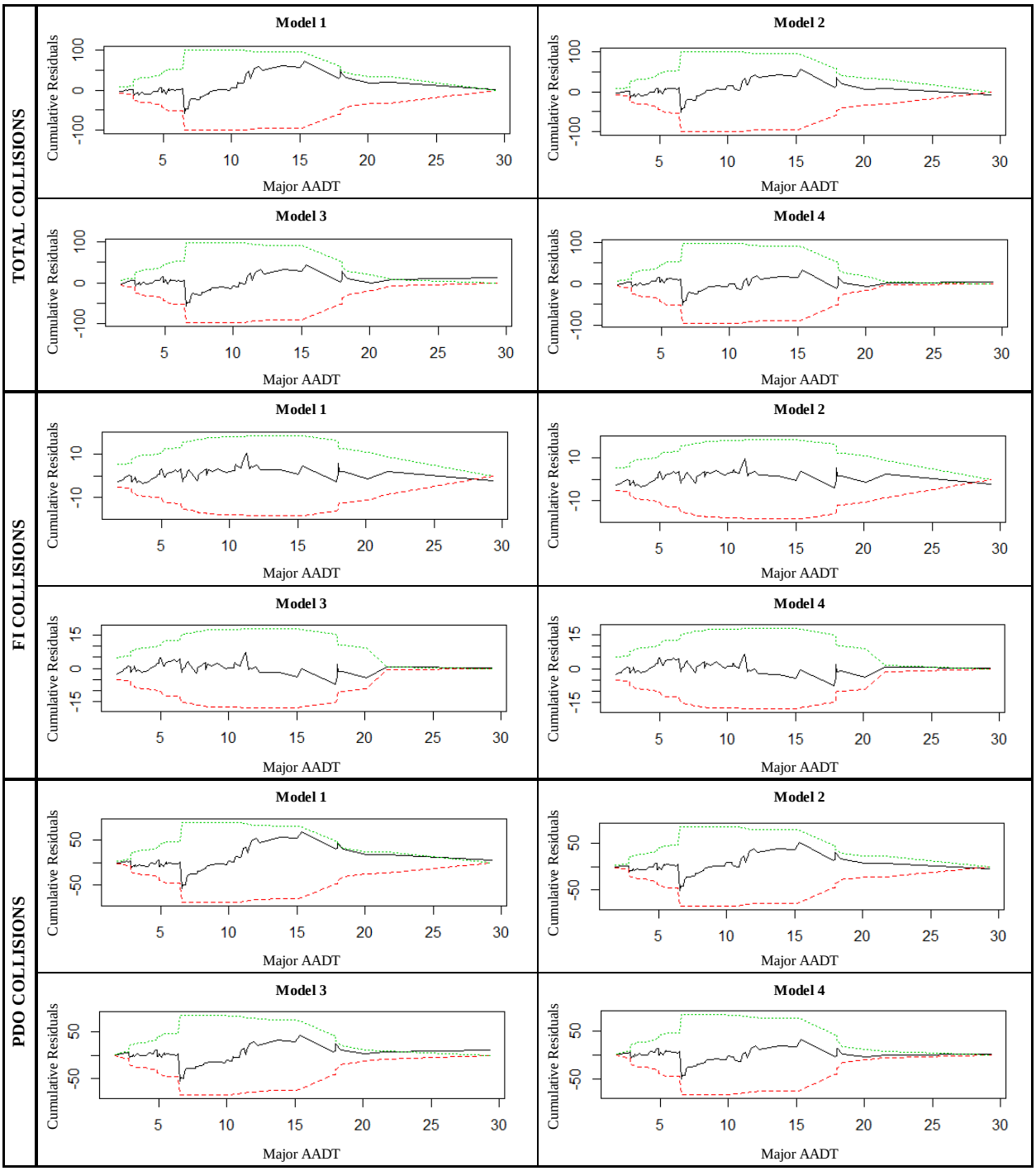

Figure 16: CURE Plots for 4-Leg Unsignalized Intersections.

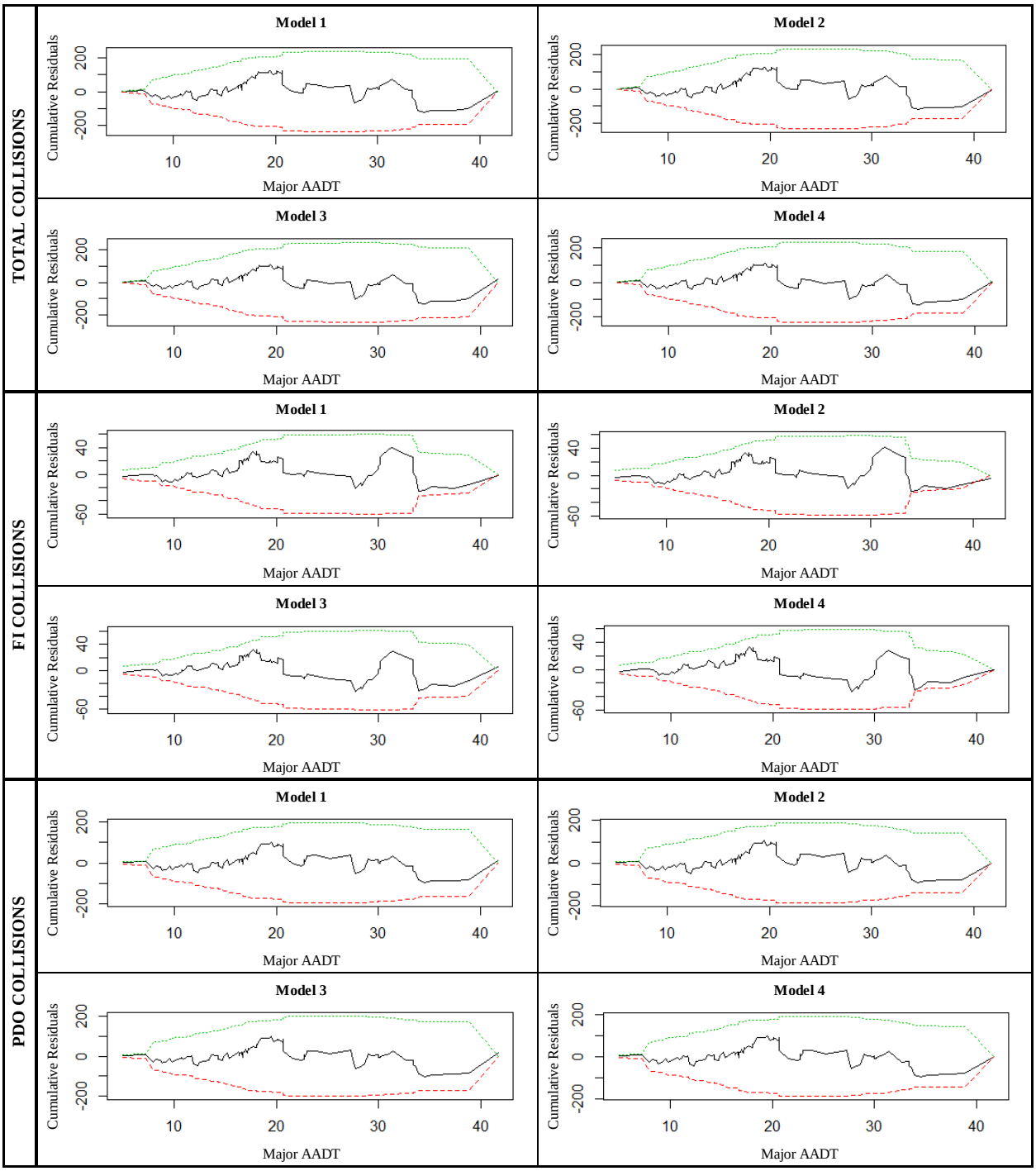

Figure 17: CURE Plots for 3 & 4-Leg Signalized Intersections.

As the tables show, the dispersion parameters, AIC and BIC values show very little difference between functional forms. For example, for total collisions at 3-leg unsignalized intersections, the dispersion parameters range between 5.525 and 5.545, the AIC values range between 493.0 and 496.7, and the BIC values range between 500.4 and 507.8. As the AIC and BIC give a relative measure of a model's statistical goodness of fit, they can still be used to determine which models may be preferable – small though the difference may be. One trend that emerged was that Model 1's AIC and BIC values were the lowest for all intersection types and severities.

The CURE plots exhibited very little difference between functional forms for each intersection type and severity. There are a few cases where the cumulative residuals fall slightly outside of the +/- two standard deviation boundaries for higher major AADT values (e.g., Model 3, total collisions on 4-leg unsignalized intersections), but generally, the cumulative residuals stay within these boundaries.

Model 1 exhibited the lowest p-values for each of the chosen variables, with all p-values significant at the 99.9% confidence level, except for minor AADT on the FI collision model for 4-leg unsignalized intersections. Based on p-values, AIC, and BIC, and CURE plots, Model 1 was selected as the best-fitting functional form for the City of Regina intersection data.

The chosen functional form (Model 1) is shown in Equation 15.

$$N = exp^{\beta_0} \cdot \left(\frac{AADT_{min}}{1000}\right)^{\beta_1} \cdot \left(\frac{AADT_{maj}}{1000}\right)^{\beta_2} \quad \text{[Equation 15]}$$

where:

N = predicted number of collisions;

$AADT_{min}$ = annual average daily traffic on the intersection's minor leg;

$AADT_{maj}$ = annual average daily traffic on the intersection's major leg; and

β_0, β_1, β_2 = regression coefficients.

The regression coefficients for all intersection types and collision severities for the chosen functional form are presented in Table 13.

Table 13: Intersection SPF Coefficients.

Intersection Type	Severity	Regression Coefficients			Overdispersion Parameter
		β_0	β_1	β_2	
3-Leg Unsignalized	Total	-1.717	0.826	0.648	0.396
	FI	-3.786	0.858	0.709	0.485
	PDO	-1.832	0.825	0.626	0.417
4-Leg Unsignalized	Total	-1.007	0.732	0.605	0.281
	FI	-3.195	0.241	0.959	0.487
	PDO	-1.138	0.799	0.559	0.257
3 & 4-Leg Signalized	Total	-0.929	0.665	0.684	0.111
	FI	-3.011	0.503	0.945	0.109
	PDO	-1.067	0.704	0.630	0.119

3.3.2. Roadway Segment SPFs

Based on the functional classifications provided by the City of Regina, the city's roadway segments were divided into a number of categories for SPF development.

Though traffic volume and collision information were available for 36 expressway locations, SPFs were not created for this road category due to the fact that the collision database didn't assign collisions to specific expressway sections (i.e., normal section, merge section, diverge section). As the roadway characteristics are markedly different at each of these sections, SPFs developed using the current collision database would exhibit inaccurate results. This situation is illustrated in Figure 18, which shows UGRID RE900009, a section of Ring Road

(shown in red) between the Winnipeg Street and McDonald Street overpasses. The entire segment length is 1,400 metres; however, the ramp influence areas on either end total approximately 725 metres, or 52% of the segment length. The collision database for this section of expressway aggregates all of the collisions, ramp influence area and normal sections alike. In order to develop accurate SPFs for expressway road segments, the individual collision records would need to be investigated, in order to assign the observed collisions to the correct locations along the expressway.

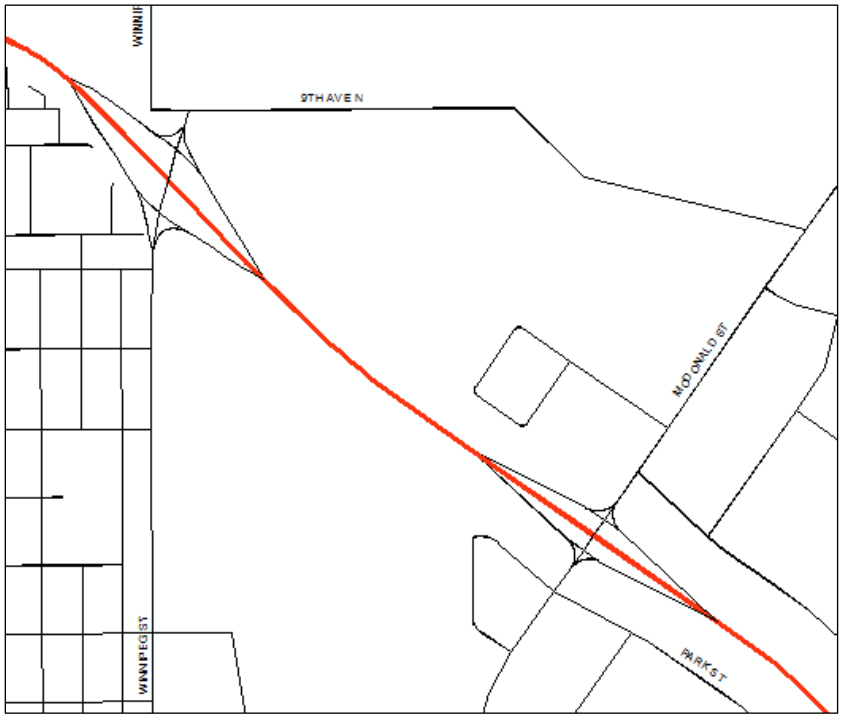

Figure 18: Freeway Section of Ring Road, Between Winnipeg Street and McDonald Street Overpasses.

The remaining roadway segments were divided into three categories, based on the functional classifications provided by the city: major arterial, minor arterial, and collector. Table 14 shows the number of segments for each category that were used for the development of SPFs.

Table 14: City of Regina Roadway Segment Categories.

Category	No. of Segments
Major Arterial	435
Minor Arterial	234
Collector	968

Similar to the intersections, each of these categories was divided into two subsections by random selection: estimation (70% of the data) and validation (30% of the data). For each of the three severity categories, four candidate model forms were developed; Table 15 shows the initial model forms that were created. Models 1 and 3 include a regression coefficient for segment length, while Models 2 and 4 assume a linear relationship between segment length and the number of collisions (similar to the HSM).

Table 15: Initial Candidate Model Forms for Roadway Segments.

Model No.	Model Form
1	$N = exp^{\beta_0} \cdot \left(\frac{AADT}{1000}\right)^{\beta_1} \cdot length^{\beta_2}$
2	$N = exp^{\beta_0} \cdot \left(\frac{AADT}{1000}\right)^{\beta_1} \cdot length$
3	$N = exp^{\beta_0} \cdot \left(\frac{AADT}{1000}\right)^{\beta_1} \cdot length^{\beta_2} \cdot exp^{\left(\beta_3 \cdot \frac{AADT}{1000}\right)}$
4	$N = exp^{\beta_0} \cdot \left(\frac{AADT}{1000}\right)^{\beta_1} \cdot length \cdot exp^{\left(\beta_2 \cdot \frac{AADT}{1000}\right)}$

Regression results for each of the three roadway segment categories are presented in Table 16 through Table 18Table 18: Regression Results for Collector Roadway Segments.. CURE plots for each of the models are shown in Figure 19 through Figure 21, with cumulative

residuals shown on the vertical axis and major AADT (in thousands) shown on the horizontal axis. In each of the figures, the green line represents the positive two standard deviation boundary, and the red line represents the negative two standard deviation boundary.

Table 16: Regression Results for Major Arterial Roadway Segments.

	Severity	Model	Regression Coefficients								Dispersion Parameter	AIC	BIC
			β_0	*p*-Value	β_1	*p*-Value	β_2	*p*-Value	β_3	*p*-Value			
Major Arterial	Total Collisions	1	-1.387	<0.001	1.077	<0.001	0.731	<0.001	NA	NA	2.461	1717.2	1724.6
		2	-0.776	<0.001	1.037	<0.001	NA	NA	NA	NA	2.337	1725.4	1731.0
		3	-0.757	<0.001	0.720	0.149	0.732	<0.001	0.021	0.450	2.453	1718.5	1727.8
		4	-0.102	<0.001	0.654	0.201	0.023	0.428	NA	NA	2.329	1726.8	1734.2
	FI Collisions	1	-4.180	<0.001	1.480	<0.001	0.953	<0.001	NA	NA	3.396	752.7	760.1
		2	-4.111	<0.001	1.483	<0.001	NA	NA	NA	NA	3.395	750.9	756.4
		3	-5.775	<0.001	2.327	0.029	0.954	<0.001	-0.045	0.415	3.520	754.1	763.3
		4	-5.721	<0.001	2.337	0.029	-0.045	0.412	NA	NA	3.518	752.2	759.6
	PDO Collisions	1	-1.430	<0.001	1.022	<0.001	0.699	<0.001	NA	NA	2.237	1656.5	1663.9
		2	-0.733	<0.001	0.973	<0.001	NA	NA	NA	NA	2.107	1665.9	1671.5
		3	-0.802	<0.001	0.666	0.202	0.700	<0.001	0.021	0.47	2.230	1657.9	1667.2
		4	-0.060	<0.001	0.589	0.272	0.023	0.447	NA	NA	2.100	1667.3	1674.7

Table 17: Regression Results for Minor Arterial Roadway Segments.

	Severity	Model	Regression Coefficients								Dispersion Parameter	AIC	BIC
			β_0	*p*-Value	β_1	*p*-Value	β_2	*p*-Value	β_3	*p*-Value			
Minor Arterial	Total Collisions	1	-1.036	<0.001	1.037	<0.001	0.880	<0.001	NA	NA	3.176	648.1	655.5
		2	-0.913	<0.001	1.086	<0.001	NA	NA	NA	NA	3.081	647.1	652.7
		3	-1.938	<0.001	2.246	0.012	0.889	<0.001	-0.194	0.155	3.351	648.3	657.5
		4	-1.874	<0.001	2.354	0.008	-0.204	0.135	NA	NA	3.260	647.1	654.5
	FI Collisions	1	-2.854	<0.001	1.122	0.017	1.120	<0.001	NA	NA	0.944	240.2	247.6
		2	-2.882	<0.001	1.031	0.019	NA	NA	NA	NA	0.957	238.5	244.0
		3	-4.782	<0.001	3.786	0.104	1.165	<0.001	-0.430	0.223	0.989	240.6	249.9
		4	-4.681	<0.001	3.469	0.127	-0.398	0.252	NA	NA	1.019	239.0	246.4
	PDO Collisions	1	-1.242	<0.001	1.026	<0.001	0.828	<0.001	NA	NA	3.499	613.3	620.7
		2	-1.057	<0.001	1.091	<0.001	NA	NA	NA	NA	3.301	613.3	618.8
		3	-2.082	<0.001	2.127	0.020	0.834	<0.001	-0.175	0.208	3.697	613.8	623.1
		4	-1.954	<0.001	2.254	0.013	-0.185	0.185	NA	NA	3.493	613.7	621.1

Table 18: Regression Results for Collector Roadway Segments.

	Severity	Model	Regression Coefficients								Dispersion Parameter	AIC	BIC
			β_0	*p* -Value	β_1	*p* -Value	β_2	*p* -Value	β_3	*p* -Value			
Collector	Total Collisions	1	0.781	<0.001	0.686	<0.001	1.358	<0.001	NA	NA	1.170	2242.9	2250.3
		2	0.068	<0.001	0.681	<0.001	NA	NA	NA	NA	1.127	2252.8	2258.4
		3	0.854	<0.001	0.128	0.539	1.354	<0.001	0.146	0.005	1.176	2238.8	2248.1
		4	0.146	<0.001	0.121	0.568	0.148	0.005	NA	NA	1.137	2248.5	2255.9
	FI Collisions	1	-2.078	<0.001	1.131	<0.001	1.566	<0.001	NA	NA	1.813	506.5	513.9
		2	-3.074	<0.001	1.099	<0.001	NA	NA	NA	NA	1.972	511.7	517.2
		3	-2.089	<0.001	1.163	0.050	1.566	<0.001	-0.007	0.955	1.809	508.5	517.7
		4	-3.095	<0.001	1.155	0.051	-0.012	0.921	NA	NA	1.970	513.7	521.1
	PDO Collisions	1	0.692	<0.001	0.648	<0.001	1.325	<0.001	NA	NA	1.074	2178.8	2186.2
		2	0.039	<0.001	0.647	<0.001	NA	NA	NA	NA	1.044	2185.9	2191.4
		3	0.769	<0.001	0.057	0.792	1.321	<0.001	0.155	0.004	1.081	2174.5	2183.8
		4	0.120	<0.001	0.057	0.795	0.156	0.004	NA	NA	1.054	2181.4	2188.8

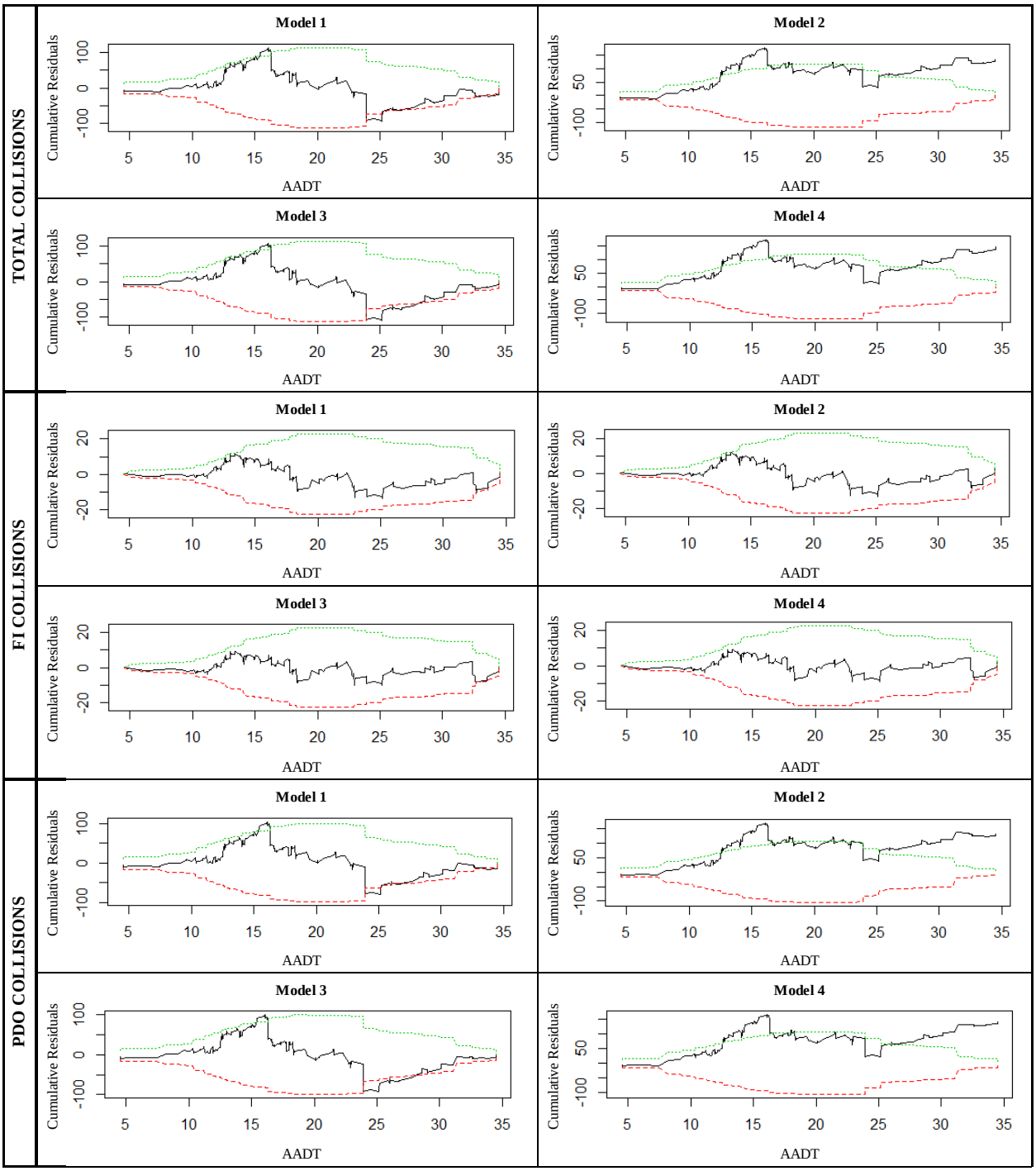

Figure 19: CURE Plots for Major Arterial Roadway Segments.

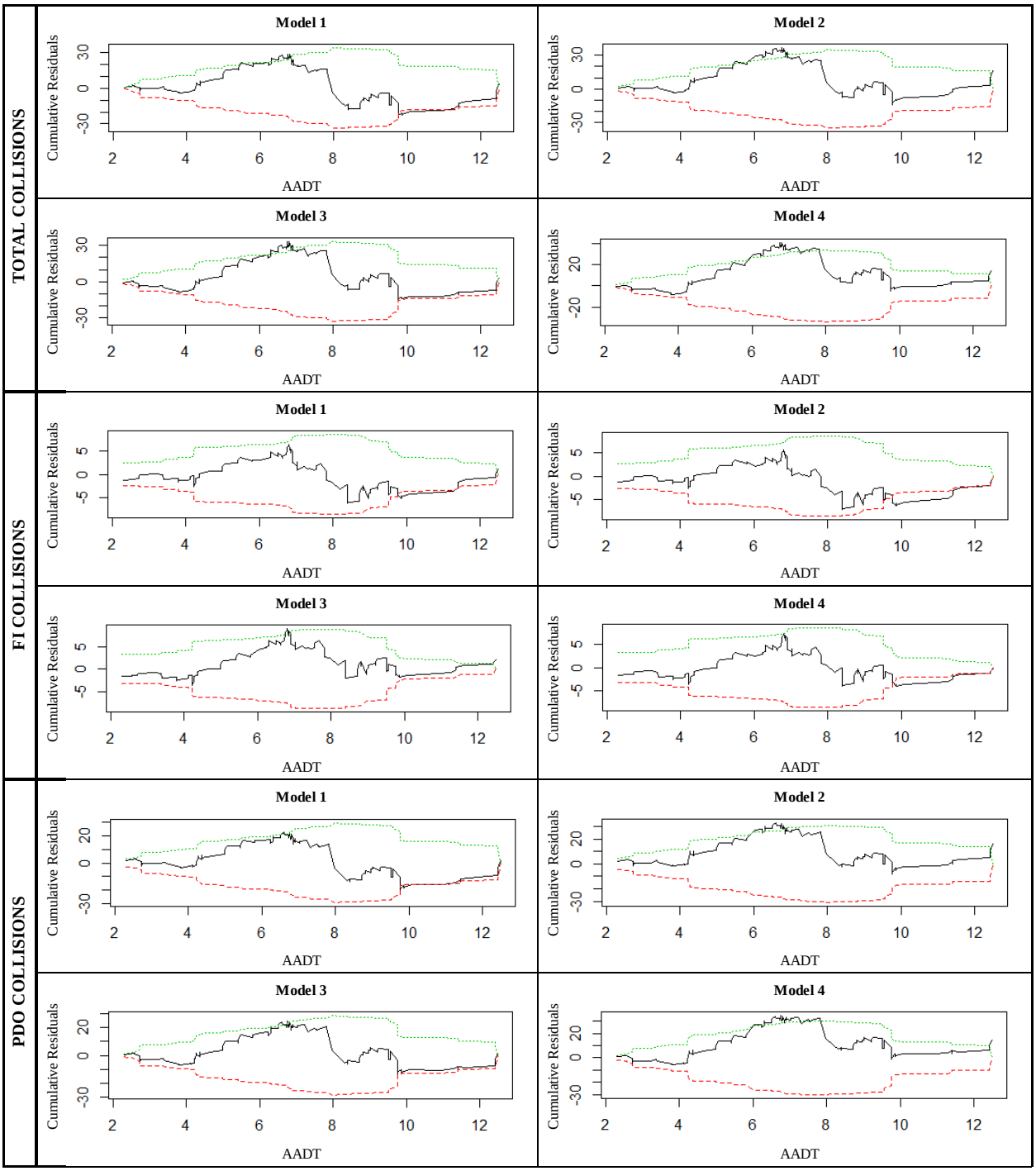

Figure 20: CURE Plots for Minor Arterial Roadway Segments.

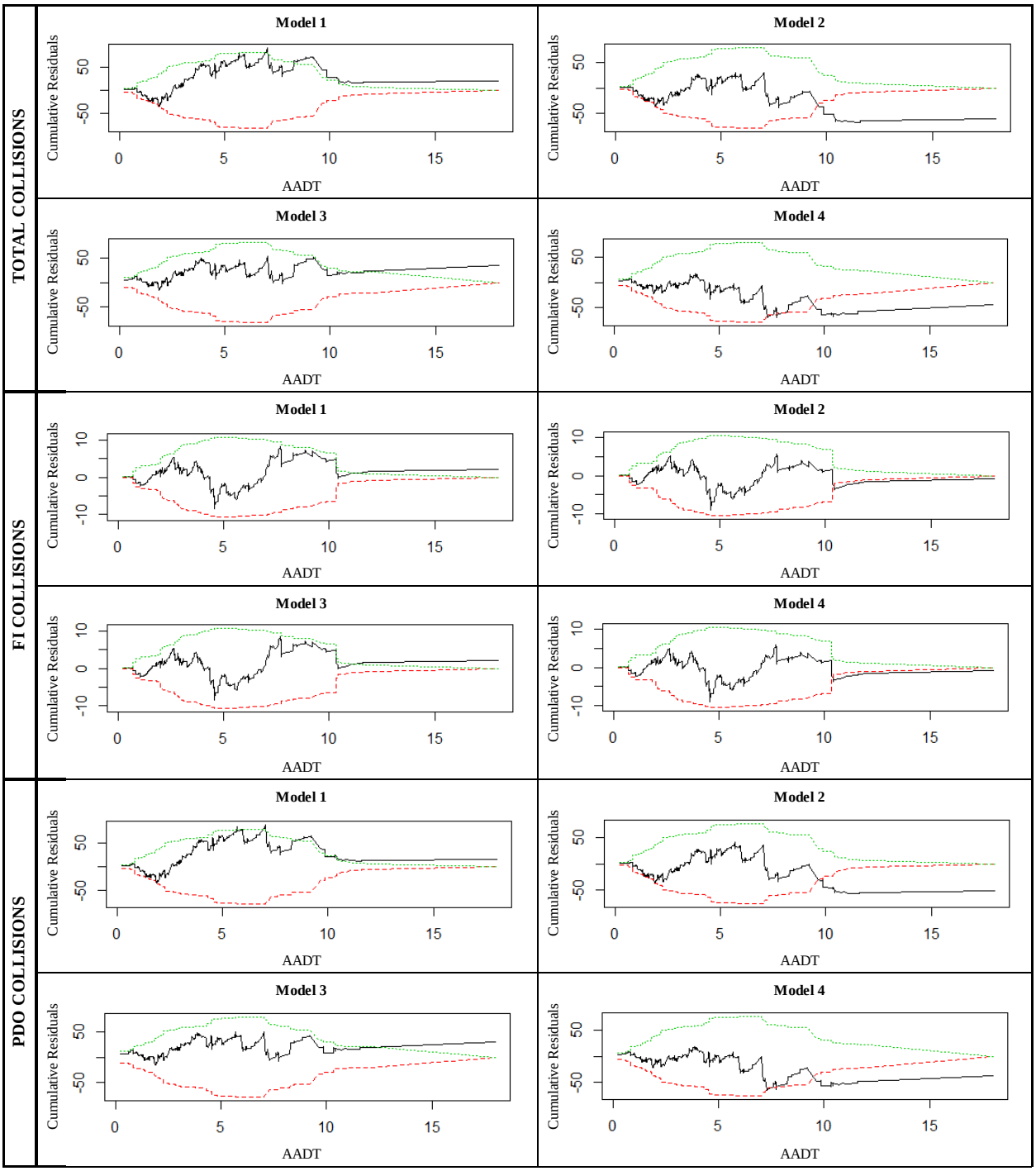

Figure 21: CURE Plots for Collector Roadway Segments.

Based on an examination of the data shown above, Model 1 appeared to show the best-fitting results for the City of Regina's roadway segment collision data. For major arterials, Model 1 exhibited the lowest AIC and BIC values for all collision severities, and all three regression coefficients were significant at the 99.9% confidence level, as shown in Table 16. The CURE plots for this roadway segment category, shown in Figure 19, show that the cumulative residuals for both Models 1 and 3 fall within the +/- two standard deviation boundaries for all severity levels; Models 2 and 4 exhibit a significant amount of deviation from these boundaries for both total and PDO collisions.

Model 1 was also chosen as the best-fitting model for minor arterial roadway segments; while this model didn't have the lowest AIC/BIC values (Model 2 did), all of the regression coefficients other than for FI collisions were significant at the 99.9% confidence level, and the CURE plots exhibited a better fit than the next-best candidate (Model 2), as shown in Figure 20.

Similarly, Model 1 was identified as the best-fitting functional form for collisions on collector roadway segments, based on p-values and CURE plots. For instance, on Figure 21, the cumulative residuals for Model 2 (the only other functional form that resulted in regression coefficients significant at the 99.9% confidence level) exhibit significant deviation from the +/- two standard deviation boundary for major AADTs with values greater than approximately 9,000 for total and PDO collisions.

The chosen functional form (Model 1) is shown in Equation 16.

$$N = exp^{\beta_0} \cdot \left(\frac{AADT}{1000}\right)^{\beta_1} \cdot L^{\beta_2} \qquad \text{[Equation 16]}$$

where:

N = predicted number of collisions;

AADT = annual average daily traffic on the roadway segment;

L = roadway segment length in kilometres; and

β_0, β_1, β_2 = regression coefficients.

The regression coefficients for all roadway segment types and collision severities for the chosen functional forms are presented in Table 19.

Table 19: Roadway Segment SPF Coefficients.

Roadway Segment Type	Severity	Regression Coefficients			Overdispersion Parameter
		β_0	β_1	β_2	
Major Arterial	Total	-1.387	1.077	0.731	0.406
	FI	-4.180	1.480	0.953	0.294
	PDO	-1.430	1.022	0.699	0.447
Minor Arterial	Total	-1.036	1.037	0.880	0.315
	FI	-2.854	1.122	1.120	1.059
	PDO	-1.242	1.026	0.828	0.286
Collector	Total	0.781	0.686	1.358	0.855
	FI	-2.078	1.131	1.566	0.552
	PDO	0.692	0.648	1.325	0.932

3.4. SPF Validation

Statistical GOF tests were performed on the validation subsets (30% of the data) for both intersections and roadway segments. The results of the validation procedures are presented in the following sections.

3.4.1. Intersection SPFs

Table 20 shows the results of the statistical GOF tests for the City of Regina's intersections. These results can be compared in order to assess the transferability of the developed models – which were developed using the estimation dataset – to the validation dataset.

Table 20: Goodness of Fit Tests for Intersection SPFs.

Category	Severity	Estimation Data (70%)		Validation Data (30%)			
		MSE	R^2_{FT}	MSPE	MPB	MAD	R^2_{FT}
3-Leg Unsignalized	Total	55.64	58%	55.09	-0.51	5.24	39%
	FI	3.10	33%	2.26	0.06	1.07	30%
	PDO	38.84	57%	42.94	-0.58	4.45	37%
4-Leg Unsignalized	Total	122.47	53%	120.05	-0.36	7.30	10%
	FI	4.12	30%	8.34	-0.65	1.84	4%
	PDO	92.94	53%	82.07	0.24	6.14	10%
3 & 4-Leg Signalized	Total	604.84	77%	502.48	0.56	16.76	73%
	FI	38.36	67%	32.72	0.00	4.65	64%
	PDO	409.85	76%	329.52	0.63	13.25	71%

The MSE and MSPE values are similar in magnitude, particularly for the unsignalized models, indicating a high level of transferability. Additionally, since the MSPE values are lower in most cases, over-fitting of the regression models is unlikely. The Freeman Tukey R-Squared values are higher for the estimation datasets than they are for the validation datasets. This may be a result of the relatively low number of sites included in the validation data; for example, the 4-leg unsignalized validation dataset included only 36 sites. Finally, the MAD test statistic, which measures the average deviation between the predicted number and observed number of collisions, is highest for 3 & 4-leg signalized intersections, and lowest for 3-leg unsignalized intersections. This is to be expected, as high volume intersections will experience higher collision frequencies, as well as more variation in the data.

Likelihood ratio R-squared values were also calculated for each of the intersection categories. As described earlier, this test statistic describes a fitted model's improvement over an intercept-only version, with even low values indicating that the selected model, with one or more independent variables, fits the dataset better than an intercept-only model. The R^2_{LR} values for the intersection SPFs are presented in Table 21.

Table 21: Likelihood Ratio R-Squared Values for Intersection SPFs.

Category	Severity	R^2_{LR}
3-Leg Unsignalized	Total	56%
	FI	35%
	PDO	53%
4-Leg Unsignalized	Total	57%
	FI	29%
	PDO	58%
3 & 4-Leg Signalized	Total	75%
	FI	65%
	PDO	73%

As the table shows, the R^2_{LR} values range between 65% and 75% for the signalized intersection SPFs, and 29% and 58% for the unsignalized intersection SPFs. This indicates that the selected SPFs show a clear improvement over intercept-only models.

3.4.2. Roadway Segment SPFs

Table 22 shows the results of the statistical GOF tests for the City of Regina's road segments. These results can be compared in order to assess the transferability of the developed models – which were developed using the estimation dataset – to the validation dataset.

Table 22: Goodness of Fit Tests for Road Segment SPFs.

Category	Severity	Estimation Data (70%)		Validation Data (30%)			
		MSE	R^2_{FT}	MSPE	MPB	MAD	R^2_{FT}
Major Arterial	Total	41.65	38%	58.89	0.14	4.51	23%
	FI	1.74	28%	2.20	-0.04	0.98	20%
	PDO	32.48	34%	44.73	0.18	4.05	19%
Minor Arterial	Total	7.06	29%	6.51	0.30	1.88	6%
	FI	0.47	14%	0.32	0.12	0.38	21%
	PDO	5.62	27%	6.08	0.17	1.81	-3%
Collector	Total	10.09	24%	27.82	0.39	1.88	20%
	FI	0.17	11%	1.01	0.01	0.32	10%
	PDO	9.19	21%	19.58	0.37	1.70	18%

For all of the road segment SPFs, the MPB varies between -0.04 for major arterial FI collisions and 0.39 for collector total collisions; as this test statistic provides a measure of the magnitude and direction of the average model bias as compared to validation data, the road segment SPFs can be said to exhibit an even better probability of predicting observed data than the intersection SPFs (which have MPB values between -0.65 and .63).

The Freeman Tukey R-Squared values are highest for major arterial SPFs, and lowest for collector SPFs. As stated by FHWA (2008), this test statistic tends to be higher for datasets with a large number of crashes per site, hence the decreasing Freeman Tukey R-Squared values for "lower" functional classifications. Additionally, the MSE and MSPE values are similar in magnitude, indicating transferability of the developed SPFs.

Likelihood ratio R-squared values were also calculated for each of the road segment categories. As described earlier, this test statistic describes a fitted model's improvement over an intercept-only version, with even low values indicating that the selected model, with one or more independent variables, fits the dataset better than an intercept-only model. The R^2_{LR} values for the road segment SPFs are presented in Table 23.

Table 23: Likelihood Ratio R-Squared Values for Road Segment SPFs.

Category	Severity	R^2_{LR}
Major Arterial	Total	38%
	FI	30%
	PDO	34%
Minor Arterial	Total	32%
	FI	11%
	PDO	30%
Collector	Total	28%
	FI	12%
	PDO	26%

As the table shows, the R^2_{LR} values range between 30% and 38% for the major arterial SPFs, 11% and 32% for the minor arterial SPFs, and 12% and 28% for the collector SPFs. This indicates that the selected SPFs show a clear improvement over intercept-only models

3.5. SPF Comparison

The following sections detail the steps that were taken in order to compare the performance of the developed SPFs to the models presented in the HSM. Comparisons were performed on both calibrated and uncalibrated versions of the provided models; the calibration results are presented in the following section.

3.5.1. Calibration of Intersection SPFs

Using the observed collision numbers for the five most recent years of City of Regina data, the HSM SPFs were calibrated according to the procedure described in the "Literature Review" section of this report. Calibration factors were calculated for each of the five years (2005 to 2009), as well as the five-year average. The results of the calibration are shown in Table 24.

Table 24: Calibration Factors for Intersection SPFs.

Category	Severity	Calibration Factor					
		2005	2006	2007	2008	2009	Avg
3-Leg Unsignalized	Total	1.67	1.28	1.37	1.46	1.54	1.47
	FI	0.60	0.62	0.72	0.64	0.68	0.65
	PDO	2.14	1.57	1.65	1.80	1.87	1.81
4-Leg Unsignalized	Total	1.57	1.47	1.43	1.65	1.97	1.63
	FI	0.61	0.69	0.58	0.79	0.63	0.66
	PDO	2.12	1.92	1.91	2.14	2.73	2.17
3 & 4-Leg Signalized	Total	2.27	1.90	2.16	2.32	2.56	2.25
	FI	1.68	1.18	1.44	1.32	1.26	1.37
	PDO	2.67	2.34	2.63	2.94	3.33	2.79

As the table shows, the majority of the average calibration factors are greater than one, indicating that the HSM SPFs under-predict the number of collisions in these categories. For 3 and 4-leg signalized intersections, the average calibration factors for total collisions and PDO collisions are 2.25 and 2.79, respectively. These results can be interpreted to say that the HSM SPFs predict 56% fewer total collisions and 64% fewer PDO collisions than actually occurred in Regina during the five-year study period.

FI collisions for both 3-leg unsignalized and 4-leg unsignalized intersections have calibration factors less than one (0.65 and 0.66, respectively), indicating that the HSM SPFs over-predict collisions in these categories. These results can be interpreted to say that the HSM SPFs predict 54% more FI collisions on 3-leg unsignalized intersections and 52% more FI collisions on 4-leg unsignalized intersections than actually occurred in Regina during the five-year study period.

For all three intersection categories, the FI calibration factor was consistently lower than the total and PDO calibration factors. For example, for 3-leg unsignalized intersections, the HSM SPFs predict 32% fewer total collisions and 45% fewer PDO collisions than actually occurred, but 54% more FI collisions than actually occurred.

There are several possible reasons for these severity-based differences between models. For one, it's possible that collisions in the City of Regina are simply less severe due to local roadway conditions, climatic effects, and/or driver behavior. For instance, Regina has longer and more severe winter seasons than Minnesota and North Carolina (where the collision data for the HSM's base SPFs were collected), and is known for icy road conditions during the long winter period. During winter, vehicles' average travel speeds on Regina streets are lower than in

summer. As severe collisions are more likely to occur in high speed collisions (i.e., high impact energy) than in low speed collisions, Regina's icy road conditions may increase the number of PDO collisions and decrease the number of FI collisions (Young& Park, 2013). The quality of local emergency medical services (EMS) also has an effect on the number of fatalities and injuries that occur.

Differences in reporting criteria between the City of Regina and the jurisdictions from which the HSM's urban/suburban intersection SPFs were developed may play a role in the models' varying results (Harwood et al., 2007). For example, the Minnesota Department of Public Safety defines a collision as "a collision that involves a motor vehicle in transport on a public traffic-way in Minnesota and results in injury, death, or at least $1,000 in property damage" (Minnesota Department of Public Safety, 2011). For the study period of 2005-2009, $1,000 was the PDO threshold for collision records to be added to the province's collision database, but this amount has recently been increased to $5,000 (SGI, 2012). Changes to reporting thresholds in Saskatchewan in 1984, 1993, and 2010 have resulted in large decreases in PDO collisions in the province's collision database, and this highlights an important consideration. Since reporting thresholds, and other collision-related criteria, are embedded in the data, jurisdiction-specific SPFs (or calibration factors for HSM SPFs) are required in order to capture these regional collision-reporting characteristics (Young & Park, 2012). Finally, in Saskatchewan, studies have shown that on average, motorists in Saskatchewan drive older vehicles than other North Americans; these older vehicles may have less advanced safety features and collision avoidance systems than the vehicles used in other states or provinces. A 2010 report by Berouk Terefe found that the oldest vehicle group made up the largest share (27%) of light vehicles. This vehicle group consists of model years of 1993 and earlier.

A statistical comparison between the HSM's SPFs (both calibrated and uncalibrated) and the jurisdiction-specific SPFs is provided in the following section.

3.5.2. Comparison of Intersection SPFs

The jurisdiction-specific SPFs were compared to the HSM SPFs (both calibrated and uncalibrated) using a number of techniques, including visual plots, statistical GOF tests, and CURE plots. As the 3 and 4-leg signalized intersection category consisted primarily of 4-leg intersection data, this category was compared to the HSM SPFs for 4-leg signalized intersections.

Graphs showing the observed collisions (five-year averages) as a function of major AADT, as well as jurisdiction-specific SPFs, HSM SPFs, and calibrated HSM SPFs, are shown in Figure 22. The average minor AADTs for each intersection type are used for the graphs.

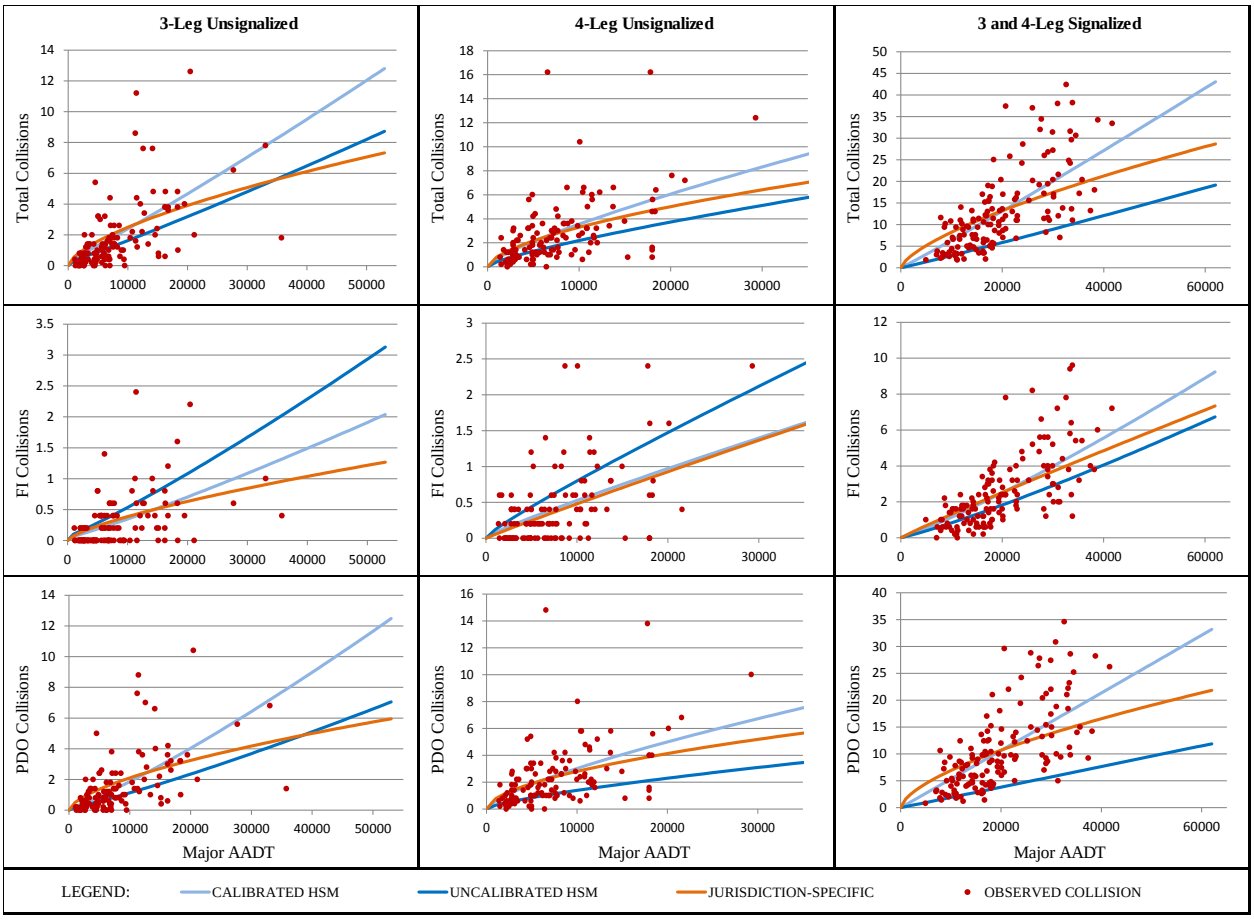

Figure 22: Total, FI, and PDO Observed Collisions and SPFs for 3-Leg Unsignalized, 4-Leg Unsignalized and 3 and 4-Leg Signalized Intersections.

For 3-leg unsignalized intersections (shown in the left column) and 4-leg unsignalized intersections (middle column), the uncalibrated HSM SPFs (dark blue) under-predict total and PDO collisions, and over-predict FI collisions. For 3 and 4-leg signalized intersections (right column), the uncalibrated HSM SPFs consistently under-predict collisions in all categories. The calibrated HSM SPFs (light blue) tend to correspond more closely to the jurisdiction-specific SPFs (orange), up until approximately 15,000 major AADT (3-leg unsignalized), 8,000 major AADT (4-leg unsignalized) and 20,000 major AADT (3 and 4-leg signalized), at which point the jurisdiction-specific SPFs exhibit a decreasing trend. Though these graphs give a general idea of

the models' fit to the observed collisions, it must be remembered that not all of the dots represent a single location (i.e., if two or more locations have similar major AADT and observed number of collisions, they will be represented by a single dot).

Statistical GOF tests were also utilized to analyze the models. It is important, when assessing a set of models using GOF tests, that several statistical tests be performed in order to identify the best-fitting model (Washington et al., 2005). Therefore, four of the statistical tests that were used to select the best-fitting functional form were also used to compare the jurisdiction-specific SPFs to the HSM SPFs. These tests include the MSPE, MPB, MAD, and Freeman Tukey R-Squared. Table 25 shows the results of this comparison.

Table 25: Statistical Comparison Between Three Sets of SPFs.

Category	Severity	Jurisdiction-Specific SPFs				HSM SPFs				Calibrated HSM SPFs			
		MSPE	MPB	MAD	R^2_{FT}	MSPE	MPB	MAD	R^2_{FT}	MSPE	MPB	MAD	R^2_{FT}
3-Leg Unsignalized	Total	54.12	-0.19	4.91	52%	75.84	-2.87	4.99	46%	60.62	0.00	4.90	51%
	FI	2.77	0.03	1.13	32%	3.89	0.71	1.40	8%	3.03	0.00	1.16	31%
	PDO	39.16	-0.23	4.20	51%	61.38	-3.44	4.61	36%	43.74	-0.69	4.03	50%
4-Leg Unsignalized	Total	118.71	-0.09	6.51	42%	161.57	-5.44	7.55	24%	119.79	0.00	6.59	40%
	FI	5.27	-0.21	1.57	22%	6.79	1.07	2.00	-8%	5.23	0.00	1.62	20%
	PDO	87.41	0.11	5.49	43%	148.25	-6.51	7.36	-4%	89.60	0.00	5.74	40%
3 & 4-Leg Signalized	Total	561.37	0.21	16.60	76%	2556.69	-36.32	36.83	-20%	753.57	0.00	20.50	66%
	FI	35.86	0.00	4.46	66%	57.78	-3.43	5.21	49%	39.71	0.00	4.69	61%
	PDO	377.09	0.28	13.49	75%	2060.92	-33.86	34.07	-61%	513.32	0.00	17.17	64%

The highlighted boxes identify the models that performed best for each statistical test. In general, the jurisdiction-specific SPFs exhibited the lowest values for MSPE (other than 4-leg unsignalized FI collisions) and MAD (other than 3-leg unsignalized total and PDO collisions). The calibrated HSM SPFs, however, exhibited the lowest MPB values in most cases. The jurisdiction-specific SPFs exhibited the highest Freeman Tukey R-Squared results for all intersections and severities. The results from these GOF tests highlight the importance of performing multiple statistical tests, as outcome from one test may not necessarily reflect the

majority of the results. Based on the results shown in Table 25, the jurisdiction-specific SPFs show the best-fitting results, based on their fit to Regina's collision data.

CURE plots were also developed for all of the intersection categories. Figure 23 shows CURE plots, as a function of major AADT, for 3-leg unsignalized, 4-leg unsignalized and 3 and 4-leg signalized intersections, based on total collisions.

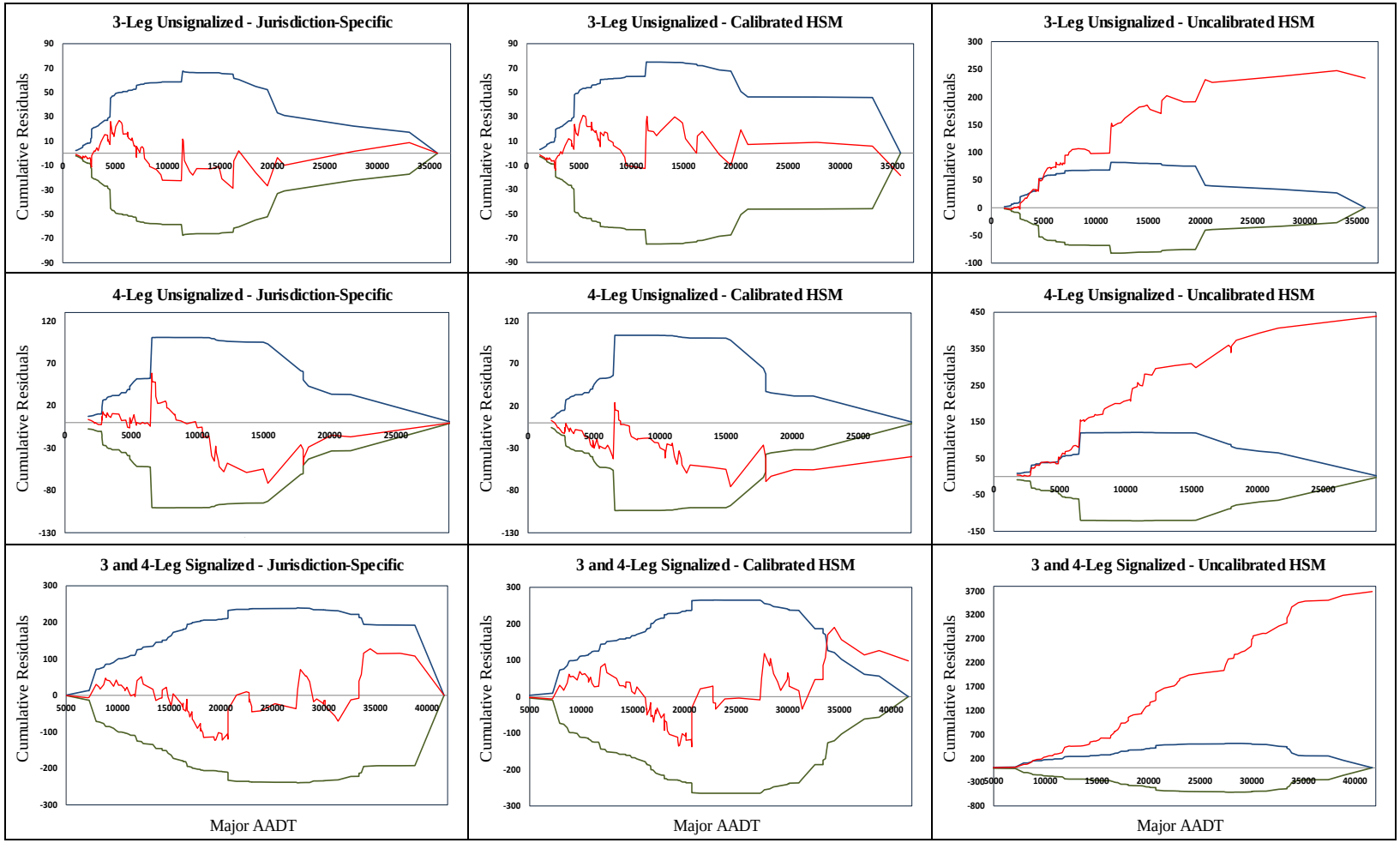

Figure 23: CURE Plots as a Function of Major AADT for 3-Leg Unsignalized, 4-Leg Unsignalized, and 3 and 4-Leg Signalized Intersections.

As the CURE plots show, the jurisdiction-specific SPFs' cumulative residuals fall within the 95% confidence interval (designated by the blue +2σ and green -2σ boundaries) for the entire range of major AADT, for both intersection categories. For these SPFs, the cumulative residuals fluctuate above and below the horizontal axis, which is representative of a good-fitting model (Hauer & Bamfo, 1997). For all three intersection categories, the uncalibrated HSM SPFs' cumulative residuals show significant deviation from the 95% confidence interval; this deviation becomes more pronounced as the major AADT increases. The calibrated HSM SPFs' proximity to the 95% confidence intervals is similar to the jurisdiction-specific SPFs, which is to be expected, as these SPFs were calibrated to the same observed collision data. However, both of the calibrated HSM SPFs shown in Figure 23 do exhibit deviation from the 95% confidence intervals for major AADTs greater than 34,000 (3-leg unsignalized), 18,000 (4-leg unsignalized intersections), and 33,000 (3 and 4-leg signalized intersections).

In addition to the cumulative residuals, information about the variation inherent in each model can be determined by examining the size of the 95% confidence interval for each model. Figure 24 shows these intervals for total collisions in the 3-leg unsignalized category, as a function of major AADT.

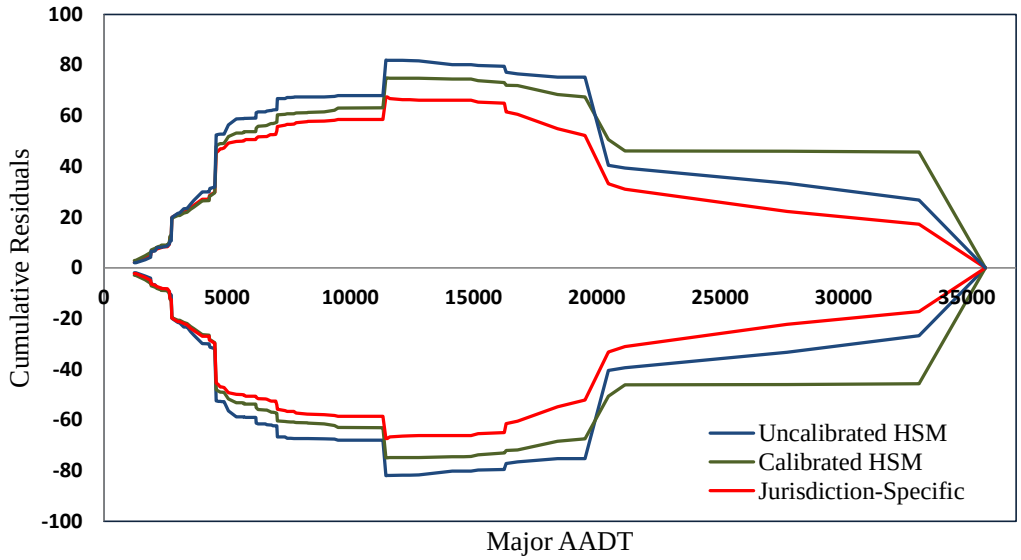

Figure 24: 95% Confidence Intervals for 3-Leg Unsignalized Intersections.

As the figure shows, the jurisdiction-specific SPF (shown in red) results in the narrowest 95% confidence interval over the entire range of major AADT values. The calibrated and uncalibrated HSM SPFs exhibit wider confidence intervals, which become pronounced at approximately 5,000 major AADT. The uncalibrated HSM SPF shows the widest confidence interval up to approximately 20,000 major AADT, at which point the calibrated HSM SPF's confidence interval expands past it. For the range between 20,000 and 35,000 major AADT, the calibrated HSM SPF's confidence interval is approximately double that of the jurisdiction-specific SPF, which indicates a higher degree of variance in the calibrated HSM SPF. As the 95% confidence interval is a function of the cumulative residuals for each model, an examination of these boundaries can also be used as a preliminary tool to determine which model best fits the observed data. Based on this comparison measure, the jurisdiction-specific SPFs displayed the best fit.

3.5.3. Calibration of Roadway Segment SPFs

Unlike the intersection SPFs, which were grouped into categories similar to the HSM's SPFs (i.e., by number of legs and control type), the road segment SPFs were grouped into categories dissimilar to the HSM SPFs. While the HSM classifies the provided SPFs by number of lanes, the SPFs developed for the City of Regina were based on functional classification. Therefore, a system had to be developed that would allow comparison between alternately-grouped datasets.

In order to perform this comparison, the City of Regina road segments were broken down by functional classification, and then within these groups, further disaggregated by number of lanes. This allowed for the creation of nine individual datasets, which are detailed in Table 26.

Table 26: Road Segment Categories Created for Comparison.

Major Arterial	No. of Segments
Two lane undivided	37
Four lane undivided	136
Four lane divided	213
Minor Arterial	**No. of Segments**
Two lane undivided	161
Four lane undivided	39
Four lane divided	34
Collector	**No. of Segments**
Two lane undivided	884
Four lane undivided	33
Four lane divided	48

Using the observed collision numbers for the five most recent years of City of Regina data, the HSM SPFs were calibrated according to the procedure described earlier in this report. Calibration factors were calculated for each of the five years (2005 to 2009), as well as the five-year average. The results of the calibration are shown in Table 27.

Table 27: Calibration Factors for Road Segments.

Category	Severity	Calibration Factor					
		2005	2006	2007	2008	2009	Avg
Major Arterial / 2-Lane Undivided	Total	2.48	0.92	1.97	2.48	2.33	2.03
	FI	1.94	0.62	0.62	1.23	0.62	1.00
	PDO	2.68	1.03	2.50	2.96	3.01	2.44
Major Arterial / 4-Lane Undivided	Total	1.31	1.26	1.51	2.10	1.88	1.61
	FI	0.82	0.74	0.79	0.54	0.65	0.71
	PDO	1.55	1.51	1.86	2.84	2.46	2.04
Major Arterial / 4-Lane Divided	Total	2.86	2.46	3.48	3.64	3.92	3.27
	FI	1.35	1.53	1.55	1.58	1.70	1.54
	PDO	3.27	2.67	4.01	4.21	4.53	3.74
Minor Arterial / 2-Lane Undivided	Total	2.02	1.82	2.16	2.04	2.52	2.12
	FI	1.05	0.64	1.02	0.55	0.96	0.85
	PDO	2.43	2.31	2.63	2.67	3.17	2.65
Minor Arterial / 4-Lane Undivided	Total	1.96	0.35	1.25	1.41	1.66	1.33
	FI	1.97	0.27	0.28	0.84	0.72	0.81
	PDO	1.98	0.38	1.71	1.70	2.12	1.59
Minor Arterial / 4-Lane Divided	Total	5.50	1.83	4.20	2.49	6.91	4.20
	FI	0.86	0.00	0.83	2.55	1.67	1.19
	PDO	6.88	2.39	5.20	2.37	8.44	5.07
Collector / 2-Lane Undivided	Total	2.73	1.85	2.81	2.90	3.29	2.74
	FI	0.68	0.50	0.78	0.71	0.70	0.68
	PDO	3.64	2.46	3.72	3.87	4.43	3.65
Collector / 4-Lane Undivided	Total	3.58	3.71	6.58	6.04	5.71	5.08
	FI	0.74	2.54	2.92	0.83	3.66	2.19
	PDO	4.95	4.30	8.36	8.56	6.72	6.48
Collector / 4-Lane Divided	Total	4.80	3.70	3.86	3.91	6.10	4.47
	FI	0.87	1.76	1.84	2.61	1.78	1.77
	PDO	5.97	4.23	4.41	4.20	7.35	5.23

As the table shows, the majority of the average calibration factors are greater than one, indicating that the HSM SPFs under-predict the number of collisions in these categories. For FI collisions in four categories (Major Arterial / 4-Lane Undivided; Major Arterial / 2 Lane Undivided; Minor Arterial / 4-Lane Undivided; and Collector / 2-Lane Undivided), the calibration factors are less than one, indicating that the HSM SPFs over-predict the number of FI

collisions in these categories. The five-year average for FI collisions on Major Arterial / 2-Lane Undivided segments is 1.00, indicating that for the study period, the HSM SPF accurately predicts the number of FI collisions on this category of roadway.

These calibration factors were applied to the SPFs provided in the HSM, and used for the comparison outlined in the following section.

3.5.4. Comparison of Roadway Segment SPFs

The jurisdiction-specific SPFs were compared to the HSM SPFs (both calibrated and uncalibrated) using a number of techniques, including visual plots, statistical GOF tests, and CURE plots. Graphs showing the observed collisions (five-year averages) as a function of AADT, as well as jurisdiction-specific SPFS, HSM SPFs, and calibrated HSM SPFs, are shown in Figure 25 through Figure 27 on the following pages. The average segment lengths for each road segment type are used for the graphs.

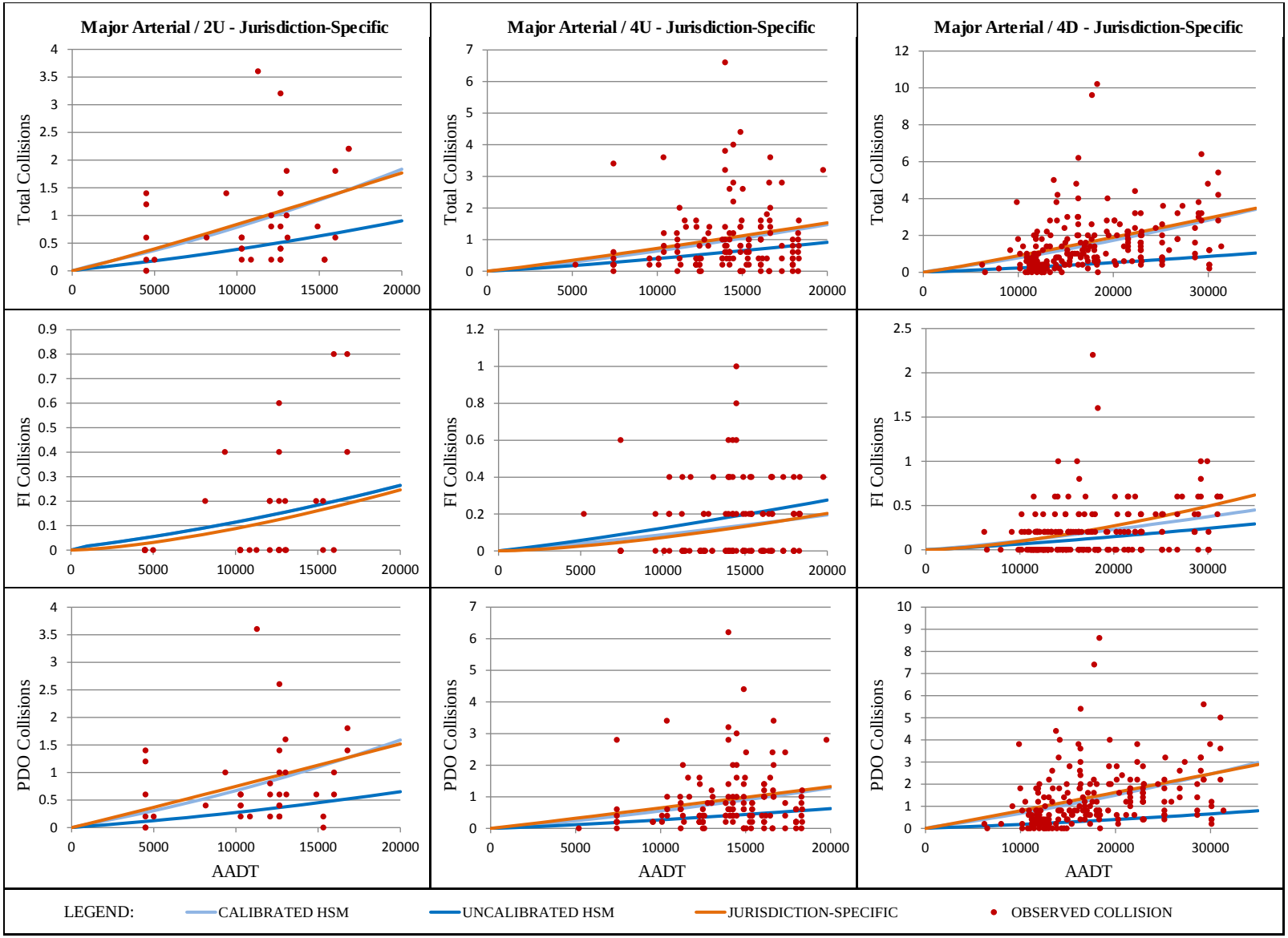

Figure 25: Total, FI, and PDO Observed Collisions and SPFs for Major Arterial Road Segments.

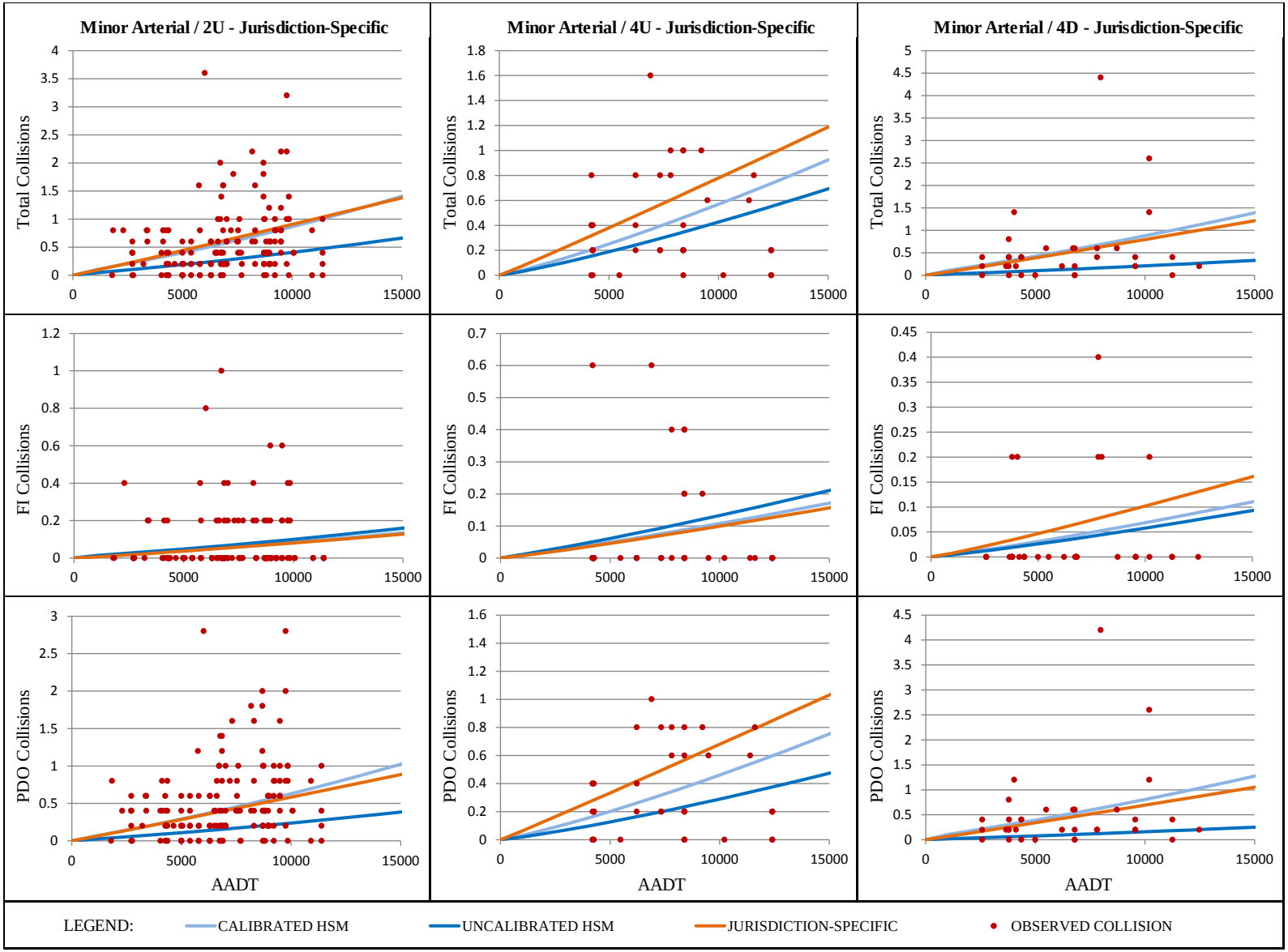

Figure 26: Total, FI, and PDO Observed Collisions and SPFs for Minor Arterial Road Segments.

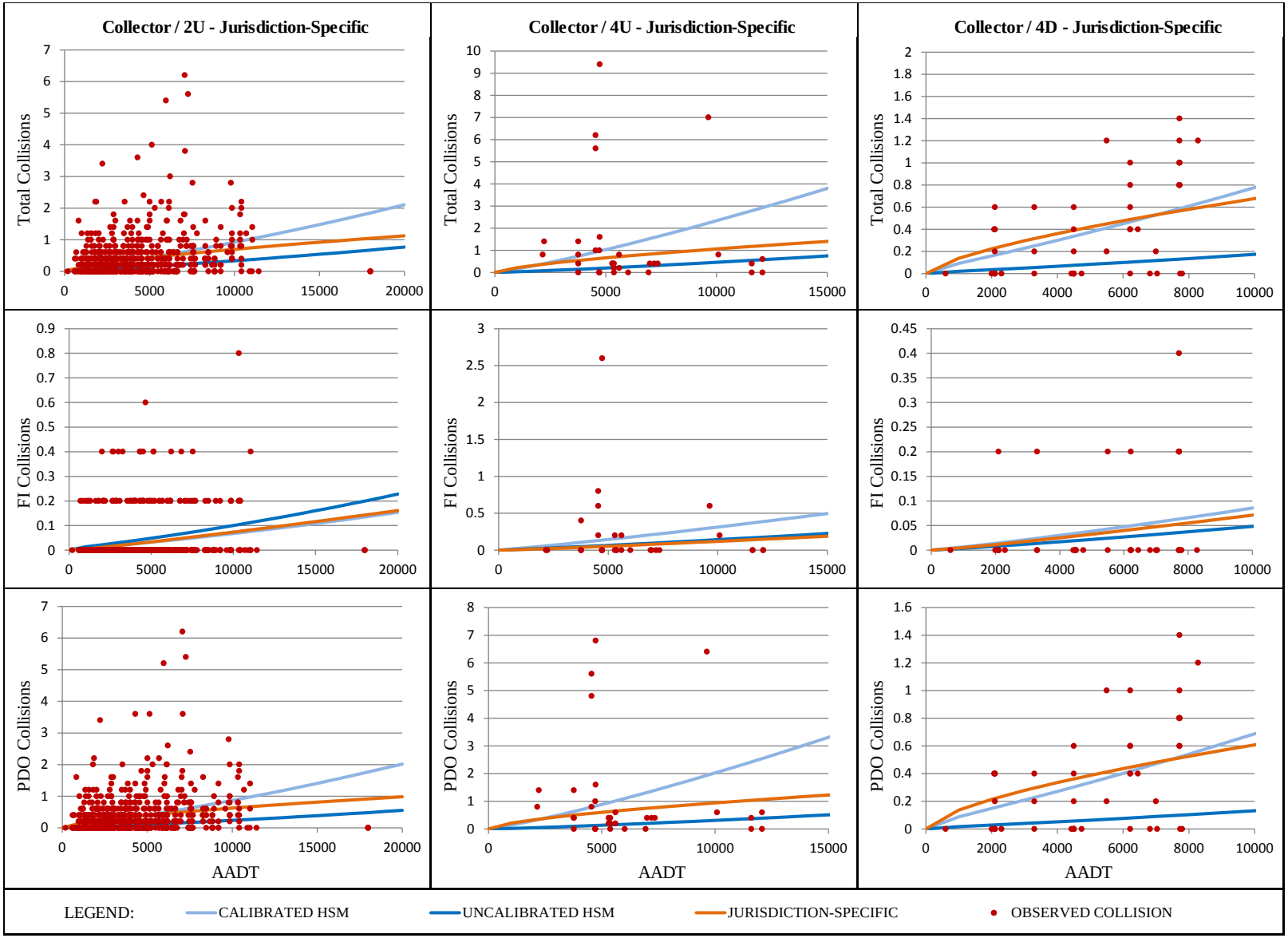

Figure 27: Total, FI, and PDO Observed Collisions and SPFs for Collector Road Segments.

As the graphs above show, the uncalibrated HSM SPFs generally under-predict the number of collisions experienced on Regina's road segments. Exceptions include FI collisions on "Major Arterial / 2-Lane Undivided & 4-Lane Undivided," "Minor Arterial / 2-Lane Undivided & 4-Lane Undivided," and "Collector / 2-Lane Undivided" segments.

The calibrated HSM SPFs generally perform comparably to the jurisdiction-specific SPFs, with a few exceptions. For several of the "4-Lane Undivided" road segment categories, the calibrated HSM SPFs diverge significantly from both the uncalibrated HSM SPFs and the jurisdiction-specific SPFs. This may be due to the fact that the "4-Lane Undivided" road segment category contains fewer locations than both the "2-Lane Undivided" and "4-Lane Divided" categories; therefore, the calibration factors were developed using a smaller dataset of historical data.

Though these graphs give a general idea of the models' fit to the observed collisions, it must be remembered that not all of the dots represent a single location (i.e., if two or more locations have similar major AADT and observed number of collisions, they will be represented by a single dot).

Statistical GOF tests were also utilized to analyze the models. These tests include the MSPE, MPB, MAD, and Freeman Tukey R-Squared. Table 28 shows the results of this comparison.

Table 28: Statistical Comparison Between Nine Sets of SPFs.

Category	Severity	Jurisdiction-Specific SPFs				HSM SPFs				Calibrated HSM SPFs			
		MSPE	MPB	MAD	R^2_{FT}	MSPE	MPB	MAD	R^2_{FT}	MSPE	MPB	MAD	R^2_{FT}
Major Arterial / 2-Lane Undivided	Total	16.08	-0.05	2.92	17%	20.45	-2.27	2.84	-13%	15.82	0.00	2.90	17%
	FI	0.99	-0.14	0.65	26%	0.95	0.00	0.70	23%	0.95	0.00	0.70	23%
	PDO	13.37	0.08	2.57	7%	17.40	-2.25	2.60	-38%	13.38	0.00	2.53	6%
Major Arterial / 4-Lane Undivided	Total	24.10	0.25	3.16	12%	28.22	-1.83	3.15	5%	24.48	0.00	3.17	11%
	FI	0.74	-0.05	0.66	18%	0.83	0.27	0.75	-2%	0.78	0.00	0.70	12%
	PDO	20.36	0.29	2.92	8%	25.39	-2.14	2.92	-10%	20.54	0.00	2.89	8%
Major Arterial / 4-Lane Divided	Total	41.70	0.43	4.39	26%	72.25	-5.22	5.52	-52%	44.31	0.00	4.34	25%
	FI	1.69	0.15	0.93	14%	1.71	-0.35	0.84	17%	1.55	0.00	0.88	19%
	PDO	32.03	0.30	3.96	23%	57.70	-4.78	5.05	-62%	35.18	0.00	3.95	20%
Minor Arterial / 2-Lane Undivided	Total	5.80	0.04	1.70	28%	8.89	-1.48	1.92	-2%	5.68	0.00	1.72	27%
	FI	0.40	0.05	0.43	21%	0.46	0.06	0.49	12%	0.47	0.00	0.47	15%
	PDO	4.64	-0.01	1.54	23%	7.53	-1.54	1.82	-25%	4.48	0.00	1.55	23%
Minor Arterial / 4-Lane Undivided	Total	4.12	0.72	1.63	-15%	3.70	-0.50	1.39	-1%	3.56	0.00	1.46	0%
	FI	0.66	-0.04	0.54	6%	0.70	0.09	0.63	-8%	0.69	0.00	0.59	-1%
	PDO	2.94	0.76	1.42	-29%	2.44	-0.60	1.20	-10%	2.18	0.00	1.20	-3%
Minor Arterial / 4-Lane Divided	Total	14.65	-0.30	2.01	22%	20.61	-2.08	2.38	-31%	14.78	0.00	2.05	18%
	FI	0.25	0.11	0.34	-6%	0.21	-0.03	0.29	7%	0.21	0.00	0.31	6%
	PDO	13.78	-0.41	1.93	21%	19.39	-2.03	2.23	-39%	13.76	0.00	2.03	18%
Collector / 2-Lane Undivided	Total	12.64	0.21	1.53	21%	8.93	-1.09	1.51	3%	7.16	0.00	1.54	17%
	FI	0.27	0.02	0.22	3%	0.15	0.06	0.26	1%	0.15	0.00	0.22	9%
	PDO	10.46	0.18	1.45	19%	8.60	-1.15	1.46	-8%	6.71	0.00	1.47	15%
Collector / 4-Lane Undivided	Total	96.74	-2.61	5.25	30%	147.76	-5.11	5.80	-19%	112.06	0.00	7.15	-2%
	FI	4.88	-0.53	0.91	26%	5.56	-0.48	1.01	9%	5.08	0.00	1.19	5%
	PDO	66.80	-2.11	4.57	28%	104.81	-4.64	5.10	-30%	76.92	0.00	6.16	-3%
Collector / 4-Lane Divided	Total	6.02	0.28	1.96	-11%	6.45	-1.55	1.84	-34%	3.94	0.00	1.65	12%
	FI	0.26	-0.01	0.33	-18%	0.21	-0.09	0.27	0%	0.21	0.00	0.33	-3%
	PDO	4.60	0.28	1.72	-10%	5.37	-1.45	1.67	-44%	3.09	0.00	1.43	12%

The highlighted boxes identify the models that performed best for each statistical test. In general, the jurisdiction-specific SPFs and calibrated HSM SPFs exhibited the lowest values for MSPE and MAD. The calibrated HSM SPFs, however, exhibited the lowest MPB values in most cases. The jurisdiction-specific SPFs exhibited the highest Freeman Tukey R-Squared results for the majority of intersections and severities. The results from these GOF tests highlight the importance of performing multiple statistical tests, as the outcome from one test may not necessarily reflect the majority of the results. Based on the results shown in Table 28, the jurisdiction-specific SPFs and calibrated HSM SPFs show the best-fitting results, based on their fit to Regina's collision data.

CURE plots were also developed for all of the road segment categories. Figure 28 through Figure 30 show CURE plots, as a function of AADT, for the nine road segment categories, based on total collisions. In each of the figures, the jurisdiction-specific SPFs are shown on the top row, calibrated HSM SPFs are shown on the middle row, and uncalibrated HSM SPFs are shown on the bottom row.

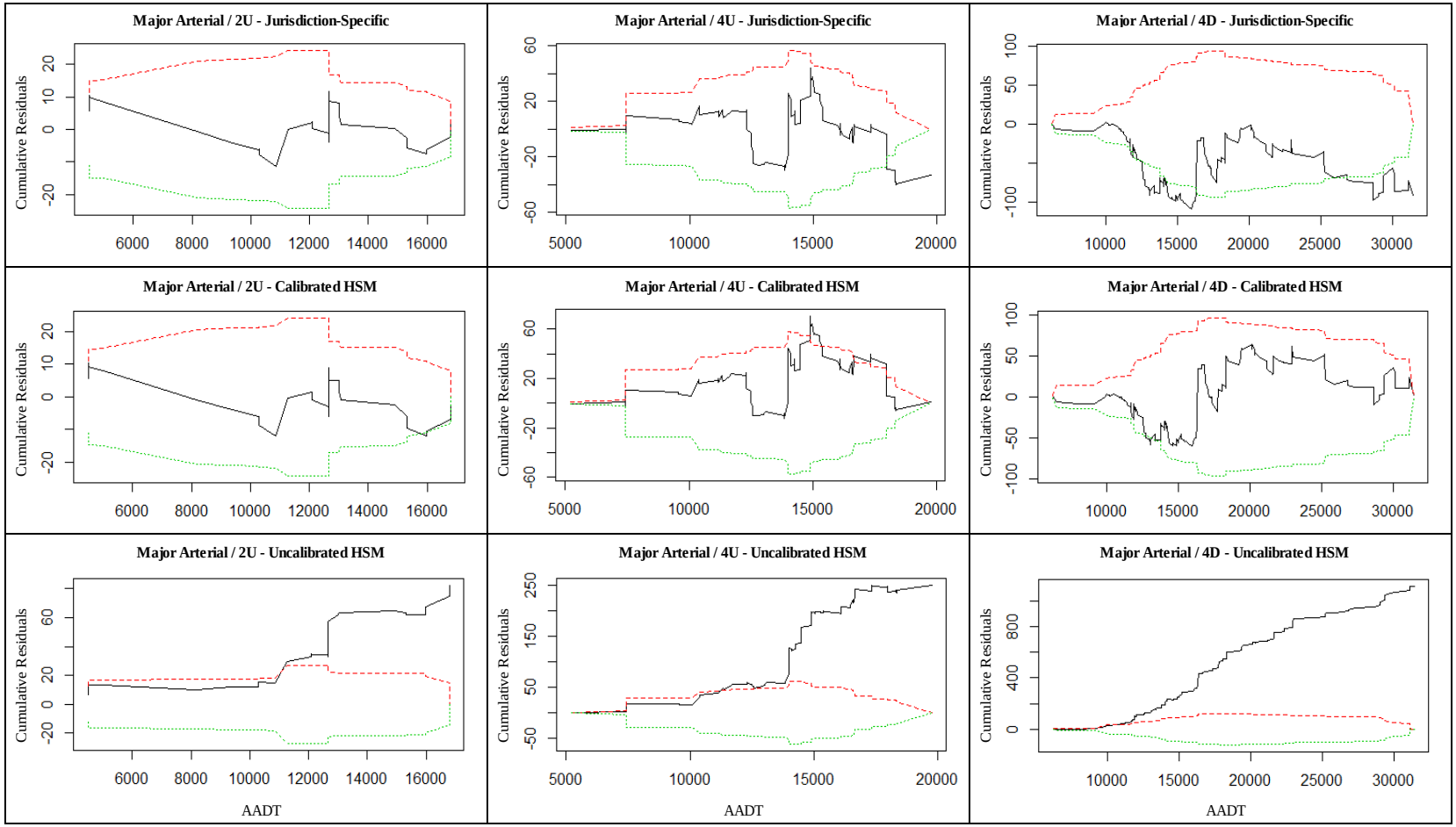

Figure 28: CURE Plots as a Function of AADT for Major Arterial Road Segments.

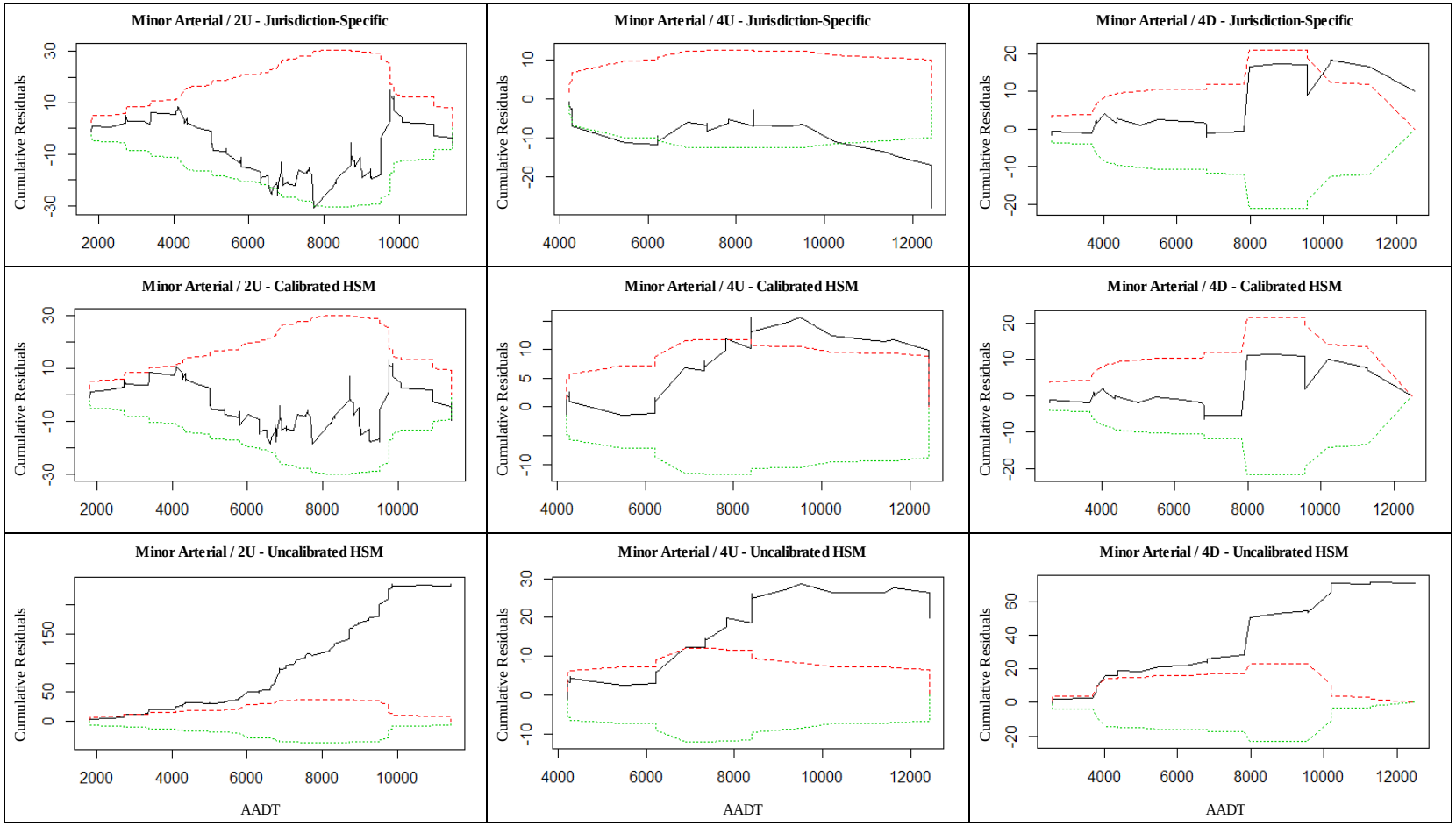

Figure 29: CURE Plots as a Function of AADT for Minor Arterial Road Segments.

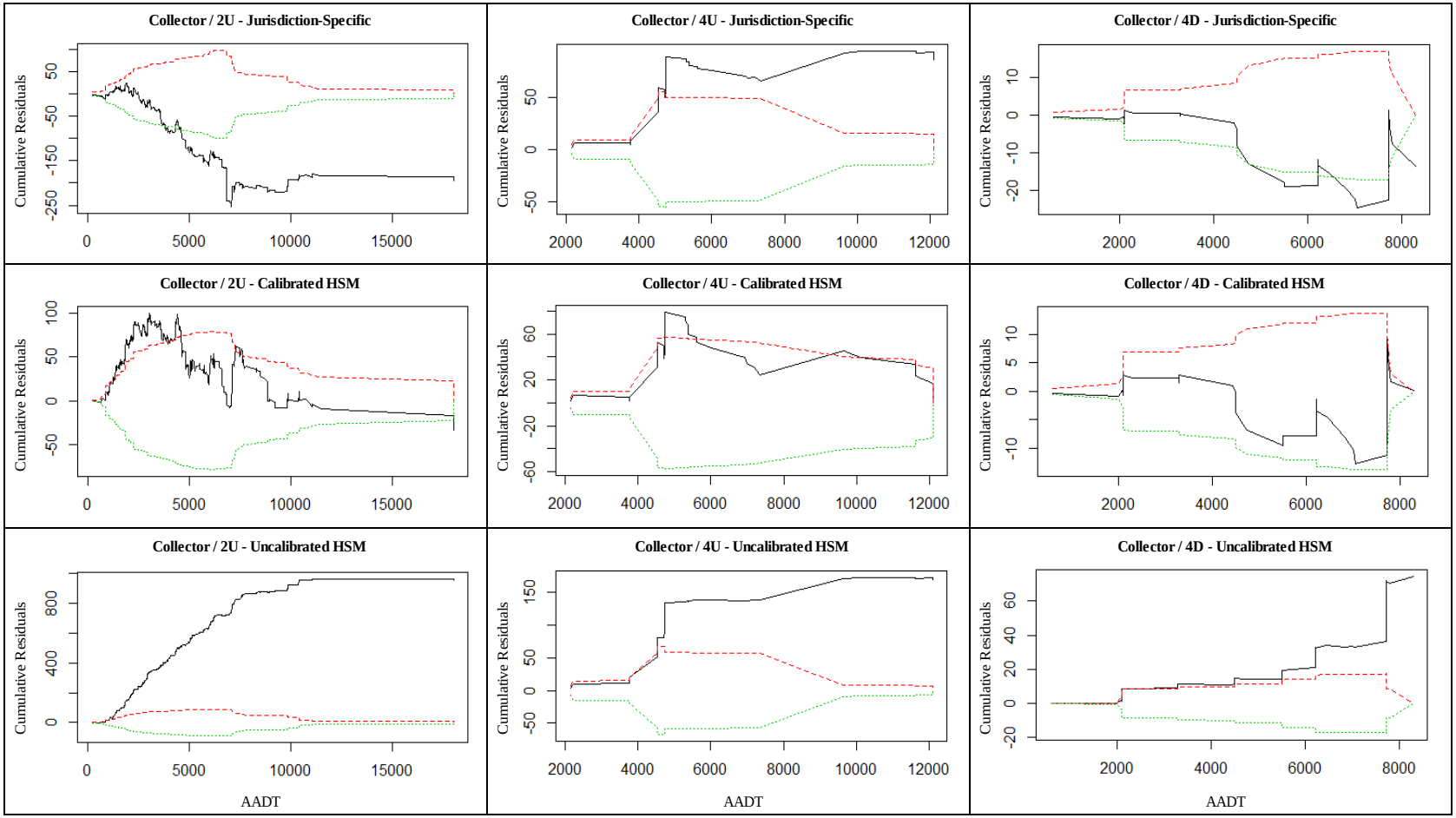

Figure 30: CURE Plots as a Function of AADT for Collector Road Segments.

As the CURE plots show, the uncalibrated HSM SPFs deviate significantly from the 95% confidence interval (designated by the blue +2σ and green -2σ boundaries) for the majority of the major AADT range. For the major arterial road segment SPFs, both the calibrated HSM SPFs and the jurisdiction-specific SPFs fall within the 95% confidence interval for the majority of major AADT ranges, with the calibrated HSM SPFs showing slightly better performance. The CURE plots for minor arterial road segments show similar results.

For the collector SPFs, the calibrated HSM SPFs stay within the 95% confidence interval for a higher major AADT range than the jurisdiction-specific SPFs. This result may be due to the fact that the HSM SPFs were calibrated to the entire dataset, whereas the jurisdiction-specific SPFs were developed using the estimation dataset only (i.e., 70% of the total data). This increase in the amount of observed collision data may contribute to the calibrated HSM SPFs' superior performance in regards to the CURE plots shown for collector road segment SPFs.

3.6. Transferability Test

The applicability of SPFs on regions other than the ones for which they were originally developed can be investigated using studies known as transferability tests, as described in Section 2.1.4.

In order to assess the transferability of the SPFs developed for Regina, the previously-described intersection models (i.e., three-leg unsignalized, four-leg unsignalized, three and four-leg signalized) were applied to collision data from the City of Saskatoon. The same statistical goodness-of-fit tests (i.e., MSPE, MPB, MAD, R^2_{FT}) used to validate the Regina SPFs were utilized to investigate the SPFs' transferability using Saskatoon data.

Two sets of calibration factors were developed for each of the intersection categories being investigated. The first set was developed for use with the HSM's base SPFs, in the same way calibration factors were developed using the Regina data: calibration factors (e.g., Ci for intersections) were obtained by calculating the ratio of total number of observed collisions to the total number of predicted collisions obtained from the base HSM SPFs. These calibration factors are shown in Table 29.

Table 29: Calibration Factors Developed for HSM SPFs Using Saskatoon Data.

Category	Severity	HSM SPF Calibration Factor					
		2005	2006	2007	2008	2009	Avg
3-Leg Unsignalized	Total	1.35	1.20	1.59	1.64	1.43	1.44
	FI	0.73	0.73	0.39	0.75	0.37	0.59
	PDO	1.52	1.32	2.00	1.89	1.77	1.71
4-Leg Unsignalized	Total	1.72	1.71	1.96	1.85	1.84	1.82
	FI	0.65	0.80	0.76	0.77	0.65	0.73
	PDO	2.33	2.23	2.64	2.46	2.52	2.44
3 & 4-Leg Signalized	Total	2.77	2.73	2.77	2.72	2.59	2.72
	FI	1.28	1.47	1.12	1.07	1.20	1.23
	PDO	3.65	3.49	3.74	3.68	3.41	3.59

As the table shows, the majority of the average calibration factors are greater than one, indicating that the HSM SPFs under-predict the number of collisions in these categories. FI collisions for both 3-leg unsignalized and 4-leg unsignalized intersections have calibration factors less than one (0.59 and 0.73, respectively), indicating that the HSM SPFs over-predict collisions in these categories. For all three intersection categories, the FI calibration factor was consistently lower than the total and PDO calibration factors; this highlights the importance of developing jurisdiction-specific SPFs (or at the very least, calibrating the HSM SPFs using local data) in order to accurately reflect region-specific variations in collision severities.

The second set of calibration factors was developed using the Regina SPFs as the base SPF input (i.e., the ratio of total number of observed collisions to the total number of predicted collisions obtained from the jurisdiction-specific SPFs was calculated). These calibration factors are shown in Table 30.

Table 30: Calibration Factors Developed Using Saskatoon Data to Calibrate Jurisdiction-Specific Regina SPFs.

Category	Severity	Regina SPF Calibration Factor					
		2005	2006	2007	2008	2009	Avg
3-Leg Unsignalized	Total	0.85	0.75	1.01	1.05	0.91	0.92
	FI	0.94	0.93	0.49	0.96	0.48	0.76
	PDO	0.84	0.72	1.11	1.06	0.99	0.95
4-Leg Unsignalized	Total	0.93	0.92	1.06	0.99	0.98	0.98
	FI	1.10	1.35	1.28	1.29	1.11	1.23
	PDO	0.90	0.86	1.02	0.94	0.97	0.94
3 & 4-Leg Signalized	Total	1.33	1.31	1.33	1.30	1.25	1.30
	FI	0.99	1.14	0.87	0.83	0.93	0.95
	PDO	1.40	1.34	1.44	1.42	1.32	1.39

As the table shows, the calibration factors that were developed using Saskatoon data to calibrate the jurisdiction-specific Regina SPFs fluctuate much closer to 1.0 than the HSM calibration factors. This is to be expected, since geographic, climatic, and driver behaviour-related similarities are much more likely to exist between Saskatoon and Regina, as opposed to Saskatoon and the American states in which the HSM SPFs were developed. The range of calibration factors varies between 0.76 and 1.39 (as opposed to the range of 0.59 and 3.59, shown in Table 29). One interesting difference to note is that for four-leg unsignalized intersections, the FI calibration factor is greater than the Total and PDO calibration factors for this category (which is in opposition to the general trends for all other categories, where the FI calibration factor was lower). This would indicate that for this category of intersections, FI

collisions occur with a relatively higher frequency in Saskatoon than in Regina (this collision severity is under-predicted using Regina SPFs).

A statistical comparison between the jurisdiction-specific Regina SPFs and the uncalibrated HSM SPFs, using Saskatoon collision data, is presented in Table 31. Highlighted cells show the best-fitting results for each category and severity, for all of the statistical tests that were used.

Table 31: Statistical Comparison Between Jurisdiction-Specific Regina SPFs and HSM SPFs.

Category	Severity	Regina SPFs				HSM SPFs			
		MSPE	MPB	MAD	R^2_{FT}	MSPE	MPB	MAD	R^2_{FT}
3-Leg Unsignalized	Total	237.36	1.14	7.84	21%	159.42	-3.78	7.60	32%
	FI	8.91	0.52	1.55	9%	8.48	1.13	1.85	-7%
	PDO	161.93	0.59	6.89	20%	127.98	-4.42	7.15	14%
4-Leg Unsignalized	Total	399.35	0.51	11.53	0%	384.85	-8.97	12.60	-2%
	FI	9.92	-0.56	1.97	14%	13.36	1.14	2.46	-9%
	PDO	309.25	1.07	10.20	-3%	326.99	-10.00	11.97	-26%
3 & 4-Leg Signalized	Total	3112.01	-20.63	34.78	59%	7648.05	-56.15	57.54	-21%
	FI	76.73	0.67	5.68	59%	107.89	-2.43	6.15	52%
	PDO	2494.53	-21.10	31.62	54%	6512.93	-54.70	55.44	-62%

As the table shows, the jurisdiction-specific Regina SPFs generally performed more accurately than the uncalibrated HSM SPFs. This result is likely due to the similarities between the two cities that were previously noted (e.g., climate, driver behaviour).

A statistical comparison between the calibrated Regina SPFs and the calibrated HSM SPFs, using Saskatoon collision data, is presented in Table 32. Highlighted cells show the best-fitting results for each category and severity, for all of the statistical tests that were used.

Table 32: Statistical Comparison Between Calibrated Jurisdiction-Specific Regina SPFs and Calibrated HSM SPFs.

Category	Severity	Calibrated Regina SPFs				Calibrated HSM SPFs			
		MSPE	MPB	MAD	R^2_{FT}	MSPE	MPB	MAD	R^2_{FT}
3-Leg Unsignalized	Total	211.75	0.00	7.82	25%	169.42	0.00	7.26	36%
	FI	6.73	0.00	1.46	22%	5.52	0.00	1.44	28%
	PDO	151.21	0.00	6.86	22%	152.01	-0.74	6.62	23%
4-Leg Unsignalized	Total	390.52	0.00	11.43	2%	316.65	0.00	11.44	14%
	FI	10.24	0.00	2.01	12%	9.94	0.00	2.01	13%
	PDO	290.68	0.00	10.01	1%	223.70	-1.29	9.64	16%
3 & 4-Leg Signalized	Total	2239.85	0.00	31.03	64%	2908.21	0.00	37.03	58%
	FI	77.88	0.00	5.60	60%	96.27	0.00	6.42	53%
	PDO	1663.91	0.00	27.17	63%	2126.65	-3.56	31.02	57%

As the table shows, the calibrated HSM SPFs generally performed better than the calibrated Regina SPFs for the two unsignalized intersection categories, while the reverse was true for signalized intersections. Another observation that can be made is that the differences in magnitude between the results shown in Table 32 are generally much smaller than the differences in magnitude shown in Table 31. This would indicate that regardless of the base SPF chosen, applying calibration factors developed using local collision data serves to increase the accuracy of the analysis results.

3.7. Chapter Summary

This chapter contained a description of the development of SPFs for the City of Regina. The study data (road network, traffic volume, and collision data) was described, as was the integrated databases that were created for the intersection and roadway segment classifications under investigation. The data was developed into two subsets: 70% for estimation, and 30% for validation. For intersections, four initial candidate model forms were developed for each level of severity; the best-fitting model was selected using AIC/BIC values, CURE plots, and the

coefficients' p-values. Four initial candidate models were also developed for roadway segments, and the best-fitting model chosen using similar criteria to the intersection models. Calibration factors were also developed for each of the intersection and roadway segment classifications.

The models were validated using statistical goodness-of-fit tests, including the mean square error, the mean prediction bias, the mean absolute deviation, the mean square prediction error, the Freeman Tukey R-Squared value, and the likelihood ratio R-squared. The jurisdiction-specific SPFs were then compared to the SPFs provided in the HSM; based on the comparison results, the jurisdiction-specific SPFs were found to exhibit a better fit to the study data.

A transferability test was performed using collision data from the City of Saskatoon; it was found that the SPFs developed for the City of Regina fit the data better than the SPFs provided in the HSM.

CHAPTER 4. NETWORK SCREENING

4.1. HSM's Network Screening Method

There are a number of performance measures commonly used for screening transportation networks for locations that are most likely to benefit from a safety improvement. The HSM recommends using multiple performance measures in order to improve the level of confidence in the results.

For this study, two network screening methods were used to investigate Regina's intersections and road segments; Appendix A contains a detailed sample calculation for both methods.

The "EPDO Average Collision Frequency with EB Adjustment" method uses weighting factors to convert FI collisions into EPDO (equivalent property damage-only) collisions, and then ranks locations by the EB-adjusted EPDO. The societal collision costs used to develop the weighting factors were taken from the HSM; these costs are given in Table 33.

Table 33: Societal Collision Costs Used in This Study.

Severity	Comprehensive Collision Cost
Fatality	$4,008,900
Injury	$82,600
PDO	$7,400

The second network screening method used was the "Excess Expected Average Collision Frequency with EB Adjustment," which ranks the locations by the difference between the predicted number of collisions (obtained using an SPF) and the EB-adjusted estimates (which take the observed number of collisions into account). The difference between expected and excess collisions is illustrated in Figure 31.

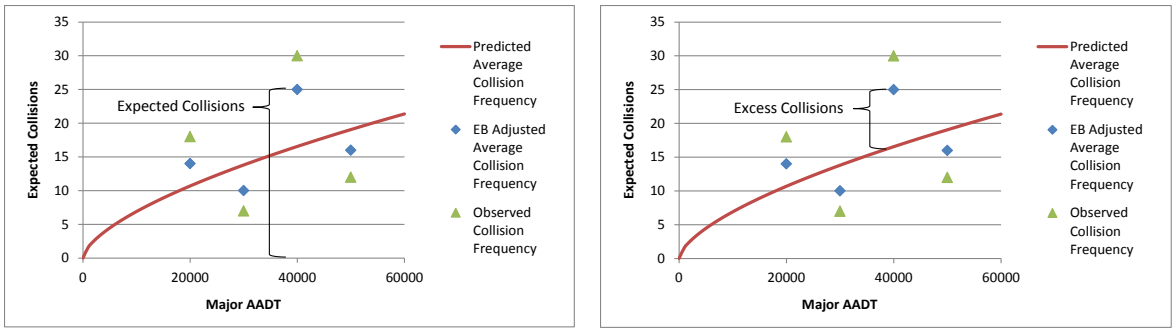

Figure 31: Expected Collisions (Left) and Excess Collisions (Right).

The network screening results from both methods were integrated into the City of Regina basemap using ArcGIS, in order to visually display the top-ranked locations. The results were published in a report to SGI entitled "Development of a Geographic Information System (GIS) to Identify Potential High Collision Locations in Regina" (Park & Young, 2012). Appendix B contains additional results of the network screening (the top 20 riskiest locations for each intersection and road segment classification).

The sections that follow present the results for Regina's intersections and road segments, showing the top ten locations for both network screening methods. The GIS maps of the top-ranked locations are also provided; the inset map for each figure has been centered on the number one ranked location.

4.2. Three and Four-Leg Signalized Intersections

The 3 and 4-leg signalized intersections were aggregated into a single category due to the small number of locations with AADT data (i.e., only 28 locations available for 3-leg signalized intersections). By aggregating the available 28 3-leg and 116 4-leg signalized intersections into a single group, the number of locations available for analysis was increased to 144. Table 34 lists

the top ten locations from both of the network screening methods, with eight locations appearing in both ranking methods.

Table 34: 3 and 4-Leg Signalized Intersections Network Screening Results.

Location	UGRID	EPDO		EPDO Rank	
		Excess	Expected	Excess	Expected
9th Ave N & McCarthy Blvd	RE688050	50.9	120.0	**1**	**9**
Dewdney Ave & Lewvan Dr	RE697760	50.1	142.3	**2**	**3**
4th Ave & Lewvan Dr	RE683430	49.3	126.8	**3**	**6**
Park St & Victoria Ave	RE706920	41.8	122.4	**4**	**7**
Prince Of Wales Dr & Victoria Ave	RE707580	40.7	139.8	**5**	**5**
Arcola Ave & Victoria Ave	RE689720	28.4	106.3	**6**	**10**
Albert St & Saskatchewan Dr	RE689010	27.3	122.4	**7**	**8**
Victoria Ave & Coleman Cres	RE696740	25.6	158.4	**8**	**2**
Albert St & Parliament Ave	RE689000	21.1	89.2	**9**	16
Victoria Ave & Winnipeg St	RE709460	19.6	85.9	**10**	17
Victoria Ave & Fleet St & University Park Dr	RE700150	-14.7	140.8	135	**4**
Pasqua St & Ring Rd & 9th Ave N	RE717710	-69.4	164.5	144	**1**

Note that two intersections: 1) Victoria Avenue & Fleet Street & University Park Drive and 2) Pasqua Street & Ring Road & 9th Avenue North have both been identified within the top ten locations when using the expected EPDO method. However, the negative excess EPDO score suggests that these locations are actually performing better than expected in terms of excess EPDO score. The results from both network screening methods are shown on the following pages.

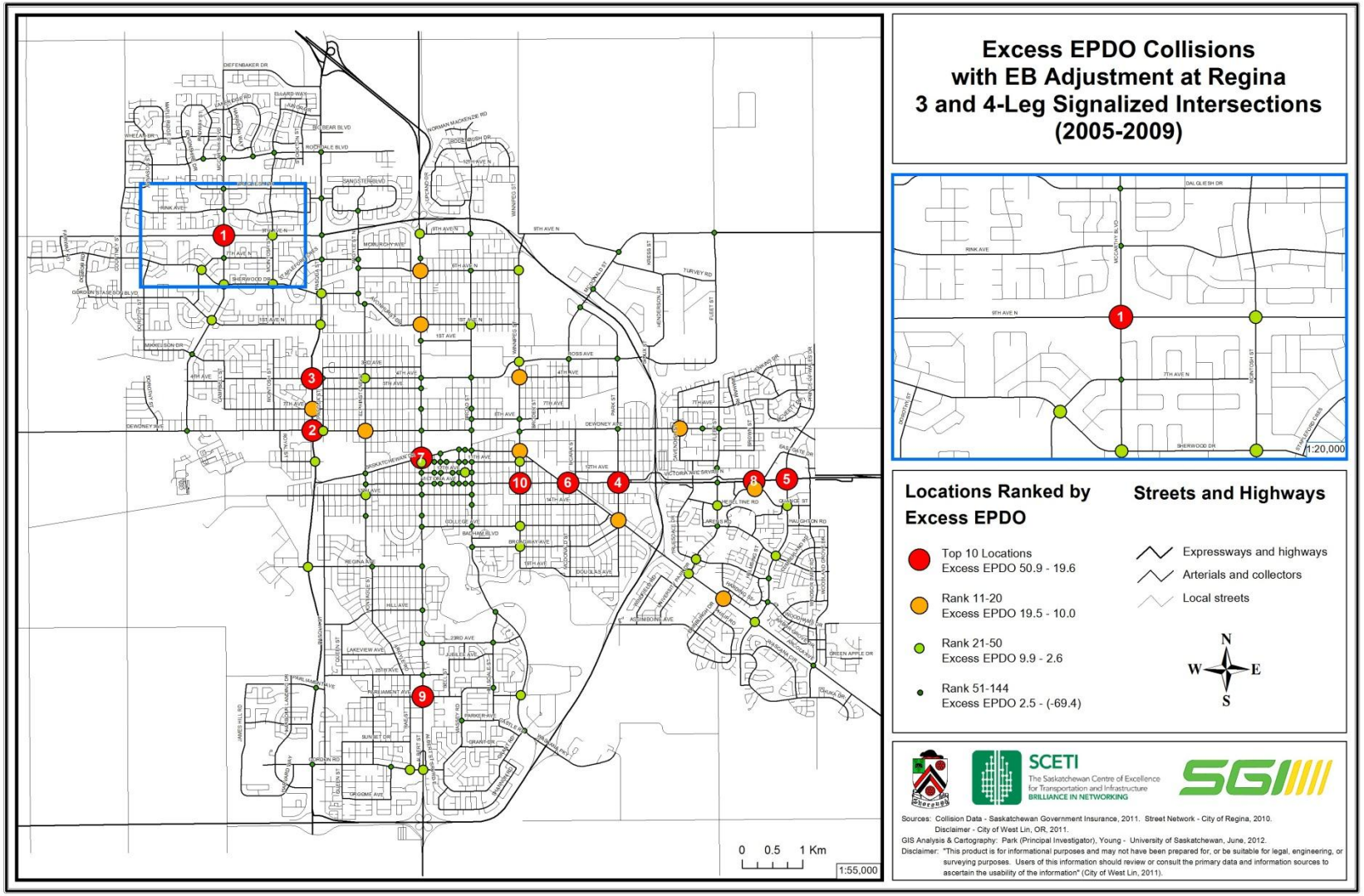

Figure 32: Excess EPDO Collisions at 3 and 4-Leg Signalized Intersections.

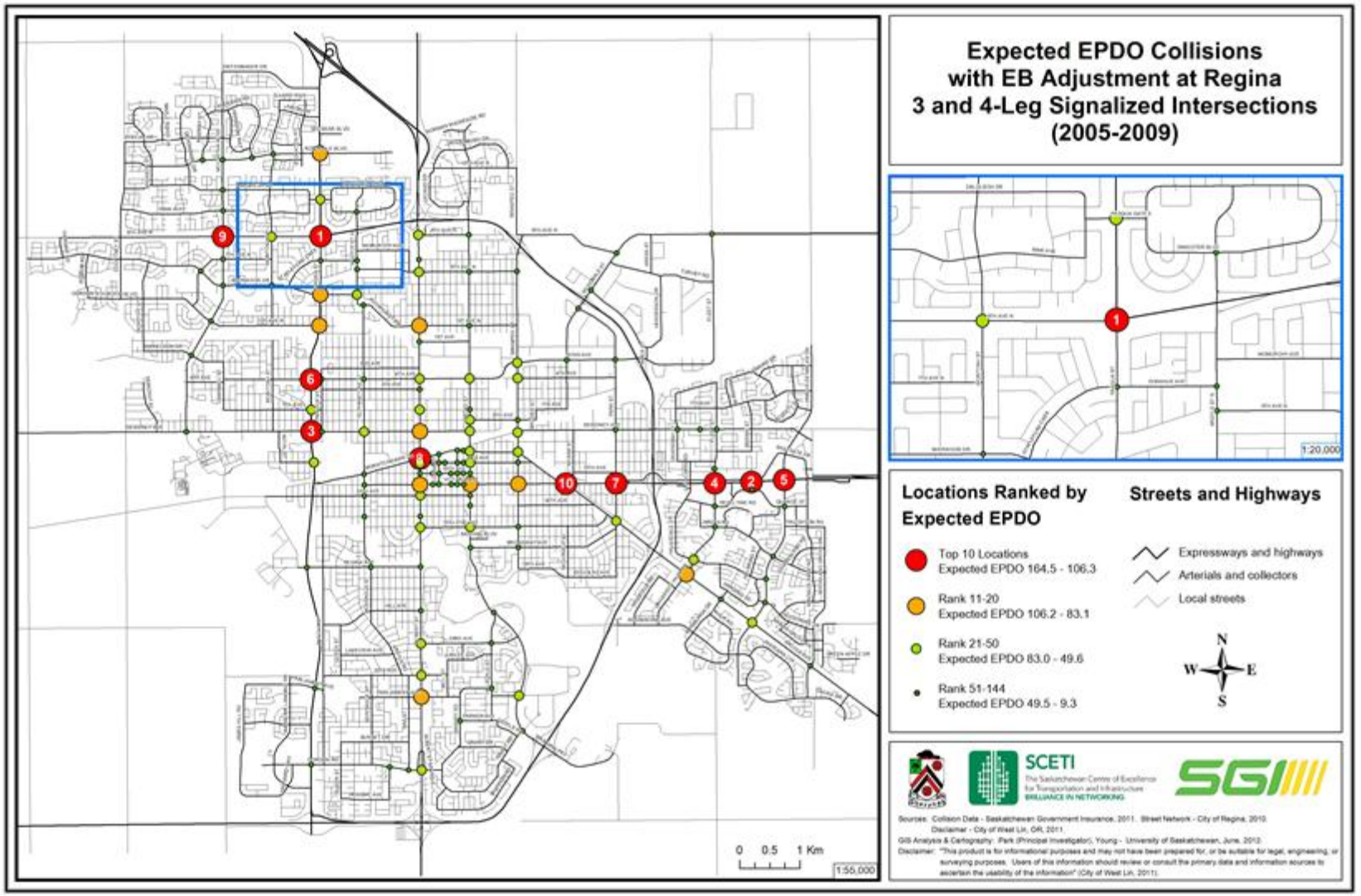

Figure 33: Expected EPDO Collisions at 3 and 4-Leg Signalized Intersections.

4.3. Three-Leg Unsignalized Intersections

Table 35 lists the top ten riskiest 3-leg unsignalized intersection locations. Of the 118 locations available for analysis, six locations appear at the top of both lists, with the top two locations being the same for both ranking methods. Note that two intersections: 1) Gordon Road & Grant Road and 2) 1st Avenue & Broad Street have both been identified within the top ten locations when using the expected EPDO method. However, the negative excess EPDO score suggests that these locations are actually performing better than expected in terms of excess EPDO score.

Table 35: 3-Leg Unsignalized Intersections Network Screening Results.

Location	UGRID	EPDO		EPDO Rank	
		Excess	Expected	Excess	Expected
Massey Rd & Parliament Ave	RE704860	18.1	29.9	**1**	**1**
Arcola Ave & College Ave	RE689800	10.0	27.9	**2**	**2**
Saskatchewan Dr & Smith St	RE708870	6.6	13.2	**3**	**5**
Quance St & Star Lite St	RE711950	6.0	9.7	**4**	12
Grant Dr & Grant Rd	RE701370	5.4	11.4	**5**	**8**
Henderson Dr & McDonald St (North Int)	RE711000	4.0	11.4	**6**	**9**
Argyle St N & Sangster Blvd (North Int)	RE712660	3.6	7.6	**7**	17
Hillsdale St & Kramer Blvd	RE702580	3.5	19.6	**8**	**3**
Cornwall St & Victoria Ave	RE696030	3.4	6.5	**9**	23
Courtney St & Rochdale Blvd	RE696110	3.3	7.1	**10**	20
1st Ave N & Winnipeg St	RE680020	1.4	13.0	17	**7**
3rd Ave & Albert St	RE682570	1.0	16.1	21	**4**
Gordon Rd & Grant Rd	RE701120	-1.0	13.1	89	**6**
1st Ave & Broad St (North Int)	RE709730	-6.7	11.0	116	**10**

The results from both network screening methods are shown on the following pages.

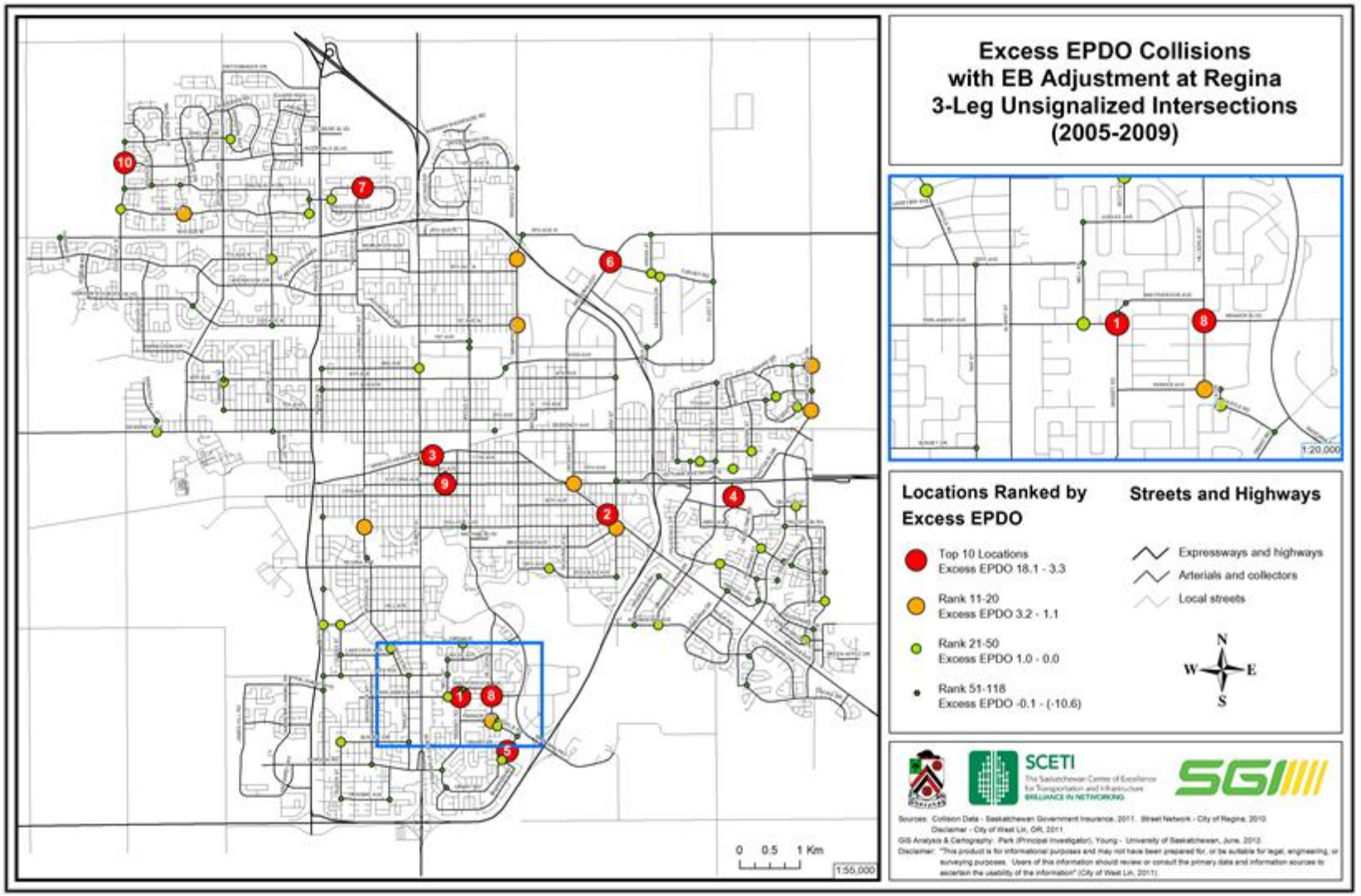

Figure 34: Excess EPDO Collisions at 3-Leg Unsignalized Intersections.

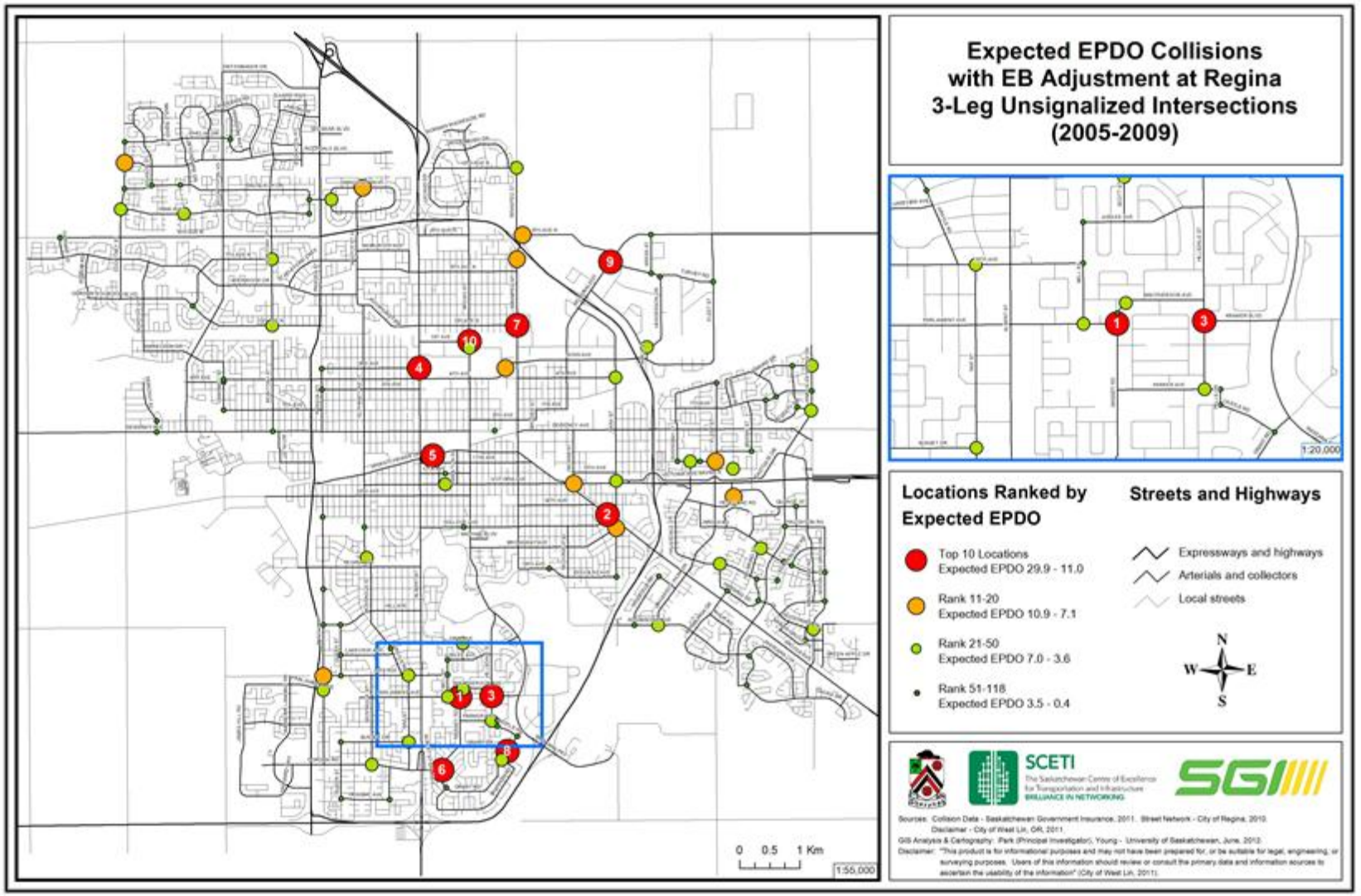

Figure 35: Expected EPDO Collisions at 3-Leg Unsignalized Intersections.

4.4. Four-Leg Unsignalized Intersections

Table 36 lists the top ten locations that have been identified for the 4-leg unsignalized intersection category. For this particular group, 125 locations were analysed; eight of these locations appear near the top of both lists. The top three locations that have the greatest excess EPDO ranking are also within the top four locations with the greatest expected EPDO score. Note that one intersection, 23rd Avenue & Broad Street & Wascana Parkway, has been identified within the top ten locations when using the expected EPDO method. However, the negative excess EPDO score suggests that this location is actually performing better than expected in terms of excess EPDO score.

Table 36: 4-Leg Unsignalized Intersections Network Screening Results.

Location	UGRID	EPDO		EPDO Rank	
		Excess	Expected	Excess	Expected
Fleet St & Victoria Ave N Srv Rd	RE700100	30.4	60.1	**1**	**1**
Glencairn Rd & Victoria Ave N Srv Rd	RE701010	22.8	34.2	**2**	**2**
14th Ave & Winnipeg St	RE677970	16.2	25.5	**3**	**4**
3rd Ave & Elphinstone St	RE682280	12.4	21.6	**4**	**8**
14th Ave & Albert St	RE677480	9.0	33.7	**5**	**3**
15th Ave & Broad St	RE678110	7.1	22.5	**6**	**6**
7th Ave & Brown St	RE686740	7.1	13.7	**7**	19
4th Ave & McIntosh St	RE683490	6.9	13.7	**8**	18
McIntyre St & Victoria Ave	RE705510	6.0	19.8	**9**	**9**
Eastgate Dr & Prince Of Wales Dr	RE699010	5.8	22.0	**10**	**7**
25th Ave & Argyle Rd & Retallack St	RE681020	1.7	17.2	26	**10**
23rd Ave & Broad St & Wascana Pky	RE680950	-3.9	22.5	110	**5**

The results from both network screening methods are shown on the following pages.

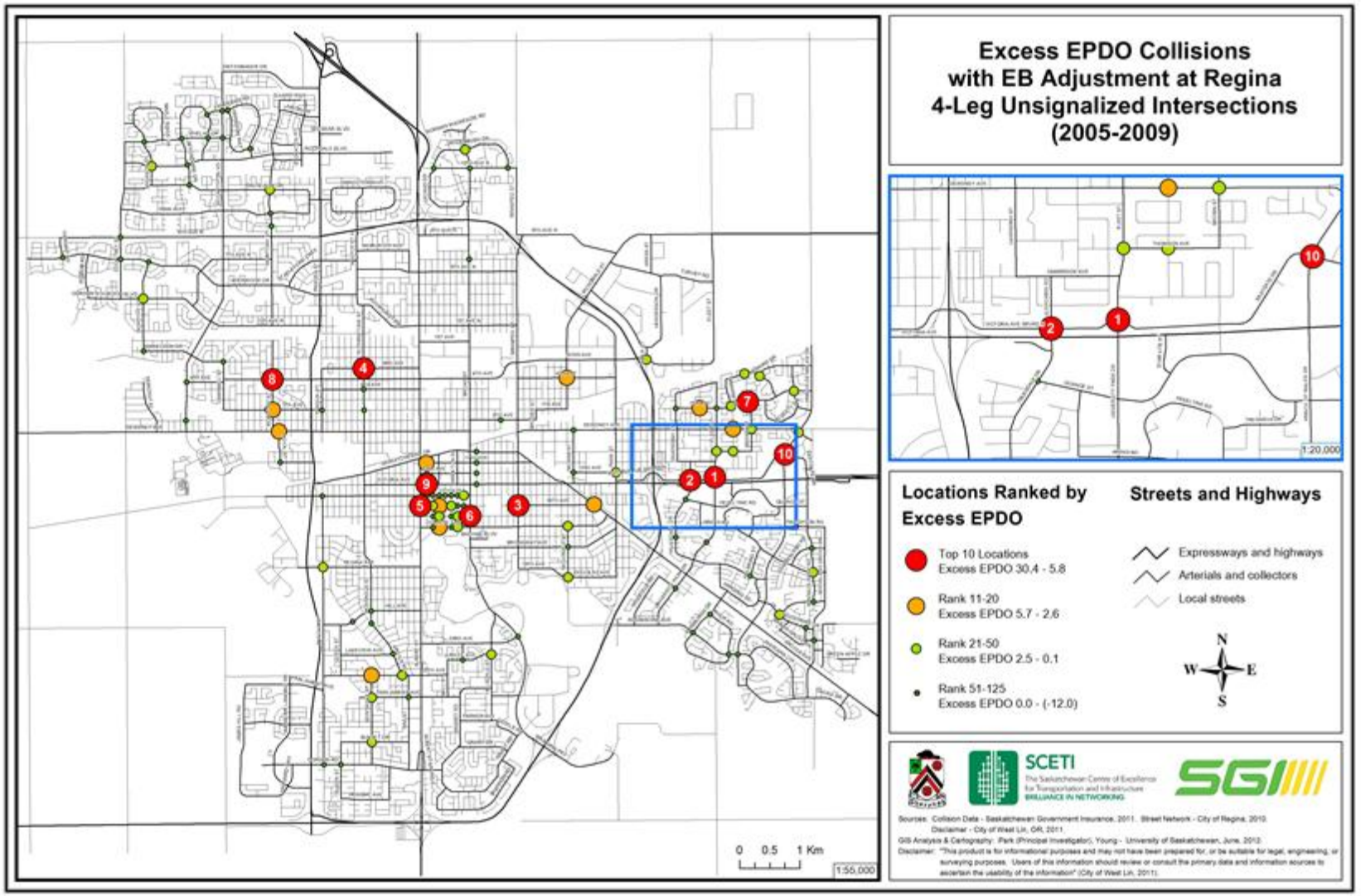

Figure 36: Excess EPDO Collisions at 4-Leg Unsignalized Intersections.

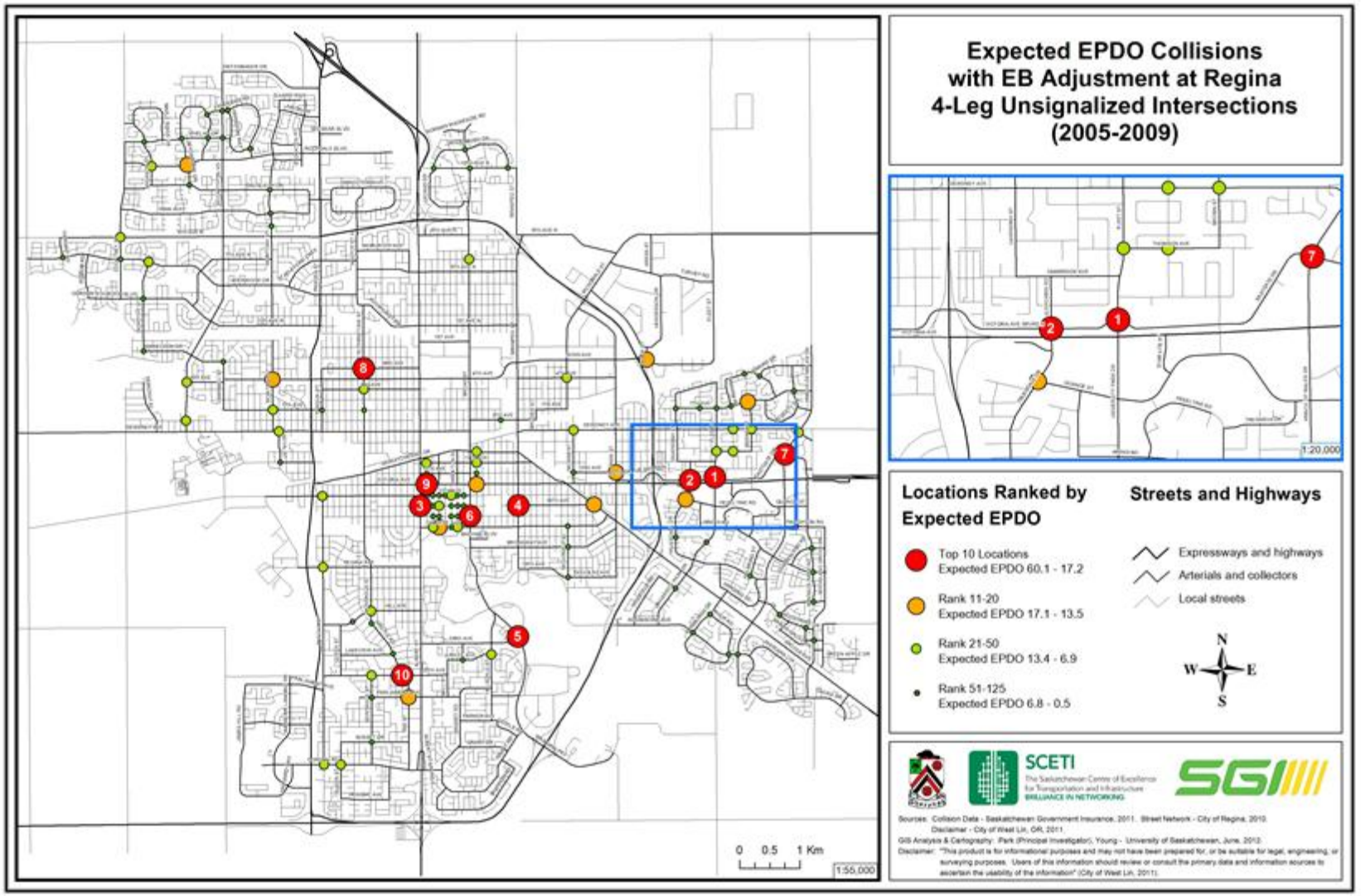

Figure 37: Expected EPDO Collisions at 4-Leg Unsignalized Intersections.

4.5. All Regina Intersections

A network screening process using the expected EPDO and excess EPDO methods was conducted on all intersections that contained the necessary data in Regina, for a total of 387 locations. This analysis focused on identifying the locations, regardless of configuration, that are most likely to benefit from a safety improvement. Table 37 contains the top ten riskiest intersections in Regina based on the two network screening methods.

Table 37: All Regina Intersections Network Screening Results.

Location	UGRID	EPDO		EPDO Rank		Int.
		Excess	Expected	Excess	Expected	Type*
9th Ave N & McCarthy Blvd	RE688050	50.9	120.0	**1**	**9**	4S
Dewdney Ave & Lewvan Dr	RE697760	50.1	142.3	**2**	**3**	4S
4th Ave & Lewvan Dr	RE683430	49.3	126.8	**3**	**6**	4S
Park St & Victoria Ave	RE706920	41.8	122.4	**4**	**7**	4S
Prince Of Wales Dr & Victoria Ave	RE707580	40.7	139.8	**5**	**5**	4S
Fleet St & Victoria Ave N Srv Rd	RE700100	30.4	60.1	**6**	33	4U
Arcola Ave & Victoria Ave	RE689720	28.4	106.3	**7**	**10**	4S
Albert St & Saskatchewan Dr	RE689010	27.3	122.4	**8**	**8**	4S
Victoria Ave & Coleman Cres	RE696740	25.6	158.4	**9**	**2**	4S
Glencairn Rd & Victoria Ave N Srv Rd	RE701010	22.8	34.2	**10**	76	4U
Victoria Ave & Fleet St & University Park Dr	RE700150	-14.7	140.8	378	**4**	4S
Pasqua St & Ring Rd & 9th Ave N	RE717710	-69.4	164.5	387	**1**	4S

Note that two intersections: 1) Victoria Avenue & Fleet Street & University Park Drive and 2) Pasqua Street & Ring Road & 9th Avenue North have both been identified within the top ten locations when using the expected EPDO method. However, the negative excess EPDO score suggest that these locations are actually performing better than expected in terms of excess EPDO score. The results from the city-wide network screening show that with the exception of two intersections, the riskiest locations are 4-leg signalized intersections. This is an expected result because SPFs for intersections are a function of traffic volumes; although the relationship is not perfectly linear, there is a tendency that the predicted number of collisions at an intersection increases with higher traffic volumes. Since traffic signals are installed at

intersections with high traffic volumes, the signalized intersections are ranked higher than unsignalized locations. The table shows the ranking results from the two ranking measures. The results from both network screening methods are shown on the following pages.

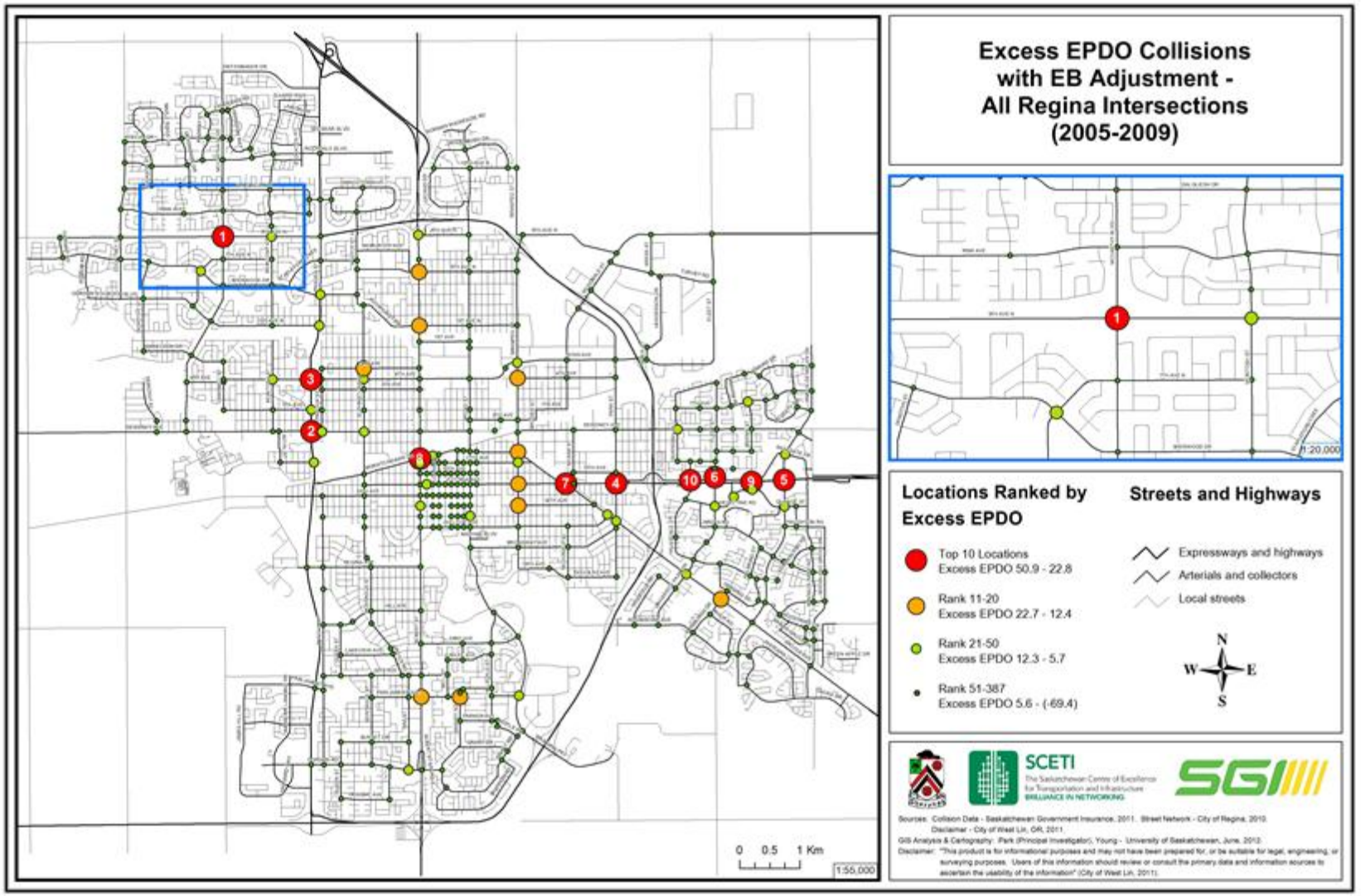

Figure 38: Excess EPDO Collisions at All Regina Intersections.

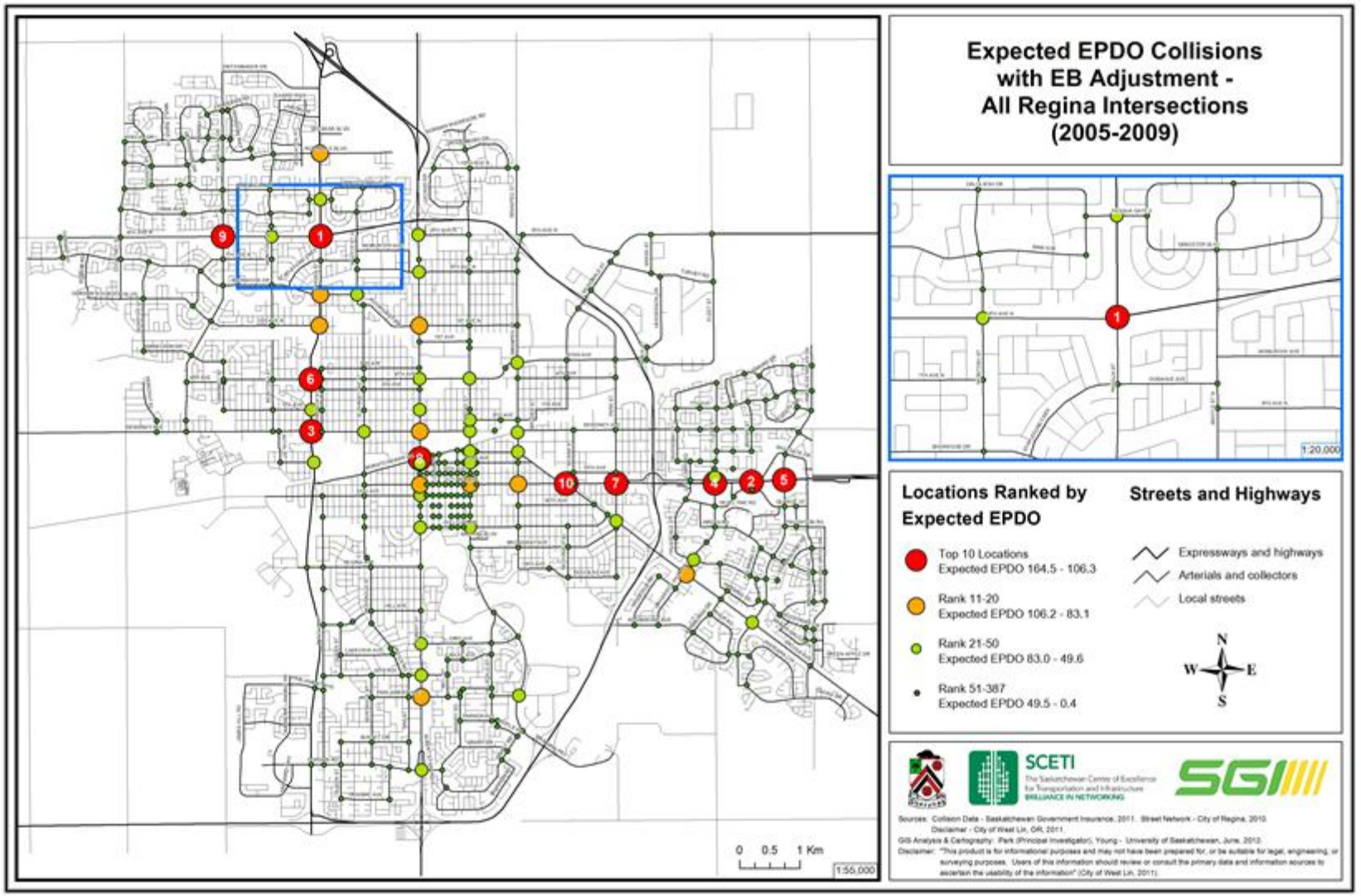

Figure 39: Expected EPDO Collisions at All Regina Intersections.

4.6. Major Arterial Road Segments

There were 435 locations available for analysis in the major arterial roadway classification. The top ten locations from the network screening results are listed in Table 38. Six locations appear in both lists, and the top five locations are the same for both ranking methods.

Table 38: Major Arterial Road Segment Network Screening Results.

Street Name	UGRID	EPDO		EPDO Rank	
		Excess	Expected	Excess	Expected
Albert St	RE3400	21.7	34.8	**1**	**1**
9th Ave N	RE900015	13.9	30.0	**2**	**2**
Albert St	RE7500	11.0	22.2	**3**	**4**
Broad St	RE38700	10.4	24.9	**4**	**3**
Albert St	RE3100	10.1	16.8	**5**	**5**
Saskatchewan Dr	RE350300	8.6	13.6	**6**	**7**
Albert St	RE3200	5.5	10.6	**7**	18
Albert St	RE5000	4.6	11.6	**8**	13
Albert St	RE6600	4.6	10.5	**9**	19
Avonhurst Dr	RE28000	4.1	7.9	**10**	36
Albert St	RE5800	3.9	13.2	14	**8**
Albert St	RE6800	-0.4	12.2	283	**10**
Pasqua St	RE298500	-8.6	13.8	434	**6**
9th Ave N	RE900014	-12.0	12.8	435	**9**

The results from both network screening methods are shown on the following pages.

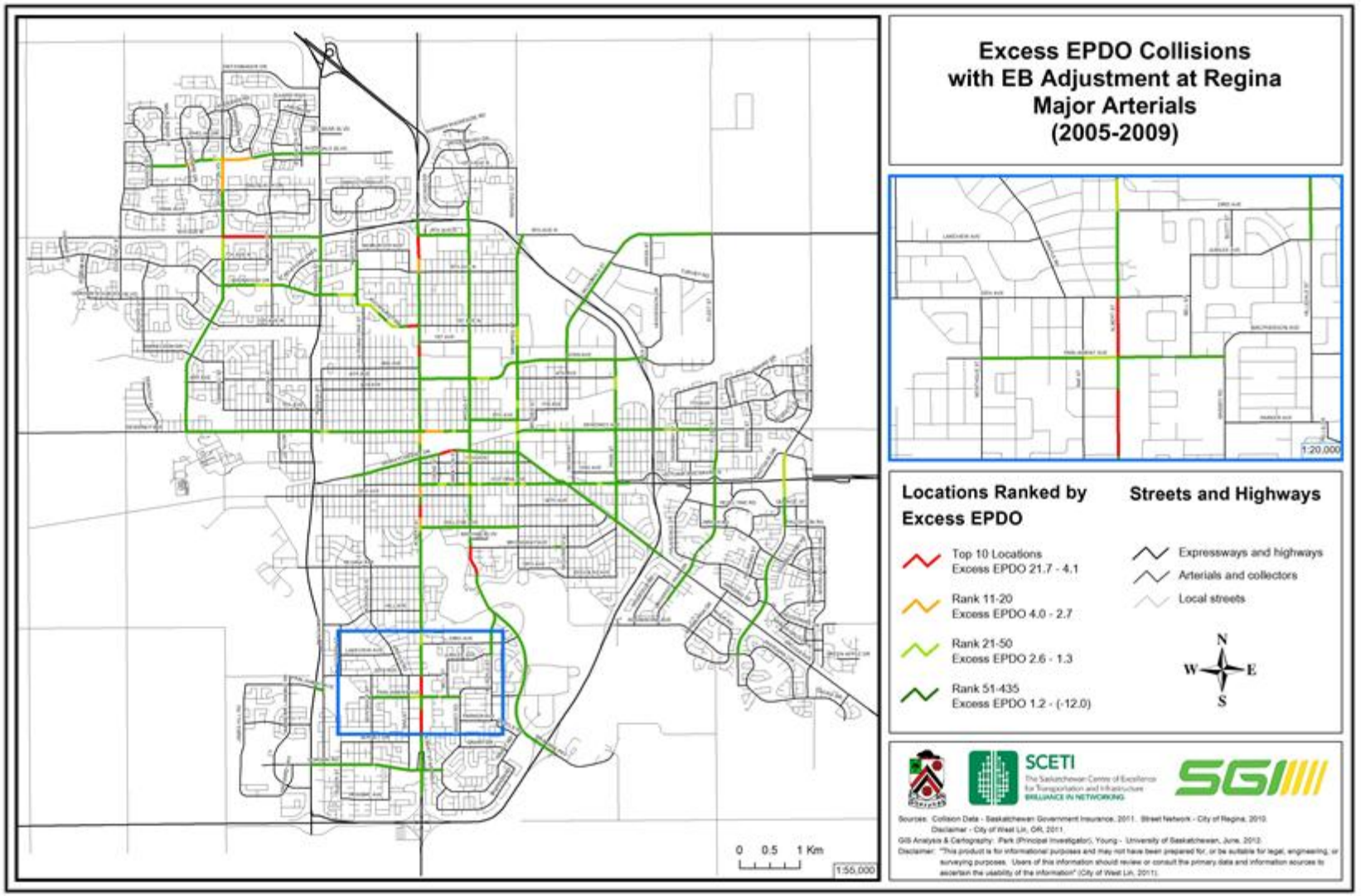

Figure 40: Excess EPDO Collisions at Major Arterial Road Segments.

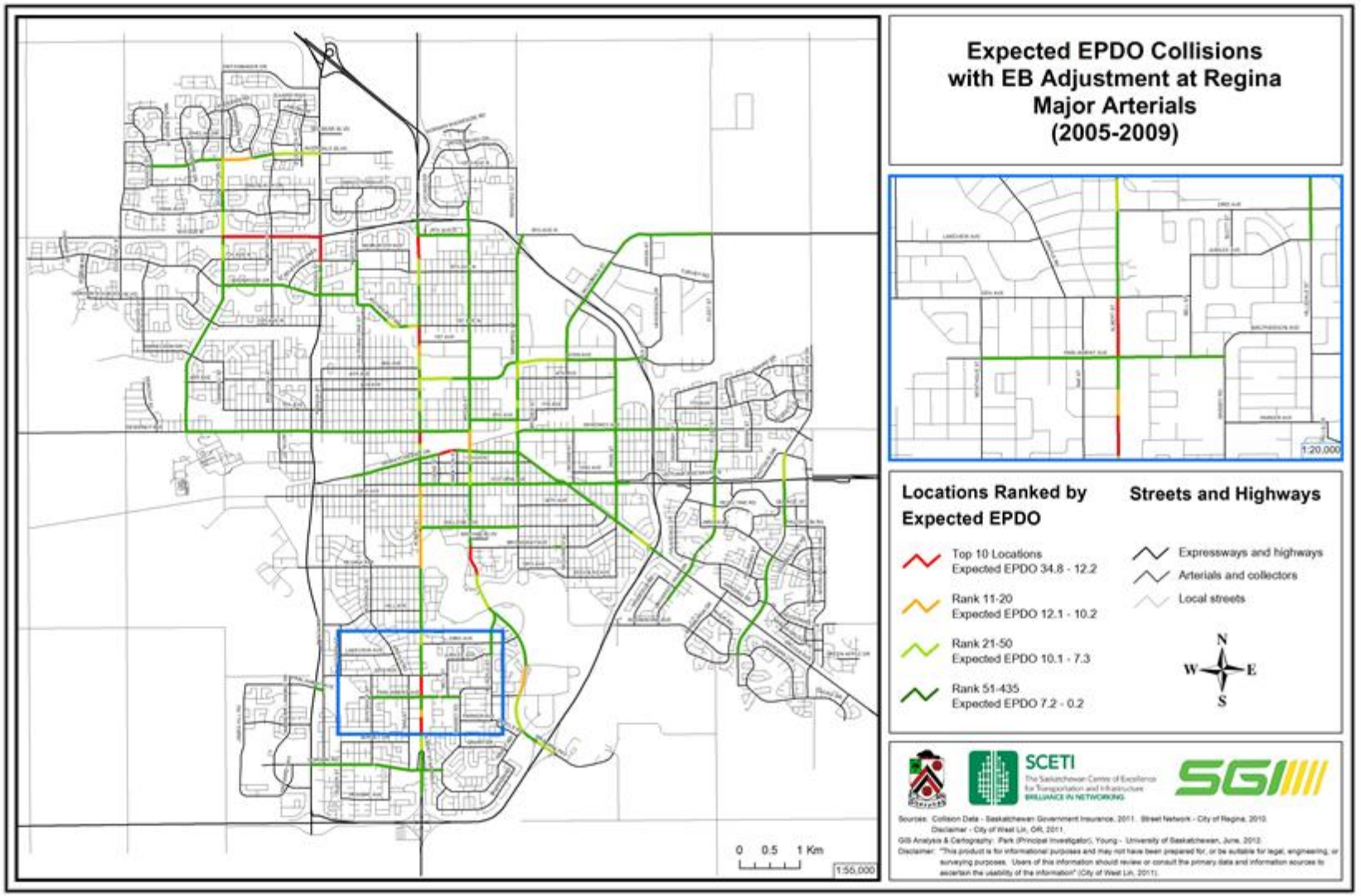

Figure 41: Expected EPDO Collisions at Major Arterial Road Segments.

4.7. Minor Arterial Road Segments

Table 39 lists the network screening results for minor arterial road segments. Of the 234 locations, four locations appear in both lists of the top ten riskiest locations. Note that two road segments: 1) RE458350 (Winnipeg Street) and 2) RE151550 (Fleet Street) have both been identified within the top ten locations when using the expected EPDO method. However, the negative excess EPDO scores suggest that these road segments are actually performing better than expected in terms of excess EPDO score.

Table 39: Minor Arterial Road Segment Network Screening Results.

Street Name	UGRID	EPDO		EPDO Rank	
		Excess	Expected	Excess	Expected
Park St	RE292000	5.0	10.5	**1**	**2**
Elphinstone St	RE125700	2.4	4.8	**2**	**7**
23rd Ave	RE434000	2.3	4.5	**3**	**8**
College Ave	RE67800	1.9	2.9	**4**	19
Montague St	RE243200	1.9	3.1	**5**	14
Winnipeg St	RE456700	1.7	3.2	**6**	13
1st Ave N	RE147900	1.6	2.6	**7**	22
1st Ave N	RE149000	1.6	3.3	**8**	12
4th Ave	RE163800	1.3	2.5	**9**	23
9th Ave N	RE279925	1.2	3.6	**10**	**10**
9th Ave N	RE279910	1.0	13.8	13	**1**
Fleet St	RE151400	0.9	4.2	16	**9**
6th Ave N	RE392300	0.7	4.9	23	**6**
Fleet St	RE151800	0.2	5.3	49	**5**
Winnipeg St	RE458350	-0.7	6.1	214	**4**
Fleet St	RE151550	-3.0	8.4	234	**3**

The results from both network screening methods are shown on the following pages.

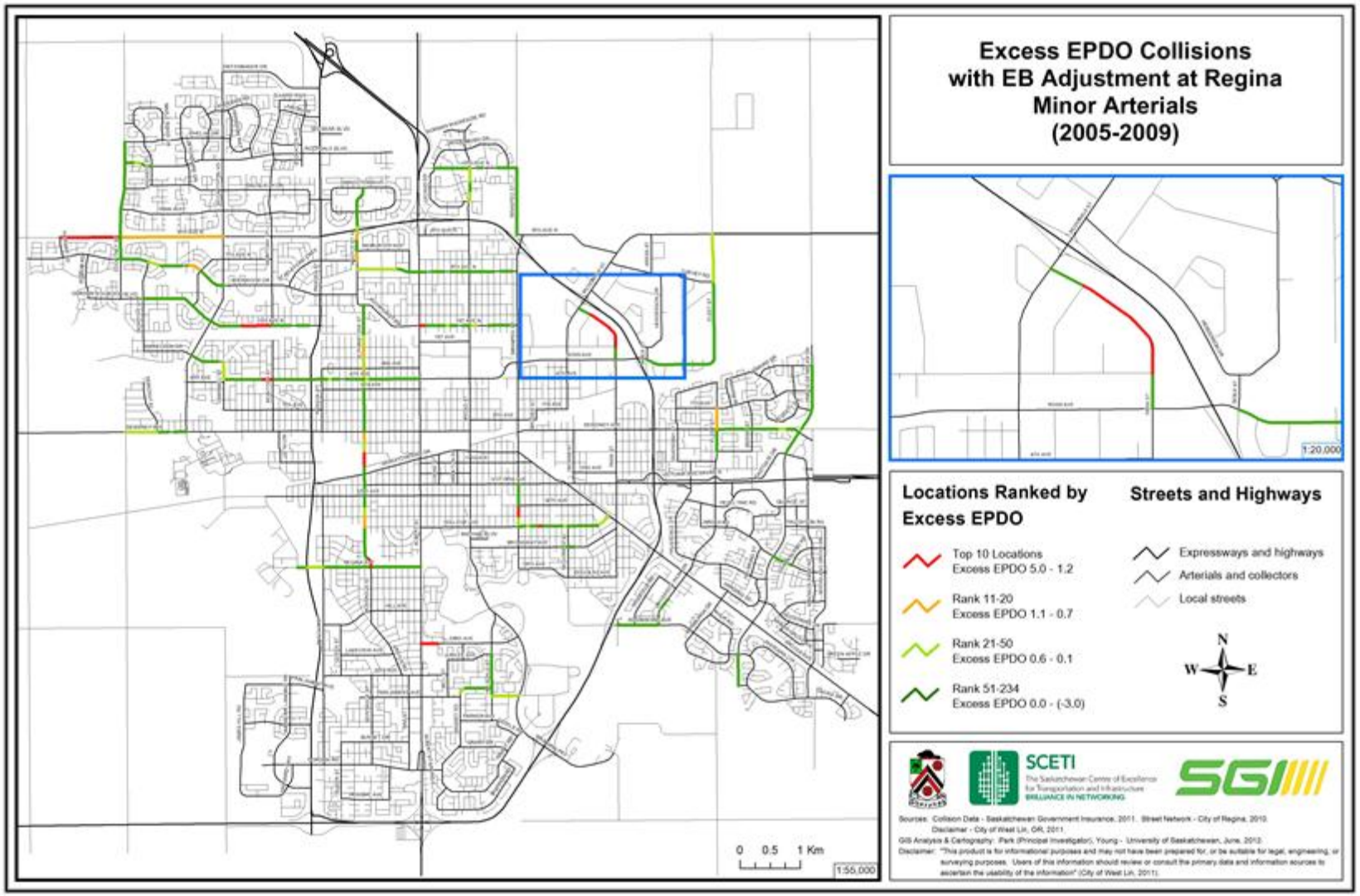

Figure 42: Excess EPDO Collisions at Minor Arterial Road Segments.

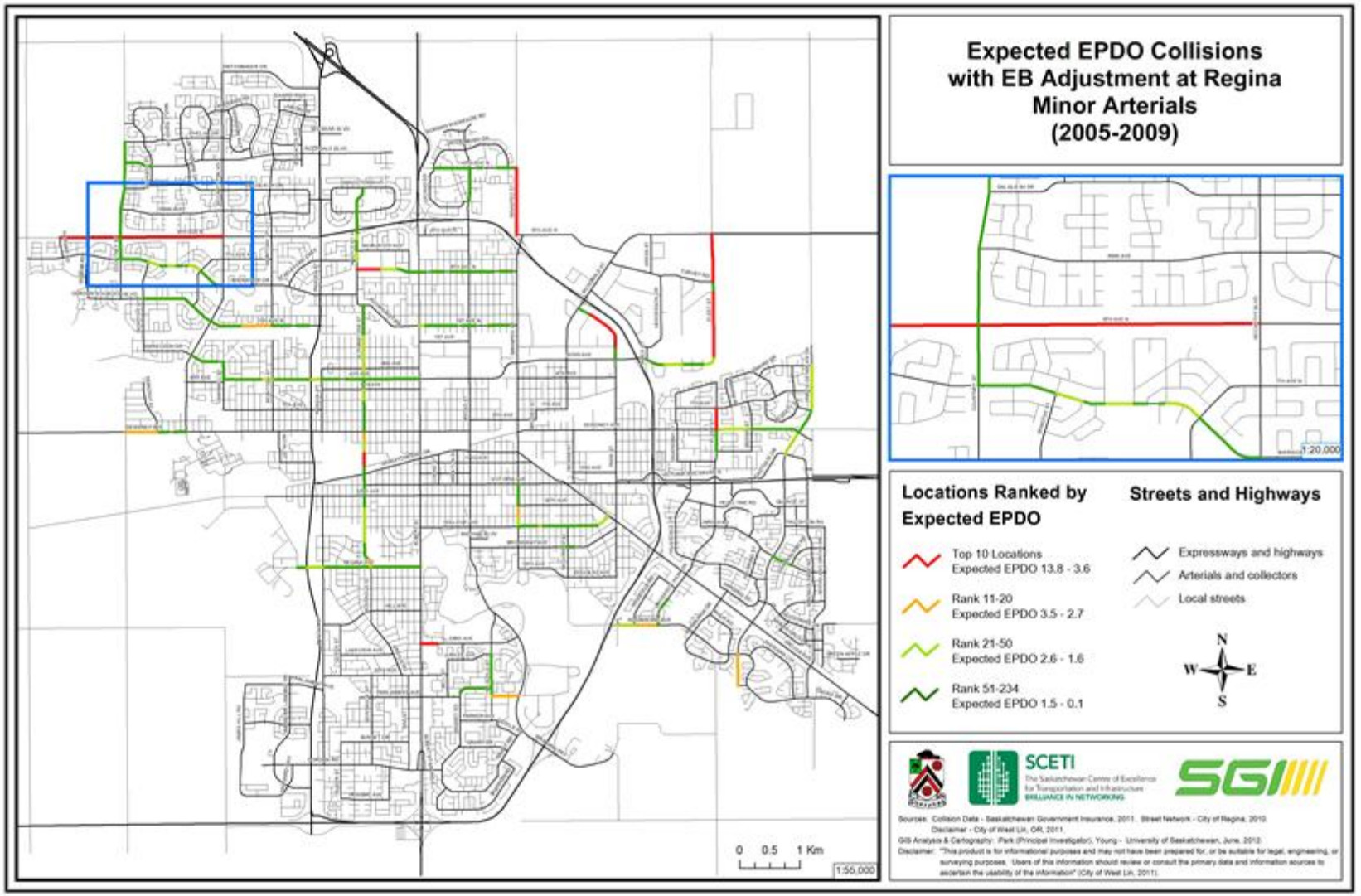

Figure 43: Expected EPDO Collisions at Minor Arterial Road Segments.

4.8. Collector Road Segments

The network screening results for the collector road segments are presented in Table 40. Of the 968 segments available for analysis, four locations appear near the top of both ranking lists; three of these locations represent road segments on Quance Street. Note that four road segments: 1) RE900044 (Victoria Avenue Service Road North), 2) RE196532 (Henderson Drive), 3) RE900045 (Victoria Avenue Service Road North), and 4) RE278975 (9th Avenue North) have been identified within the top ten locations when using the expected EPDO method. However, the negative excess EPDO scores suggest that these road segments are actually performing better than expected in terms of excess EPDO score.

Table 40: Collector Road Segment Network Screening Results.

Street Name	UGRID	EPDO		EPDO Rank	
		Excess	Expected	Excess	Expected
Quance St	RE308275	16.7	22.5	**1**	**1**
Quance St	RE308225	8.6	13.8	**2**	**2**
Quance St	RE308255	4.3	6.4	**3**	**6**
Quance St	RE308230	3.9	4.9	**4**	15
Massey Rd	RE233400	3.8	5.4	**5**	11
Hamilton St	RE190400	3.5	4.6	**6**	16
Hamilton St	RE190500	2.8	4.0	**7**	20
Hamilton St	RE190300	2.5	4.1	**8**	18
Broadway Ave	RE44400	2.4	5.9	**9**	**9**
Massey Rd	RE233500	2.2	4.6	**10**	17
Victoria Ave Srv Rd N	RE900043	1.4	12.4	15	**4**
Rae St	RE314700	1.3	6.1	17	**8**
Victoria Ave Srv Rd N	RE900044	-1.4	5.5	951	**10**
Henderson Dr	RE196532	-1.7	6.2	957	**7**
Victoria Ave Srv Rd N	RE900045	-4.7	12.8	967	**3**
9th Ave N	RE278975	-29.5	8.2	968	**5**

The results from both network screening methods are shown on the following pages.

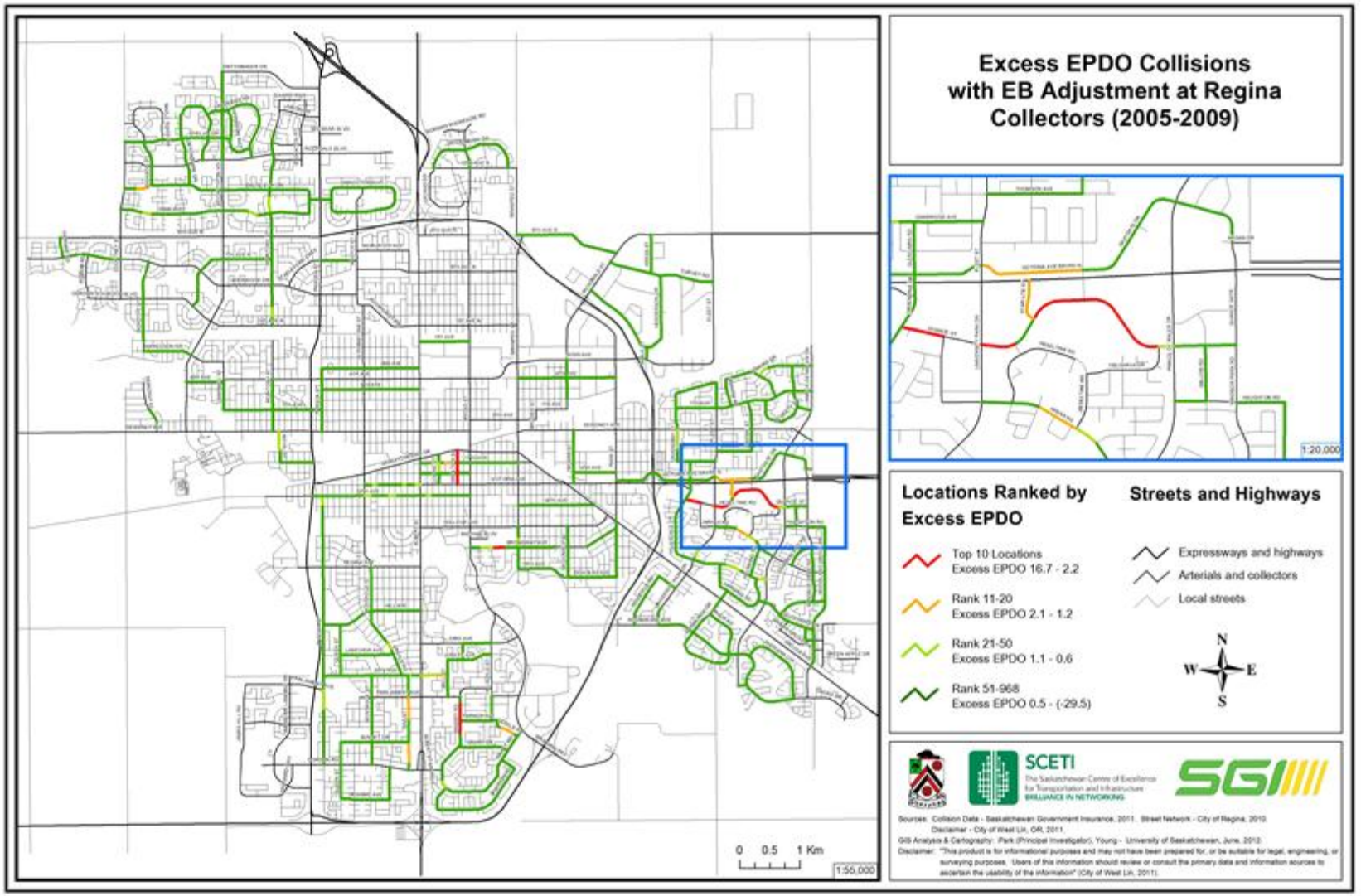

Figure 44: Excess EPDO Collisions at Collector Road Segments.

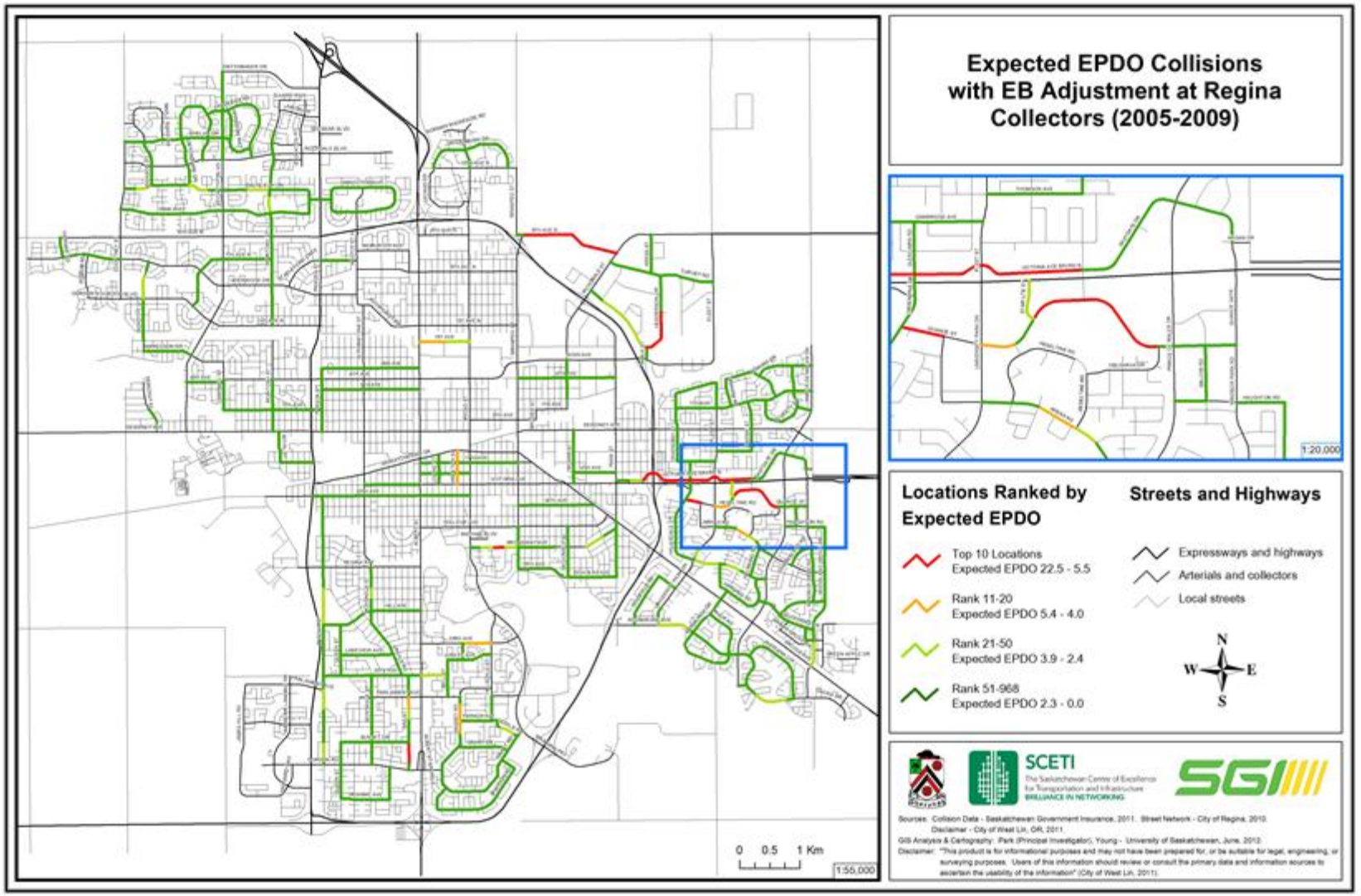

Figure 45: Expected EPDO Collisions at Collector Road Segments.

4.9. All Regina Road Segments

Depending on the City's desired method for selecting the top ranked locations, it may be beneficial to simply identify those locations that are most likely to benefit from a safety improvement, regardless of roadway classification. Table 41 lists the top ranked segments from both network screening methods; it is now possible to identify segments in the City of Regina that are expected to experience the greatest amount of EPDO collisions and show room for further improvements. This analysis included 1,637 road segments. It can be seen that eight out of the top ten road segments are common to both ranking methods.

Table 41: All Regina Road Segments Network Screening Results.

Location	UGRID	EPDO		EPDO Rank		Road
		Excess	Expected	Excess	Expected	Class*
Albert St	RE3400	21.7	34.8	**1**	**1**	MAJ
Quance St	RE308275	16.7	22.5	**2**	**4**	COLL
9th Ave N	RE900015	13.9	30.0	**3**	**2**	MAJ
Albert St	RE7500	11.0	22.2	**4**	**5**	MAJ
Broad St	RE38700	10.4	24.9	**5**	**3**	MAJ
Albert St	RE3100	10.1	16.8	**6**	**6**	MAJ
Quance St	RE308225	8.6	13.8	**7**	**8**	COLL
Saskatchewan Dr	RE350300	8.6	13.6	**8**	**10**	MAJ
Albert St	RE3200	5.5	10.6	**9**	23	MAJ
Park St	RE292000	5.0	10.5	**10**	25	MIN
9th Ave N	RE279910	1.0	13.8	96	**9**	MIN
Pasqua St	RE298500	-8.6	13.8	1635	**7**	MAJ

The results from both network screening methods are shown on the following pages.

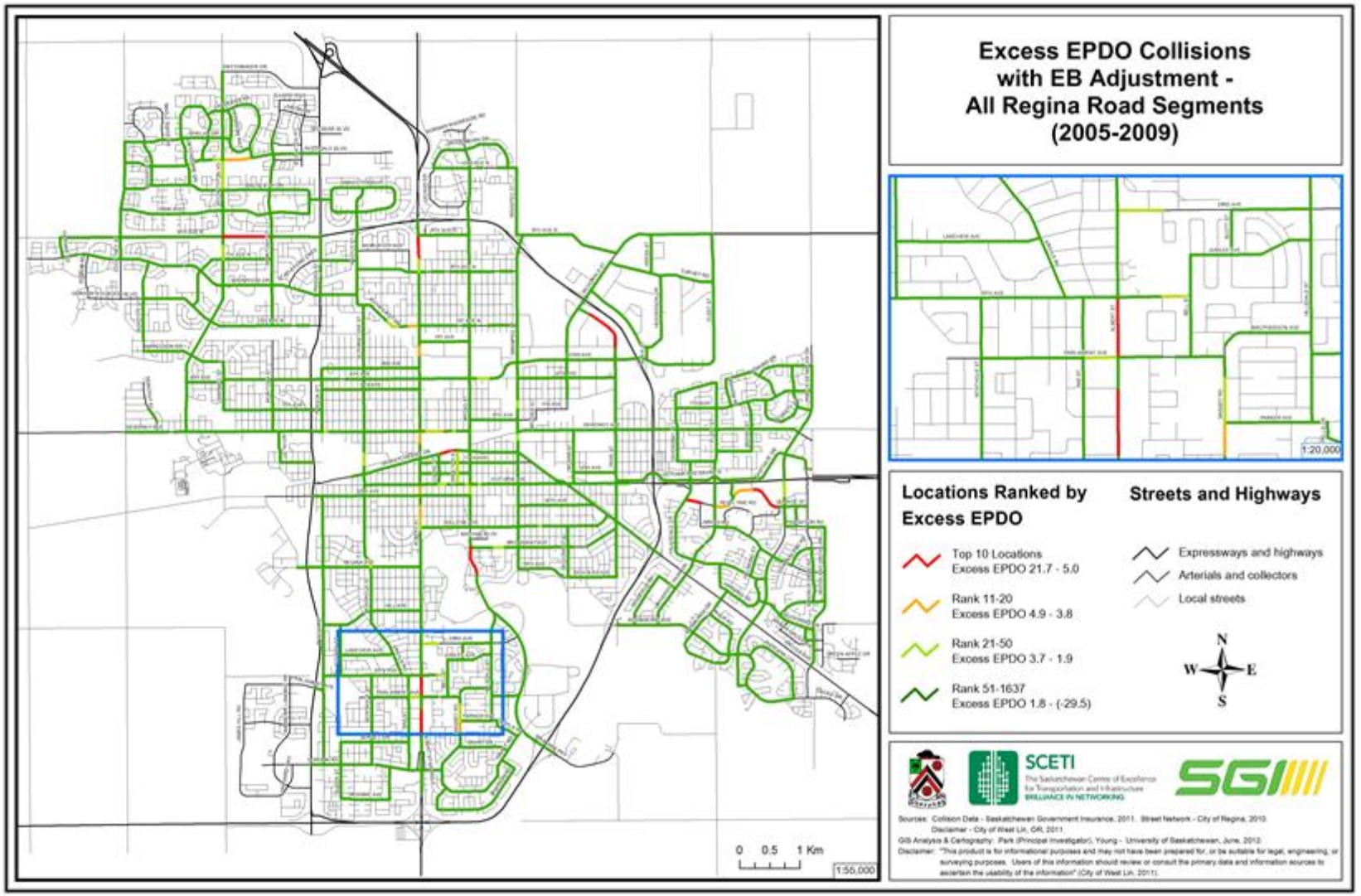

Figure 46: Excess EPDO Collisions at All Regina Road Segments.

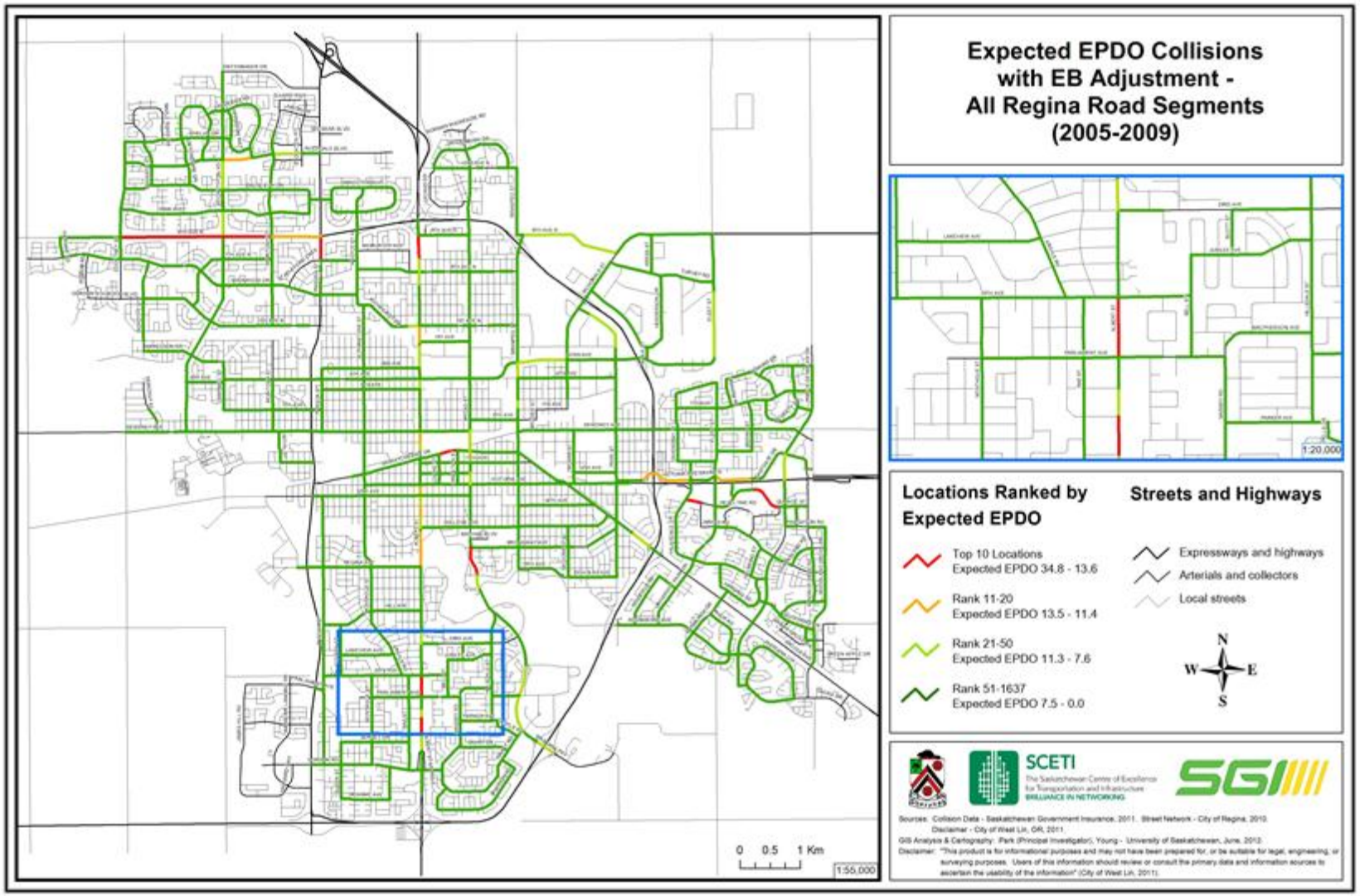

Figure 47: Expected EPDO Collisions at All Regina Road Segments.

4.10. All Regina Road Segments and Intersections

A visual analysis of combined road segment and intersection network screening results may result in the identification of collision-prone corridors with the potential for significant safety improvements. Figure 48 and Figure 49 on the following pages present the network screening results for all road segments and intersections which were investigated in this study, for both network screening methods.

As Figure 48 shows, the intersection of 9th Avenue North & McCarthy Boulevard (RE688050), and one of the adjacent segments (RE900015) were both ranked highly using the Excess EPDO performance measure (number one and number three, respectively). This site represents a location where safety improvements (e.g., advanced warning beacons, additional lanes) may have a positive effect on both the road segments and nearby intersection. A detailed collision diagnosis would be required in order to effectively recommend a suitable treatment.

Also on Figure 48, it can be seen that the intersection of Albert Street and Parliament Avenue (RE689000) and adjacent sections of Albert Street between 25th Avenue and 31st Avenue are both ranked relatively highly, and could benefit from related safety improvements.

Figure 49, which visually displays the highest-ranked expected EPDO road segments and locations, shows that a number of nearby road segments (RE900014, RE900015, and RE279910) and intersections (RE688050 and RE717710) were ranked highly using this network screening measure. These locations represent a corridor close to the Ring Road expressway which may benefit from safety improvements related to speed adaptation. Speed adaptation, described as the experience of leaving a freeway after a long period of driving and having difficulty adjusting to

reduced speed limits, has been shown to last up to five minutes after leaving a freeway, and to occur even after very short periods of traveling at high speeds (Schmidt & Tiffin, 1969).

Finally, it can be seen from Figure 49 that five intersections along Victoria Drive (RE689720, RE696740, RE700150, RE706920, and RE707580) were identified within the top ten ranked intersections using the Expected EPDO ranking measure. By investigating the causes of collisions at these locations (and also analyzing the nearby segments), it may be possible to reduce collisions at several locations by implementing comprehensive safety improvements.

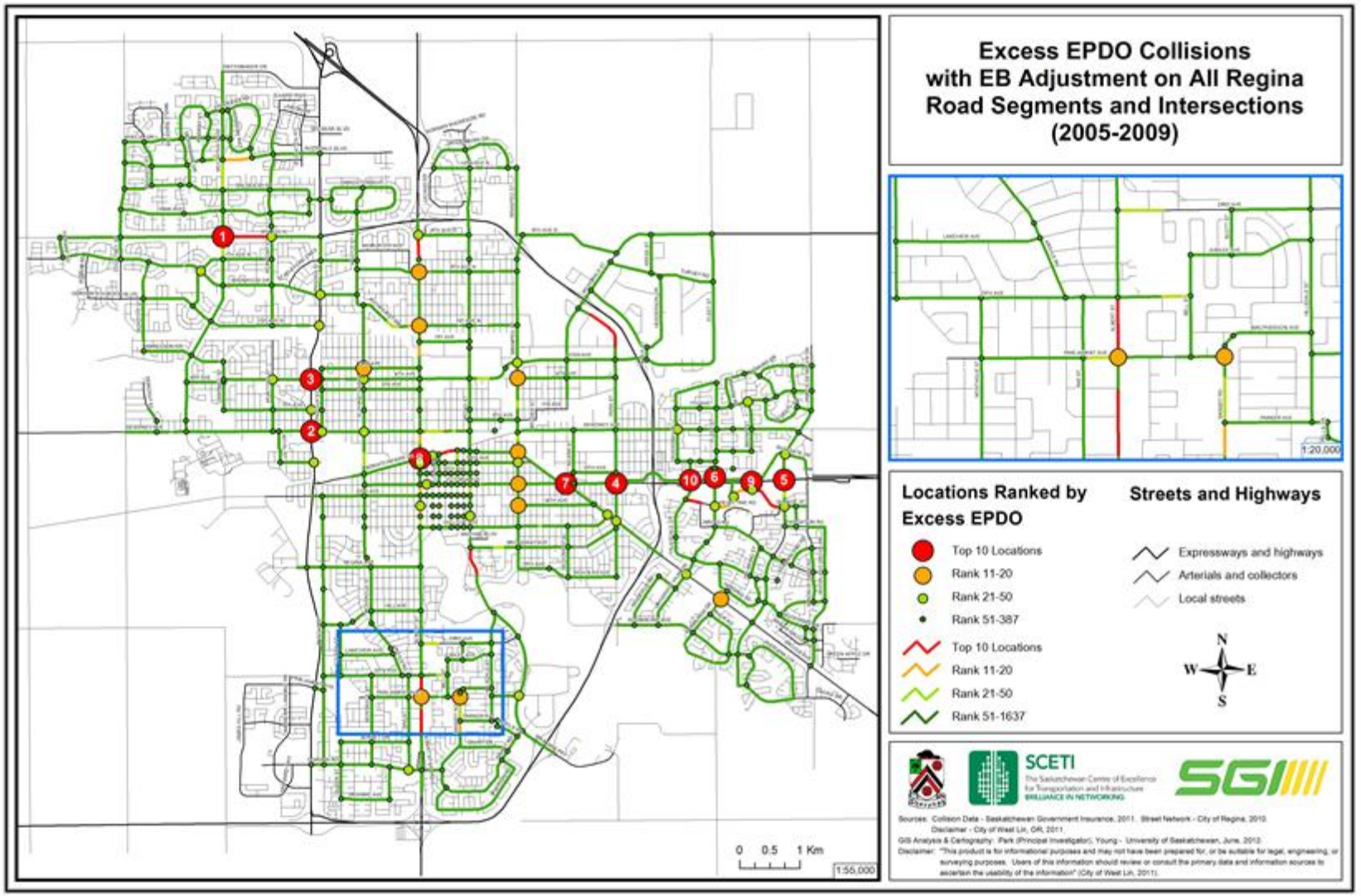

Figure 48: Excess EPDO Collisions at All Regina Road Segments and Intersections.

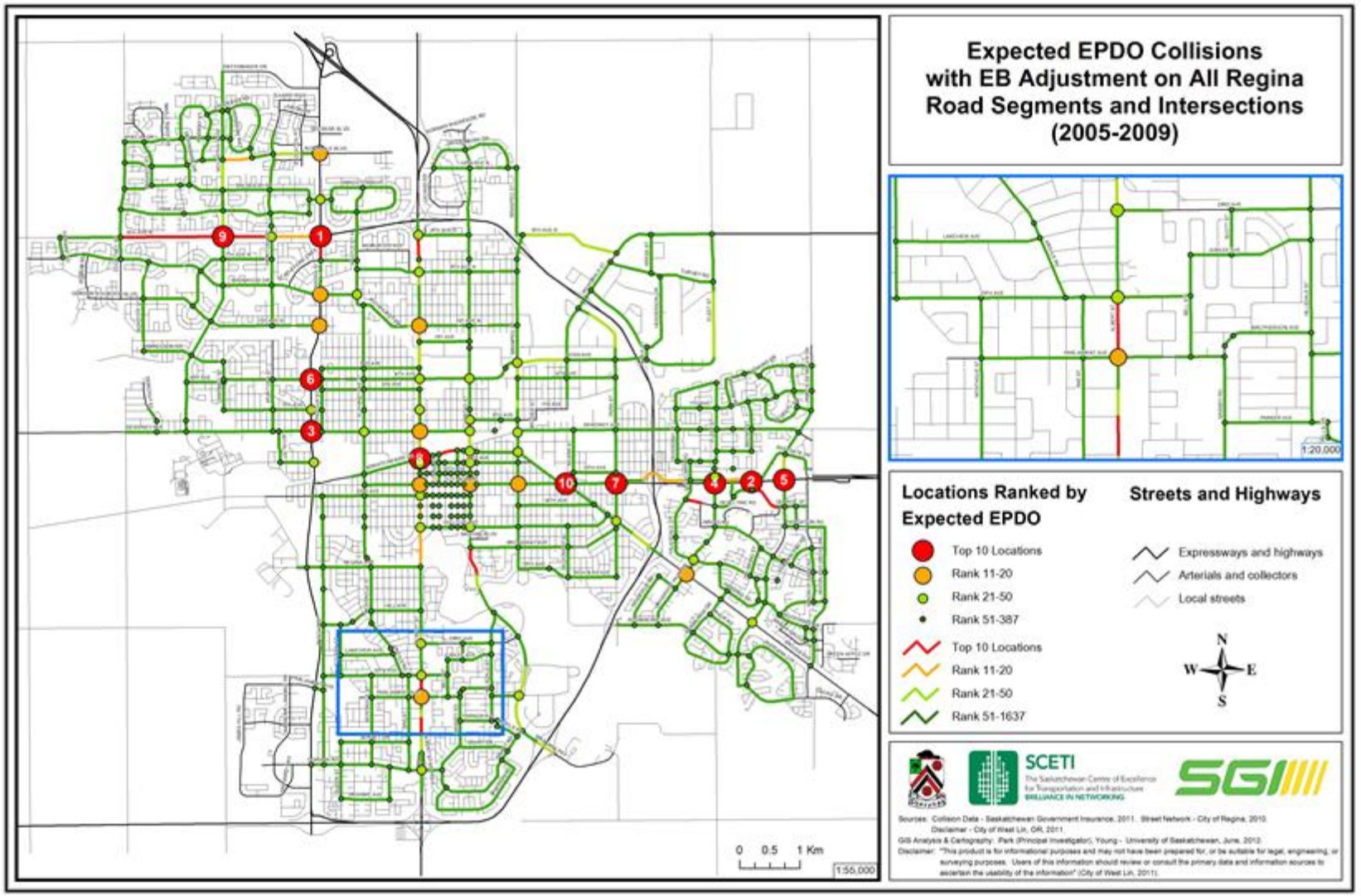

Figure 49: Expected EPDO Collisions at All Regina Road Segments and Intersections.

4.11. Chapter Summary

This chapter presented the results of the network screening that was performed on the City of Regina's intersections (three and four-leg signalized, three leg unsignalized, and four leg unsignalized), as well as road segments (major arterials, minor arterials, and collectors). Two ranking measures were used in this study: excess EPDO collisions, and expected EPDO collisions. The top ten locations for each ranking measure were presented in tabular format; GIS maps of the top-ranked locations were also provided.

CHAPTER 5. POST-NETWORK SCREENING ANALYSIS

5.1. Network-Constrained KDE

Network-constrained KDE was used to examine the spatial association of collisions on Regina's roadway network. The output of this analysis (a collision density map) shows peak density road segments, such as a group of neighboring hotspots, that can be regarded as hotzones that have potential for systemic safety improvements.

The software package used was Spatial Analysis along Networks (SANET), an ArcGIS-based network-constrained KDE tool. SANET's kernel function is presented in Equation 17 (Okabe et al., 2009):

$$K_y(x) = \begin{cases} k(x)\ for\ -h \le x \le 2d-h, \\ k(x) - \frac{n-2}{n} k(2d-x)\ for\ 2d-h \le x \le d, \\ \frac{2}{n} k(x)\ for\ d \le x \le h. \end{cases} \quad \text{[Equation 17]}$$

Where:

k(x) = the base kernel function;

y = the kernel center;

x = a point located on the network;

h = the bandwidth (m);

n = the degree of the node; and

d = the shortest path distance from *y* to *x* (m).

Figure 50 provides a simplified graphical illustration of Equation 17. In the illustration, node *v* has three links. As the figure shows, the kernel function is split at node v, and the function is split evenly between the three links.

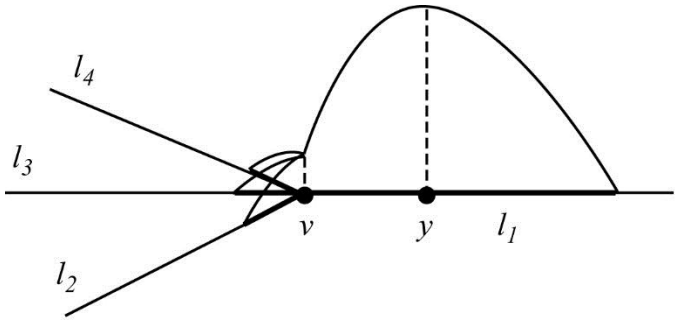

Figure 50: Simplified Example of Network Kernel Function.

Figure 51 provides a visual example of the three distinct ranges described in Equation 17. Only one of the three links of Figure 50 is shown.

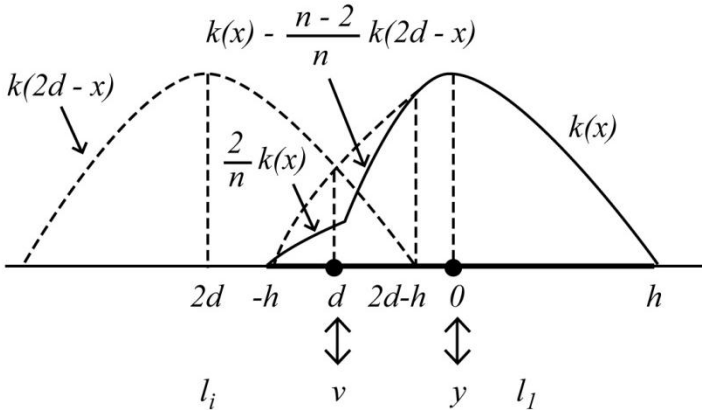

Figure 51: The Three Ranges of the Network Kernel Function.

5.2. Bandwidth Selection

The user's selection of bandwidth has a major impact on network-constrained KDE results. If the bandwidth is too small, the contour map will merely highlight individual hotspots separately instead of revealing any spatial association amongst neighboring hotspots. On the other hand, too large a bandwidth may result in a lack of differentiation between areas of interest (i.e., hotzones in our case) since many hotspots will simply be grouped together and presented by only a few

hotzones that could include too many hotspots. In either case, the results will not offer useful information for decision makers (O'Sullivan & Unwin, 2003).

Unfortunately, there is very little research on the selection of optimal bandwidth. Studies in recent years have primarily relied on an iterative approach to selecting the bandwidth. The approach used by Anderson (2009) and Plug et al. (2011), for example, has practical appeal. They suggested a trial and error technique (a kind of sensitivity analysis) to meet the purpose and unique characteristics of their respective studies. This investigation followed their suggestion and tested a range of bandwidths (100m to 1,000m). Figure 52 shows some of the results of the sensitivity analysis, using collisions on major arterials as the reference collision dataset.

(a) 100m (b) 200m

(c) 400m (d) 600m

(e) 800m (f) 1,000m

Figure 52: Sensitivity Analysis of Bandwidths for Network-Constrained KDE Analysis.

As expected, small bandwidths (e.g., 100m) resulted in a collision contour map that simply focuses on the collision densities in the immediate area. The results isolate individual hotspots (the red areas) and sometimes select high-collision areas that are only one roadway segment. This bandwidth clearly does not take advantage of the network-constrained KDE approach. Large bandwidths (e.g., 1,000m) resulted in a collision contour map that included collision densities over a wide area. The results select entire corridors as hotzones, making it difficult to identify the true areas of safety concern. These results suggested that a bandwidth of 400m was optimal for this study. In order to stay consistent, this bandwidth was used in the analyses of all road categories (i.e., major arterials, minor arterials, and collectors).

5.3. Post-Network Screening Analysis

In order to compare the performance of the proposed post-network screening analysis using network-constrained KDE, several analyses were carried out for each of the road network categories: observed collision count, observed EPDO, expected EPDO, and a hotzone selection technique that uses standard deviations of the expected number of collisions. These methods are discussed in the following paragraphs; the two main reasons for discussing these measures are: 1) this study uses the output of existing network screenings as an input to the post-network screening analysis; and 2) this study applies network screening methods (not a GIS technique) to take collision severity and RTM bias issues into account.

The observed collision count simply uses the total number of collisions as the network-constrained KDE input. Fatal collisions, injury collisions, and PDO collisions are weighted equally; therefore, severity is not taken into account. This analysis is similar to the technique used in recent KDE studies (Erdogan et al., 2011; Plug et al., 2011), as it used only observed collision counts and did not include severity-weighted collision information.

The next method that was used, referred to here as the observed EPDO (and in the HSM as the "Equivalent Property Damage Only (EPDO) Average Crash Frequency"), allocates a weight based on collision severity to each observed collision at the location, and then combines all the observed weighted collisions to produce a single EPDO score for each location. The societal costs of collisions are often used to generate the different weights for each severity level. Societal cost estimates take into account the costs of medical care, emergency services, property damage, and so on. Various studies have estimated the monetary value of the societal cost of each collision severity (Vodden et al., 2007; Truong and Somenahalli, 2011). Our study used the monetary values currently reported in the HSM and originally estimated by Council et al. (2005). As a result, this method gives a much higher weighting to fatal (541.7) and injury (11.2) collisions than to PDO collisions (1.0), as shown in Table 42.

Table 42: Societal Collision Cost Estimates by Severity (2001 Dollar Values).

Collision Severity	Comprehensive Societal Collision Cost	EPDO Score
Fatal	$4,008,900	541.7
Injury	$82,600	11.2
PDO	$7,400	1.0

The observed EPDO exercise was repeated for the each of the roadway segments included in this study. The segments were then ranked from the riskiest to the least risky by the magnitude of the observed EPDO scores.

The expected EPDO measure, described in the "Network Screening" chapter, also uses societal costs related to collision severity. The major difference is that the expected EPDO measure uses the long term average (expected) number of collisions whereas the observed EPDO measure simply uses the observed number of collisions that occurred in a short term or pre-set

time period. RTM bias can be reduced by using the expected number of collisions rather than the observed number. The current state-of-the-industry method for estimating the expected number of collisions applies a generalized regression model coupled with the empirical Bayes (EB) technique (Harwood et al., 2010; Hauer et al., 2002; Hauer et al., 2004). This method used the SPFs that were developed for each road segment category; individual locations were then ranked from the riskiest (those with the highest expected EPDO score) to the least risky locations.

The final analysis undertaken for each road segment category was the identification of hotzones. The input for this step was the outcome of the HSM network screening procedure described earlier. In order to identify spatially-related hotzones within the roadway network, specific point locations with high EPDO collision densities must first be identified. Any number of high EPDO collision density points could be selected, but this study focused on the top five points. With the high EPDO collision density points identified, it is then possible to define the extent of each hotzone. This study selected a threshold value for the selection process using a procedure similar to the one suggested by Larsen (2010). Roadway segments adjacent to the highest EPDO collision density points were selected if their EPDO collision density values were greater than two standard deviations from the mean.

The following sections present the results of these analyses on the following road segment categories for the City of Regina: major arterials, minor arterials, and collectors.

5.4. Major Arterial Post-Network Screening

Though the City of Regina contains 456 major arterial roadway segments, traffic volumes and collision information were only available for 435 segments. Figure 53 shows the locations of

these segments. As not all of the major arterial roadway segments contained enough data to be included in this study, a few major arterial roadway segments appear to be isolated.

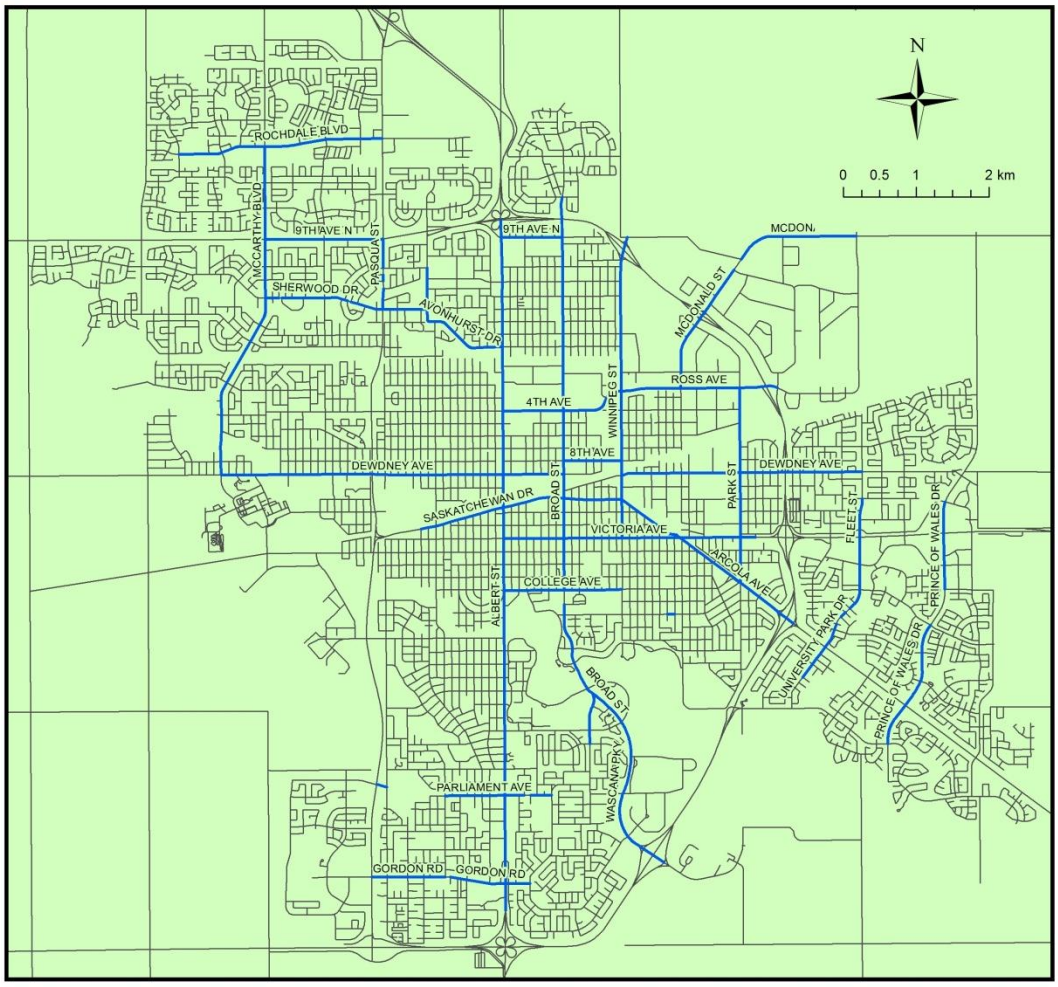

Figure 53: Study Network With 435 Major Arterial Segments.

The first step of the network-constrained KDE analysis used observed collision counts. Figure 54 shows the two collision density maps, one in 2D (the top map) and one in 3D (the bottom map). As the legend for Figure 54 shows, the collision densities were classified into ten groups. The groups were divided using the Natural Breaks (Jenks) classification technique which seeks to minimize each group's average deviation from the group mean while maximizing each group's deviation from the neighboring groups' means (Jenks, 1967). The KDE values at each

point along the study segments represent the collision density using the chosen bandwidth of 400m.

Figure 54 shows that the City of Regina's high-density collision hotzones (shown in red) are primarily located along two major arterial roadways: Albert Street which runs north/south, and Victoria Avenue which runs east/west. The highest EPDO collision densities are located near the south end of Albert Street (on the left edge of the 3D collision density map) where the peak approaches 18 EPDO collisions.

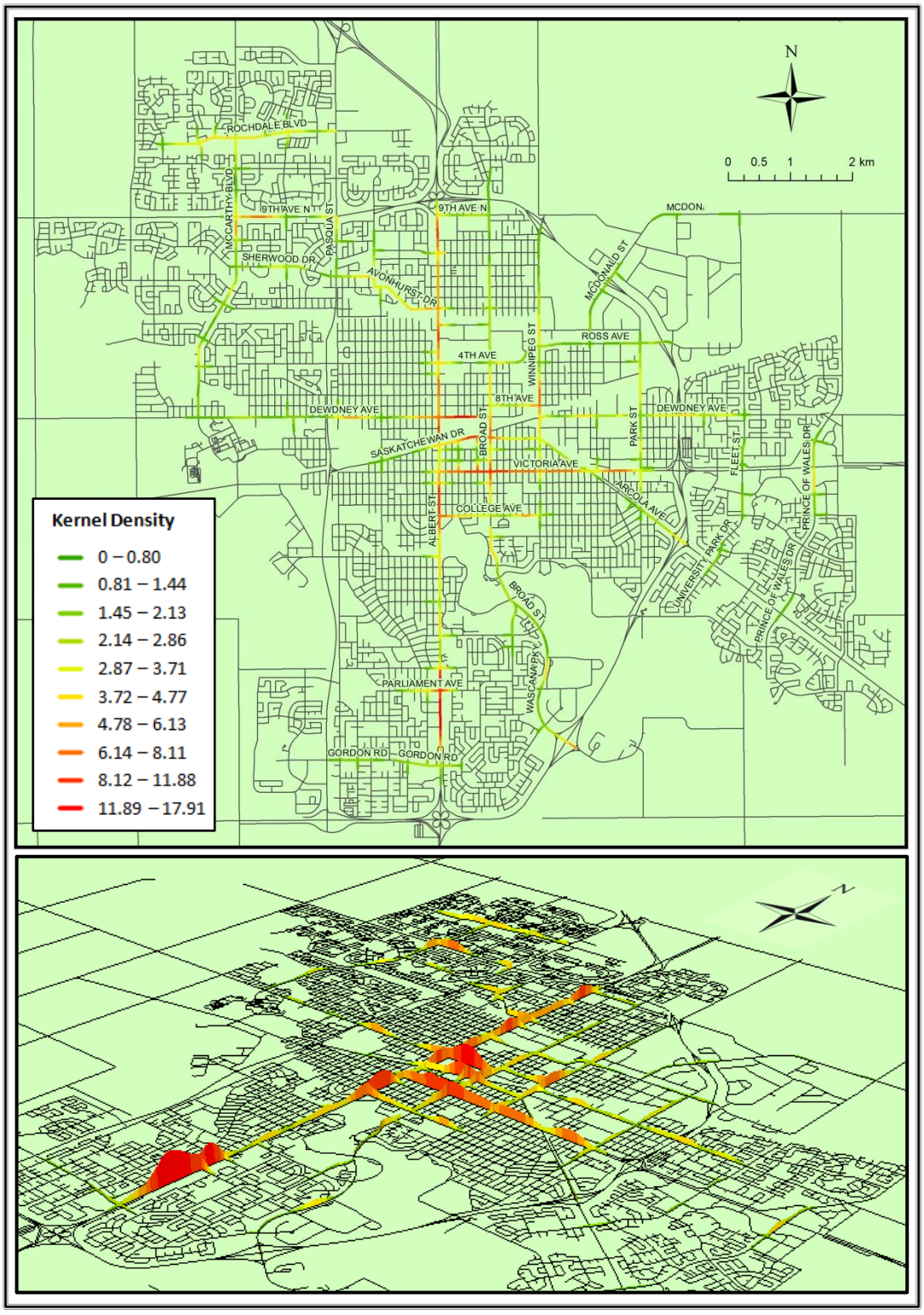

Figure 54: Network-Constrained KDE Results for Major Arterials Based on Observed Collision Counts (400m Bandwidth).

The second step of the network-constrained KDE analysis used severity-weighted collisions (i.e., the observed EPDO) instead of the simple collision counts discussed in the previous section. Figure 55 shows the two collision density maps.

Most high-density collision hotzones (shown in red) were located along Albert Street and Victoria Avenue (as in the observed collisions analysis), but there is a significant peak on McCarthy Boulevard on the city's west side. This peak is due to a fatal collision at that location (the only fatal collision that occurred on major arterials during the study period). As one fatal collision is equivalent to 541.7 PDO collisions, a single fatal collision affects the analysis dramatically.

The Albert Street corridor shows that the use of severity-weighted (observed EPDO) counts rather than simple observed collision counts clearly affects the identification of hotzones in the KDE analysis. The severity-weighted (observed EPDO) counts identified the same six hotzones as the observed collision counts (Figure 54), but the magnitude of each peak identified by the severity-weighted (observed EPDO) counts is increased due to the scaling-up effect of applying EPDO scores to fatal and injury collisions. For example, the peak area of Albert Street had an approximate collision density of 18 using the unweighted observed collision counts compared with a peak value of approximately 35 EPDO collisions, nearly double the unweighted value, when EPDO scores are applied.

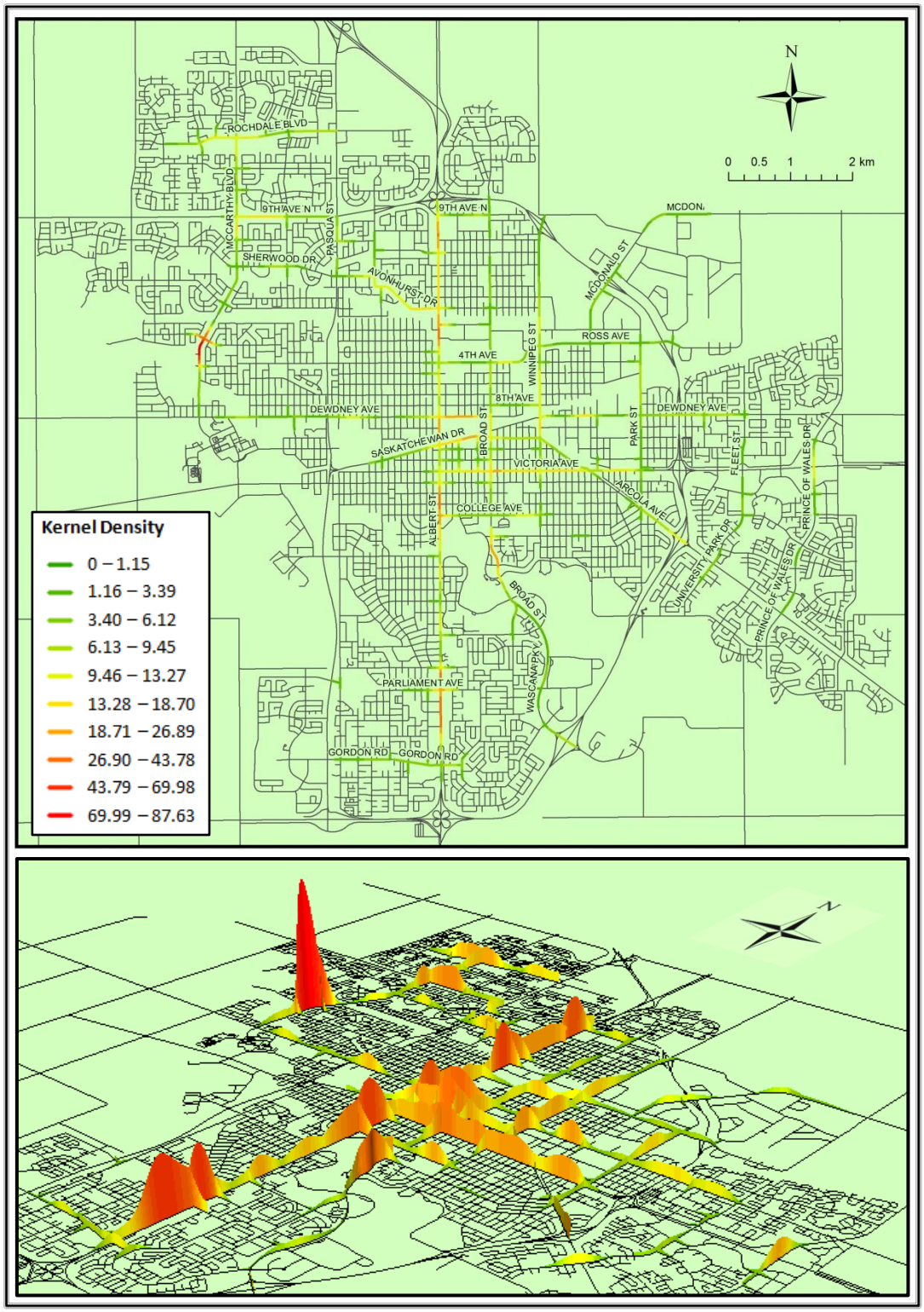

Figure 55: Network-Constrained KDE Results for Major Arterials Based on Observed EPDO (400m Bandwidth).

Expected EPDO values are products of the network screening process and make use of the long term average (expected) number of collisions. Expected EPDO values were calculated and used to generate a set of network-constrained KDE maps. Figure 56 shows the results.

Figure 56 shows that, in general, the magnitude of the expected EPDO densities was somewhat smaller than the densities obtained from the observed EPDO analysis shown in Figure 55. The expected EPDO densities show no unusually high peaked areas, a marked difference from the observed EPDO results shown in Figure 55, and a clear indication that the EB technique (used to generate the expected EPDO values) reduced the effects of the fatal collision that occurred during the study period. The results shown in Figure 56 indicate that unusual collision patterns, such as a fatal collision or a higher than usual number of injury collisions, do not influence the expected EPDO network screening results as much as they influence the observed EPDO results. This reduction in RTM bias is an important and desirable outcome.

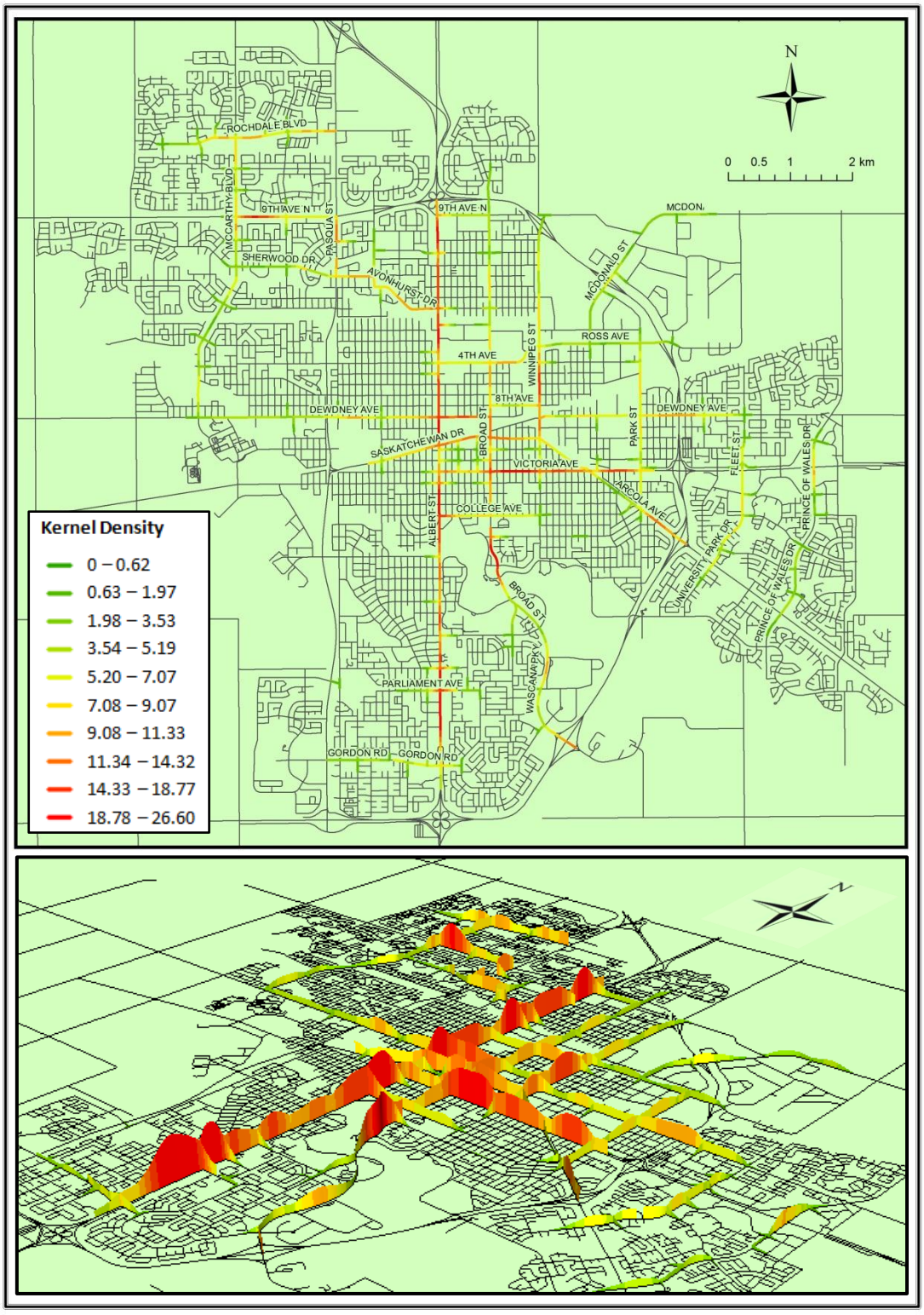

Figure 56: Network-Constrained KDE Results for Major Arterials Based on Expected EPDO (400m Bandwidth).

Corridors of safety concern can be identified using the results obtained in this analysis. For example, since multiple segments along Albert Street contained high EPDO collision densities, this section of roadway could be considered for corridor-level safety improvements. However, road safety decision makers may be interested in identifying specific hotzones (i.e., spatially-related groups of hotspots) within corridors, where targeted safety improvements could be made in order to reduce collisions.

The input for this step is the outcome of the HSM network screening procedure described earlier. Figure 57 shows the top five locations identified using the HSM's approach. The five locations in the figure are individual segments, and each one does not take into consideration the safety levels of neighboring roadway segments.

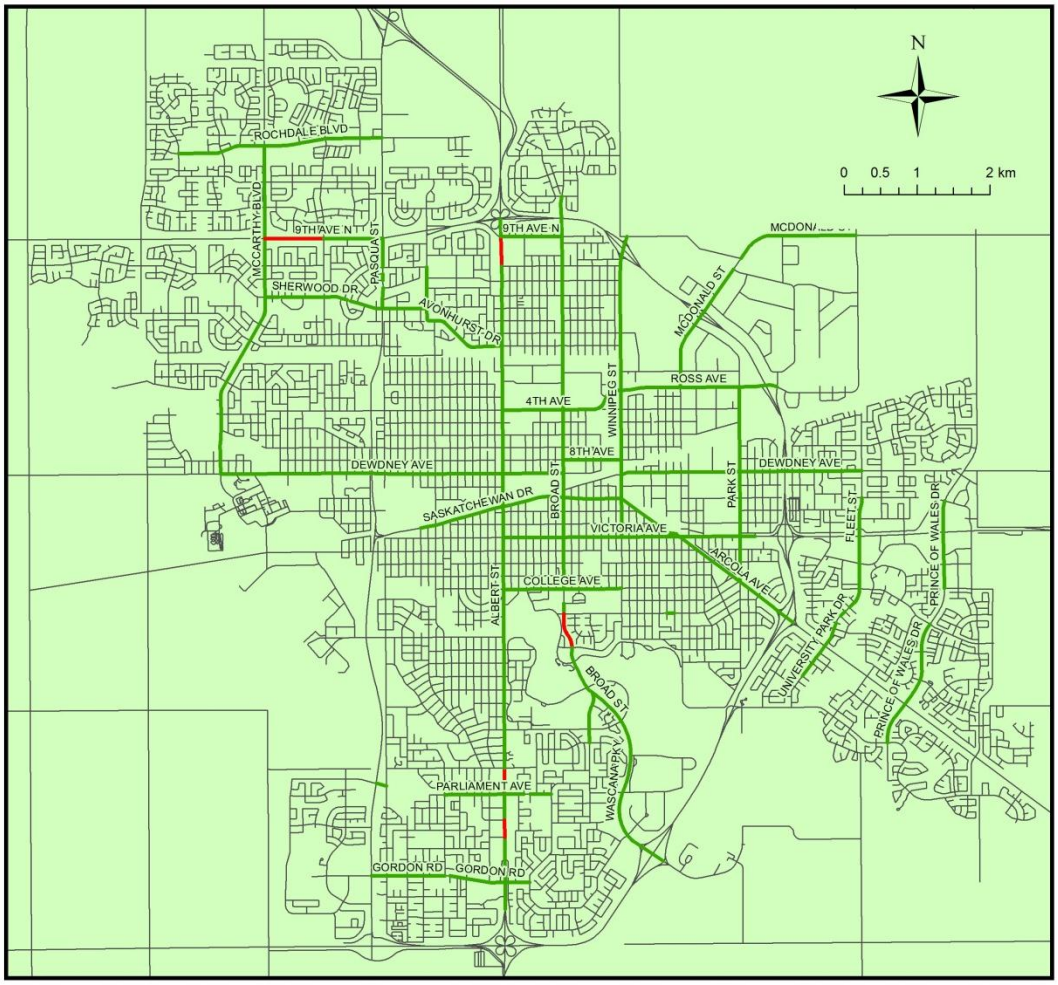

Figure 57: Top Five Riskiest Locations (Shown in Red) Based on HSM Network Screening Using Expected EPDO Results for 435 Major Arterial Segments.

In order to identify spatially-related hotzones within the roadway network, specific point locations with high EPDO collision densities must first be identified. Figure 58 shows two high EPDO collision density points along Albert Street. These points were identified using expected EPDO data and network-constrained KDE. It should be noted that these points are neither complete segments nor hotzones; they are simply the points with high EPDO collision densities. Any number of high EPDO collision density points could be selected, but this study focused on the top five points.

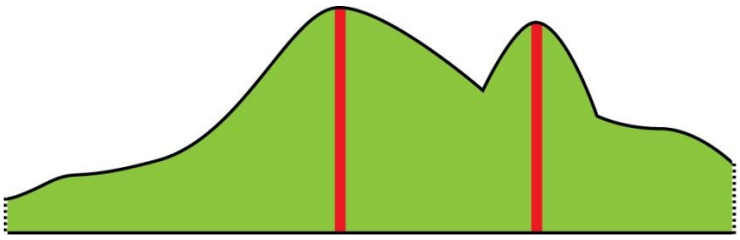

Figure 58: Two Points Showing High EPDO Collision Densities on Albert Street.

Figure 59 shows the top five points on the City of Regina's road network. Four of the points are on Albert Street, and one is on Broad Street.

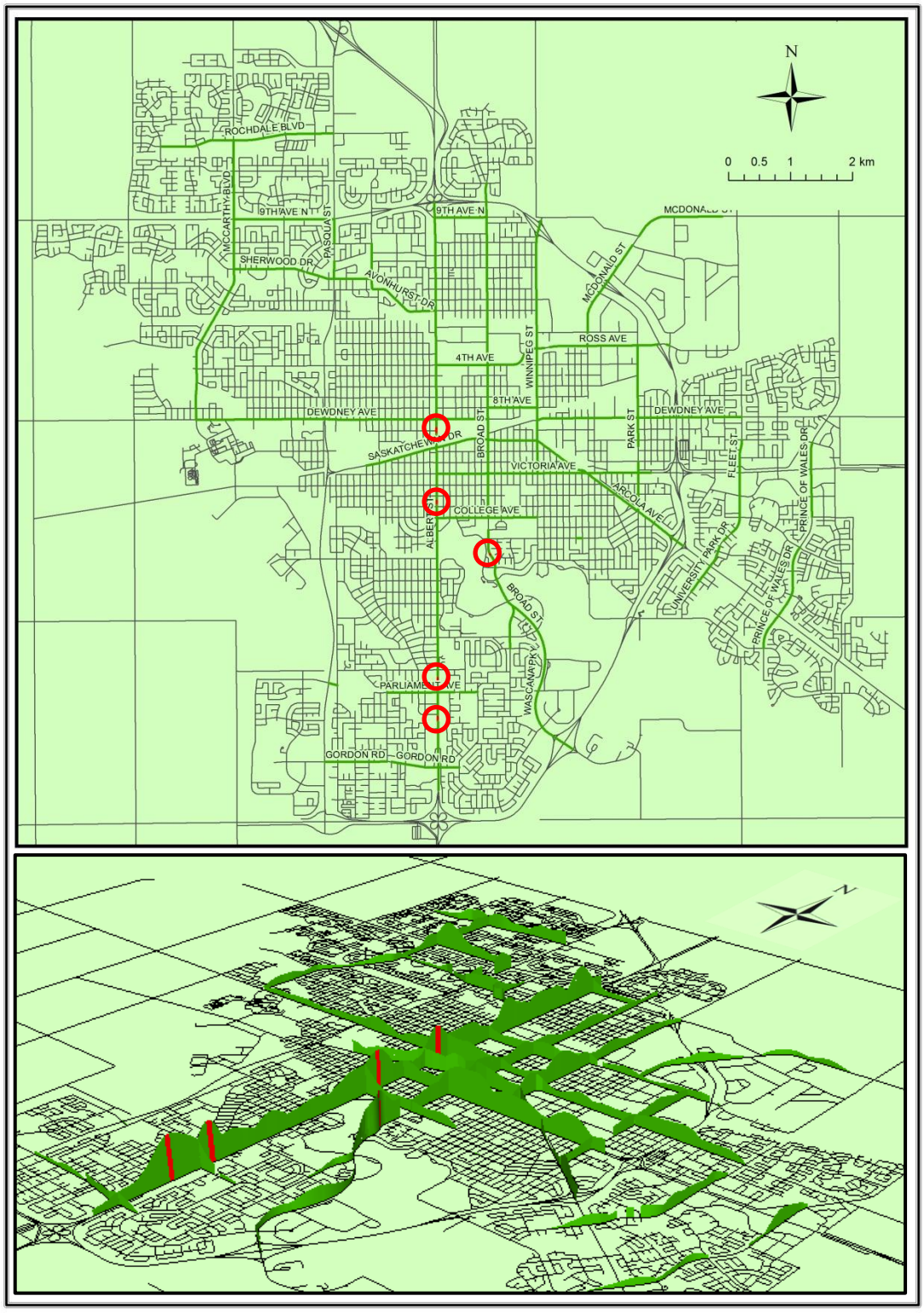

Figure 59: Top Five High EPDO Collision Density Points (Shown in Red) Based on Expected EPDO and Network-Constrained KDE Results for Major Arterials.

With the high EPDO collision density points identified, it is now possible to define the extent of each hotzone. This study selected a threshold value for the selection process using a procedure similar to the one suggested by Larsen (2010). Major arterial roadway segments adjacent to the highest EPDO collision density points were selected if their EPDO collision density values were greater than two standard deviations from the mean. Figure 60 shows the effect of applying a threshold value of two standard deviations to the two high EPDO collision density points shown in Figure 58.

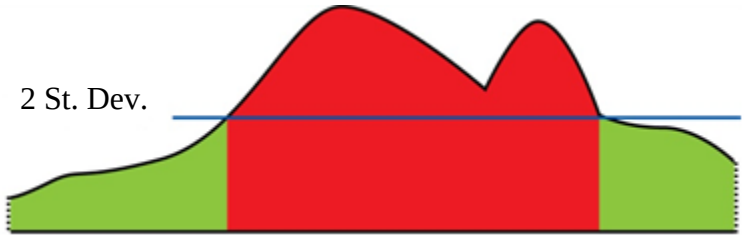

Figure 60: Hotzone Based on Two Standard Deviation Threshold on Albert Street.

As Figure 60 shows, once the threshold value is applied, the two high EPDO collision points shown in Figure 58 become part of the same hotzone. Figure 61 shows the four hotzones identified on the City of Regina's roadway network, three on Albert Street, and one on Broad Street. The two high EPDO collision density points identified towards the south end of Albert Street are joined in one hotzone. These findings are discussed in the "Results" section at the end of this chapter.

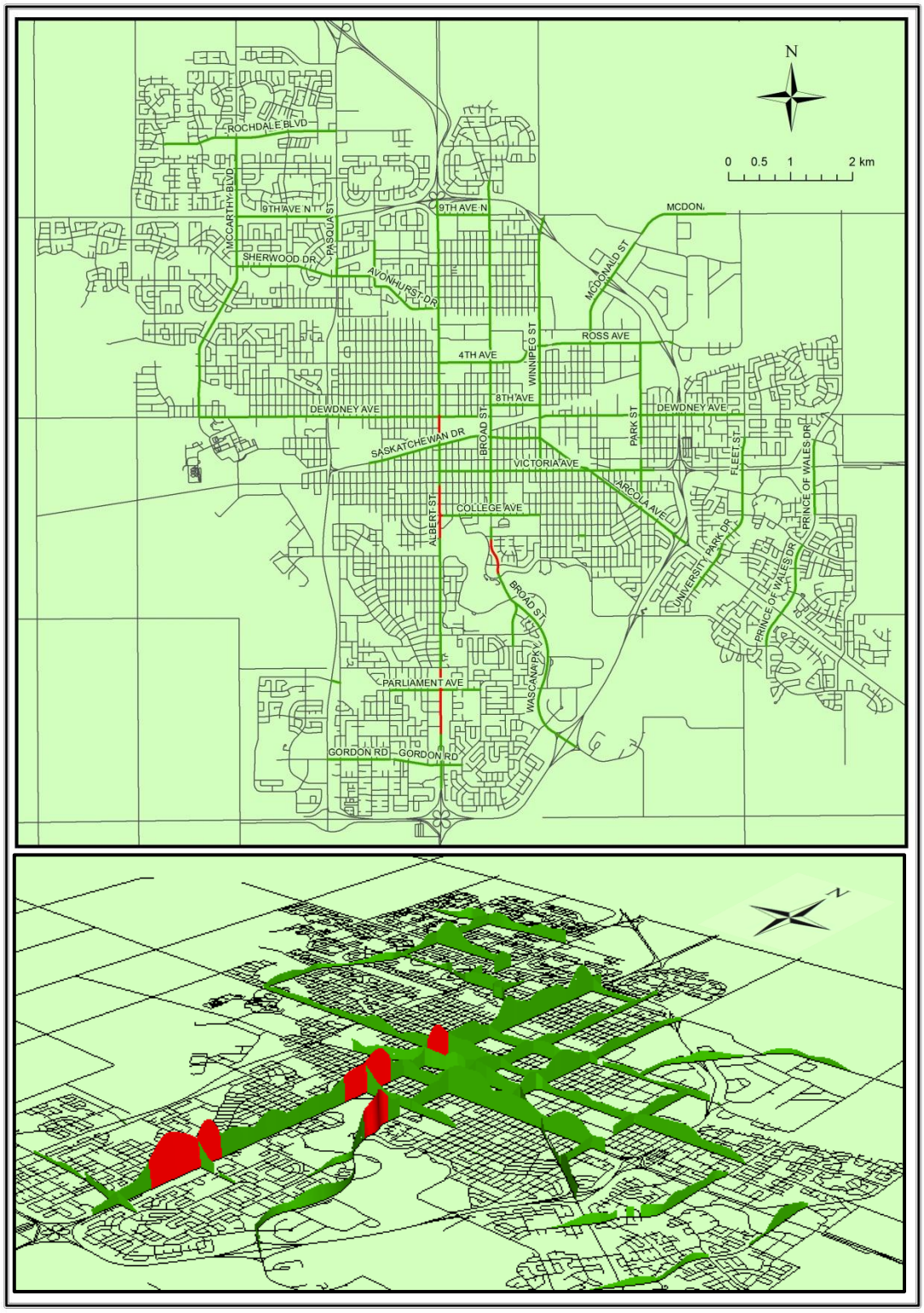

Figure 61: Top Four Hotzones (Shown in Red) Based on Expected EPDO and Network-Constrained KDE Results for Major Arterials.

5.5. Minor Arterial Post-Network Screening

Though the City of Regina contains 269 minor arterial roadway segments, traffic volumes and collision information were only available for 234 segments. Figure 62 shows the locations of these segments. As not all of the minor arterial roadway segments contained enough data to be included in this study, a few minor arterial roadway segments appear to be isolated.

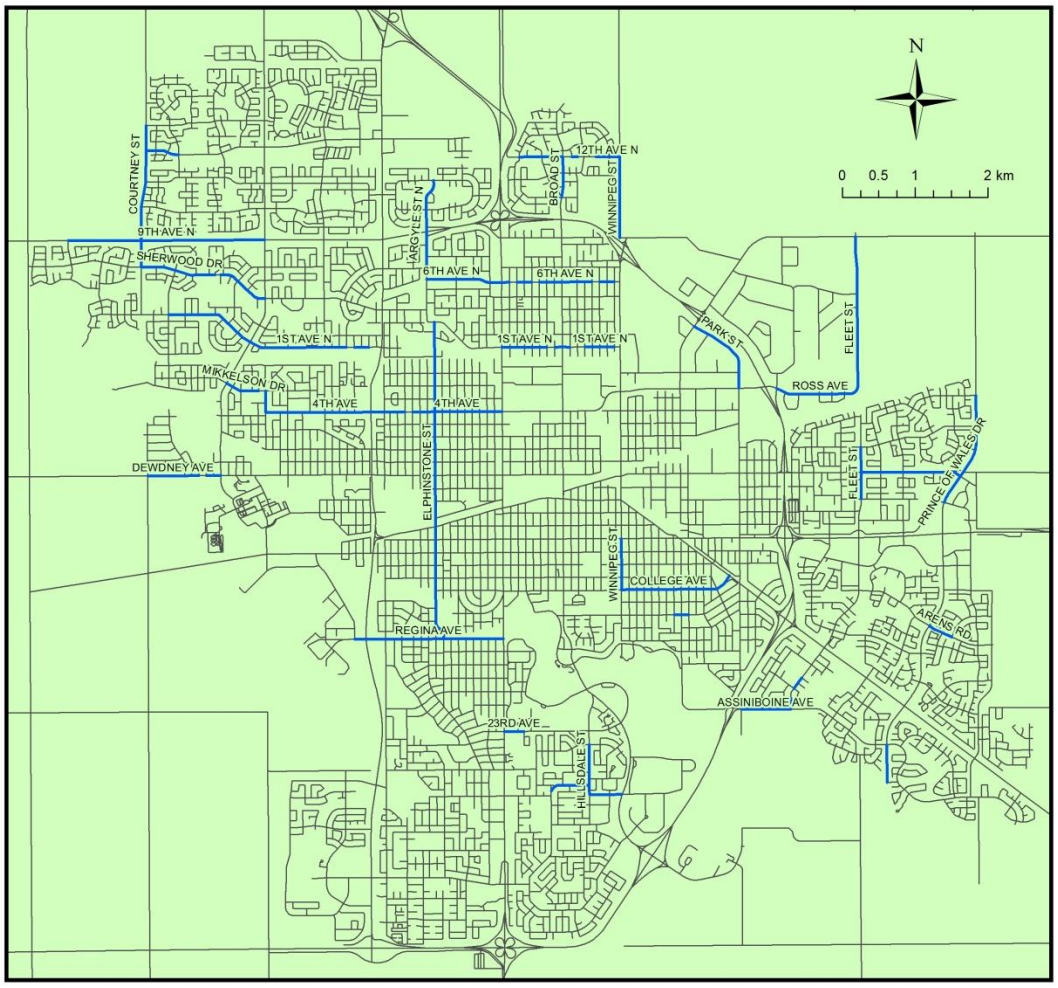

Figure 62: Study Network with 234 Minor Arterial Segments.

Figure 63 shows the results of the network-constrained KDE performed on minor arterial roadways, using observed collision counts, which do not take collision severity into account. As the figure shows, the relatively disconnected minor arterial roadways feature high density

regions scattered throughout the city; the most collision-prone areas are located on Elphinstone Street and College Avenue.

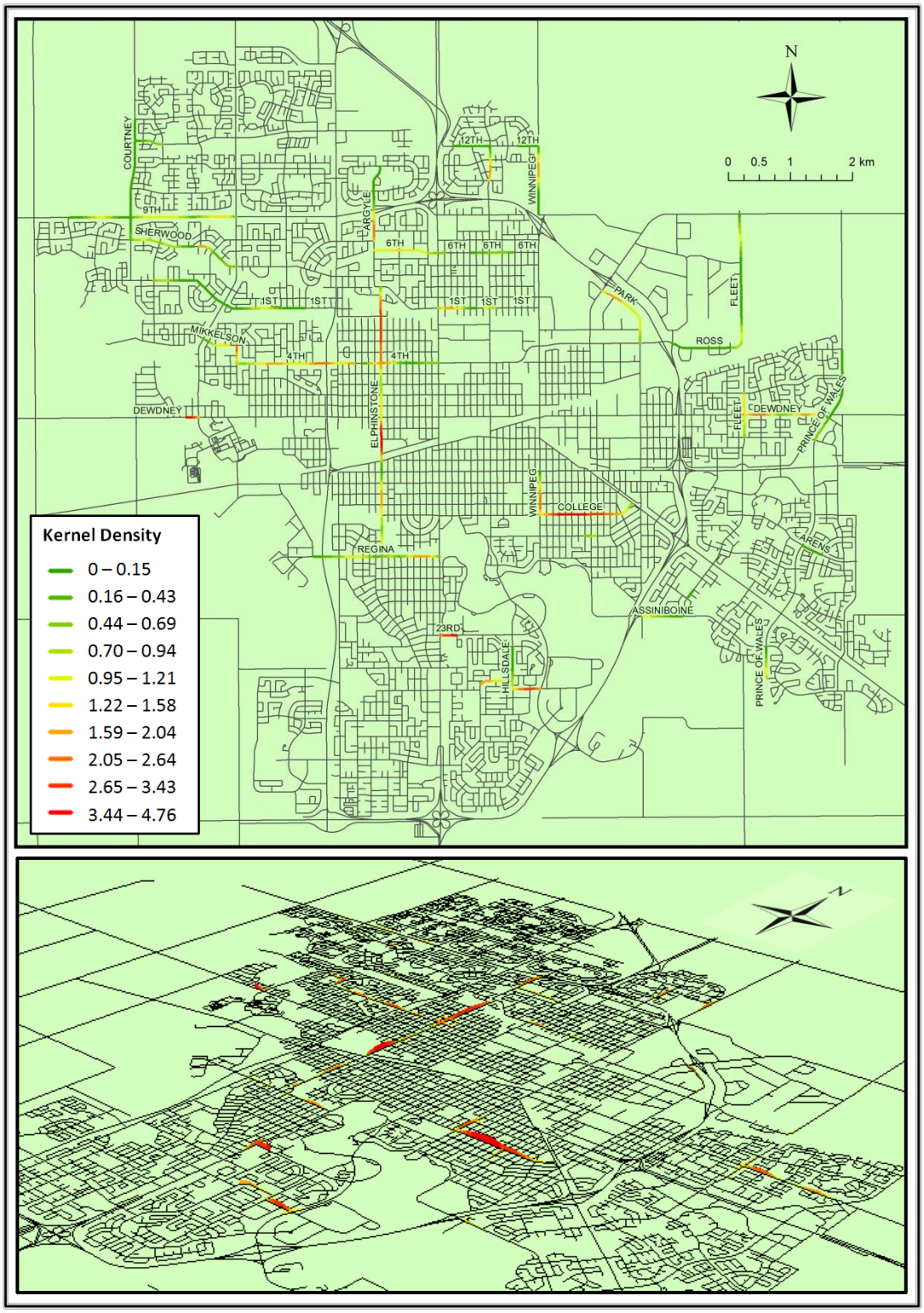

Figure 63: Network-Constrained KDE Results for Minor Arterials Based on Observed Collision Counts (400m Bandwidth).

Figure 64, which shows the KDE performed using observed EPDO collisions on minor arterials, shows higher collision densities, as should be expected from the "scaling-up" effect of applying collision severity factors. While the majority of the locations follow the same general trend as the observed collision count analysis shown in Figure 63, there are a couple of regions that have become more or less pronounced, due to the severity of collisions in these areas. For example, the high collision area on Argyle Street (near the top of the map) increased in density with the application of severity factors, while the northern-most high collision area on Elphinstone Street appears to have decreased, due to the collisions that occurred there being of a lesser severity.

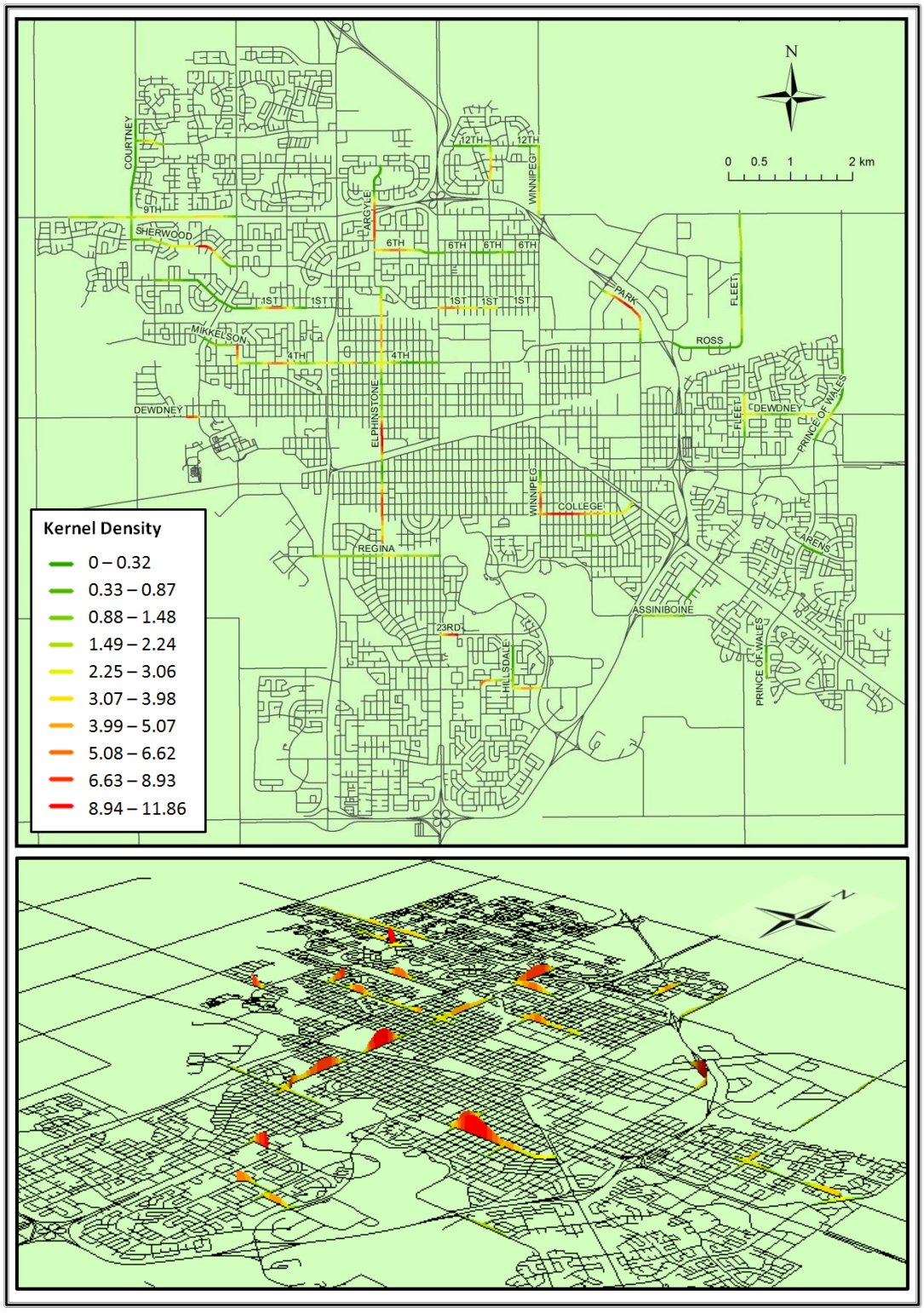

Figure 64: Network-Constrained KDE Results for Minor Arterials Based on Observed EPDO (400m Bandwidth).

Figure 65 shows the expected EPDO results for minor arterials. By comparing this figure to Figure 56, which presented the expected EPDO results for major arterials, a couple of observations can be made. First, the collision densities are much smaller for minor arterials than for major arterials. One reason for this is simply that fewer collisions occur on minor arterial roadways than major arterial roadways, due to a lower level of exposure. Another interesting conclusion that can be made is that since KDE takes into account the collision densities of neighbouring roadway segments, a less-connected road network (e.g., minor arterials) may result in lower overall collision densities than a more-connected road network (e.g., major arterials), where adjacent road segments with similar classifications serve to increase the resulting collision densities.

Also of interest is that depending on the alignment of a roadway network, usability problems related to the 3D visualization of density maps may arise. As the 2D map in Figure 65 shows, there is a relatively-highly ranked region on Park Street, near the north-east portion of the map. However, since this road segment exists at a diagonal alignment (as opposed to a north-south or east-west alignment), this particular road is difficult to see on the 3D map, which is rotated at an angle that coincides with this segment's alignment angle. Possible solutions may include: showing 3D KDE results at multiple angles; including specific inset maps for each locations; and adjusting the rotation angle of 3D visualizations. For the purposes of this study, the 3D rotation angle was held constant across all maps to keep the maps consistent, and aid in comparison. It should also be noted that the hotzone selection method proposed in this study serves to reduce dependency on visual inspections of data, and will help to avoid human observation biases such as the one described here.

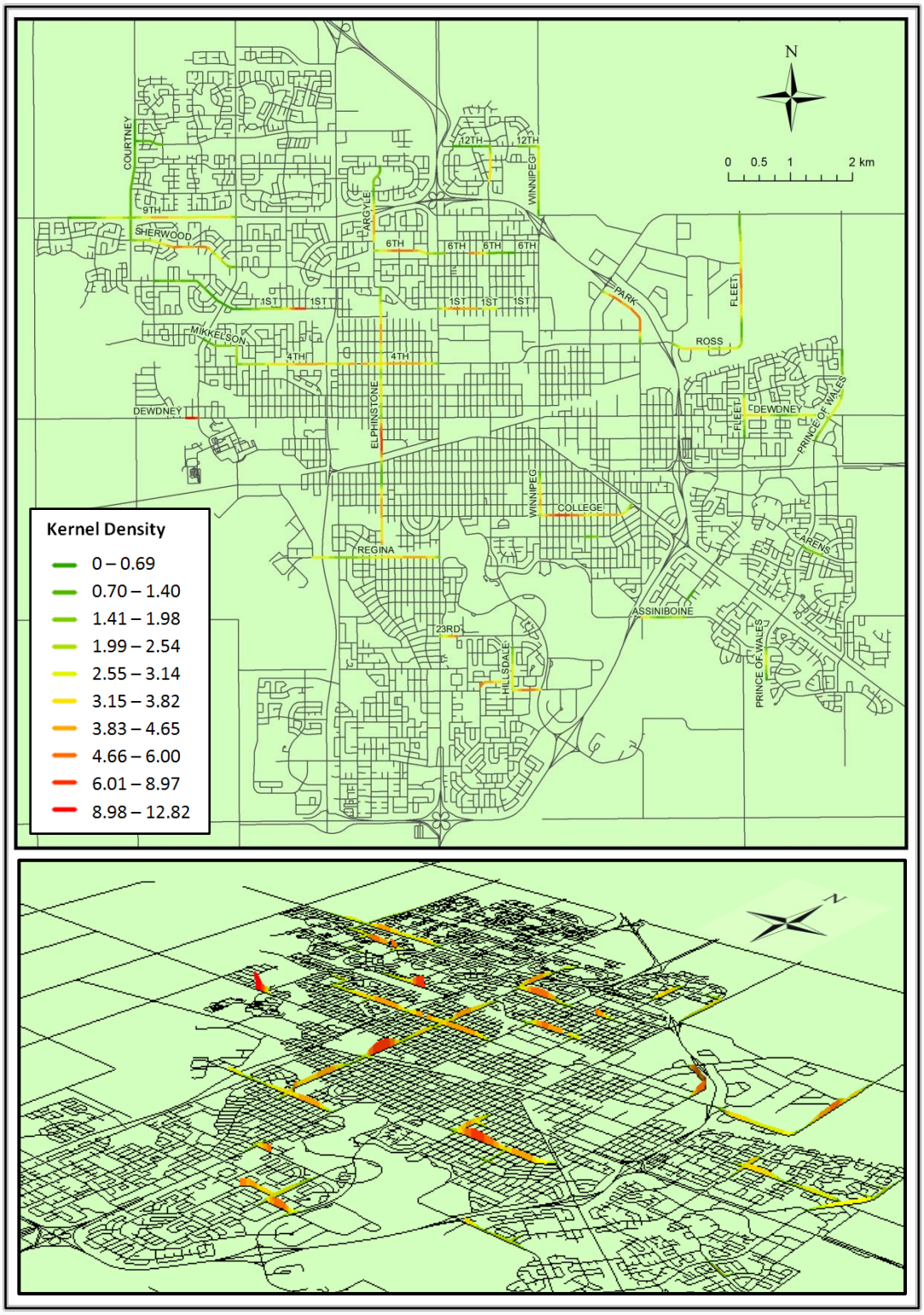

Figure 65: Network-Constrained KDE Results for Minor Arterials Based on Expected EPDO (400m Bandwidth).

The input for the hotzone selection step is the outcome of the HSM network screening procedure described earlier. Figure 66 shows the top five locations identified using the HSM's approach. The five locations in the figure are individual segments, and each one does not take into consideration the safety levels of neighboring roadway segments.

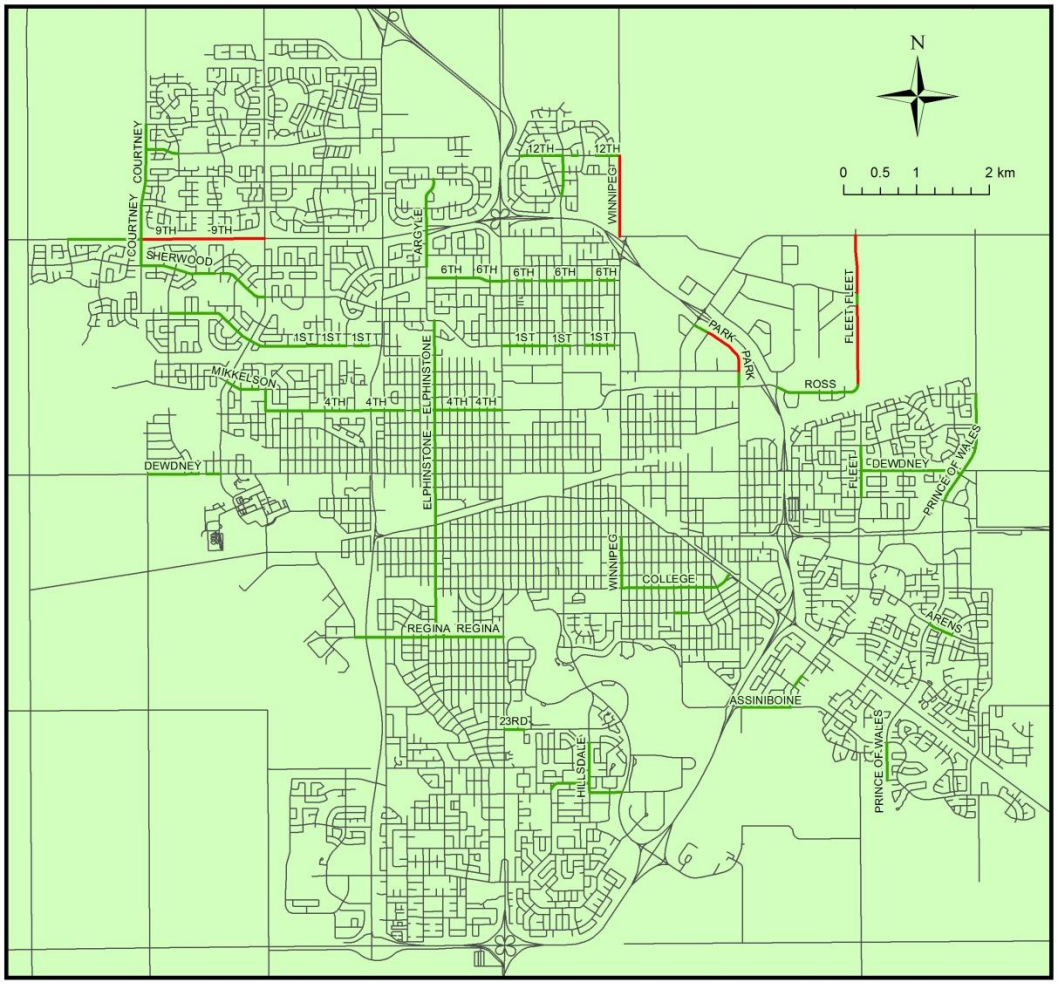

Figure 66: Top Five Riskiest Locations (Shown in Red) Based on HSM Network Screening Using Expected EPDO Results for 234 Minor Arterial Segments.

In order to identify spatially-related hotzones within the roadway network, specific point locations with high EPDO collision densities must first be identified. Figure 67 shows the top five points on the City of Regina's minor arterial road network.

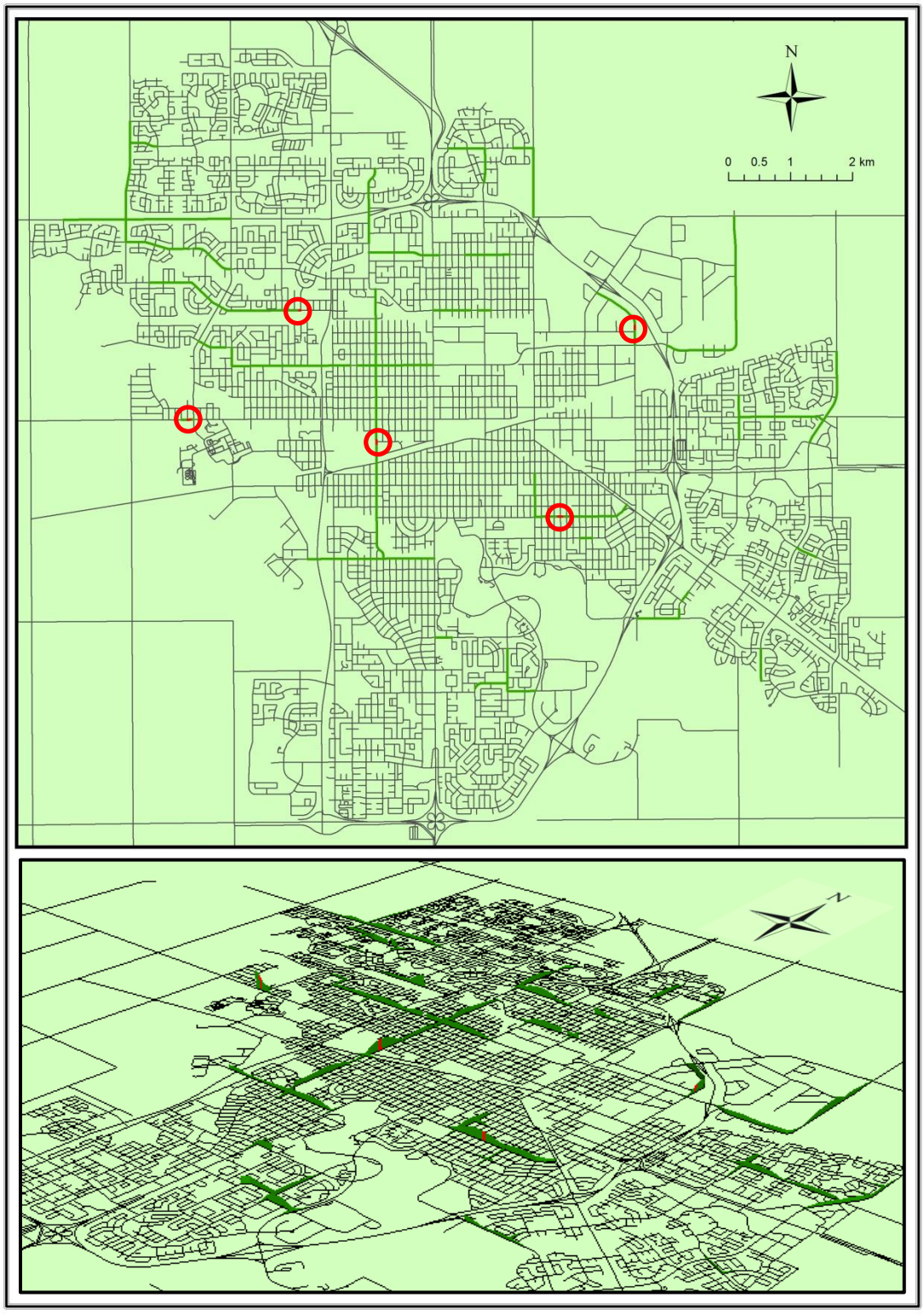

Figure 67: Top Five High EPDO Collision Density Points (Shown in Red) Based on Expected EPDO and Network-Constrained KDE Results for Minor Arterials.

Figure 68 shows the five hotzones that were identified using the two standard deviation hotzone selection approach. Hotzones were identified on Elphinstone Street, Park Street, College Avenue, Dewdney Avenue, and 1st Avenue North.

The identified hotzones contain between two and eight individual minor arterial roadway segments; the expected EPDO results for each hotzone range between 1.2 EPDO collisions and 11.8 EPDO collisions. These findings are discussed in the "Results" section at the end of this chapter.

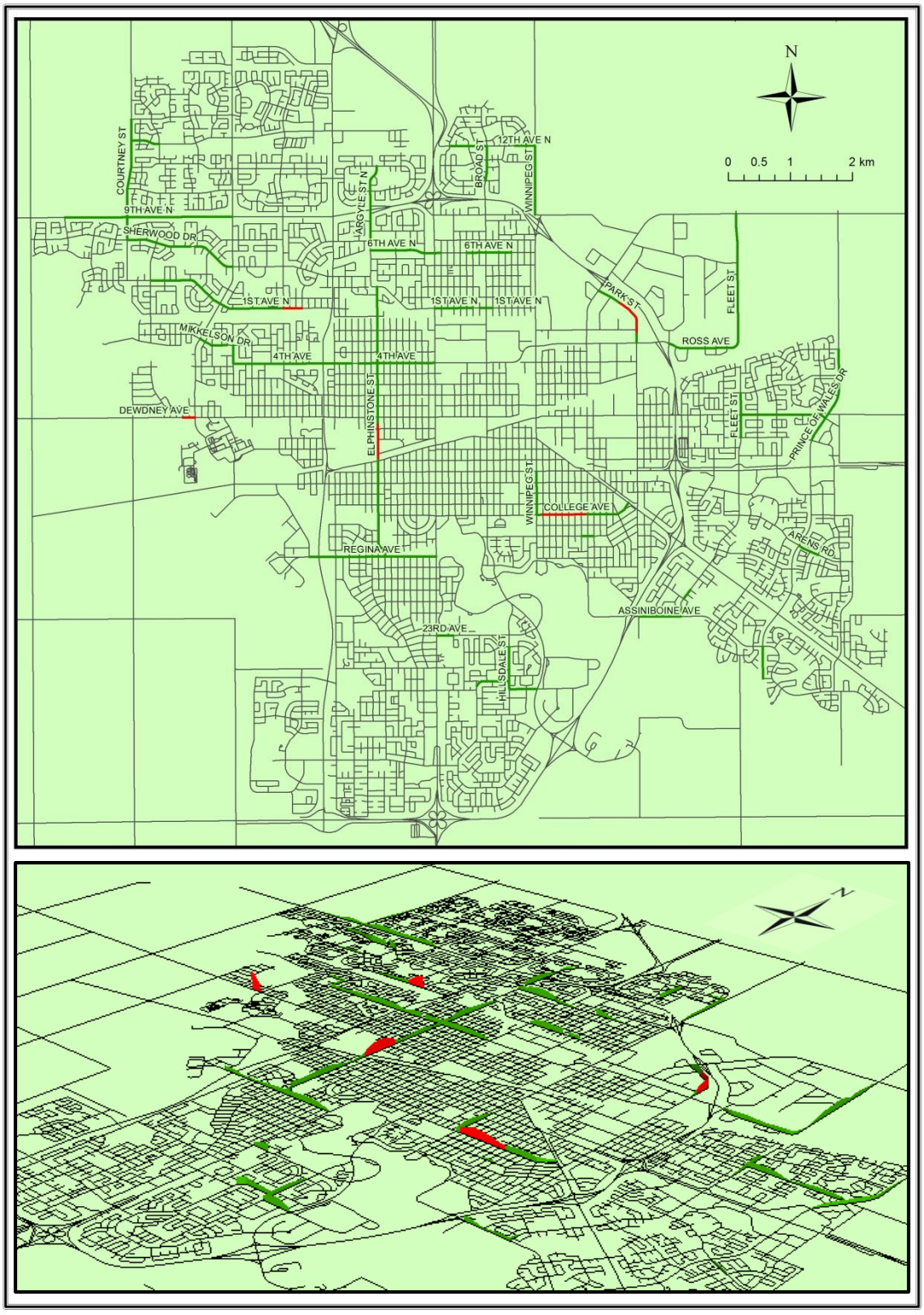

Figure 68: Top Five Hotzones (Shown in Red) Based on Expected EPDO and Network-Constrained KDE Results for Minor Arterials.

5.6. Collector Post-Network Screening

Though the City of Regina contains 1,157 collector roadway segments, traffic volumes and collision information were only available for 968 segments. Figure 69 shows the locations of these segments. As not all of the collector roadway segments contained enough data to be included in this study, a few collector roadway segments appear to be isolated.

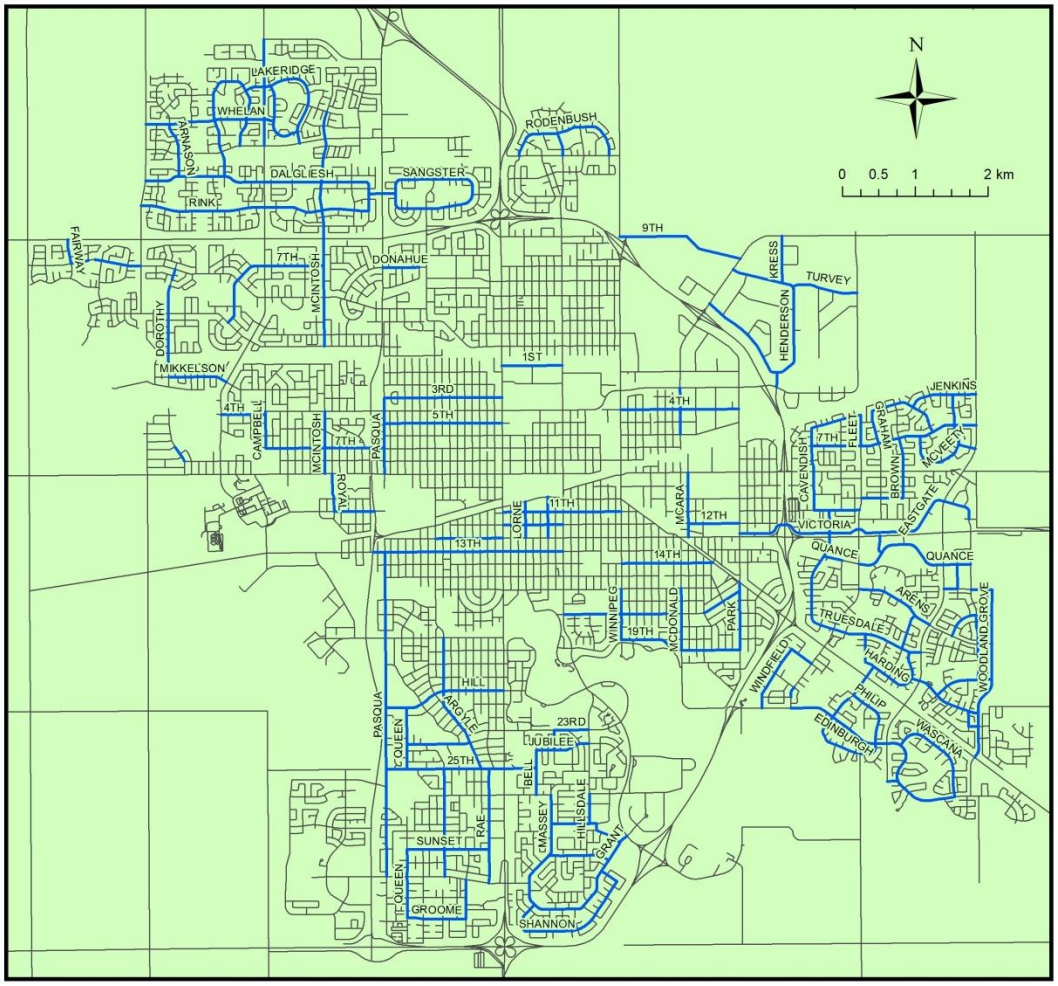

Figure 69: Study Network With 968 Collector Segments.

Figure 70 shows the results of the network-constrained KDE performed on collector roadways, using observed collision counts, which do not take collision severity into account. As

the figure shows, high collision density locations are focused in three regions: downtown, the east side, and the south side.

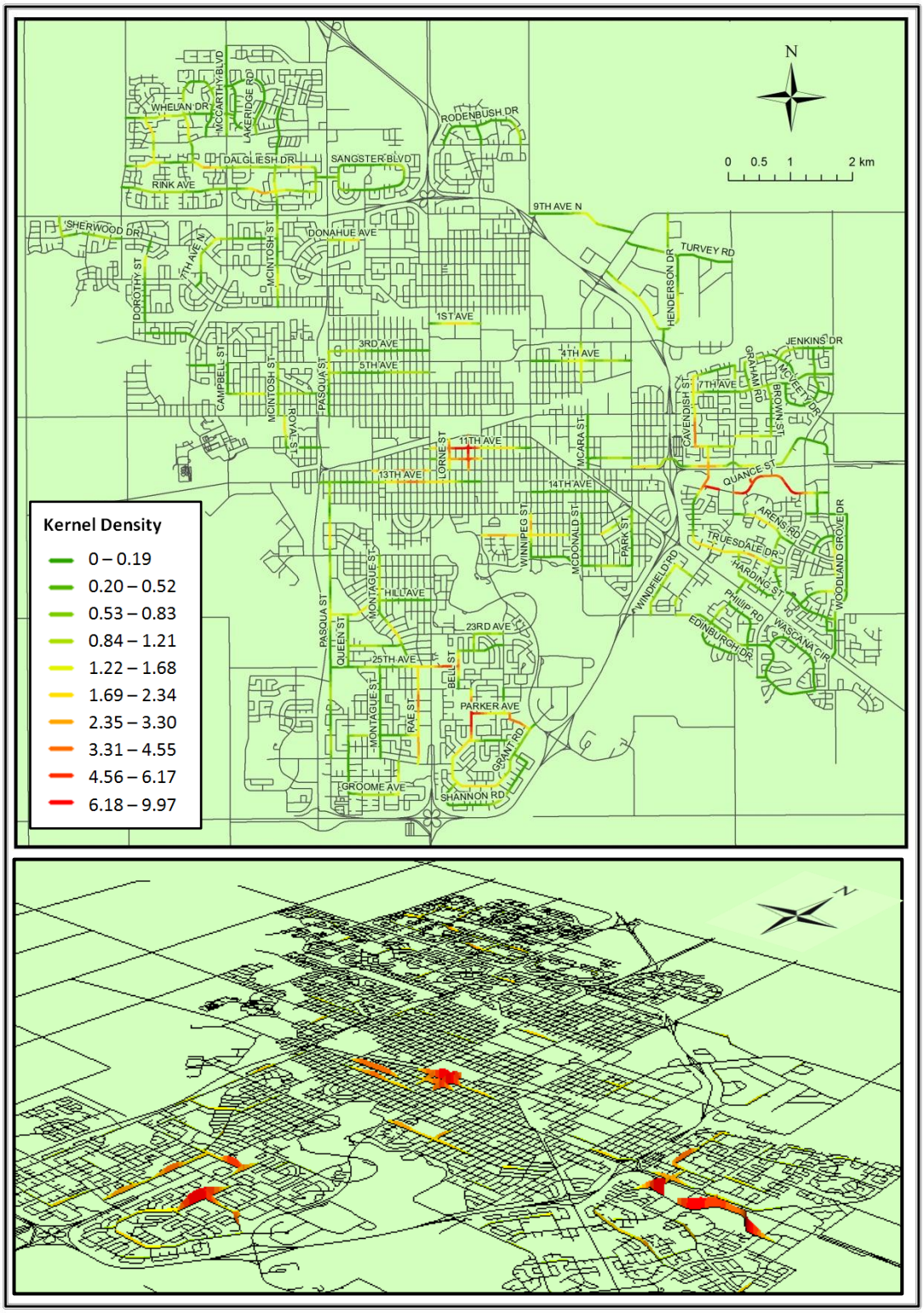

Figure 70: Network-Constrained KDE Results for Collectors Based on Observed Collision Counts (400m Bandwidth).

Figure 71 presents the results of the severity-based observed EPDO KDE on collector road segments. In this case, the eastern-most hotspots located on Quance Street emerge as clear peaks, with collision densities over 26 EPDO along these collector segments.

One benefit of the proposed KDE approach is the clear delineation between higher-ranked and lower-ranked locations. Unlike the HSM's approach, which simply presents a ranked list of locations, the visual output of a KDE analysis presents the user with an easily-identifiable hierarchy of high-collision locations. Rather than having to sort through tables of numbers, a user can simply refer to a colourized collision density map, such as the one shown in Figure 71, and immediately get an idea of which locations are deserving of further analysis and potential safety improvements.

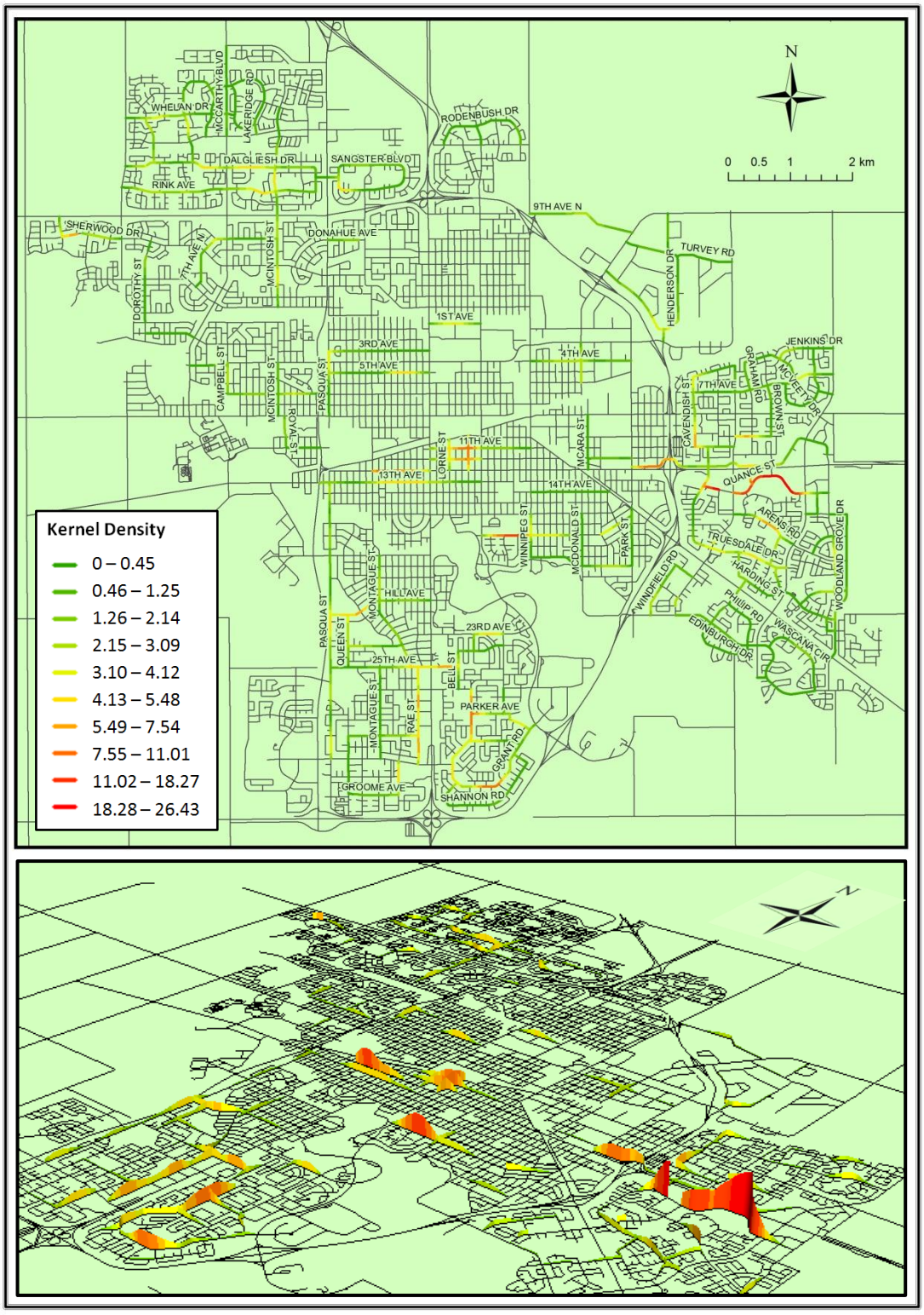

Figure 71: Network-Constrained KDE Results for Collectors Based on Observed EPDO (400m Bandwidth).

Figure 72 shows the expected EPDO results of a KDE analysis on collector roadways. Unlike the two previous analyses, which used observed collisions as inputs, the results of this investigation are much more dispersed, with medium- to high-collision density locations present throughout the roadway network. With scattered results such as these, the importance of an organized, consistent means of selecting hotzones becomes apparent.

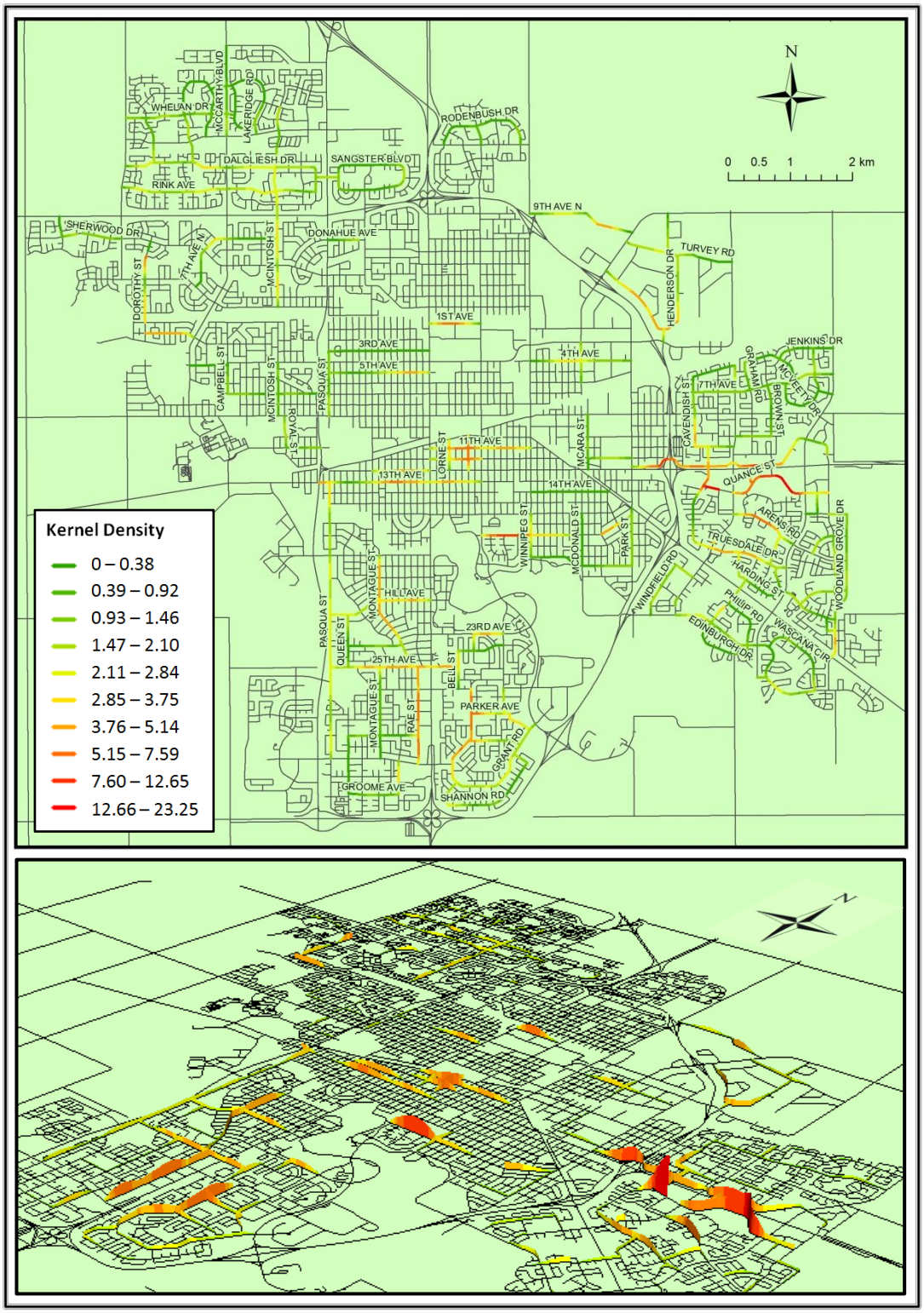

Figure 72: Network-Constrained KDE Results for Collectors Based on Expected EPDO (400m Bandwidth).

The input for the hotzone selection step is the outcome of the HSM network screening procedure described earlier. Figure 73 shows the top five locations identified using the HSM's approach. The five locations in the figure are individual segments, and each one does not take into consideration the safety levels of neighboring roadway segments.

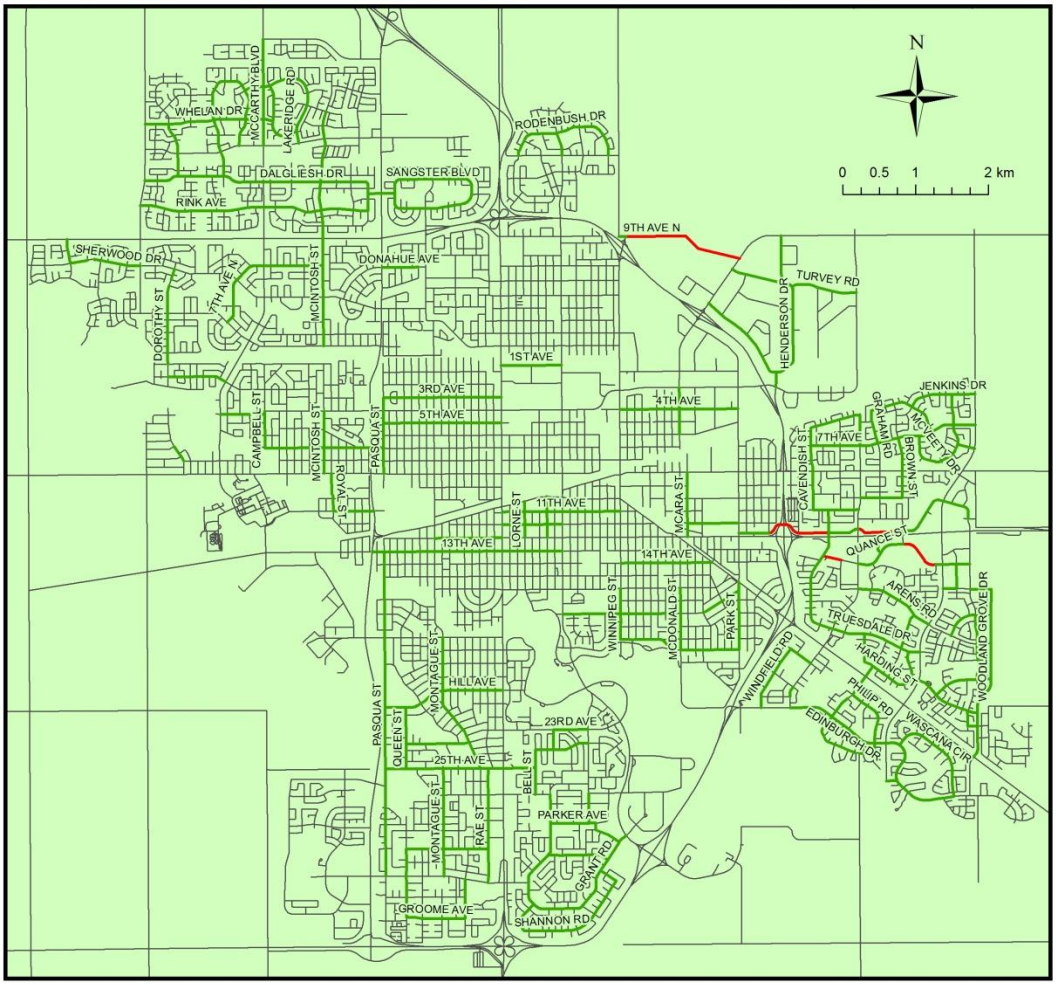

Figure 73: Top Five Riskiest Locations (Shown in Red) Based on HSM Network Screening Using Expected EPDO Results for 968 Collector Segments.

In order to identify spatially-related hotzones within the roadway network, specific point locations with high EPDO collision densities must first be identified. Figure 74 shows the top five points on the City of Regina's collector road network.

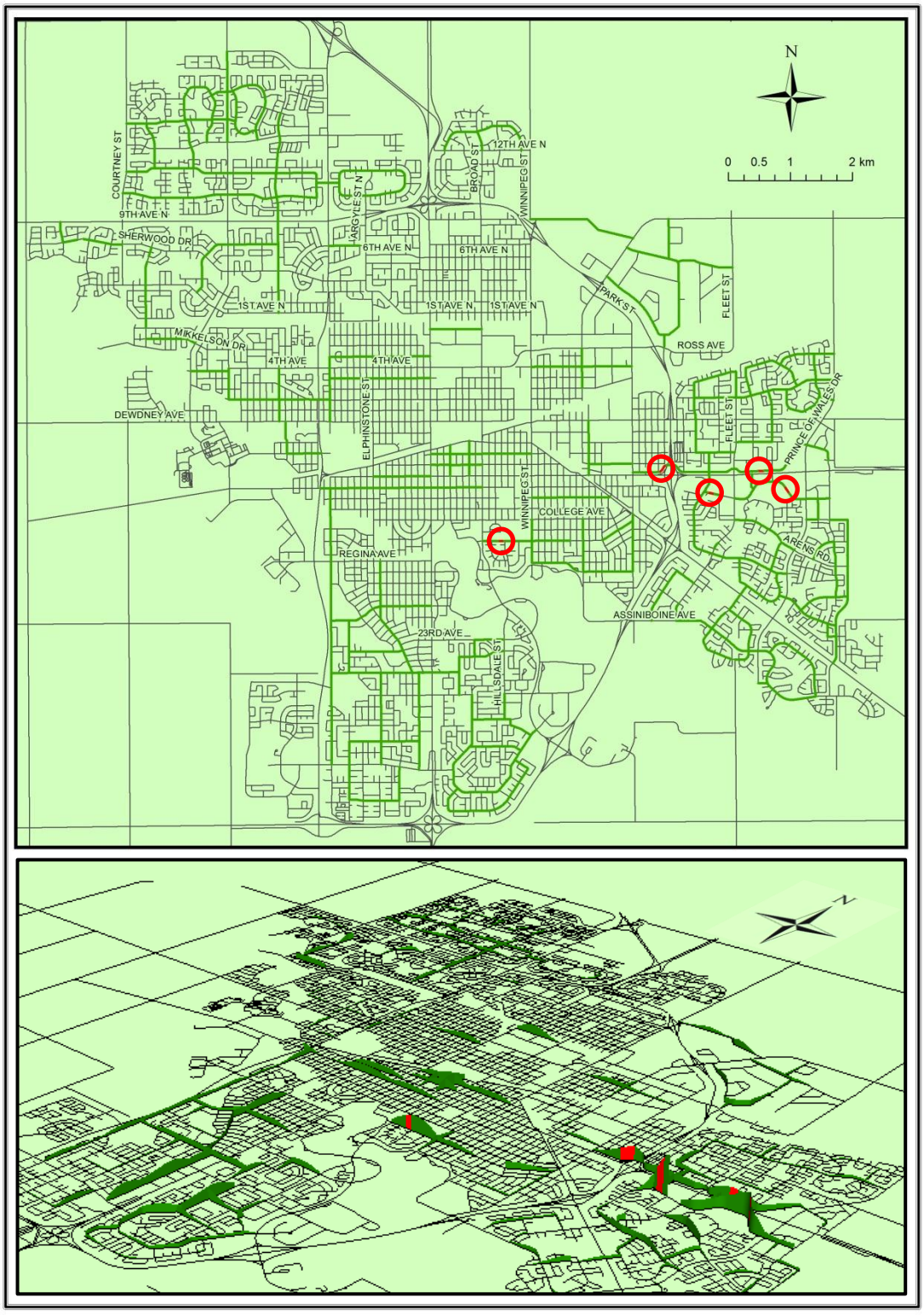

Figure 74: Top Five High EPDO Collision Density Points (Shown in Red) Based on Expected EPDO and Network-Constrained KDE Results for Collectors.

Figure 75 shows the five hotzones that were identified using the two standard deviation hotzone selection approach. Hotzones were identified on Quance Street (two), North Service Road (two), and Broadway Avenue. The identified hotzones contain between one and four individual collector roadway segments; the expected EPDO results for each hotzone range between 13.3 EPDO collisions and 29.9 EPDO collisions. These findings are discussed in the "Results" section at the end of this chapter.

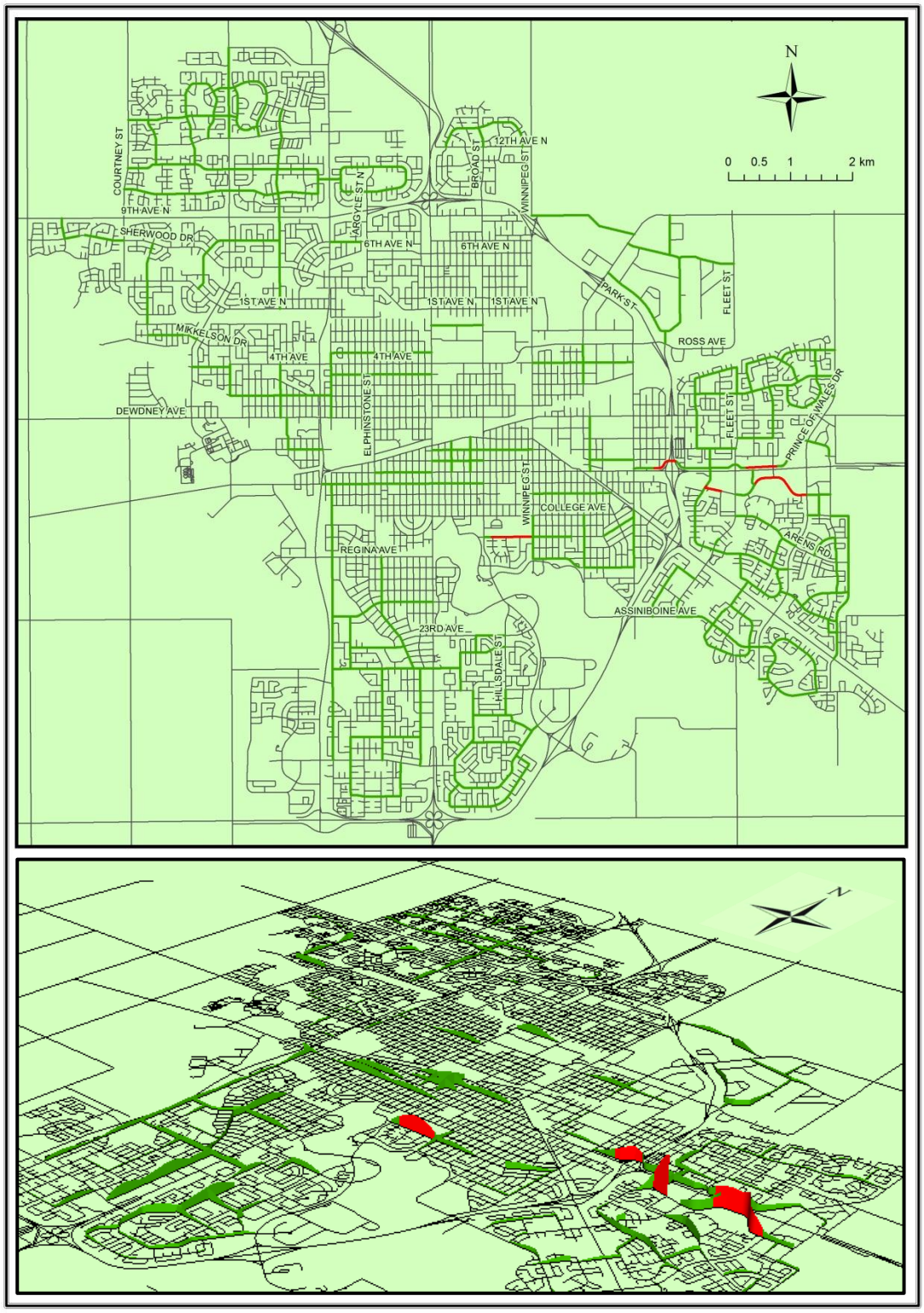

Figure 75: Top Five Hotzones (Shown in Red) Based on Expected EPDO and Network-Constrained KDE Results for Collectors.

5.7. Post-Network Screening Results

This section discusses the findings of the network-constrained KDE analysis undertaken on the following three road segment classifications in the City of Regina: major arterials, minor arterials, and collectors.

For major arterial roadways, only three of the five hotspots identified using the HSM's approach were included in the selected four hotzones. Table 43 compares the top five segments identified using the HSM network screening approach with the top four hotzones identified using the network-constrained KDE procedure as part of the proposed two-step approach.

Table 43: Comparison Between HSM Network Screening Results and Network-Constrained KDE Hotzone Results for Major Arterials.

Ranking	HSM Network Screening		Network-Constrained KDE Hotzones	
	Number of Segments	Expected EPDO	Number of Segments	Expected EPDO
1	1	34.8	5	77.3
2	1	30.0	5	46.0
3	1	24.9	3	32.7
4	1	22.2	3	24.7
5	1	16.8	-	-
Total	**5**	**128.7**	**16**	**180.7**

The table shows that the top five segments identified using the HSM approach accounted for five segments with 16.8 to 34.8 expected EPDO collisions per segment, giving a total of 128.7 EPDO collisions. The four hotzones identified using the proposed two-step approach accounted for 16 segments in four hotzones with 24.7 to 77.3 expected EPDO collisions per hotzone, giving a total of 180.7 expected EPDO collisions (approximately 40% more expected EPDO collisions than the HSM result).

The next road segment classification that was analyzed was minor arterials. Table 44 compares the top five segments identified using the HSM network screening approach with the top five hotzones identified using the network-constrained KDE procedure as part of the proposed two-step approach.

Table 44: Comparison Between HSM Network Screening Results and Network-Constrained KDE Hotzone Results for Minor Arterials.

Ranking	HSM Network Screening		Network-Constrained KDE Hotzones	
	Number of Segments	Expected EPDO	Number of Segments	Expected EPDO
1	1	13.8	2	11.8
2	1	10.5	4	10.7
3	1	8.4	8	10.6
4	1	6.1	4	5.8
5	1	5.3	2	1.2
Total	**5**	**44.1**	**20**	**40.0**

The table shows that the top five segments identified using the HSM approach give a total of 44.1 EPDO collisions. The five hotzones identified using the proposed two-step approach accounted for 20 segments with a total of 40.0 EPDO collisions. These results highlight an important factor inherent in network-constrained KDE: the connectivity of the network. As can be seen in the classification-specific maps shown in Figure 53 (major arterials) and Figure 62 (minor arterials), there exists a significant difference in the connectivity exhibited by these two road networks. While the major arterial network is highly connected, with many instances of road segments crossing each other, the minor arterial road network is relatively disconnected, with minor arterials divided into a number of isolated, non-intersecting sections. As with any form of spatial analysis, the effectiveness of a spatially-based approach is directly related to the

geographic relationships of the features under consideration. In the case of minor arterials in the City of Regina, which are relatively disconnected, network-constrained KDE may not be as appropriate an analysis technique as a non-spatially-related method, such as the methodology outlined in the HSM. However, as road networks become more fine-grained, with higher levels of connectivity (in larger metropolitan areas, for example), spatial analysis techniques such as network-constrained KDE may prove to be of greater utility.

The final road segment classification that was investigated was collectors. Table 45 compares the top five segments identified using the HSM network screening approach with the top five hotzones identified using the network-constrained KDE procedure as part of the proposed two-step approach.

Table 45: Comparison Between HSM Network Screening Results and Network-Constrained KDE Hotzone Results for Collectors.

Ranking	HSM Network Screening		Network-Constrained KDE Hotzones	
	Number of Segments	Expected EPDO	Number of Segments	Expected EPDO
1	1	22.5	3	29.9
2	1	13.8	2	15.2
3	1	12.8	4	14.9
4	1	12.4	1	13.8
5	1	8.2	2	13.3
Total	**5**	**69.7**	**12**	**87.1**

The table shows that the top five segments identified using the HSM approach give a total of 69.7 EPDO collisions. The five hotzones identified using the proposed two-step approach accounted for 12 segments with a total of 87.1 EPDO collisions. As the collector road segment

network contained a high level of connectivity, with multiple collector segments located in close proximity, the expected EPDO total is higher than the HSM approach, as expected.

5.8. Safety Improvement Example

The benefit of the proposed two-step post-network screening analysis can be shown by performing a theoretical safety improvement on one of the hotzones identified in the previous sections.

By using the societal collision costs presented in the HSM, a relationship between the AADT on a road segment and the associated cost can be developed. A plot showing this relationship for major arterial roadways is shown in Figure 76, using the jurisdiction-specific SPF and a segment length of 1 kilometre.

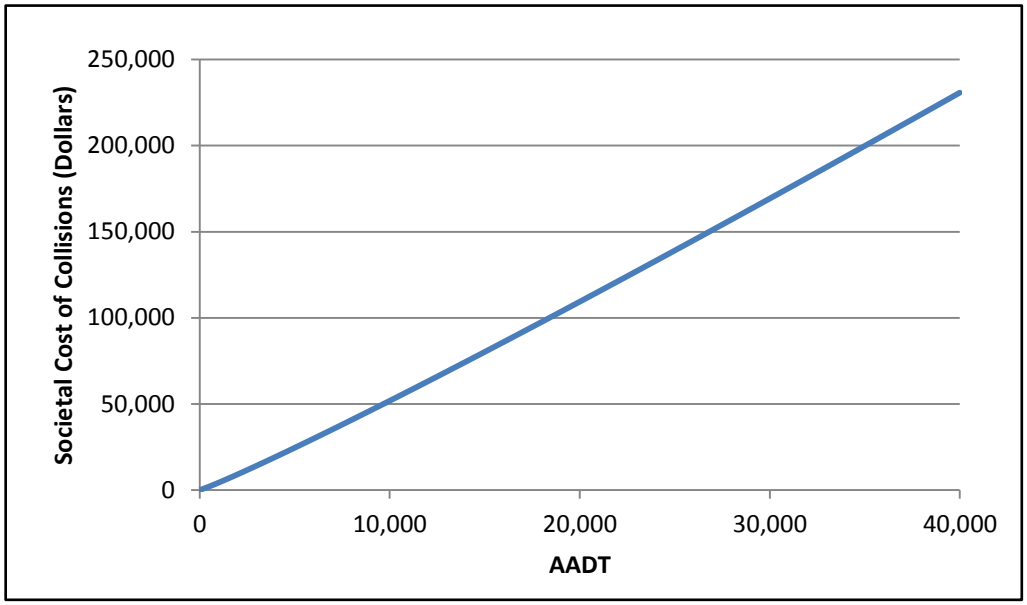

Figure 76: AADT Vs. Societal Cost of Collisions for Major Arterial Road Segments.

The highest-ranked hotzone identified on major arterial roadways, located near the south end of Albert Street, is shown in Figure 61, and described in Table 43. In 2009, the AADT on

this one kilometre road segment was 27,400. The estimated societal cost of collisions for this hotzone is $153,500. This value is represented in Figure 77 with a blue circle.

Derek Murray Consulting and Associates (2010) provided an annual population growth factor for the City of Regina of 1.12%. By applying this population growth factor, the traffic volume within the hotzone on Albert Street was estimated to be 28,650 for the year 2013. This AADT results in a societal cost of collisions of $161,100, which is represented in Figure 77 with a red square.

For this particular hotzone, one potential safety improvement would be reducing the number of access points. A study published by Lee et al. (2011) found that limiting the number of access points along an urban arterial will result in a collision modification factor (CMF) of 0.56. A CMF of 0.56 can be interpreted to mean a 44% reduction in collisions. By applying this CMF to the expected number of collisions, as estimate can be found for the number of collisions that would occur should this treatment be utilized. In the case of this particular hotzone, reducing the number of access points would result in a societal cost of collisions of $90,200 in 2013. This value is represented in Figure 77 with a green triangle. The potential reduction in safety that would be achieved through the implementation of this countermeasure in the Albert Street hotzone would be $70,900.

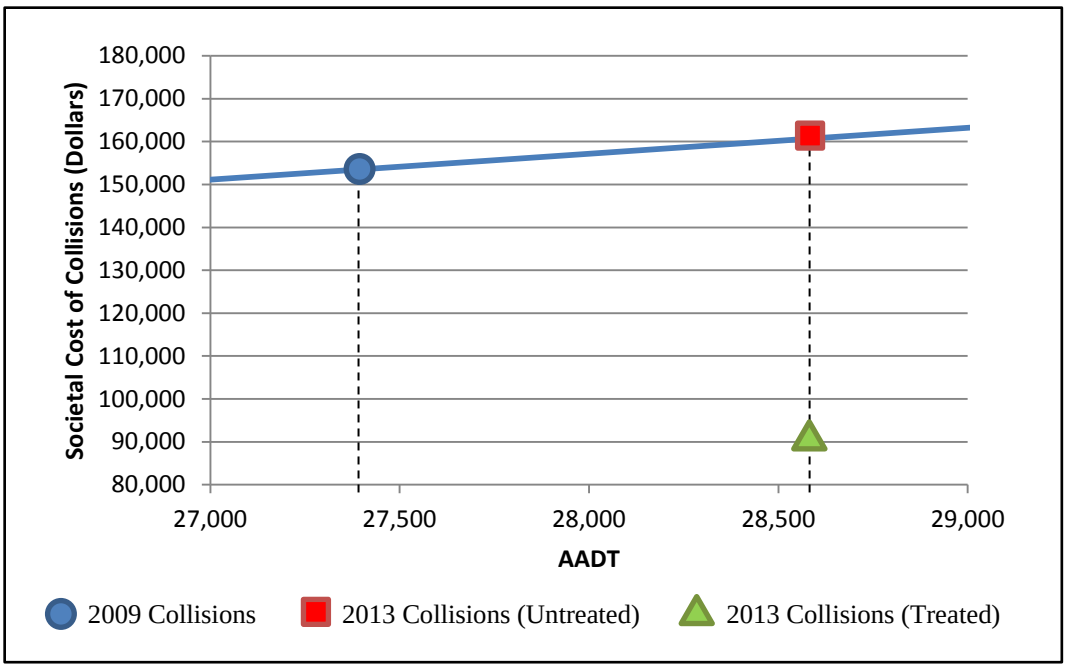

Figure 77: Societal Collision Costs for the Selected Hotzone.

As the above example shows, the locations identified using the proposed two-step post-network screening analysis can be used to estimate the expected reduction in collisions, and associated societal cost of collisions, in future years.

5.9. Chapter Summary

This chapter contained a description of the kernel function that was used for this research, as well as an overview of the bandwidth selection process (400m was selected as the optimal bandwidth for this study). In order to compare the performance of the proposed post-network screening analysis using network-constrained KDE, several analyses were performed for each of the road network categories, including observed collision count, observed EPDO, expected EPDO, and a hotzone selection technique that used two standard deviations of the expected number of collisions. The benefits of using this approach are as follows: the spatial relationships between collision locations are taken into account; regression-to-the-mean bias is accounted for;

and collision severity is factored in to the results. The results of this analysis were compared with the results of the HSM's network screening approach, and it was found that the proposed two-step post-network screening analysis captured a higher number of expected collisions within the top five hotzones. Finally, a case study was performed using one of the hotzones that was identified on the City of Regina's major arterial road network. By using the jurisdiction-specific SPF, along with a growth factor for the City of Regina, a comparison could be made for the expected societal cost of collisions in future years, both with and without making a safety improvement to the hotspot.

CHAPTER 6. SUMMARY AND CONCLUSION

6.1. Safety Performance Functions for the City of Regina

SPFs were developed for roadway segments and intersections in the City of Regina, Saskatchewan. The categories included major arterials, minor arterials, collectors, three-leg unsignalized intersections, four-leg unsignalized intersections, and three and four-leg signalized intersections. These SPFs were developed using three types of information: road network information, traffic volume (AADT), and collision data (including severity and configuration information). As traffic counts are not performed every year, for every segment, the estimation procedure described in the HSM was followed in order to generate volume information for missing years.

Calibration factors were generated for each roadway category, based on the method outlined in the HSM. This allowed the researcher to compare the performance of jurisdiction-specific SPFs with calibrated HSM models.

For each of the three severity categories, four candidate model forms were developed. A number of methods were used to select the most appropriate form of SPFs for each category, including investigation of each model's p-values, Akaike information criterion (AIC), Bayesian information criterion (BIC), cumulative residual (CURE) plots, and dispersion parameters.

Based on the results of this study, the jurisdiction-specific SPFs outperformed the HSM SPFs (both the uncalibrated and calibrated models).

In order to assess the transferability of the SPFs developed for Regina, the previously-described intersection models (i.e., three-leg unsignalized, four-leg unsignalized, three and four-leg signalized) were applied to collision data from the City of Saskatoon. The same statistical

goodness-of-fit tests (i.e., MSPE, MPB, MAD, R^2_{FT}) used to validate the Regina SPFs were utilized to investigate the SPFs' transferability using Saskatoon data. This transferability test showed that in general, the uncalibrated Regina SPFs performed better than the uncalibrated HSM SPFs. For calibrated SPFs, however, the results were mixed: the calibrated HSM SPFs generally performed better than the calibrated Regina SPFs for the two unsignalized intersection categories, while the reverse was true for signalized intersections.

6.2. Network Screening for the City of Regina

For this study, two network screening methods were used to investigate the City of Regina's intersections and road segments. The "EPDO Average Collision Frequency with EB Adjustment" method uses weighting factors to convert FI collisions into EPDO (equivalent property damage-only) collisions, and then ranks locations by the EB-adjusted EPDO. The second network screening method used was the "Excess Expected Average Collision Frequency with EB Adjustment," which ranks the locations by the difference between the predicted number of collisions (obtained using an SPF) and the EB-adjusted estimates (which take the observed number of collisions into account).

Ranked lists for each road segment and intersection category were generated, as well as collision maps. In addition to presenting these results, the output of this step of the research was used in the following section ("Post-Network Screening Using Network-Constrained KDE").

6.3. Post-Network Screening Using Network-Constrained KDE

This research introduced a two-step post-network screening approach for identifying corridor hotzones within a roadway network. The proposed approach combines the network screening procedure outlined in AASHTO's HSM with a GIS-based network-constrained KDE analysis. The approach was tested using collision data for five years (2005-2009) for 435 major arterial

roadway segments, 234 minor arterial roadway segments, and 968 collector roadway segments in the City of Regina, Saskatchewan.

The study investigated how the identification of hotzones is affected by 1) taking the severity of collisions into account, and 2) ensuring that RTM bias is reduced. The study then compared the hotzone results obtained from the proposed two-step approach to results obtained using the HSM's standard approach.

The effect of taking the severity of collisions into account was tested by comparing the results obtained from an analysis using simple observed collision counts (which do not take collision severity into account) with the results obtained from an analysis using observed EPDO counts (which give weightings based on severity). It was clear that the expected EPDO collision density results identified by the two approaches were similar. The difference was that the observed EPDO counts could very dramatically emphasize a small number of fatal or injury collisions. This emphasis might be useful in certain situations, but it might also be misleading if the fatal or injury collisions were "rare and random" in nature rather than associated with the surface infrastructure conditions. The emphasis on locations with a small number of fatal or injury collisions would be especially problematic if the collisions occurred primarily because of driver error (e.g., impaired driving) in which case improvements to the surface infrastructure might not be helpful.

The effect of ensuring that RTM bias is reduced was tested by comparing results obtained from an analysis using the observed EPDO (which does not consider RTM bias) with the results obtained from an analysis using the expected EPDO (which does consider RTM bias). It was clear that analysis using the expected EPDO successfully "dampened" the effects of unusual

collisions such as the fatal collision. This is important if we are to avoid expenditures that appear to improve safety, when in reality the improvement was due to regression to the mean.

The comparison between the hotzone results obtained from the proposed two-step approach with the results obtained using the HSM's standard approach showed some interesting differences. In the proposed two-step approach, segments adjacent to the five highest EPDO collision density points were selected for inclusion in a hotzone if their EPDO collision density values were greater than two standard deviations from the mean. For major arterial roadway segments, this approach reduced the five high expected EPDO collision density points to four hotzones. The HSM's network screening method's top five major arterial segments accounted for 128.7 expected EPDO collisions whereas the four hotzones identified using the proposed two-step method accounted for 16 major arterial segments and 180.7 expected EPDO collisions.

Finally, a case study was performed using one of the hotzones that was identified on the City of Regina's major arterials, with the impact of applying a safety improvement treatment converted into a monetary amount using the societal collision costs provided in the HSM.

The study's findings suggest that the proposed two-step network screening method using network-constrained KDE can successfully reduce the effects of RTM and successfully identify hotzones where appropriate safety improvements should be identified and investigated. As the proposed two-step method takes into account the EPDO collision densities of adjacent roadways, and aggregates multiple individual segments into spatially-associated hotzones, transportation safety decision-makers are not confined to isolated roadway segment definitions when considering safety improvements, but can see the larger safety picture and have an opportunity to allocate their limited transportation safety resources more efficiently.

6.4. Future Work and Recommendations

The areas of KDE and road safety analysis are rife with areas for future exploration. This study proposed a two-step post-network screening approach for urban roadway segments, including major arterials, minor arterials, and collectors. Future work could apply this approach to other configurations of roadways, including freeways, ramps, and intersections.

The development of a scientific approach to the selection of the bandwidth used in the KDE analysis is also recommended. Though this study (and numerous other studies) used a trial and error method in selecting the optimal bandwidth, a more rigorous and statistical method would give researchers a more consistent way of applying the spatial analysis methods used in this study.

REFERENCES

Akaike, Hirotugu (1974). *A new look at the statistical model identification*, IEEE Transactions on Automatic Control 19 (6): 716–723.

Alluri, P. & Ogle, J. (2012). *Effect of Variations of CMFs on Predicted Crash Frequency on Rural Two-1 Lane Highways: Sensitivity Analysis*, Proceedings from the 2012 TRB 91st Annual Meeting. Washington, D.C. January 2012.

Alluri, P. & Ogle, J. (2012). *Effects of state-specific SPFs, AADT estimations, and overdispersion parameters on crash predictions using SafetyAnalyst*, Proceedings from the 2012 TRB 91st Annual Meeting. Washington, D.C. January 2012.

American Association of State Highway and Transportation Officials (AASHTO). (2010). *Highway Safety Manual – First Edition*, American Association of State Highway and Transportation Officials. Washington, DC.

Anderson, T. K., (2009). *Kernel density estimation and K-means clustering to profile road accident hot spots*, Accident Analysis & Prevention 41(3), 359–364.

Banihashemi, M. (2011). *Highway Safety Manual, New Model Parameters vs. Calibration of Crash Prediction Models*, Annual Meeting of the Transportation Research Board (TRB), Washington DC.

Bornheimer, C., Schrock, S., Wang, M. & Lubliner, H. (2012). *Developing a Regional Safety Performance Function for Rural Two-Lane Highways*, Proceedings from the 2012 TRB 91st Annual Meeting. Washington, D.C. January 2012.

Brimley, B., Saito, M., & Schultz, G. (2012). *Calibration of the Highway Safety Manual Safety Performance Function and Development of New Models for Rural Two-Lane Two-Way Highways*, Proceedings from the 2012 TRB 91st Annual Meeting. Washington, D.C. January 2012.

City of Regina. (2007). *Regina Road Network Plan*, City of Regina Engineering and Works Department.

City of Saskatoon, *2011 Business Plan and Preliminary Budget*, 2011.

City of Saskatoon. (2011). *Traffic Signals*, City of Saskatoon Website. Retrieved July 2011 from: "http://www.saskatoon.ca/DEPARTMENTS/Infrastructure%20Services/Transportation/Pages/TrafficSignals.aspx"

Colorado Department of Transportation. (2009). *Safety Performance Functions for Intersections*, Colorado Department of Transportation DTD Applied Research and Innovation Branch. Denver, CO.

Council, F.M., Zaloshnja, E., Miller, T., Persaud, B., (2005*). Crash Cost Estimates by Maximum Police Reported Injury Severity within Selected Crash Geometries*, Publication No. FHWA-HRT-05-051, Federal Highway Administration, U.S. Department of Transportation.

Dai, D., (2012). *Identifying clusters and risk factors of injuries in pedestrian–vehicle crashes in a GIS environment*, Journal of Transport Geography, in press.

De Pauw, E., Daniels, S., Brijs, T., Elke, H., Geert, W., (2011). *The Magnitude Of The Regression To The Mean Effect In Traffic Crashes*, Presented at the 24th Annual International Co-operation on Theories and Concepts in Traffic Safety, Warsaw, Poland.

Derek Murray Consulting and Associates, (2010). *Population, Employment and Economic Analysis of Regina,* Report Prepared for City of Regina Planning and Sustainability Department. Retrieved August 2013 from: http://www.regina.ca/opencms/export/sites/regina.ca/residents/urban-planning/.media/pdf/population-employment-full.pdf

de Smith, M., Goodchild, M. & Longley, P. (2012). *Geospatial Analysis*, Third Edition, Retrieved July 4, 2012 from: http://www.spatialanalysisonline.com/

Dufays T., Flahaut B., Steenberghen T., & Thomas I. (2004) *Intra-urban location and clustering of road accidents using GIS: a Belgian example*, International Journal of Geographical Information Systems, Vol 18, pp. 169-181. Retrieved July 4, 2012 from: http://www.scribd.com/doc/47878524/Intra-urban-location-and-clustering-of-road-accidents-using-GIS

Elvik, R. (2010). *Sources of uncertainty in estimated benefits of road safety programmes*, Accident Analysis and Prevention, Volume 42, Issue 6, pp 2171–2178.

Elvik, R. (2010). *Strengthening incentives for efficient road safety policy priorities: The roles of cost–benefit analysis and road pricing*, Safety Science 48.

Elvik, R., Vaa, T. (eds.), (2004), *The Handbook of Road Safety Measures*, Amsterdam: Elsevier.

Erdogan, S., Yilmaz, I., Baybura, T., Gullu, M., (2008). *Geographical information systems aided traffic accident analysis system case study: city of Afyonkarahisar*, Accident Analysis and Prevention. 40, 174–181.

ESRI. (2012). *How Multi-Distance Spatial Cluster Analysis Works: Ripley's k-function (Spatial Statistics),* ArcGIS Resource Center. Retrieved July 3, 2012 from:

http://resources.esri.com/help/9.3/arcgisdesktop/com/gp_toolref/spatial_statistics_tools/how_multi_distance_spatial_cluster_analysis_colon_ripley_s_k_function_spatial_statistics_works.htm

Federal Highway Administration (FHWA). (1998). *Life-Cycle Cost Analysis in Pavement Design,* Pavement Division Interim Technical Bulletin.

Federal Highway Administration (FHWA). (2000). *Prediction of the Expected Safety Performance of Rural Two-Lane Highways,* Publication No. FHWA-RD-99-207.

Federal Highway Administration (FHWA). (2003). *Economic Analysis Primer*. Retrieved January 2012 from: http://www.fhwa.dot.gov/infrastructure/asstmgmt/primer.pdf

Federal Highway Administration (FHWA). (2008). *Safety Evaluation of Flashing Beacons at STOP-Controlled Intersections*, Publication No. FHWA-HRT-08-044.

Flahaut, B., Mouchart, M., San Martin, E., Thomas, I., (2003). *The local spatial autocorrelation and the kernel method for identifying black zones: a comparative approach,* Accident Analysis and Prevention 35(6), 991–1004.

Fridstrom, J. Ifver, S. Ingebrigtsen, R. Kulmala, & L.K. Thomsen. (1995). *Measuring the Contribution of Randomness, Exposure, Weather, and Daylight to the Variation in Road Accident Counts,* Accident Analysis and Prevention, Vol. 27(1), pp. 1-20.

Garber, N. & G. Rivera. (2010). *Safety performance functions for intersections on highways maintained by the Virginia Department of Transportation,* Final Contract Report. Retrieved January 2012 from: http://www.virginiadot.org/vtrc/main/online_reports/pdf/11-cr1.pdf

Garber, N., Rivera, G. & Lim, I. (2011). *Safety Performance Functions for Intersections in Virginia,* Proceedings from the 2011 TRB 90th Annual Meeting. Washington, D.C. January 2011.

Hamidi, A., Fontaine, M., & Demetsky, M. (2010). *A Planning-Level Methodology for Identifying High-Crash Sections of Virginia's Primary System,* Virginia Transportation Research Council Research Report.

Harwood, D., Bauer, K., Richard, K., Gilmore, D., Graham, J., Potts, I., Torbic, D., Hauer, E. (2007). *Methodology to Predict the Safety Performance of Urban and Suburban Arterials.* National Cooperative Highway Research Program Project 17-26. Retrieved April 2, 2012 from http://onlinepubs.trb.org/onlinepubs/nchrp/nchrp_w129p1&2.pdf

Harwood, D., Council,F., Hauer, E., Hughes, W. & Vogt, A. (2000). *Prediction of the Expected Safety Performance of Rural Two-Lane Highways.* Publication No. FHWA-RD-99-207.

Retrieved April 2, 2012 from http://www.fhwa.dot.gov/publications/research/safety/99207/99207.pdf

Harwood, D., Torbic, D., Richard, K., Meyer, M., (2010). *SafetyAnalyst: Software Tools for Safety Management of Specific Highway Sites*, Final Report of the Federal Highway Administration, FHWA-HRT-10-063.

Hauer, E. & Bamfo, J. (1997). *Two tools for finding what function links the dependent variable to the explanatory variables,* Proceedings of ICTCT 97: International Cooperation on Theories and Concepts in Traffic Safety (pp. 1–7), Lund, Sweden.

Hauer, E. (2011). *Computing what the public wants: Some issues in road safety cost–benefit analysis,* Accident Analysis and Prevention 43.

Hauer, E., Allery, B., Kononov, J., Griffith, M., (2004). *How Best to Rank Sites with Promise.* Transportation Research Record: Journal of the Transportation Research Board, No. 1897, TRB, National Research Council, Washington, D.C., pp. 48–54.

Hauer, E., Harwood, D., Council, F., Griffith, M., (2002). *Estimating Safety by the Empirical Bayes Method: A Tutorial*, Transportation Research Record 1784, 126–131, Transportation Research Board, Washington, DC.

Hilbe, J. (2008). *Negative Binomial Regression*. Cambridge University Press. Cambridge University Press, Cambridge, UK.

Kuo, P., Zeng, X., Lord, D., (2012). *Guidelines for Choosing Hot-Spot Analysis Tools Based on Data Characteristics, Network Restrictions, and Time Distributions*. 91st Annual Transportation Research Board Meeting. Washington, D.C.

Larsen, M., (2010). *Philadelphia Traffic Accident Cluster Analysis using GIS and SANET*, Master of Urban Spatial Analytics Capstone Project, Penn Institute for Urban Research.

Lee, C., Xu, X., & Nguyen, V, (2011). *Non-intersection-related Crashes at Mid-block in an Urban Divided Arterial Road with High Truck Volume,* Presented at the 90th Meeting of the Transportation Research Board, Washington, D.C.

Li, R. & Rose, G. (2011). *Incorporating uncertainty into short-term travel time predictions.* Transportation Research Part C: Emerging Technologies, Vol. 19, No. 6.

Loo, B. (2009). *The Identification of Hazardous Road Locations: A Comparison of the Blacksite and Hot Zone Methodologies in Hong Kong*, The University of Hong Kong, International Journal of Sustainable Transportation, Vol. 3, Issue 3, pp. 187-202.

Lord, D., Geedipally, S., Persaud, B., Washington, S., van Schalkwyk, I., Ivan, J., Lyon, C. & Jonsson, T. (2008*). Methodology to Predict the Safety Performance of Rural Multilane*

Highways, Contractor's Final Report for NCHRP Project 17-29. Retrieved April 2, 2012 from http://onlinepubs.trb.org/onlinepubs/nchrp/nchrp_w126.pdf

Lord, D., Mannering, F., (2010). *The Statistical Analysis of Crash-Frequency Data: A Review and Assessment of Methodological Alternatives*, Transportation Research, Part A, Vol. 44 (5), pp. 291-305.

Lu, J., Gan, A., Haleem, K., Alluri, P. & Liu, K. (2012). *Comparing Locally-Calibrated and SafetyAnalyst-Default Safety Performance Functions for Florida's Urban Freeways*, Proceedings from the 2012 TRB 91st Annual Meeting. Washington, D.C. January 2012.

Lyon, C., Haq, A., Persaud, B. & Kodama, S. (2005). *Safety Performance Functions for Signalized Intersections in Large Urban Areas: Development and Application to Evaluation of Left-Turn Priority Treatment,* Transportation Research Record: Journal of the Transportation Research Board, Volume 1908, pp. 165-171.

Magee, L. (1990). *R^2 Measures Based on Wald and Likelihood Ratio Joint Significance Tests*, The American Statistician, Vol. 44, No. 3 (Aug., 1990), pp. 250-253. Published by: American Statistical Association. Retrieved March 15, 2012 from: http://www.jstor.org/stable/2685352

Marleau, M. & E. Hildebrand. (2010). *Collision Prediction for Two Lane Rural Roads Using IHSDM: A Canadian Experience.* Proceedings of the 20th Canadian Multidisciplinary Road Safety Conference. Niagra Falls, ON.

Miller, H. & Shaw, S. (2001). *Geographic Information Systems for Transportation: Principles and Applications*, Oxford University Press, USA.

Minnesota Department of Public Safety. (2011). *Minnesota Motor Vehicle Crash Facts.* Retrieved March 2012 from: https://dps.mn.gov/divisions/ots/educational-materials/Documents/CRASH-FACTS-2010.pdf

Mishra, S., S. Khasnabis, & S. Swain. (2011). *An approach to incorporate uncertainty and risk in transportation investment decision making: Detroit River International Crossing case study,* Annual Meeting of the Transportation Research Board (TRB), Washington DC.

Mohaymany, A., Shahri, M., & Mirbagheri, B. (2013). *GIS-based method for detecting high-crash-risk road segments using network kernel density estimation.* Geo-spatial Information Science. February 2013 Issue.

Moons, E., Brijs, T., & Wets, G. (2009). *Identifying Hazardous Road Locations: Hot Spots versus Hot Zones*, Transactions on Computational Science VI, Lecture Notes in Computer Science Volume 5730, 2009, pp 288-300.

Ng, M., Zhang, Z., & Waller, S. (2011). *The price of uncertainty in pavement infrastructure management planning: An integer programming approach.* Transportation Research Part 27 C: Emerging Technologies, Vol. 19, No. 6.

O'Sullivan, D., Unwin, D.J., (2003). *Geographic Information Analysis*. John Wiley & Sons, Inc., Hoboken.

Okabe, A., Satohb, T. & Sugiharac, K. (2009). *A kernel density estimation method for networks, its computational method and a GIS-based tool*, International Journal of Geographical Information Science, Volume 23, Issue 1, 2009. Retrieved July 4, 2012 from: http://www.tandfonline.com/doi/ref/10.1080/13658810802475491#tabModule

Park, C.S. (2007). *Contemporary Engineering Economics*, Pearson/Prentice Hall. Upper Saddle River, NJ.

Park, P., Lord, D. (2010). *Investigating Regression to the Mean in Before-and-After Speed Data Analysis*, Transportation Research Record: Journal of the Transportation Research Board, Issue 2165, pp 52-58.

Park, P., Sahaji, R. (2013). *Safety network screening for municipalities with incomplete traffic volume data*, Accident Analysis and Prevention 50, 2013, 1062-1072.

Park, P, Young, J. (2012). *Development of a Geographic Information System (GIS) to Identify Potential High Collision Locations in Regina*. Final Report for SGI, Regina Operations Centre.

Persaud, B., Lord, D., Palmisano, J. (2002). *Calibration and Transferability of Accident Prediction Models for Urban Intersections.* Transportation Research Record: Journal of the Transportation Research Board Iss. 1784, pp. 57-64.

Plug, C., Xiab, J., Caulfield, C., (2011). *Spatial and temporal visualization techniques for crash analysis.* Accident Analysis and Prevention 43, 1937–1946.

Sacchi, E., Persaud, B. & Bassani, M. (2012). *Assessing International Transferability of the Highway Safety Manual Crash Prediction Algorithm and its Components*, Proceedings from the 2012 TRB 91st Annual Meeting. Washington, D.C. January 2012.

Saskatchewan Government Insurance (SGI). (2007*). Saskatchewan Traffic Accident Information System (TAIS) Data Dictionary*. Government of Saskatchewan. Regina, Saskatchewan.

Saskatchewan Government Insurance (SGI). (2011). *2009 Saskatchewan Traffic Accident Facts,* Retrieved January 2012 from: http://www.sgi.sk.ca/pdf/tais/ TAIS_2009_Annual_Report.pdf

Saskatchewan Government Insurance (SGI). (2012). *2010 Saskatchewan Traffic Accident Facts.* Retrieved January 2012 from: http://www.sgi.sk.ca/pdf/tais/TAIS_2010_Annual_Report.pdf

Schmidt, F. & Tiffin, J. (1969). *Distortion of drivers estimates of automobile speed as a function of speed adaptation*. Journal of Applied Psychology, Vol. 53, 1969.

Schwarz, G. (1978). *Estimating the Dimension of a Model,* Annals of Statistics. Volume 6, Number 2, pp. 461-464.

Statistics Canada. (2010). *Population of Census Metropolitan Areas*. Retrieved January 2012 from: http://www.statcan.gc.ca/tables-tableaux/sum-som/l01/cst01/demo05a-eng.htm

Steenberghen, T., Aerts, K., Thomas, I., (2010). *Spatial clustering of events on a network.* Journal of Transport Geography 18, 411–418.

Steenberghen, T., Thomas, I. & Wets, G. (2005). *Innovative Spatial Analysis Techniques for Traffic Safety, Scientific Support Plan for a Sustainable Development Policy*. Retrieved July 3, 2012 from: http://www.belspo.be/belspo/organisation/Publ/pub_ostc/CPtrans/rappCP34_en.pdf

Tegge, R., Jo, J. & Ouyang, Y. (2010). *Development and Application of Safety Performance Functions for Illinois,* Research Report for Illinois Center for Transportation.

Terefe, B. (2010). *Greenhouse Gas Emissions from Private Vehicles in Canada, 1990 to 2007.* 2010. Retrieved March 15, 2012 from: http://www.statcan.gc.ca/pub/16-001-m/2010012/part-partie1-eng.htm

Transport and Rural Infrastructure Services Learning and Sharing Programme (TRISP) (2005). *Risk and Uncertainty Analysis,* Economic Evaluation Notes TRN-7, UK Department for International Development and the World Bank.

Truong, L., Somenahalli, S., (2011). *Using GIS to Identify Pedestrian-Vehicle Crash Hot Spots and Unsafe Bus Stops,* Journal of Public Transportation 14, No. 1.

Vodden, K., Smith, D., Eaton, F., Mayhew, D., (2007). *Analysis and Estimation of the Social Cost of Motor Vehicle Collisions in Ontario,* Transport Canada Final Report TP 14800F.

Washington, S., Persaud, B., Lyon, C., & Oh, J. (2005). *Validation of Accident Models for Intersections.* FHWA Report, Publication No. FHWA-RD-03-037.

Wilson, G. (1994). *Guide to Benefit-Cost Analysis in Transport Canada.* Retrieved January 2012 from: http://www.tc.gc.ca/media/documents/corporate-services/bca.pdf

Xie, F., Gladhill, K., Dixon, K., & Monsere, C. (2011). *Calibrating the Highway Safety Manual Predictive Models for Oregon State Highways*, Annual Meeting of the Transportation Research Board (TRB), Washington DC.

Xie, Z. & Yan, J. (2008). *Kernel Density Estimation of Traffic Accidents in a Network Space*. Computers, Environment, and Urban Systems, 35 (5), 396-406. Retrieved July 4, 2012 from: http://digitalcommons.wku.edu/geog_fac_pub/3

Yamada, I. & Thill, J., (2004). *Comparison of planar and network K-functions in traffic accident analysis*. Journal of Transport Geography 12, 149–158.

Young, J. & Park, P. (2012). *Comparing the Highway Safety Manual's Safety Performance Functions with Jurisdiction-Specific Functions for Intersections in Regina.* Proceedings from the 2012 Annual Conference of the Transportation Association of Canada, Fredericton, New Brunswick. October 2012.

Young, J. & Park, P. (2013). *Benefits of small municipalities using jurisdiction-specific safety performance functions rather than the Highway Safety Manual's calibrated or uncalibrated safety performance functions.* Canadian Journal of Civil Engineering, 10.1139/cjce-2012-0501. In Press. Published on the Web March 25, 2013.

APPENDIX A

SAMPLE CALCULATION FOR NETWORK SCREENING METHODS

EPDO Average Collision Frequency with EB Adjustment

A sample calculation is provided for a 4-leg signalized intersection. The selected intersection is UGRID RE688050, 9th Avenue North & McCarthy Boulevard.

Step 1: Calculate Weighting Factors for Collision Severity

The first step accounts for the severity of the collision based on the societal collision cost for a particular collision severity relative to a PDO collision.

$$f_{y(weight)} = \frac{CC_y}{CC_{PDO}}$$

Where:

$f_{y(weight)}$ = EPDO weighting factor based on collision severity, y;

CC_y = Collision cost for each severity, y; and,

CC_{PDO} = Collision cost for PDO collision severity.

This study used the societal costs provided in the HSM:

Severity	Societal Cost
Fatal	$4,008,900.00
Injury	$82,600.00
PDO	$7,400.00

$$f_{Fatal(weight)} = \frac{\$4{,}008{,}900}{\$7{,}400}$$

$$f_{Fatal(weight)} = 541.7$$

$$f_{Injury(weight)} = \frac{\$82{,}600}{\$7{,}400}$$

$$f_{Injury(weight)} = 11.2$$

Step 2: Calculate the Predicted Average Collision Frequency from an SPF

Step 2.1: Calibrate SPF

$$C_r = \frac{\sum_{all\ sites} observed\ collisions}{\sum_{all\ sites} predicted\ collisions}$$

$$N_{predicted,y} = C_r \times N_y$$

Where:

C_r = Calibration factor;

$N_{predicted,y}$ = Predicted number of collisions for severity, y; and,

N_y = Uncalibrated predicted number of collisions for severity, y.

$$C_{r(tot)} = \frac{9{,}481}{9{,}527}$$

$$C_{r(tot)} = 0.995$$

$$C_{r(FI)} = \frac{1{,}827}{1{,}835}$$

$$C_{r(FI)} = 0.996$$

$$C_{r(PDO)} = \frac{7{,}654}{7{,}701}$$

$$C_{r(PDO)} = 0.994$$

Step 2.2: Determine and Apply the Appropriate SPF for the Facility Type

$$N_{(total)} = C_{r(tot)} \times a \times \left(\frac{MajAADT}{1000}\right)^b \times \left(\frac{MinAADT}{1000}\right)^c$$

$$N'_{(FI)} = C_{r(FI)} \times a \times \left(\frac{MajAADT}{1000}\right)^b \times \left(\frac{MinAADT}{1000}\right)^c$$

$$N'_{(PDO)} = C_{r(PDO)} \times a \times \left(\frac{MajAADT}{1000}\right)^{b} \times \left(\frac{MinAADT}{1000}\right)^{c}$$

$$N_{(FI)} = N_{(total)} \times \left(\frac{N'_{(FI)}}{N'_{FI} + N'_{PDO}}\right)$$

$$N_{(PDO)} = N_{(total)} - N_{(FI)}$$

Where:

$N_{(total)}$ = Predicted total collisions;

$N'_{(FI)}$ = Fatal and injury component of the total collisions;

$N'_{(PDO)}$ = PDO component of the total collisions;

$N_{(FI)}$ = Predicted fatal and injury collisions; and,

$N_{(PDO)}$ = Predicted PDO collisions.

$$N_{(total)} = 0.995 \times 0.395 \times \left(\frac{19{,}500}{1000}\right)^{0.684} \times \left(\frac{16{,}100}{1000}\right)^{0.665}$$

$$N_{(total)} = 19.04$$

$$N'_{(FI)} = 0.996 \times 0.049 \times \left(\frac{19{,}500}{1000}\right)^{0.945} \times \left(\frac{16{,}100}{1000}\right)^{0.503}$$

$$N'_{(FI)} = 3.28$$

$$N'_{(PDO)} = 0.994 \times 0.344 \times \left(\frac{19{,}500}{1000}\right)^{0.630} \times \left(\frac{16{,}100}{1000}\right)^{0.704}$$

$$N'_{(PDO)} = 15.75$$

$$N_{(FI)} = 19.04 \times \left(\frac{3.28}{3.28 + 15.75}\right)$$

$$N_{(FI)} = 3.28$$

$$N_{(PDO)} = 19.04 - 3.28$$

$$N_{(PDO)} = 15.76$$

Step 3: Calculate Annual Correction Factor

Annual correction factors are then applied to the SPFs to account for annual changes in traffic volume.

$$C_{n(total)} = \frac{N_{predicted,n(total)}}{N_{predicted,1(total)}} \; and \; C_{n(FI)} = \frac{N_{predicted,n(FI)}}{N_{predicted,1(FI)}}$$

Where:

$C_{n(total)}$ = Annual correction factor for total collisions;

$C_{n(FI)}$ = Annual correction factor for fatal and injury collisions;

$N_{predicted,n(total)}$ = Predicted number of total collisions for year, n;

$N_{predicted,1(total)}$ = Predicted number of total collisions for year 1;

$N_{predicted,n(FI)}$ = Predicted number of fatal and injury collisions for year, n; and,

$N_{predicted,1(FI)}$ = Predicted number of fatal and injury collisions for year 1.

$$C_{5(total)} = \frac{22.65}{19.04}$$

$$C_{5(total)} = 1.19$$

$$C_{5(FI)} = \frac{3.90}{3.28}$$

$$C_{5(FI)} = 1.19$$

Step 4: Calculate Weighted Adjustment

The EB weight factor is then calculated for each location. The weight factor is dependent on the overdispersion parameter, study period, and the predicted number of collisions obtained from the calibrated SPF. An increase in any of these variables will cause a decrease in the weight factor.

$$w_y = \frac{1}{1 + k \times \left(\sum_{Study\ Period} N_{predicted,y}\right)}$$

Where:

w_y = Empirical Bayes weight for severity, y;

k = Overdispersion parameter from the appropriate SPF; and,

$N_{predicted,y}$ = Predicted average collision frequency for severity type, y.

$$w_{total} = \frac{1}{1 + 0.111 \times (19.04 + 19.13 + 22.65 + 22.76 + 22.65)}$$

$$w_{total} = 0.078$$

$$w_{FI} = \frac{1}{1 + 0.109 \times (3.28 + 3.30 + 3.90 + 3.90 + 3.90)}$$

$$w_{FI} = 0.334$$

Step 5: Calculate First Year EB-Adjusted Expected Average Collision Frequency

The EB-adjusted expected average collision frequency is obtained by applying the weight factor to the predicted and observed collision frequencies. As the weight factor increases, more emphasis will be placed on the predicted collision frequency obtained from the SPFs. Based on the definition of the weight factor, more emphasis will be placed on the SPF for lower overdispersion parameters, shorter study periods and fewer predicted number of collisions.

$$N_{expected,n(total)} = w_{total} \times N_{predicted,n(total)} + (1 - w_{total}) \times \left(\frac{\sum_{n=1}^{j} N_{observed,n(total)}}{\sum_{n=1}^{j} C_{n(total)}} \right)$$

$$N_{expected,n(FI)} = w_{FI} \times N_{predicted,n(FI)} + (1 - w_{FI}) \times \left(\frac{\sum_{n=1}^{j} N_{observed,n(FI)}}{\sum_{n=1}^{j} C_{n(FI)}} \right)$$

Where:

$N_{expected,n,(total)}$ = EB-adjusted expected total average collision frequency for year, n;

$N_{predicted,n(total)}$ = Calibrated predicted total average collision frequency from SPF;

$N_{observed,n(total)}$ = Observed number of total collisions for year, n;

$w_{(total)}$ = Weight factor for total collisions;

$C_{n(total)}$ = Annual correction factor for total collisions;

$N_{expected,n,(FI)}$ = EB-adjusted expected fatal and injury average collision frequency for year, n;

$N_{predicted,n(FI)}$ = Calibrated predicted fatal and injury average collision frequency from SPF;

$N_{observed,n(FI)}$ = Observed number of fatal and injury collisions for year, n;

$w_{(FI)}$ = Weight factor for fatal and injury collisions;

$C_{n(FI)}$ = Annual correction factor for fatal and injury collisions; and,

j = Number of years in the study.

$$N_{expected,1(total)} = 0.078 \times 19.04 + (1 - 0.078) \times \left(\frac{187}{1.00 + 1.00 + 1.19 + 1.20 + 1.19}\right)$$

$$N_{expected,1(total)} = 32.39$$

$$N_{expected,1(FI)} = 0.334 \times 3.28 + (1 - 0.334) \times \left(\frac{39}{1.00 + 1.00 + 1.19 + 1.19 + 1.19}\right)$$

$$N_{expected,1(FI)} = 5.76$$

Step 6: Calculate Final Year EB-Adjusted Average Collision Frequency

The ranking of locations is based on the most recent year in the study period. The final year expected collision frequency is calculated by multiplying the SPF predicted collision frequency by the annual correction factor for the final year in the study.

$$N_{expected,n(total)} = N_{expected,1(total)} \times C_{n(total)}$$

$$N_{expected,n(FI)} = N_{expected,1(FI)} \times C_{n(FI)}$$

$$N_{expected,n(PDO)} = N_{expected,n(total)} - N_{expected,n(FI)}$$

Where:

$N_{expected,n(total)}$ = EB-adjusted expected total average collision frequency for final year, n;

$N_{expected,1(total)}$ = EB-adjusted expected total average collision frequency for year 1;

$N_{expected,n(FI)}$ = EB-adjusted expected fatal and injury average collision frequency for final year, n;

$N_{expected,1(FI)}$ = EB-adjusted expected fatal and injury average collision frequency for year 1;

$N_{expected,n(PDO)}$ = EB-adjusted expected PDO average collision frequency for final year, n; and,

C_n = Annual correction factor for year, n

$$N_{expected,5(total)} = 32.39 \times 1.19$$

$$N_{expected,5(total)} = 38.52$$

$$N_{expected,5(FI)} = 5.76 \times 1.19$$

$$N_{expected,5(FI)} = 6.84$$

$$N_{expected,5(PDO)} = 38.52 - 6.84$$

$$N_{expected,5(PDO)} = 31.68$$

*small discrepancies in the numbers are due to rounding.

Step 7: Calculate the Proportion of Fatal and Injury Collisions

Since the predicted fatal and injury collisions are combined into a single SPF, the weight factor that is applied to calculate an EPDO score must be relative to the proportion of the observed fatal and injury collisions.

$$P_F = \frac{\sum N_{observed,(F)}}{\sum N_{observed,(FI)}}$$

$$P_I = \frac{\sum N_{observed,(I)}}{\sum N_{observed,(FI)}}$$

Where:

P_F = Proportion of observed number of fatal collisions out of FI collisions;

P_I = Proportion of observed number of injury collisions out of FI collisions;

$N_{observed,(F)}$ = Observed number of fatal collisions;

$N_{observed\ ,(I)}$ = Observed number of injury collisions; and,

$N_{observed,(FI)}$ = Observed number of fatal and injury collisions.

$$P_F = \frac{6}{1{,}827}$$

$$P_F = 0.003$$

$$P_I = \frac{1{,}821}{1{,}827}$$

$$P_I = 0.997$$

Step 8: Calculate the Weight of Fatal and Injury Collisions

The EPDO weight factor for fatal/injury collisions is obtained by summing the product of the proportion of fatal and injury collisions with their respective EPDO collision cost.

$$w_{EPDO,FI} = P_F \times f_{F(weight)} + P_I \times f_{inj(weight)}$$

Where:

$w_{EPDO,FI}$ = EPDO weight factor for fatal and injury collisions;

$f_{inj(weight)}$ = EPDO injury weight factor;

$f_{F(weight)}$ = EPDO fatal weight factor;

P_F = Proportion of observed number of fatal collisions out of FI collisions; and,

P_I = Proportion of observed number of injury collisions out of FI collisions;

$$w_{EPDO,FI} = 0.003 \times 541.7 + 0.997 \times 11.2$$

$$w_{EPDO,FI} = 12.90$$

*small discrepancies in the numbers are due to rounding.

Step 9: Calculate the Final Year EPDO Expected Average Collision Frequency

The final year EPDO expected average collision frequency is calculated by summing the expected PDO collision frequency with the EPDO weighted, expected fatal/injury collisions.

$$N_{expected,n(EPDO)} = N_{expected,n(PDO)} + w_{EPDO,FI} \times N_{expected,n(FI)}$$

Where:

$N_{expected,n(EPDO)}$ = EPDO expected average collision frequency for year, n;

$N_{expected,n(PDO)}$ = EB-adjusted expected PDO average collision frequency for year, n;

$w_{EPDO,FI}$ = EPDO weight factor for fatal and injury collisions; and,

$N_{expected,n(FI)}$ = EB-adjusted expected fatal and injury average collision frequency for year, n.

$$N_{expected,5(EPDO)} = 31.68 + 12.90 \times 6.84$$

$$N_{expected,5(EPDO)} = 119.97$$

Step 10: Rank Sites by EB-Adjusted EPDO Score

Sites are then ranked from highest to lowest EPDO score to identify the locations from most likely to least likely to benefit from a safety improvement.

Excess Expected Average Collision Frequency with EB Adjustment

The Excess Expected Average Collision Frequency with EB Adjustment is used to rank locations based on the difference between estimates provided by the SPFs and the EB-adjusted estimates.

This procedure is intended to identify those locations sites which experience more collisions than expected for other locations with similar characteristics (AASHTO, 2010). To calculate the excess collision frequency, the EB adjusted collision frequency must be calculated as described previously (i.e., follow steps 1-8 listed above). The procedure for calculating the excess collision frequency is listed below.

A sample calculation is provided for a 4-leg signalized intersection. The selected intersection is UGRID RE688050, 9th Avenue North & McCarthy Boulevard.

Step 9: Calculate the Excess Expected Average Collision Frequency

The excess collision frequency is the difference between the EB-adjusted collision frequency and the predicted collision frequency obtained from the SPF. A positive excess collision frequency indicates that a location is not performing as well as other locations with similar traffic volumes and geometric characteristics.

$$Excess_y = \left(N_{expected,n(PDO)} - N_{predicted,n(PDO)}\right) + \left(N_{expected,n(FI)} - N_{predicted,n(FI)}\right)$$

Where:

$Excess_n$ = Excess expected collisions for year, n;

$N_{expected,n}$ = EB-adjusted expected average collision frequency for year, n; and,

$N_{predicted,n}$ = SPF predicted average collision frequency for year, n.

$$Excess_5 = (31.68 - 18.75) + (6.84 - 3.90)$$

$$Excess_5 = 15.88$$

Step 10: Calculate EPDO Excess

The excess collisions can be converted into EPDO scores in order to account for the severity of the collisions. This is accomplished through applying a weighting factor.

$$Excess_y = \left(N_{expected,n(PDO)} - N_{predicted,n(PDO)}\right) + \left(N_{expected,n(FI)} - N_{predicted,n(FI)}\right) \times w_{EPDO}$$

Where:

$Excess_y$ = Excess expected collisions for year, n;

$N_{expected,n}$ = EB-adjusted expected average collision frequency for year, n; and,

$N_{predicted,n}$ = SPF predicted average collision frequency for year, n; and,

$w_{EPDO,FI}$ = EPDO weight factor for fatal and injury collisions.

$$Excess_5 = (31.68 - 18.75) + (6.84 - 3.90) \times 12.90$$

$$Excess_5 = 50.88$$

Step 11: Rank Sites by Excess EB-Adjusted EPDO Score

Sites are then ranked from highest to lowest excess EPDO score to identify the locations from most likely to least likely to benefit from a safety improvement.

APPENDIX B

Network Screening Results for 3 and 4-Leg Signalized Intersections

Network Screening Results for 3-Leg Unsignalized Intersections

Network Screening Results for 4-Leg Unsignalized Intersections

Network Screening Results for All Regina Intersections

Network Screening Results for Major Arterial Road Segments

Network Screening Results for Minor Arterial Road Segments

Network Screening Results for Collector Road Segments

Network Screening Results for All Regina Road Segments

Network Screening Results for 3 and 4-Leg Signalized Intersections

Location	UGRID	Int. Type	Major AADT					Minor AADT					Fatal					Injury					PDO					EPDO		EPDO Rank	
			2005	2006	2007	2008	2009	2005	2006	2007	2008	2009	2005	2006	2007	2008	2009	2005	2006	2007	2008	2009	2005	2006	2007	2008	2009	Excess	Expected	Excess	Expected
9th Ave N & McCarthy Blvd	RE688050	4S	19500	19500	21500	21500	21500	16100	16100	18900	18900	18900	0	0	0	0	0	11	3	9	7	9	26	17	28	29	48	50.9	120.0	1	9
Dewdney Ave & Lewvan Dr	RE697760	4S	33800	33800	33900	33900	33900	13900	13900	15700	15700	15700	0	0	0	0	0	12	11	9	7	9	22	26	28	44	23	50.1	142.3	2	3
4th Ave & Lewvan Dr	RE683430	4S	33400	33400	33400	33400	33400	11600	11600	11700	11700	11700	1	0	0	0	0	11	9	12	6	8	21	24	25	23	18	49.3	126.8	3	6
Park St & Victoria Ave	RE706920	4S	25900	25900	25900	25900	26200	18400	18400	18400	18400	18400	0	0	0	0	0	9	6	10	6	10	19	22	27	36	40	41.8	122.4	4	7
Prince Of Wales Dr & Victoria Ave	RE707580	4S	28450	29500	29500	29500	37600	11400	15100	15100	15100	15200	0	0	0	0	0	5	8	4	10	9	23	17	22	35	57	40.7	139.8	5	5
Arcola Ave & Victoria Ave	RE689720	4S	27600	27600	27600	27600	28200	15400	15400	15400	15400	15400	0	0	0	0	0	2	8	9	6	8	24	14	19	30	52	28.4	106.3	6	10
Albert St & Saskatchewan Dr	RE689010	4S	32300	32300	32300	33100	33100	20800	20800	20800	17200	17200	0	0	0	0	0	8	5	7	8	11	23	31	33	32	54	27.3	122.4	7	8
Victoria Ave & Coleman Cres	RE696740	4S	29800	32200	32200	32200	52400	5800	5800	5800	5800	15400	0	0	0	0	0	7	5	3	6	6	13	14	11	24	13	25.6	158.4	8	2
Albert St & Parliament Ave	RE689000	4S	27500	27500	27500	27400	27400	13900	13900	13900	12600	12600	0	0	0	0	0	3	8	12	4	1	24	20	30	26	32	21.1	89.2	9	16
Victoria Ave & Winnipeg St	RE709460	4S	23100	23100	23100	23100	27900	11700	11700	11700	11700	11700	0	0	0	0	0	7	4	5	1	5	14	20	23	34	30	19.6	85.9	10	17
6th Ave N & Albert St	RE684570	4S	26600	26600	25600	25600	25600	9800	9800	9900	9900	9900	0	0	0	0	0	1	7	8	5	5	24	8	15	16	12	17.0	73.2	11	25
4th Ave & Winnipeg St	RE683680	4S	15350	15100	15100	15100	22900	2850	2700	2700	2700	4500	0	0	0	0	0	3	2	4	1	2	8	7	7	17	10	16.6	49.6	12	50
Arcola Ave & Doan Dr & Edinburgh Dr	RE689760	4S	17400	18800	18800	18800	18800	5000	5000	5000	5000	5000	0	0	0	0	0	5	4	5	6	1	5	3	3	5	6	14.5	44.1	13	58
Albert St & 1st Ave N & Avonhurst Dr	RE688930	4S	34700	34700	33600	32600	32600	13400	13400	15200	15200	15200	0	0	0	0	0	10	5	5	5	7	21	16	23	31	25	14.1	101.8	14	11
Winnipeg St & Saskatchewan Dr & Arcola Ave	RE708860	4S	18300	18300	18300	18300	18300	16850	16300	16300	16300	18200	1	0	0	0	0	8	3	3	3	2	19	15	17	20	34	12.6	71.5	15	27
Dewdney Ave & Elphinstone St	RE697250	4S	16100	16100	16100	16100	16100	9800	9800	9800	9700	9700	0	0	0	0	0	4	3	4	4	2	10	18	15	14	11	12.4	49.6	16	49
Arcola Ave & Park St	RE689910	4S	21600	21500	21500	21500	21500	13100	13000	13000	13000	13000	0	0	0	0	0	7	1	2	6	3	25	20	18	26	21	11.5	67.7	17	29
Cavendish St & Dewdney Ave	RE694640	4S	16700	16700	16700	16700	19900	7100	7100	7100	7100	5800	0	0	0	0	0	2	2	2	7	2	10	15	5	15	17	11.5	45.2	18	57
7th Ave & Lewvan Dr	RE686020	4S	31200	31200	32400	32400	32400	6000	6000	4700	4700	4700	0	0	0	0	0	8	5	2	3	4	12	10	5	10	10	11.3	56.9	19	39
Quance St & Coleman Cres	RE716770	3S	5950	6600	5800	5800	15400	5800	5800	3400	3400	4700	0	0	0	0	0	1	1	1	2	0	9	13	9	11	11	10.0	34.0	20	75
Lewvan Dr & 1st Ave N	RE714000	4S	33400	33400	33400	33400	33400	12450	12400	12400	12400	12400	0	0	0	0	0	2	4	6	9	8	26	11	12	16	27	9.7	89.7	23	15
Lewvan Dr & Pasqua St & Sherwood Dr	RE707260	4S	28200	28200	29600	29600	29600	15400	15400	17400	17400	17400	0	0	0	0	1	9	4	6	2	6	22	25	19	19	21	7.9	94.8	27	14
Arcola Ave & University Park Dr	RE689780	4S	26750	28700	28700	28700	28700	15650	16900	16900	16900	19800	0	0	0	0	0	6	6	9	3	4	25	14	21	17	25	7.5	98.3	29	12
Albert St & Dewdney Ave	RE689110	4S	34500	34500	34500	34500	34500	16100	16100	16100	16100	16100	0	0	0	0	0	7	8	3	7	2	22	26	24	16	38	0.3	95.3	66	13
Albert St & Victoria Ave	RE689030	4S	30900	30900	30900	28600	28600	18000	18000	18000	18100	18100	0	0	0	0	0	7	4	6	5	4	19	22	28	26	15	-0.5	85.7	71	18
Victoria Ave & Fleet St & University Park Dr	RE700150	4S	35550	35400	35400	35400	52400	19450	20500	20500	20500	20500	0	0	1	0	0	9	5	6	5	4	25	11	28	36	41	-14.7	140.8	135	4
Rochdale Blvd & Pasqua St	RE718810	4S	24500	24500	24500	44800	31400	20800	20800	21500	36200	23100	0	0	0	0	0	3	3	5	4	5	23	17	30	28	39	-22.7	84.2	140	19
Broad St & Victoria Ave	RE693030	4S	29000	29000	29000	29000	29000	20000	20000	20000	20000	27900	0	0	0	0	0	3	4	3	5	5	16	11	15	16	19	-27.7	83.1	143	20
Pasqua St & Ring Rd & 9th Ave N	RE717710	4S	32300	32300	32300	61100	50300	28000	28000	28000	50300	45800	0	0	0	0	0	3	11	4	6	12	22	20	19	25	45	-69.4	164.5	144	1

Int. Type	Description
3S	3-Leg Signalized
4S	4-Leg Signalized

Network Screening Results for 3-Leg Unsignalized Intersections

Location	UGRID	Int. Type	Major AADT					Minor AADT					Fatal					Injury					PDO					EPDO		EPDO Rank	
			2005	2006	2007	2008	2009	2005	2006	2007	2008	2009	2005	2006	2007	2008	2009	2005	2006	2007	2008	2009	2005	2006	2007	2008	2009	Excess	Expected	Excess	Expected
Massey Rd & Parliament Ave	RE704860	3U	10600	10600	10600	12700	12700	7100	7100	7100	6900	6900	0	0	0	0	0	2	2	3	1	4	5	10	7	11	11	18.1	29.9	1	1
Arcola Ave & College Ave	RE689800	3U	20350	20500	20500	20500	20500	9600	9600	9600	9600	7700	0	0	0	0	0	0	4	2	2	3	15	12	9	8	8	10.0	27.9	2	2
Saskatchewan Dr & Smith St	RE708870	3U	20800	20800	20800	14650	14650	3100	3100	3100	3100	3100	0	0	0	0	0	1	3	2	1	1	3	5	2	4	2	6.6	13.2	3	5
Quance St & Star Lite St	RE711950	3U	5950	6600	3400	3400	5800	700	700	700	3250	3400	0	0	0	0	0	0	0	1	2	1	6	0	3	2	1	6.0	9.7	4	12
Grant Dr & Grant Rd	RE701370	3U	6300	6300	6300	6000	6000	5800	5800	5800	5800	5800	0	0	0	0	0	0	5	1	0	1	1	3	1	3	1	5.4	11.4	5	8
Henderson Dr & McDonald St (North Int)	RE711000	3U	13300	13300	13300	13300	9700	4500	4500	4500	4500	5000	0	0	0	0	0	0	1	1	0	1	5	11	2	9	8	4.0	11.4	6	9
Argyle St N & Sangster Blvd (North Int)	RE712660	3U	4500	4500	4600	4600	4600	4300	4300	4400	4400	4400	0	0	0	0	0	0	1	0	0	1	3	1	4	9	8	3.6	7.6	7	17
Hillsdale St & Kramer Blvd	RE702580	3U	11300	11300	11300	11200	11200	9600	9600	9600	11100	11100	0	0	0	0	0	3	0	0	2	0	10	7	4	10	7	3.5	19.6	8	3
Cornwall St & Victoria Ave	RE696030	3U	18000	18000	18000	13800	13800	1300	1300	1300	1300	1300	0	0	0	0	0	0	1	1	0	1	3	1	7	4	6	3.4	6.5	9	23
Courtney St & Rochdale Blvd	RE696110	3U	4700	4700	5300	5300	5300	3950	3900	3700	3700	3700	0	0	0	0	0	1	0	0	1	2	1	2	0	8	1	3.3	7.1	10	20
McIntyre St & Saskatchewan Dr	RE705500	3U	20800	20800	20800	14650	14650	1300	1300	1300	1300	1450	0	0	0	0	0	0	1	0	1	1	3	3	2	1	7	2.9	6.3	11	25
Broadway Ave & Park St (North Int)	RE693300	3U	8400	6700	6700	6700	6700	5500	5500	5500	5500	5500	0	0	0	0	0	0	0	2	1	0	7	2	5	3	2	2.5	8.7	12	14
7th Ave N & Winnipeg St	RE685970	3U	13100	12500	12500	12500	13300	2850	2800	3100	3100	3100	0	0	0	0	0	1	0	1	0	1	2	0	4	2	6	2.2	8.4	13	15
Prince Of Wales Dr. & Jenkins Dr.	RE678740	3U	1900	1900	1900	1900	6200	1200	1200	1200	1200	2600	0	0	0	0	0	0	0	0	0	0	3	2	2	1	2	1.6	4.8	14	34
Lansdowne Dr & Rink Ave	RE703860	3U	7800	7800	7200	7200	7200	2400	2400	1800	1800	1800	0	0	0	0	0	0	0	2	1	0	2	1	2	2	0	1.6	4.2	15	44
McAra St & Victoria Ave	RE705000	3U	27600	27600	27600	27600	28200	3250	3300	3300	3300	2400	0	0	0	0	0	0	0	1	2	0	5	10	4	4	5	1.5	9.9	16	11
1st Ave N & Winnipeg St	RE680020	3U	14500	14200	14200	14200	14200	5400	5400	6000	6000	6200	0	0	0	0	0	1	0	1	1	1	5	3	4	5	3	1.4	13.0	17	7
Hillsdale St & Parker Ave	RE702630	3U	5300	5300	5300	5500	5500	4800	4800	4800	5400	5400	0	0	0	0	0	1	0	0	0	1	2	2	4	3	2	1.3	6.7	18	22
Creekside Rd & Prince Of Wales Dr	RE696760	3U	5950	6500	6500	6500	7600	2200	2200	2200	2200	2700	0	0	0	0	0	0	0	0	0	2	3	2	0	0	1	1.2	4.9	19	33
College Ave & Elphinstone St	RE695420	3U	7300	7300	7300	6900	6900	2000	2000	2000	1800	1800	0	0	0	0	0	0	0	0	0	1	4	3	1	2	2	1.1	3.6	20	53
3rd Ave & Albert St	RE682570	3U	35000	35000	34100	30600	30600	5300	5300	4500	4500	4500	0	0	0	0	0	1	1	0	1	2	6	3	5	9	11	1.0	16.1	21	4
Ross Ave & Toronto St	RE708610	3U	16250	15800	15800	16700	16700	2800	2800	3200	3200	3200	0	0	0	0	0	0	0	0	0	1	7	2	6	0	3	-0.2	7.2	60	19
Cambridge Ave & Fleet St	RE693930	3U	12800	12800	12800	12800	23300	2400	2400	2400	2400	2700	0	0	0	0	0	1	0	0	0	0	3	0	1	3	4	-0.6	7.5	79	18
9th Ave N & Winnipeg St (E Leg)	RE698690	3U	10600	10600	10900	10900	10900	6500	6500	7300	7300	6600	0	0	0	0	0	2	1	1	0	0	1	0	2	2	2	-0.6	9.6	80	13
Gordon Rd & Grant Rd	RE701120	3U	11500	11500	11500	11500	11500	6400	6400	6400	9300	9300	0	0	0	0	0	1	1	0	0	1	5	9	2	0	3	-1.0	13.1	89	6
25th Ave & Pasqua St	RE681130	3U	6600	6600	6600	11500	11500	6100	6100	6100	6600	6600	0	0	0	0	0	0	0	0	0	1	2	1	2	0	7	-2.8	7.8	109	16
1st Ave & Broad St (North Int)	RE709730	3U	19400	19400	20400	19200	19200	6400	6400	6400	8000	8000	0	0	0	0	0	0	0	1	1	0	2	0	2	6	8	-6.7	11.0	116	10

Int. Type	Description
3U	3-Leg Unsignalized

Network Screening Results for 4-Leg Unsignalized Intersections

Location	UGRID	Int. Type	Major AADT					Minor AADT					Fatal					Injury					PDO					EPDO		EPDO Rank	
			2005	2006	2007	2008	2009	2005	2006	2007	2008	2009	2005	2006	2007	2008	2009	2005	2006	2007	2008	2009	2005	2006	2007	2008	2009	Excess	Expected	Excess	Expected
Fleet St & Victoria Ave N Srv Rd	RE700100	4U	17600	15600	15600	15600	24700	4000	4400	4400	4400	9400	0	0	0	0	0	3	3	2	2	2	12	16	11	17	13	30.4	60.1	1	1
Glencairn Rd & Victoria Ave N Srv Rd	RE701010	4U	6050	5800	5800	5800	9400	4500	4600	4600	4600	6200	0	0	0	0	0	0	0	1	3	3	15	14	12	17	16	22.8	34.2	2	2
14th Ave & Winnipeg St	RE677970	4U	10400	10200	10200	9800	9800	3150	3700	3700	3700	3700	0	0	0	0	0	0	2	3	4	3	2	6	11	11	10	16.2	25.5	3	4
3rd Ave & Elphinstone St	RE682280	4U	8800	8800	8500	8700	8700	5300	5300	4500	4500	4500	0	0	0	0	0	1	2	2	5	2	1	3	3	3	11	12.4	21.6	4	8
14th Ave & Albert St	RE677480	4U	30100	30100	30100	28100	28100	4900	4900	4900	4900	4900	0	0	0	0	0	4	4	1	1	2	5	12	11	8	14	9.0	33.7	5	3
15th Ave & Broad St	RE678110	4U	19500	19500	19500	21100	21100	2800	2800	2800	2800	2800	0	0	0	0	0	1	1	2	3	1	9	6	4	7	4	7.1	22.5	6	6
7th Ave & Brown St	RE686740	4U	4900	4900	4900	4900	5300	2100	2500	2500	2500	5200	0	0	0	0	0	4	0	1	1	0	4	6	0	1	4	7.1	13.7	7	19
4th Ave & McIntosh St	RE683490	4U	11600	11600	11600	11600	10600	2200	2200	1600	1600	1600	0	0	0	0	0	4	1	1	1	0	5	3	0	5	10	6.9	13.7	8	18
McIntyre St & Victoria Ave	RE705510	4U	18000	18000	18000	18100	18100	2700	2700	2700	2900	2900	0	0	0	0	0	2	2	0	4	0	3	4	2	7	4	6.0	19.8	9	9
Eastgate Dr & Prince Of Wales Dr	RE699010	4U	10750	11800	11800	11800	15200	3000	2900	2900	2900	5800	0	0	0	0	0	3	0	0	0	2	9	5	1	7	4	5.8	22.0	10	7
Bentley Dr & Dewdney Ave	RE691940	4U	7800	8200	8200	8200	10500	1600	1600	1600	1600	2200	0	0	0	0	0	1	2	0	3	0	2	2	0	1	1	5.6	13.4	11	21
14th Ave & Lorne St	RE677710	4U	4900	4900	4900	4900	4900	2200	2200	2200	2200	2200	0	0	0	0	0	2	0	0	0	1	5	5	8	3	6	4.4	8.6	12	44
7th Ave & McIntosh St	RE686410	4U	6000	6000	4700	4700	4700	3250	3400	3200	3200	3400	0	0	0	0	0	0	3	0	1	1	1	2	5	0	9	4.2	9.2	13	37
4th Ave & McDonald St	RE683480	4U	4750	4400	4400	4400	4700	3200	3000	3000	3000	4500	0	0	0	0	0	0	0	1	1	0	4	3	9	3	7	3.9	9.6	14	34
11th Ave & McIntyre St	RE675810	4U	7600	7600	7600	7600	7600	1600	1600	1600	1600	1600	0	0	0	0	0	0	0	1	2	2	1	1	2	0	2	3.4	8.6	15	43
College Ave & Lorne St	RE695650	4U	16300	16300	16300	17500	17500	2200	2200	2200	2200	2200	0	0	0	0	0	1	0	2	1	2	4	4	2	3	0	3.1	15.0	16	13
25th Ave & Millar Cres & Montague St	RE681120	4U	8300	8300	8300	8300	8300	3600	3600	3600	4000	4000	0	0	0	0	0	2	1	1	1	0	2	2	2	5	2	3.1	11.5	17	26
Arcola Ave & 14th Ave & Fleury St	RE689850	4U	11900	11900	11900	11900	11900	3150	3700	3700	3700	3700	0	0	0	0	0	2	1	0	2	1	2	1	2	2	3	2.6	13.5	18	20
7th Ave & Cannon St	RE685470	4U	2500	2500	2500	2500	4300	2250	2300	2300	2300	2300	0	0	0	0	0	0	1	0	0	1	3	2	5	2	2	2.6	6.5	19	57
Dewdney Ave & Royal St	RE697900	4U	16000	16000	14300	14300	14300	2000	2000	1800	1800	1800	0	0	0	0	0	2	0	1	1	1	1	2	3	3	5	2.6	11.8	20	25
12th Ave & Park St	RE676650	4U	18400	18400	18400	18400	18400	2200	2200	2200	2200	2200	0	0	0	0	0	1	2	0	1	0	3	9	5	5	6	1.9	14.2	22	16
25th Ave & Argyle Rd & Retallack St	RE681020	4U	11200	11200	11200	11800	11800	7300	7300	7300	8200	8200	0	0	0	0	0	1	2	1	0	2	7	1	6	3	5	1.7	17.2	26	10
Ross Ave & (Se Ramp) & Sioux St	RE718510	4U	10300	10300	10300	10300	11400	6650	7300	7300	7300	8200	0	0	0	0	0	1	0	1	2	0	6	8	3	0	12	0.9	16.0	33	12
Devonshire Dr & Rochdale Blvd	RE697150	4U	14000	14000	13600	13600	13600	5600	5600	5800	5800	5800	0	0	0	0	0	1	0	1	0	2	3	5	2	9	10	-0.1	14.8	55	15
23rd Ave & Broad St & Wascana Pky	RE680950	4U	13000	13000	13000	13300	18400	11600	11600	11600	12000	12000	0	0	0	0	0	2	0	0	1	2	8	5	6	5	9	-3.9	22.5	110	5
Parliament Ave & Rae St	RE707050	4U	8900	8900	8900	12700	12700	8900	8900	8900	12600	12600	0	0	0	0	0	1	0	0	1	0	5	2	6	7	9	-5.4	14.9	115	14
Osler St & Victoria Ave	RE706810	4U	20000	20000	20000	20000	27900	5000	5000	5000	5000	5000	0	0	0	0	0	0	0	0	1	1	5	10	8	5	6	-8.5	16.3	122	11
Quance St & Truesdale Dr	RE708050	4U	11500	11500	11500	11500	14600	8400	8400	8400	8400	14400	0	0	0	0	0	2	0	0	0	0	6	2	2	1	7	-10.3	13.7	124	17

Int. Type	Description
4U	4-Leg Unsignalized

Network Screening Results for All Regina Intersections

Location	UGRID	Int. Type	Major AADT					Minor AADT					Fatal					Injury					PDO					EPDO		EPDO Rank	
			2005	2006	2007	2008	2009	2005	2006	2007	2008	2009	2005	2006	2007	2008	2009	2005	2006	2007	2008	2009	2005	2006	2007	2008	2009	Excess	Expected	Excess	Expected
9th Ave N & McCarthy Blvd	RE688050	4S	19500	19500	21500	21500	21500	16100	16100	18900	18900	18900	0	0	0	0	0	11	3	9	7	9	26	17	28	29	48	50.9	120.0	1	9
Dewdney Ave & Lewvan Dr	RE697760	4S	33800	33800	33900	33900	33900	13900	13900	15700	15700	15700	0	0	0	0	0	12	11	9	7	9	22	26	28	44	23	50.1	142.3	2	3
4th Ave & Lewvan Dr	RE683430	4S	33400	33400	33400	33400	33400	11600	11600	11700	11700	11700	1	0	0	0	0	11	9	12	6	8	21	24	25	23	18	49.3	126.8	3	6
Park St & Victoria Ave	RE706920	4S	25900	25900	25900	25900	26200	18400	18400	18400	18400	18400	0	0	0	0	0	9	6	10	6	10	19	22	27	36	40	41.8	122.4	4	7
Prince Of Wales Dr & Victoria Ave	RE707580	4S	28450	29500	29500	29500	37600	11400	15100	15100	15100	15200	0	0	0	0	0	5	8	4	10	9	23	17	22	35	57	40.7	139.8	5	5
Fleet St & Victoria Ave N Srv Rd	RE700100	4U	17600	15600	15600	15600	24700	4000	4400	4400	4400	9400	0	0	0	0	0	3	3	2	2	2	12	16	11	17	13	30.4	60.1	6	33
Arcola Ave & Victoria Ave	RE689720	4S	27600	27600	27600	27600	28200	15400	15400	15400	15400	15400	0	0	0	0	0	2	8	9	6	8	24	14	19	30	52	28.4	106.3	7	10
Albert St & Saskatchewan Dr	RE689010	4S	32300	32300	32300	33100	33100	20800	20800	20800	17200	17200	0	0	0	0	0	8	5	7	8	11	23	31	33	32	54	27.3	122.4	8	8
Victoria Ave & Coleman Cres	RE696740	4S	29800	32200	32200	32200	52400	5800	5800	5800	5800	15400	0	0	0	0	0	7	5	3	6	6	13	14	11	24	13	25.6	158.4	9	2
Glencairn Rd & Victoria Ave N Srv Rd	RE701010	4U	6050	5800	5800	5800	9400	4500	4600	4600	4600	6200	0	0	0	0	0	0	0	1	3	3	15	14	12	17	16	22.8	34.2	10	76
Albert St & Parliament Ave	RE689000	4S	27500	27500	27500	27400	27400	13900	13900	13900	12600	12600	0	0	0	0	0	3	8	12	4	1	24	20	30	26	32	21.1	89.2	11	16
Victoria Ave & Winnipeg St	RE709460	4S	23100	23100	23100	23100	27900	11700	11700	11700	11700	11700	0	0	0	0	0	7	4	5	1	5	14	20	23	34	30	19.6	85.9	12	17
Massey Rd & Parliament Ave	RE704860	3U	10600	10600	10600	12700	12700	7100	7100	7100	6900	6900	0	0	0	0	0	2	2	3	1	4	5	10	7	11	11	18.1	29.9	13	92
6th Ave N & Albert St	RE684570	4S	26600	26600	25600	25600	25600	9800	9800	9900	9900	9900	0	0	0	0	0	1	7	8	5	5	24	8	15	16	12	17.0	73.2	14	25
4th Ave & Winnipeg St	RE683680	4S	15350	15100	15100	15100	22900	2850	2700	2700	2700	4500	0	0	0	0	0	3	2	4	1	2	8	7	7	17	10	16.6	49.6	15	51
14th Ave & Winnipeg St	RE677970	4U	10400	10200	10200	9800	9800	3150	3700	3700	3700	3700	0	0	0	0	0	0	2	3	4	3	2	6	11	11	10	16.2	25.5	16	105
Arcola Ave & Doan Dr & Edinburgh Dr	RE689760	4S	17400	18800	18800	18800	18800	5000	5000	5000	5000	5000	0	0	0	0	0	5	4	5	6	1	5	3	3	5	6	14.5	44.1	17	59
Albert St & 1st Ave N & Avonhurst Dr	RE688930	4S	34700	34700	33600	32600	32600	13400	13400	15200	15200	15200	0	0	0	0	0	10	5	5	5	7	21	16	23	31	25	14.1	101.8	18	11
Winnipeg St & Saskatchewan Dr & Arcola Ave	RE708860	4S	18300	18300	18300	18300	18300	16850	16300	16300	16300	18200	1	0	0	0	0	8	3	3	3	2	19	15	17	20	34	12.6	71.5	19	27
3rd Ave & Elphinstone St	RE682280	4U	8800	8800	8500	8700	8700	5300	5300	4500	4500	4500	0	0	0	0	0	1	2	2	5	2	1	3	3	3	11	12.4	21.6	20	120
Lewvan Dr & 1st Ave N	RE714000	4S	33400	33400	33400	33400	33400	12450	12400	12400	12400	12400	0	0	0	0	0	2	4	6	9	8	26	11	12	16	27	9.7	89.7	29	15
Lewvan Dr & Pasqua St & Sherwood Dr	RE707260	4S	28200	28200	29600	29600	29600	15400	15400	17400	17400	17400	0	0	0	0	1	9	4	6	2	6	22	25	19	19	21	7.9	94.8	34	14
Arcola Ave & University Park Dr	RE689780	4S	26750	28700	28700	28700	28700	15650	16900	16900	16900	19800	0	0	0	0	0	6	6	9	3	4	25	14	21	17	25	7.5	98.3	36	12
Albert St & Dewdney Ave	RE689110	4S	34500	34500	34500	34500	34500	16100	16100	16100	16100	16100	0	0	0	0	0	7	8	3	7	2	22	26	24	16	38	0.3	95.3	149	13
Albert St & Victoria Ave	RE689030	4S	30900	30900	30900	28600	28600	18000	18000	18000	18100	18100	0	0	0	0	0	7	4	6	5	4	19	22	28	26	15	-0.5	85.7	215	18
Victoria Ave & Fleet St & University Park Dr	RE700150	4S	35550	35400	35400	35400	52400	19450	20500	20500	20500	20500	0	0	1	0	0	9	5	6	5	4	25	11	28	36	41	-14.7	140.8	378	4
Rochdale Blvd & Pasqua St	RE718810	4S	24500	24500	24500	44800	31400	20800	20800	21500	36200	23100	0	0	0	0	0	3	3	5	4	5	23	17	30	28	39	-22.7	84.2	383	19
Broad St & Victoria Ave	RE693030	4S	29000	29000	29000	29000	29000	20000	20000	20000	20000	27900	0	0	0	0	0	3	4	3	5	5	16	11	15	16	19	-27.7	83.1	386	20
Pasqua St & Ring Rd & 9th Ave N	RE717710	4S	32300	32300	32300	61100	50300	28000	28000	28000	50300	45800	0	0	0	0	0	3	11	4	6	12	22	20	19	25	45	-69.4	164.5	387	1

Int. Type	Description
3S	3-Leg Signalized
4S	4-Leg Signalized
3U	3-Leg Unsignalized
4U	4-Leg Unsignalized

Network Screening Results for Major Arterial Road Segments

Street Name	UGRID	Length (m)	Traffic Volume					Fatal Collisions					Injury Collisions					PDO Collisions					EPDO		EPDO Rank	
			2005	2006	2007	2008	2009	2005	2006	2007	2008	2009	2005	2006	2007	2008	2009	2005	2006	2007	2008	2009	Excess	Expected	Excess	Expected
Albert St	RE3400	362	27500	27500	27500	27400	27400	0	0	0	0	0	3	3	4	3	1	10	10	8	17	15	21.7	34.8	1	1
9th Ave N	RE900015	810	16100	16100	18900	18900	18900	0	0	0	0	0	1	0	1	4	5	10	4	5	8	10	13.9	30.0	2	2
Albert St	RE7500	406	22800	22800	22700	22700	22700	0	0	0	0	0	0	3	0	1	5	5	2	9	9	11	11.0	22.2	3	4
Broad St	RE38700	488	21700	21700	21700	25300	24400	0	0	0	0	0	4	1	2	3	1	3	0	1	2	10	10.4	24.9	4	3
Albert St	RE3100	231	25100	25100	25100	22100	22100	0	0	0	0	0	0	1	3	2	0	13	10	9	11	10	10.1	16.8	5	5
Saskatchewan Dr	RE350300	315	20800	20800	20800	14600	14600	0	0	0	0	0	0	1	3	2	2	10	6	10	10	7	8.6	13.6	6	7
Albert St	RE3200	171	25100	25100	25100	22100	22100	0	0	0	0	0	1	1	0	0	2	7	6	8	5	7	5.5	10.6	7	18
Albert St	RE5000	172	30100	30100	30100	28100	28100	0	0	0	0	0	0	3	0	0	1	4	8	4	6	6	4.6	11.6	8	13
Albert St	RE6600	135	35000	35000	34100	29000	29000	0	0	0	0	0	3	1	1	0	2	3	5	4	0	0	4.6	10.5	9	19
Avonhurst Dr	RE28000	210	13400	13400	15200	15200	15200	0	0	0	0	0	0	1	2	0	2	3	1	2	4	5	4.1	7.9	10	36
Dewdney Ave	RE89100	102	14000	14000	14000	14000	14000	0	0	0	0	0	0	0	1	0	1	3	5	5	10	8	4.0	5.8	11	77
Rochdale Blvd	RE334480	487	16600	16600	15800	15800	15800	0	0	0	0	0	0	2	1	2	0	2	4	5	5	3	3.9	12.1	12	11
Albert St	RE5200	183	30900	30900	30900	28600	28600	0	0	0	0	0	0	1	2	0	2	2	2	4	6	5	3.9	11.5	13	14
Albert St	RE5800	185	32300	32300	32300	33100	33100	0	0	0	0	0	2	0	2	1	0	0	6	6	5	2	3.9	13.2	14	8
Victoria Ave	RE441500	107	18000	18000	18000	13850	13850	0	0	0	0	0	0	1	0	1	2	2	4	5	11	5	3.8	5.6	15	82
Rochdale Blvd	RE334650	144	14000	14000	13600	13600	13600	0	0	0	0	0	0	0	1	1	1	9	3	4	3	3	3.4	5.8	16	78
Albert St	RE7400	208	22800	22800	22700	22700	22700	0	0	0	0	0	2	0	0	1	1	3	1	3	5	3	3.0	9.3	17	24
Dewdney Ave	RE89200	204	14000	14000	14000	14000	14000	0	0	0	0	0	0	3	0	0	0	3	0	5	3	5	2.8	6.0	18	72
Albert St	RE4900	183	30100	30100	30100	28100	28100	0	0	0	0	0	0	2	3	0	0	3	1	1	1	5	2.7	10.2	19	20
McCarthy Blvd	RE253500	499	14100	14100	14100	14100	14100	0	0	0	0	0	2	0	1	0	2	1	2	2	2	2	2.7	9.8	20	21
Wascana Pky	RE449300	523	13000	13000	13000	13300	18400	0	0	0	0	0	1	0	0	0	0	1	3	5	6	5	0.3	10.9	111	17
Albert St	RE6800	267	34700	34700	33600	32600	32600	0	0	0	0	0	1	2	0	0	0	4	2	5	6	5	-0.4	12.2	283	10
Albert St	RE4700	281	31500	31500	31500	30400	30400	0	0	0	0	0	0	1	0	0	2	4	2	5	1	6	-0.6	11.4	322	15
Broad St	RE39600	332	27300	27300	27300	27300	27300	0	0	0	0	0	1	0	1	1	0	2	1	7	2	3	-1.0	11.1	366	16
Albert St	RE4800	328	31500	31500	31500	30400	30400	0	0	0	0	0	2	0	0	0	0	5	3	6	5	6	-1.9	11.8	404	12
Pasqua St	RE298500	403	27500	27500	25300	38300	38300	0	0	0	0	0	0	1	1	0	1	2	1	0	1	0	-8.6	13.8	434	6
9th Ave N	RE900014	812	24000	24000	26100	26100	26100	0	0	0	0	0	1	0	0	0	1	3	2	5	1	5	-12.0	12.8	435	9

Network Screening Results for Minor Arterial Road Segments

Street Name	UGRID	Length (m)	Traffic Volume					Fatal Collisions					Injury Collisions					PDO Collisions					EPDO		EPDO Rank	
			2005	2006	2007	2008	2009	2005	2006	2007	2008	2009	2005	2006	2007	2008	2009	2005	2006	2007	2008	2009	Excess	Expected	Excess	Expected
Park St	RE292000	726	6450	6600	6600	6600	7400	0	0	0	0	0	1	1	1	1	1	0	0	2	2	1	5.0	10.5	1	2
Elphinstone St	RE125700	233	9800	9800	9800	9700	9700	0	0	0	0	0	2	0	0	0	0	2	5	2	4	1	2.4	4.8	2	7
23rd Ave	RE434000	275	8100	8100	8100	7800	7800	0	0	0	0	0	0	0	1	0	0	8	2	4	1	6	2.3	4.5	3	8
College Ave	RE67800	103	9500	9500	9500	9500	9500	0	0	0	0	0	0	0	0	1	2	4	0	0	2	2	1.9	2.9	4	19
Montague St	RE243200	180	6900	6900	6900	6900	6900	0	0	0	0	0	2	0	0	1	0	0	0	1	2	2	1.9	3.1	5	14
Winnipeg St	RE456700	174	8150	8200	8200	8200	8200	0	0	0	0	0	0	0	0	1	1	1	1	2	2	3	1.7	3.2	6	13
1st Ave N	RE147900	109	8000	8000	9600	9600	9600	0	0	0	0	0	1	0	2	0	0	0	1	1	0	1	1.6	2.6	7	22
1st Ave N	RE149000	499	4550	5700	3600	3600	3600	0	0	0	0	0	2	0	0	1	0	0	0	0	1	0	1.6	3.3	8	12
4th Ave	RE163800	205	6800	7100	7100	7100	6200	0	0	0	0	0	1	0	0	0	1	0	2	3	0	1	1.3	2.5	9	23
9th Ave N	RE279925	1001	2200	2200	2300	2300	2500	0	0	0	0	0	0	1	0	1	0	1	0	0	1	0	1.2	3.6	10	10
Elphinstone St	RE125875	186	9800	9800	9800	9700	9700	0	0	0	0	0	0	0	1	0	0	2	0	4	2	2	1.1	3.0	11	17
Argyle St N	RE19900	161	8300	8300	7500	7500	7500	0	0	0	0	0	1	0	0	0	1	1	0	1	0	1	1.0	2.2	12	30
9th Ave N	RE279910	1700	5300	5300	6200	6200	7100	0	0	0	0	0	1	0	0	1	2	2	3	0	6	3	1.0	13.8	13	1
Sherwood Dr	RE382900	109	7800	7800	8800	8800	8800	0	0	0	0	0	0	1	0	1	0	0	0	0	3	0	1.0	1.9	14	37
Elphinstone St	RE126300	178	7800	7800	7000	7000	7000	0	0	0	0	0	0	0	0	0	1	1	1	1	1	4	0.9	2.1	15	34
Fleet St	RE151400	351	6500	6200	6200	6200	9200	0	0	0	0	0	1	0	0	0	0	2	2	0	0	3	0.9	4.2	16	9
Elphinstone St	RE125100	171	7300	7300	7300	6600	6600	0	0	0	0	0	0	0	2	0	0	0	0	0	0	1	0.8	1.9	17	38
Argyle St N	RE20100	140	8300	8300	7500	7500	7500	0	0	0	0	0	1	0	0	1	0	0	0	1	0	0	0.8	1.8	18	41
Sherwood Dr	RE382800	121	7800	7800	8800	8800	8800	0	0	0	0	0	0	0	1	0	1	0	0	0	0	0	0.8	1.8	19	42
Elphinstone St	RE126500	172	8800	8800	8500	8700	8700	0	0	0	0	0	0	0	1	0	0	1	1	0	1	3	0.7	2.2	20	29
Kramer Blvd	RE211000	175	9600	9600	9600	11100	11100	0	0	0	0	0	0	0	0	0	0	0	1	3	3	6	0.7	2.7	21	20
Dewdney Ave	RE93500	511	3500	3500	4400	4400	4400	0	0	0	0	0	0	0	0	1	0	0	0	1	2	3	0.7	2.9	22	18
6th Ave N	RE392300	408	9800	9800	9900	9900	9900	0	0	0	0	0	0	1	1	0	0	2	0	2	0	1	0.7	4.9	23	6
Kramer Blvd	RE211100	276	9600	9600	9600	11100	11100	0	0	0	0	0	0	0	0	0	1	0	1	3	1	1	0.3	3.5	37	11
Fleet St	RE151800	793	2150	2800	2800	2800	6300	0	0	0	0	0	0	0	0	0	1	2	1	0	0	0	0.2	5.3	49	5
Prince Of Wales Dr	RE305758	519	900	900	900	900	5600	0	0	0	0	0	0	0	0	0	0	1	0	3	0	0	0.1	3.0	52	15
Winnipeg St	RE458350	1112	5400	5400	6000	6000	6000	0	0	0	0	0	0	0	2	0	0	3	0	1	1	1	-0.7	6.1	214	4
Assiniboine Ave	RE30651	398	7350	7400	7400	7400	9000	0	0	0	0	0	1	0	0	0	0	0	0	0	0	0	-0.7	3.0	216	16
Fleet St	RE151550	1092	2550	3000	3000	3000	9800	0	0	0	0	0	0	1	0	0	0	1	0	0	1	1	-3.0	8.4	234	3

Network Screening Results for Collector Road Segments

Street Name	UGRID	Length (m)	Traffic Volume					Fatal Collisions					Injury Collisions					PDO Collisions					EPDO		EPDO Rank	
			2005	2006	2007	2008	2009	2005	2006	2007	2008	2009	2005	2006	2007	2008	2009	2005	2006	2007	2008	2009	Excess	Expected	Excess	Expected
Quance St	RE308275	575	5950	6600	3200	3200	4700	0	0	0	0	0	0	3	3	1	6	7	2	9	8	8	16.7	22.5	1	1
Quance St	RE308225	262	8400	8400	8400	8400	14600	0	0	0	0	0	0	2	0	0	1	8	3	7	7	7	8.6	13.8	2	2
Quance St	RE308255	348	5950	6600	3400	3400	3400	0	0	0	0	0	0	1	1	0	2	2	3	5	7	7	4.3	6.4	3	6
Quance St	RE308230	205	5950	6600	3400	3400	3400	0	0	0	0	0	1	0	1	0	1	3	6	4	10	5	3.9	4.9	4	15
Massey Rd	RE233400	193	7300	7300	7300	7000	6500	0	0	0	0	0	0	0	0	0	0	5	5	5	9	7	3.8	5.4	5	11
Hamilton St	RE190400	174	6300	6300	6300	5500	5500	0	0	0	0	0	0	0	1	0	0	3	2	7	4	10	3.5	4.6	6	16
Hamilton St	RE190500	210	8000	8000	8000	8000	4400	0	0	0	0	0	0	0	0	1	0	6	4	5	3	9	2.8	4.0	7	20
Hamilton St	RE190300	182	7100	7100	7100	7100	7100	0	0	0	0	0	0	0	0	0	1	2	3	3	5	5	2.5	4.1	8	18
Broadway Ave	RE44400	221	8900	8900	8900	12500	12500	0	0	0	0	0	1	0	0	2	1	1	1	0	0	0	2.4	5.9	9	9
Massey Rd	RE233500	269	6300	6300	6300	6100	6100	0	0	0	0	0	1	0	0	0	1	5	1	0	2	5	2.2	4.6	10	17
25th Ave	RE429900	171	4300	4300	4300	4300	4300	0	0	0	0	0	0	0	0	0	0	1	8	4	2	3	2.1	3.0	11	31
Castle Rd	RE60000	209	2300	2300	2300	2300	2000	0	0	0	0	0	0	0	0	0	0	3	0	5	4	5	1.8	2.4	12	50
Arens Rd	RE14880	263	5200	5200	5200	5200	10000	0	0	0	0	0	0	1	0	0	0	4	2	3	0	1	1.6	5.3	13	12
Dalgliesh Dr	RE82400	301	1400	1400	2100	2100	2100	0	0	0	0	0	0	1	0	0	0	2	1	3	2	2	1.5	2.6	14	44
Victoria Ave Srvrd N	RE900043	629	3500	3900	3900	3900	8100	0	0	0	0	0	0	0	2	0	1	5	0	1	1	2	1.4	12.4	15	4
Rae St	RE315400	184	8900	8900	8900	12700	12700	0	0	0	0	0	0	0	0	1	0	2	1	2	1	4	1.4	4.1	16	19
Rae St	RE314700	366	7300	7300	7300	7900	7900	0	0	0	0	0	0	1	0	1	0	4	0	3	1	4	1.3	6.1	17	8
11th Ave	RE119200	102	10200	10200	10200	10200	8200	0	0	0	0	0	0	0	0	0	0	0	4	2	4	4	1.3	2.1	18	69
Rae St	RE315300	170	8900	8900	8900	12700	12700	0	0	0	0	0	0	1	0	0	0	0	3	4	1	1	1.3	3.7	19	23
Star Lite St	RE396770	254	700	700	700	3250	5800	0	0	0	0	0	0	0	0	0	0	3	0	2	1	1	1.2	3.3	20	26
1st Ave	RE143800	415	6400	6400	6400	8000	8000	0	0	0	0	0	1	0	0	0	0	2	0	0	5	1	-1.0	4.9	946	14
Victoria Ave Srvrd N	RE900044	418	4000	4400	4400	4400	9400	0	0	0	0	0	0	0	0	0	0	2	0	3	3	2	-1.4	5.5	951	10
Henderson Dr	RE196532	718	2950	3400	3400	3400	4600	0	0	0	0	0	0	1	0	0	0	1	3	4	0	2	-1.7	6.2	957	7
23rd Ave	RE434100	478	8000	8000	8000	8700	8700	0	0	0	0	0	1	0	1	0	0	0	0	0	1	0	-2.6	5.2	964	13
Victoria Ave Srvrd N	RE900045	915	4500	4600	4600	4600	7400	0	0	0	0	0	0	1	0	0	1	7	3	0	6	2	-4.7	12.8	967	3
9th Ave N	RE278975	1650	6500	6500	7300	7300	6600	0	0	0	0	0	0	0	1	1	0	2	0	0	2	2	-29.5	8.2	968	5

Network Screening Results for All Regina Road Segments

Street Name	UGRID	Length (m)	Traffic Volume					Fatal Collisions					Injury Collisions					PDO Collisions					EPDO		EPDO Rank		Road Class
			2005	2006	2007	2008	2009	2005	2006	2007	2008	2009	2005	2006	2007	2008	2009	2005	2006	2007	2008	2009	Excess	Expected	Excess	Expected	
Albert St	RE3400	362	27500	27500	27500	27400	27400	0	0	0	0	0	3	3	4	3	1	10	10	8	17	15	21.7	34.8	1	1	MAJ
Quance St	RE308275	575	5950	6600	3200	3200	4700	0	0	0	0	0	0	3	3	1	6	7	2	9	8	8	16.7	22.5	2	4	COLL
9th Ave N	RE900015	810	16100	16100	18900	18900	18900	0	0	0	0	0	1	0	1	4	5	10	4	5	8	10	13.9	30.0	3	2	MAJ
Albert St	RE7500	406	22800	22800	22700	22700	22700	0	0	0	0	0	0	3	0	1	5	5	2	9	9	11	11.0	22.2	4	5	MAJ
Broad St	RE38700	488	21700	21700	21700	25300	24400	0	0	0	0	0	4	1	2	3	1	3	0	1	2	10	10.4	24.9	5	3	MAJ
Albert St	RE3100	231	25100	25100	25100	22100	22100	0	0	0	0	0	0	1	3	2	0	13	10	9	11	10	10.1	16.8	6	6	MAJ
Quance St	RE308225	262	8400	8400	8400	8400	14600	0	0	0	0	0	0	2	0	0	1	8	3	7	7	7	8.6	13.8	7	8	COLL
Saskatchewan Dr	RE350300	315	20800	20800	20800	14600	14600	0	0	0	0	0	0	1	3	2	2	10	6	10	10	7	8.6	13.6	8	10	MAJ
Albert St	RE3200	171	25100	25100	25100	22100	22100	0	0	0	0	0	1	1	0	0	2	7	6	8	5	7	5.5	10.6	9	23	MAJ
Park St	RE292000	726	6450	6600	6600	6600	7400	0	0	0	0	0	1	1	1	1	1	0	0	2	2	1	5.0	10.5	10	25	MIN
Albert St	RE5000	172	30100	30100	30100	28100	28100	0	0	0	0	0	0	3	0	0	1	4	8	4	6	6	4.6	11.6	11	18	MAJ
Albert St	RE6600	135	35000	35000	34100	29000	29000	0	0	0	0	0	3	1	1	0	2	3	5	4	0	0	4.6	10.5	12	24	MAJ
Quance St	RE308255	348	5950	6600	3400	3400	3400	0	0	0	0	0	0	1	1	0	2	2	3	5	7	7	4.3	6.4	13	72	COLL
Avonhurst Dr	RE28000	210	13400	13400	15200	15200	15200	0	0	0	0	0	0	1	2	0	2	3	1	2	4	5	4.1	7.9	14	44	MAJ
Dewdney Ave	RE89100	102	14000	14000	14000	14000	14000	0	0	0	0	0	0	0	1	0	1	3	5	5	10	8	4.0	5.8	15	90	MAJ
Rochdale Blvd	RE334480	487	16600	16600	15800	15800	15800	0	0	0	0	0	0	2	1	2	0	2	4	5	5	3	3.9	12.1	16	16	MAJ
Quance St	RE308230	205	5950	6600	3400	3400	3400	0	0	0	0	0	1	0	1	0	1	3	6	4	10	5	3.9	4.9	17	130	COLL
Albert St	RE5200	183	30900	30900	30900	28600	28600	0	0	0	0	0	0	1	2	0	2	2	2	4	6	5	3.9	11.5	18	19	MAJ
Albert St	RE5800	185	32300	32300	32300	33100	33100	0	0	0	0	0	2	0	2	1	0	0	6	6	5	2	3.9	13.2	19	11	MAJ
Massey Rd	RE233400	193	7300	7300	7300	7000	6500	0	0	0	0	0	0	0	0	0	0	5	5	5	9	7	3.8	5.4	20	106	COLL
Victoria Ave Srvrd N	RE900043	629	3500	3900	3900	3900	8100	0	0	0	0	0	0	0	2	0	1	5	0	1	1	2	1.4	12.4	69	14	COLL
9th Ave N	RE279910	1700	5300	5300	6200	6200	7100	0	0	0	0	0	1	0	0	1	2	2	3	0	6	3	1.0	13.8	96	9	MIN
Albert St	RE6800	267	34700	34700	33600	32600	32600	0	0	0	0	0	1	2	0	0	0	4	2	5	6	5	-0.4	12.2	1371	15	MAJ
Albert St	RE4700	281	31500	31500	31500	30400	30400	0	0	0	0	0	0	1	0	0	2	4	2	5	1	6	-0.6	11.4	1452	20	MAJ
Albert St	RE4800	328	31500	31500	31500	30400	30400	0	0	0	0	0	2	0	0	0	0	5	3	6	5	6	-1.9	11.8	1594	17	MAJ
Victoria Ave Srvrd N	RE900045	915	4500	4600	4600	4600	7400	0	0	0	0	0	0	1	0	0	1	7	3	0	6	2	-4.7	12.8	1630	12	COLL
Pasqua St	RE298500	403	27500	27500	25300	38300	38300	0	0	0	0	0	0	1	1	0	1	2	1	0	1	0	-8.6	13.8	1635	7	MAJ
9th Ave N	RE900014	812	24000	24000	26100	26100	26100	0	0	0	0	0	1	0	0	0	1	3	2	5	1	5	-12.0	12.8	1636	13	MAJ

Road Class	Description
MAJ	Major Arterial
MIN	Minor Arterial
COLL	Collector